The dynamics and roles of CD4+ T cells during *H. polygyrus* infection

Caitlin Margaret McManus

BSc (Hons)

Submitted in fulfilment of the requirement for the Degree of Doctor of Philosophy

Institute of Infection, Immunity and Inflammation

College of Medical, Veterinary and Life Sciences

University of Glasgow

January 2022

Abstract

Around one quarter of the world's population is infected with helminth parasites, which are masters at modulating their host immune system. Expansion of the T regulatory cell (Treg) compartment is seen in many helminth infections and may prevent T helper 2 (Th2) cells from mediating worm clearance. As the Treg and Teffector cell balance may determine resistance versus susceptibility, this thesis focuses on these populations during infection. The model helminth *Heligmosomoides polygyrus* was studied in two mouse strains with different susceptibilities to infection, Th2-biased BALB/c mice which expel infection, and Th1-skewed C57BL/6 with a more regulatory response that fails to clear. Using single cell RNA sequencing and flow cytometric analysis, the CD4+ T cell populations within the two strains were compared. At the RNA level, Th2 cells fell into 5 subsets, some showing signs of anergy, and others with stronger TCR, co-stimulation and cytokine signalling; overall BALB/c T cells were more highly activated. However, both strains showed high levels of regulatory IL-10 signalling when infected. Treg populations were also characterised, defining 5 subsets. Tregs from infected BALB/c were more transcriptionally active than their naïve counterparts, although C57BL/6 mice showed greater proportions of *Maf*+ and *Ly6e*+ subsets that might explain their susceptibility. Treg responses were further characterised at the protein level using flow cytometry, including some markers suggested by subset delineation in scRNAseq analysis. There was a marked increase in co-expression of GATA3 with Foxp3, consistent with the Th2 environment. However, in contrast to published work, RORγt+ Tregs were not more frequent and were not affected by blockade of IL-6 in vivo. The expression of co-inhibitory receptors CTLA-4, PD-1 and TIGIT were also assessed on Tregs and Teffector cells, with CTLA-4 upregulated on both Tregs and Teffector cells post infection whereas PD-1 and TIGIT were only upregulated on effectors. Finally, a novel approach was taken to identify the epitopes recognised by CD4+ T cells during H. polygyrus infection, using the novel mouse line Nr4a3-Tocky which allows temporal and sensitive tracking of TCR engagement and thus antigen recognition. However, only a small proportion of CD4+ T cells recognised excretory-secretory (HES) antigens, even when isolated from H. polygyrus experienced mice, and there were components in HES which activated naive CD4+ T cells. More studies are required to further understand the antigen specific response to H. polygyrus. Overall, the thesis demonstrates that the adaptive response to H. polygyrus differs in resistant versus susceptible individuals at the transcriptomic, signalling and cell population levels; further functional investigation into the dynamics and role of each subset is required in future research.

Table of Contents

Chapter 1 ..... Introduction ***1***

1.1 Helminth Infections 1

1.2 Anthelminthic therapies 3

1.3 Immune response to human helminth infection 5

1.4 Vaccination 7

1.4.1 Vaccination with irradiated helminths 8

1.4.2 Vaccination with helminth excretory secretory products 8

1.4.3 Vaccination with recombinant helminth molecules 9

1.5 The relationship between helminthiases and autoimmune and allergic disorders 11

1.5.1 The Hygiene Hypothesis 11

1.5.2 The Old Friends Hypothesis 12

1.6 Helminth therapy for allergic and autoimmune diseases 13

1.7 Use of helminth products for inflammatory disease treatment 15

1.8 Mouse models of helminthiases 16

1.8.1 Heligmosomoides polygyrus 17

1.9 Immune Regulation by H. polygyrus 19

1.9.1 Tregs 20

1.9.2 Dendritic cells 24

1.10 Immune regulators from H. polygyrus 25

1.10.1 TGF-ß Mimic 26

1.10.2 Hp-ARI 28

1.11 CD4+ T cell activation: from exogenous protein to activation 31

1.12 Thesis Aims 33

Chapter 2 ..... Materials and Methods ***37***

2.1 Methods 37

2.1.1 Mice 37

2.1.2 Parasites and Antigens 38

2.1.3 Tissue Processing 38
2.1.4 Flow cytometry 41
2.1.5 Cytokine Analysis 43
2.1.6 Cell Sorting 44
2.1.7 Cell Culture 44
2.1.8 Single Cell RNA Sequencing 47
2.1.9 Statistical analysis 49
2.2 Materials 51
2.2.1 Media table 51
2.2.2 Antibody table 53
Chapter 3..... Single Cell RNA analysis of T cell responses to helminth infection ***55***
3.1 Introduction 55
3.1.1 Diverse immune responses to the same parasite 55
3.2 Single cell RNA sequencing 56
3.2.1 Cell Hashing 58
3.2.2 Demuxlet 58
3.3 Aims 59
3.4 Results 59
3.4.1 Experimental design of single cell RNA sequencing 59
3.4.2 Viability and purity of CD3+ T cells sorted for single cell RNA sequencing . 61
3.4.3 Clustering of CD3+ T cells from naïve and H. polygyrus d7 infected mice .. 63
3.4.4 Clustering of Th2 cells from naïve and H. polygyrus infected mice 66
3.4.5 Pathway analysis of Th2 cells from naïve and H. polygyrus infected mice.. 68
3.4.6 Clustering of Tregs from naïve and H. polygyrus infected mice 72
3.4.7 Pathway analysis of Tregs from naïve and H. polygyrus infected mice..... 76
3.4.8 Purity and viability of CD4+ T cells sorted for single cell RNA sequencing.. 78
3.4.9 Assigning cell identities using cell hashing..... 80
3.4.10 Clustering of CD4+ T cells in naïve and H. polygyrus infected mice 82
3.4.11 Pathway analysis of CD4+ T cells from naïve and H. polygyrus infected mice 84
3.4.12 Clustering of Th2 cells from naïve and H. polygyrus infected mice..... 87
3.4.13 Pathway analysis of Th2 cells from naïve and H. polygyrus infected mice 90
3.4.14 Differential expression of genes in Th2 cells from naïve and H. polygyrus infected mice 93

3.4.15 Clustering of Tregs from naïve and H. polygyrus infected mice 96
3.4.16 Pathway analysis of Tregs from naïve and H. polygyrus infected mice ... 98
3.4.17 Differential expression of genes in Tregs from naïve and H. polygyrus infected mice 101
3.4.18 Validation of Treg gene hits from single cell RNA sequencing at the protein level..... 103
3.5 Discussion 106
3.6 Summary 111
Chapter 4 ..... Treg Characterisation ***113***
4.1 Introduction 113
4.1.1 Treg subtypes..... 113
4.1.2 Co-expression of transcription factors..... 113
4.1.3 The importance of IL-6 during H. polygyrus infection..... 117
4.1.4 Expression of co-inhibitory molecules by Tregs 118
4.2 Aims..... 123
4.3 Results..... 124
4.3.1 Dynamics of Treg expansion at d7 and d14 post H. polygyrus infection ... 124
4.3.2 Dynamics of Th2 cells at d7 and d14 post H. polygyrus infection..... 127
4.3.3 Location of Treg expansion during H. polygyrus infection..... 129
4.3.4 Dynamics of T-bet+ T cells during H. polygyrus infection..... 132
4.3.5 Dynamics of GATA3+ CD4+ T cells during H. polygyrus infection 135
4.3.6 Dynamics of RORγt+ CD4+ T cells during H. polygyrus infection..... 137
4.3.7 IL-6 antibody blockade effect on H. polygyrus infection..... 138
4.3.8 The effect of IL-6 blockade on RORγt+ CD4+ T cells during H. polygyrus infection 141
4.3.9 The effect of IL-6 blockade on GATA3 expression in Tregs during H. polygyrus infection 143
4.3.10 The effect of IL-6 blockade on T cell activation during H. polygyrus infection 145
4.3.11 The expression of CD44 on Teffector cells from H. polygyrus infected mice after IL-6 blockade..... 147
4.3.12 The effect of IL-6 blockade on the cytokine production of MLN T cells 149
4.3.13 The expression of CTLA-4 on T cells from H. polygyrus infected mice.. 151
4.3.14 The expression of PD-1 on CD4+ T cells during H. polygyrus infection.. 153
4.3.15 The expression of TIGIT on CD4+ T cells during H. polygyrus infection. 155

4.4 Discussion 157
4.4.1 Summary 165

Chapter 5..... T Cell antigen specificity during H. polygyrus infection ***167***

5.1 Introduction 167
5.1.1 Potential T cell epitopes during H. polygyrus infection 167
5.1.2 MHC II Epitope Prediction Methods 169
5.1.3 Experimental Markers of TCR engagement 170
5.2 Aims 174
5.3 Results 175
5.3.1 Hp-VAL-1.1 epitope predictions for C57BL/6 and BALB/c mice 175
5.3.2 Hp-VAL-2.1 epitope predictions for C57BL/6 and BALB/c mice 179
5.3.3 Hp-VAL-3 epitope predictions for C57BL/6 and BALB/c mice 181
5.3.4 Hp-VAL-4 epitope predictions for C57BL/6 and BALB/c mice 185
5.3.5 Comparison of BMDC:CD4+ T cell cocultures versus whole MLN restimulation of T cells in vitro 188
5.3.6 CD69 as a marker of in vitro TCR stimulation in Teffector cells 191
5.3.7 CD69 as a marker of in vitro TCR stimulation in Tregs 194
5.3.8 CD154 as a marker of in vitro TCR stimulation in Teffector cells 196
5.3.9 Nr4a3-Tocky mice as a marker of T cell restimulation in vitro 198
5.3.10 Restimulation of Nr4a3-Timer CD4+ T cells after 14 or 21 days of H. polygyrus infection 201
5.3.11 Restimulation of Nr4a3-Timer CD4+ T cells after secondary infection with H. polygyrus 203
5.3.12 Restimulation of Nr4a3-Timer CD4+ T cells after clearing H. polygyrus infection 206
5.3.13 Restimulation of Nr4a3-tocky CD4+ T cells with heat inactivated HES (hiHES) 209
5.3.14 Restimulation of Nr4a3-tocky CD4+ T cells with various Hp-VAL proteins 211
5.4 Discussion 213
5.5 Summary 217

Chapter 6..... Discussion ***219***

List of Tables

Table 2.1 Media used throughout the project 51-52

Table 2.2 Antibodies used throughout the project.....53

Table 5.1 Peptide predictions from NetMHCII and IEDB for *Hp*-VAL-1.1.....178

Table 5.2 Peptide predictions from NetMHCII and IEDB for *Hp*-VAL-2.1.....181

Table 5.3 Peptide predictions from NetMHCII and IEDB for *Hp*-VAL-3.....184

Table 5.4 Peptide predictions from NetMHCII and IEDB for *Hp*-VAL-4.....187

List of Figures

Figure 1.1 Life cycle of *Heligmosomoides polygyrus*.....19
Figure 1.2 The immune response to H. polygyrus and its immunomodulation.....30
Figure 3.1 Experimental workflow for single cell RNA sequencing.....60
Figure 3.2 Purity and viability of sorted cells for single cell RNA sequencing.....62
Figure 3.3 Guided clustering of CD3+ T cells from naïve and *H. polygyrus* infected mice.....65
Figure 3.4 Guided clustering of Th2 cells from naïve and *H. polygyrus* infected mice.....67
Figure 3.5 Pathway analysis of Th2 cells from naïve and *H. polygyrus* infected mice.....71
Figure 3.6 Guided clustering of Tregs from naïve and *H. polygyrus* infected mice.....75
Figure 3.7 Pathway analysis of Tregs from naïve and *H. polygyrus* infected mice.....77
Figure 3.8 Purity and viability of sorted cells for single cell RNA sequencing.....79
Figure 3.9 Assigning strain IDs to each cell and excluding doublets using Cell hashing.....81
Figure 3.10 Guided clustering of CD4+ T cells from naïve and *H. polygyrus* infected mice.....83
Figure 3.11 Pathway analysis of CD4+ T cells from naïve and *H. polygyrus* infected mice.....86
Figure 3.12 Guided clustering of Th2 cells from naïve and *H. polygyrus* infected mice.....89
Figure 3.13 Pathway analysis of Th2 cells from naïve and *H. polygyrus* infected mice.....92
Figure 3.14 Differentially expressed genes in the Th2 cell cluster during *H. polygyrus* infection.....95
Figure 3.15 Guided clustering of Tregs from naïve and *H. polygyrus* infected mice.....97
Figure 3.16 Pathway analysis of Tregs from naïve and *H. polygyrus* infected mice.....100
Figure 3.17 Differentially expressed genes in the Treg cluster during *H. polygyrus* infection.....102

Figure 3.18 Confirmation of gene hits at the protein level.....105
Figure 4.1 The dynamics of Treg expansion at d7 and d14 *H. polygyrus* infection.....126
Figure 4.2 The dynamics of Th2 expansion at d7 and d14 *H. polygyrus* infection.....128
Figure 4.3 The locations of Treg expansion during *H. polygyrus* infection.....131
Figure 4.4 The dynamics of T-bet expansion at d7 and d14 *H. polygyrus* infection.....134
Figure 4.5 The dynamics of GATA3 expansion at d7 and d14 *H. polygyrus* infection.....136
Figure 4.6 The dynamics of RORγt expansion at d7 and d14 *H. polygyrus* infection.....138
Figure 4.7 Th2 cells induced by *H. polygyrus* are further expanded in IL-6 blockade.....140
Figure 4.8 Dynamics of RORγt during *H. polygyrus* infection during IL-6 blockade.....142
Figure 4.9 Dynamics of GATA3+ Tregs during *H. polygyrus* infection during IL-6 blockade.....144
Figure 4.10 Dynamics of CD44 expression on Tregs during *H. polygyrus* infection during IL-6 blockade.....146
Figure 4.11 Dynamics of CD44 expression on different Teffector populations during *H. polygyrus* infection during IL-6 blockade.....148
Figure 4.12 Cytokine output from anti-CD3 treated whole MLN is affected by IL-6 blockade during infection.....150
Figure 4.13 The expression of CTLA-4 on Tregs and Th2 cells from *H. polygyrus* infected mice.....152
Figure 4.14 The expression of PD-1 on Tregs and Th2 cells from *H. polygyrus* infected mice.....154
Figure 4.15 The expression of TIGIT on Tregs and Th2 cells from *H. polygyrus* infected mice.....156
Figure 5.1 Dynamics of Nr4a3-tocky mice after TCR stimulation.....174
Figure 5.2 Peptide predictions from NetMHCII and IEDB for Hp-VAL-1.1.....177
Figure 5.3 Peptide predictions from NetMHCII and IEDB for Hp-VAL-2.1.....180
Figure 5.4 Peptide predictions from NetMHCII and IEDB for Hp-VAL-3.....183

Figure 5.5 Peptide predictions from NetMHCII and IEDB for Hp-VAL-4.....186
Figure 5.6 In vitro restimulation of CD4+ T cells using whole MLN culture versus BMDC:T cell coculture.....190
Figure 5.7 The expression of CD69 on Teffector cells after 16 hours restimulation with HES and some components.....193
Figure 5.8 The expression of CD69 on Foxp3+ Treg cells after 16 hours restimulation with HES and some components.....195
Figure 5.9 The expression of CD154 on Teffector cells after 16 hours restimulation with HES and some components.....197
Figure 5.10 The expression of CD69 and Timer proteins in CD4+ T cells.....200
Figure 5.11 In vitro restimulation of d14 and d21 *H. polygyrus* infected MLN cells with HES.....202
Figure 5.12 The experimental set up for *H. polygyrus* secondary infection and restimulation in vitro.....204
Figure 5.13 In vitro restimulation of MLN cells with HES from mice reinfected with *H. polygyrus*.....205
Figure 5.14 The experimental set up for *H. polygyrus* clearance and restimulation in vitro.....207
Figure 5.15 In vitro restimulation of MLN cells with HES from mice previously infected with *H. polygyrus*.....208
Figure 5.16 In vitro restimulation of MLN cells with heat inactivated HES (hiHES) from mice previously infected with *H. polygyrus*.....210
Figure 5.17 In vitro restimulation of MLN cells with Hp-VAL proteins from mice previously infected with *H. polygyrus*. 212
Figure 6.1 T cell response to *H. polygyrus* in BALB/c and C57BL/6 mice.....228

Acknowledgements

My time as a PhD student in Glasgow has been an incredible experience, meeting new people and enjoying life in a new city all the while doing fun and novel experiments with my favourite lab pet – *H. polygyrus*.

First, I would like to thank my fantastic supervisor Professor Rick Maizels who took me in and welcomed me to the laboratory with open arms. His advice, patience and support has been instrumental in my success as a student as well as my personal development. I would like to especially thank him for his patience in the thesis project, through panic, stress and countless drafts Rick has been a fantastic support that helped me believe in myself and my abilities. Working with Rick has brought me so many opportunities from international conferences, to cutting edge science and sourcing novel mouse lines and I cannot thank him enough. So again Rick, thank you, I couldn't have done this without you!

Next, I would like to thank the members of Maizels lab past and present who trained me up and made sure to make being part of the lab a fun experience. With your support on busy days and help with processing tissues on experiment days, you saved me lots of stress, time and painful fingers! Special thanks to Anne Donachie, Nicola Hamilton and Claire Ciancia for maintaining the life cycle of *H. polygyrus* and making sure I had heaps of HES to use. Also thank you to Tiffany Campion, Claire Drurey and Patrizia Di Crescenzio for the supply of various VAL proteins produced and purified by the wonderful team protein. My biggest thanks go to Danielle Smyth who took me under her wing, made sure I was taking care of myself and helped me with so many techniques from gut preps to monoclonal antibody purification – I'll miss our pub trips, diet coke breaks and plant shopping! Anne, I also owe you a huge thank you for your experimental and moral support, you make every lab day brighter.

Thanks are also due to my second supervisor Dr Georgia Perona-Wright who always made time to meet with me to discuss my project and gave great advice and suggestions. Also, thank you Georgia for your help and patience during the PhD application process, you gave me the confidence to 'go for it'. Thomas Otto was instrumental to the single cell sequencing analysis and planning, thank you

Thomas, you helped an immunologist think like a bioinformatician! I would also like to thank the College of Medical, Veterinary and Life Sciences who funded my PhD through their Doctoral Training Program and gave me the freedom and opportunity to choose my own laboratory and project.

Finally, I would like to thank my wonderful family who have been by my side with love through every high and low of this project. My partner Alex has been by my side every day with coffee, advice, hugs and unconditional support. He has taken the role of proof-reader and therapist and has been my rock throughout this endeavour so thank you Alex, you're my favourite. Thank you to my mum and dad have supported me throughout my whole educational career and have been my biggest cheerleaders, even when they had no idea what I was doing! My sister Erin and her 3 wonderful children Brodie, Luke and Maeve have made sure I stay smiling and showered me with love, thank you for making sure I look after myself and providing unlimited hugs. And to my incredible grandparents, thank you for all of your support, love and belief in me, I couldn't have done it without you both. I would also like to thank my in-laws the Brouwers who have supported me all the way from the Netherlands and treated me like their own. And finally, my work from home desk-mate and emotional support animal Finlaggan the cat who never failed to make me smile and reminded me to take breaks (to play!). Again, to all my family thank you, I hope I can continue to make you all proud.

Author's Declaration

I declare that this thesis is the result of my own work, except where reference is made to the contributions of others, and has not been submitted for any other degree at the University of Glasgow or any other institution.

Signature: Name: Caitlin Margaret McManus

Abbreviations

20F3	IL-6 blocking monoclonal antibody
Ab	Antibody
ADL	Adenolymphangitis
Ag	Antigen
AIDS	Acquired immune deficiency syndrome
AIP-2	Anti-inflammatory protein 2
ANN	Artificial Neural Network
APC	Antigen presenting cell
AR	Antihelminthic resistance
BCR	B cell receptor
BMDC	Bone marrow dendritic cell
CCP	Complement control protein
CD	Chron's Disease
CDC	Centre for Disease Control
CK2	Casein kinase 2
ConA	Concanavalin A
CTLA-4	Cytotoxic T lymphocyte antigen-4
CXCR3	C-X-C Motif Chemokine Receptor 3
DALY	Disability adjusted life year
DC	Dendritic cell
DEREG	Depletion of Regulatory T cells
DNA	Deoxyribonucleic acid
DSS	Dextran sulphate sodium
DTR	Diphtheria toxin receptor
EAE	Experimental autoimmune encephalomyelitis
ES	Excretory/secretory products
EV	Extracellular vesicle
GALT	Gut associated lymphoid tissue
GATA3	GATA Binding Protein 3
GM-CSF	Granulocyte-macrophage colony-stimulating factor
HES	Heligmosomoides polygyrus excretory/secretory products
HEx	Heligmosomoides polygyrus extract
HIV	Human immunodeficiency virus
Hp	Heligmosomoides polygyrus
HSV	Herpes Simplex Virus
HTO	Hashtag oligonucleotide
IBD	Inflammatory bowel disease
ICOS	Inducible costimulatory (CD278)
IEDB	The Immune Epitope Database
IFNγ	Interferon gamma
IgG	Immunoglobulin G
IgM	Immunoglobulin M
IL-2C	IL-2 complex

ILC2	Type 2 innate lymphoid cells
iLN	Inguinal lymph node
IPEX	Immunodysregulation polyendocrinopathy enteropathy X-linked syndrome
iTreg	Induced Treg
KO	Knock out
MDA	Mass drug administration
MFI	Mean fluorescence intensity
MHC II	Major histocompatibility complex II
MLN	Mesenteric lymph node
Na	Necator americanus
NFAT	Nuclear factor of activated T-cells
NFAT	Nuclear factor of activated T-cells
NIF	Neutrophil inhibitory factor
NOD	Non-obese diabetic
non-siMLN	Non-Small intestine draining MLN
NTD	Neglected tropical disease
nTreg	Natural Treg
OVA	Ovalbumin
PBS	Phosphate buffered saline
PD-1	Programmed cell death 1, CD279
PD-L1/PD-L2	Programmed cell death ligand 1/2
PEC	Peritoneal exudate cells
PP	Peyer's patch
pTreg	Peripheral Treg
RANTES	Regulated upon Activation, Normal T Cell Expressed and Presumably Secreted
RARi	Retinoic acid receptor inhibitor
RNA	Ribonucleic acid
RORγt	Retineic-acid-receptor-related orphan nuclear receptor gamma
SCP	sperm coating protein
scRNAseq	Single cell RNA sequencing
SILP	Small intestine lamina propria
siMLN	Small intestine draining MLN
SNP	Single nucleotide polymorphism
ST2	Interleukin 33 receptor
STH	Soil-transmitted helminth
T-bet	T-box expressed in T cells
TCR	T cell receptor
Teffs	T effector cells
Tfh	T follicular helper cell
Tg	Transgenic
TGFß	Transforming growth factor beta
TgTCR	Transgenic TCR
Th	T helper

TIGIT	T-cell immunoreceptor with Ig and ITIM domains
Tr1	T regulatory type 1
tSNE	t-distributed stochastic neighbour embedding
TSO	*Trichuris suis* ova
tTreg	Thymic Treg
UC	Ulcerative colitis
UMAP	Uniform manifold approximation and projection
VAL	Vennom allergen like
WHO	World Health Organisation
IVC	Individually ventilated cage
LAL	Limulus amebocyte lysate
TCM	T cell media
PCR	Polymerase chain reaction
cDNA	Complementary DNA
GEM	Gel beads in emulsion
GANP	Germinal centre-associated nuclear protein
GITR	Glucocorticoid-induced tumour necrosis factor receptor-related protein
IGF	Insulin-like growth factor
IDO	Indoleamine 2,3- dioxygenase
PVR	Polio virus receptor
hiHES	Heat inactivated HES

Chapter 1 Introduction

1.1 Helminth Infections

Helminths or parasitic worms are a huge source of morbidity in both human and livestock populations worldwide. However, helminth infections are often overlooked despite one quarter of the worlds population being currently infected with helminths (World Health Organisation, 2021). Nine of the 20 neglected tropical diseases (NTD) set out by the World Health Organisation (WHO) and Centre for Disease Control (CDC) are helminth infections – Cysticercosis (pork tapeworm), Echinococcosis (hydatid tapeworm), Fascioliasis (liver fluke), Dracunculiasis (Guinea worm), Food-borne trematode infection, Lymphatic Filariasis (elephantiasis), Onchocerciasis (river blindness), Schistosomiasis (Bilharzia) and the Soil Transmitted Helminths (STH) (Centre for Disease Control, 2021; World Health Organisation, 2021).

While helminthiases do not often lead to death of the host, these infections are generally chronic and can lead to significant morbidities in patients with a high worm burden. One major comorbidity caused by worm infection is malnutrition. In the case of hookworms like *Necator americanus* and *Ancyclostoma duodenale*, the helminths bite into the intestinal wall resulting in compromised intestinal absorption and loss of blood leading to anaemia (Albonico *et al.*, 1998; Hotez *et al.*, 2004). In children in particular, the loss of nutrient uptake can lead to malnutrition and developmental delays which also carry socioeconomic costs (Hotez *et al.*, 2004). There is also evidence that pregnancy and foetal development can be negatively affected by helminth infection whereby infants born to mothers infected with a helminth have lower birth weights and even increased neonatal and maternal fatality (Friedman, Mital, Kanzaria, Olds, & Kurtis, 2007; Mpairwe, Tweyongyere, & Elliott, 2014).

Helminth infections can also cause immunopathology, where the immune response to infection causes pathology rather than the infective agent itself . Infection with *Wuchereria bancrofti, Brugia malayi* or *Brugia timori* can lead to lymphatic filariasis, a condition which is associated with an overzealous CD4+ T cell response and inflammatory damage to the lymphatics resulting in lymph

stasis and oedema (S. Babu & Nutman, 2014). The pathological manifestations of lymphatic filariasis include lymphoedema or the build up of lymph in the soft tissues, hydrocoele or lymph accumulation around the scrotum, and elephantiais which is hyperplasia of the skin and subcutaneous tissues as the result of lymphoedema and secondary microbial infections (S. Babu & Nutman, 2014). As a result of these pathologies, mobility is often limited and this leads to loss of work and social interactions which can lead to financial problems which can also greatly impact quality of life (Asiedu et al., 2021; Zeldenryk, Gray, Speare, Gordon, & Melrose, 2011). In addition, those with lymphatic filariasis can suffer from ADL (adenolymphangitis) attacks, a sudden filarial fever which can incapacitate the patient and cause physical injury, often leading to a social stigma in the community (S. Babu & Nutman, 2014; B. v. Babu, Nayak, & Dhal, 2005; Kumari, Harichandrakumar, Das, & Krishnamoorthy, 2005). Hence, lymphatic filariasis, an immunopathology, causes loss of quality of life in terms of pathology, finances, social interactions and can lead to mental health problems.

Another helminth infection which causes immunopathology with significant impact on the quality of life of the host is Schistosomiasis. Infection with *Schistosoma mansoni* and *Schistosoma japonicum* can lead to accumulation of helminth eggs and granuloma formation in the intestine and liver, while infection with *Schistosoma haematobium* can lead to accumulation of ova in the urogenital tract (Burke *et al.*, 2009; Mei, 2020). In hepatosplenic schistosomiasis, in which ova are deposited in the liver, the development of granulomas around the eggs leads to increased production of collagen in the liver and fibrosis; consequent blocking of the portal veins can lead to splenomegaly and even death due to intestinal bleeding (Burke *et al.*, 2009). *S. haematobium* ova accumulate in the urogenital tract and granuloma formation also occurs to encase the eggs. The granulomatous response can lead to lesions in the genitals which increases risk of sexually-transmitted infections and can also in rare cases affect the uterus, fallopian tubes and ovaries, leading in some cases to infertility (Burke *et al.*, 2009). The formation of the granulomas and the resulting fibrosis are associated with Th2 cells and Th17 cells whereas acute infection without ova accumulation is associated with a Th1 or Treg led response (Zheng *et al.*, 2020). This suggests that the T cell response to schistosomiasis is

the main cause of immunopathology due to Th2-driven granulomatous and fibrotic responses to the accumulatiing ova which can significantly affect quality of life and even lead to death (Burke *et al.*, 2009; Zheng *et al.*, 2020).

The overall effects of helminth infection can be captured by the metric Disability-Adjusted Life Years (DALYs), which calculates the number of years of healthy life lost to disability and morbidity, to give a numerical value to the health burden caused by helminthiases (C. H. King, 2015). Currently, most tropical disease funding goes towards researching the 'Big Three' – malaria, tuberculosis and HIV/AIDS and a much smaller proportion goes towards the study of helminthiases. While the "Big Three" diseases are indeed severe and have a high mortality, when considering the morbidity in terms of DALYs (excluding mortalities), helminthiases lead to the loss of almost four times as many DALYs compared to malaria (C. H. King, 2015). This suggests that while helminthiases are often not fatal, their impact on the everyday life of their host is very severe.

With this is mind, it is of the upmost importance that helminth infections are understood fully and controlled for the protection of the human population.

1.2 Anthelminthic therapies

Currently, the treatments used to treat helminth infections are a short-term solution to a long-term problem. In a study published in 1987, a group of school students in St Lucia had their worm burden assessed using egg counts in the faeces and given the anthelminthic drug mebendazole, which was effective at clearing their intestinal parasites. After 17 months, however, the students had a similar worm burden to their starting burden, suggesting that the drug was only effective in the short term and demonstrating that reinfection is a big hurdle for any long-term control strategy (Bundy et al., 1987). In the 35 years between this paper and the present, little has changed and we still do not have an effective long-term treatment for helminth infections. In fact, data compiled from more recent studies seem to confirm that within 12 months of treatment with antihelminthics, individuals have worm burdens similar to those pre-treatment. In one study, on the roundworm *Ascaris lumbricoides,* reinfection was reported to reach 94% of the pre-treatment burden in 12 months. Similarly, whipworm

(*Trichuris trichiura)* and hookworm patients were found to be reinfected with 82% and 54% of their initial worm burdens respectively 12 months post-anthelminthic treatment (Jia, Melville, Utzinger, King, & Zhou, 2012). This also shows that despite reinfection, there is no lasting acquired immunity to the infection (Bethony et al., 2006; Maizels, 2021).

Anthelminthic resistance (AR) has already emerged in soil-transmitted livestock STHs such as *Haemonchus contortus*, a natural nematode of ruminants (Kotze & Prichard, 2016; Tinkler, 2019). *H. contortus* has become extremely efficient in developing resistance to different anthelminthics with AR becoming rampant. In some cases, resistance has developed within 10 years of the introduction of a new drug (Kotze and Prichard, 2016), perhaps reflecting the high intensity of infection and frequent drug administration in the veterinary setting. In fact, *H. contortus* is now resistant to three of the four main classes of anthelminthic and is showing rising resistance to amino-acetonitrile derivatives, the only remaining class of anthelminthic which retains efficacy (Kotze & Prichard, 2016). The future of ruminant farming is now at great risk as *H. contortus* begins to develop resistance to the last effective anthelminthic in our arsenal (Kotze & Prichard, 2016).

This problem has not yet reached the human infecting STH population and hence its importance is often unappreciated (Vercruysse, Levecke and Prichard, 2012). However, due to the sigmoidal pattern through which anthelminthic resistance emerges, small outbreaks of resistance can spread through the entire population and lead to the loss of effective drug treatment (Tinkler, 2019). As such, anthelminthic use in humans should be assessed and monitored to prevent the widespread anthelminthic resistance we see in livestock species.

There are many risk factors for the development of AR which include the biology of the STH, the epidemiology and life cycle of the helminth, the dynamics between the STH and its host and the way in which we use antihelminthics including treatment frequency and strategy (Tinkler, 2019). The WHO has been carrying out a mass drug administration of school-aged children to control the spread of human helminthiases. In regions with >50% prevalence, children are given between 2 and 4 doses of anthelminthics per year and those in regions

with between 20-50% prevalence are treated yearly (Bradbury & Graves, 2016). Repeated treatments with the same drug (or from the same family of anthelminthics) also imposes a selective pressure for resistance in helminth populations (Tinkler, 2019). Currently, the two most commonly administered drugs are mebendazole and albendazole, both of which belong to the Benzimidazole drug family (Tinkler, 2019).

While interventions can slow the spread of AR, the field is in desperate need of new anthelminthic drugs and, most importantly, new intervention strategies that would offer longer-lasting freedom from infection.

1.3 Immune response to human helminth infection

The immune response to human hookworm may hold the answer to new therapeutic strategies to control helminth infection. Human hookworm infection represents infection with *Necator americanus* or *Ancyclostoma duodenale* which infect via the skin. Both worms burrow through the exposed skin of their human host and enter the circulation. The larvae then enter the capillaries in the lungs and burrow into the lung to be coughed up and swallowed. The larvae then travel to the intestine where they commence feeding, mature, and begin producing eggs (Hotez *et al.*, 2004; Loukas *et al.*, 2016). This life cycle is damaging to the host in three barrier sites; the skin, lung and gastrointestinal tract where the worm takes its blood meal which causes alarmin release from the epithelial cells lining these tissues. The damage caused by the worm burrowing can also allow translocation of the microbiota into the sub-epithelial layers, also causing an immune response (George *et al.*, 2012). The response to this bacterial translocation can lead to activation of the type 1 and type 3 responses alongside the type 2 response. It has also been shown that there are IFNγ positive cells within the granulomas which encyst *H. polygyrus* larvae in the intestinal epithelium and the reprogramming of the intestinal stem cells to allow rapid proliferation during helminth infection is also dependent on IFNγ, showing the importance of not only the type 2 response, but also the type 1 response (Nusse *et al.*, 2018). The interplay and mutual suppression between the type 1 and type 2 response is also important during helminth infection as IFNγ-/- mice have increased worm expulsion, showing that loss of the type 1 response leads to

a loss of suppression of the type 2 response (Reynolds, Filbey, & Maizels, 2012). In fact, in many human helminth infections, a type 1 dominant response leads to greater infection burdens and chronicity of infection, further showing the importance of this response to the anti-helminth response (Klementowicz *et al.*, 2012). The release of alarmin cytokines IL-25 and IL-33 from damaged epithelial cells is thought to activate antigen presenting cells and type 2 innate lymphoid cells (ILC2) which can produce cytokines to support the immune response (Loukas *et al.*, 2016). These cytokines include IL-22 which increases epithelial cell turnover to repair damage and increases differentiation into goblet cells which produce mucus as part of the weep and sweep response to clear helminth infection. IL-33 is also able to induce production of IL-4, IL-5 and IL-13 from ILC2s, Th2 cells, basophils and mast cells, amplifying the type 2 response to infection (Loukas *et al.*, 2016).

There is also a response against the hookworm itself and its excretory-secretory (ES) products. Antigen-presenting cells like dendritic cells take up these molecules and present them to naïve CD4+ T cells which differentiate into Th2 cells, producing high levels of IL-4, IL-5 and IL-13 or Tregs which control the immune response (Loukas *et al.*, 2016). IL-4 and IL-13 also induces class switching in B cells to produce IgE (Junttila, 2018) that activates basophils and mast cells to trigger histamine release (Stone, Prussin, & Metcalfe, 2010). Type 2 cytokines IL-4 and IL-13 are also able to induce M2 macrophage differentiation, M2 macrophages have been shown to directly kill *Nippostrongylous brasiliensis* larvae, a murine hookworm similar to *N. americanus* and *A. duodenale, in vitro*, suggesting these M2 macrophages may also directly attack the human parasite (F. Chen et al., 2014; Filbey et al., 2019). Studies suggest that the Th2 response in particular is important in anti-helminth immunity and limits the number of parasites in the host (Filbey et al., 2014; Reynolds, Filbey, & Maizels, 2012). Together, this shows that there are multiple immune pathways which contribute to the control of hookworm infections in humans, leaving many immunological targets for therapeutic treatments of human helminthiases.

1.4 Vaccination

Currently, there is no vaccine approved for treatment of any human helminthiases, although some trials have been undertaken for schistosome and hookworm species. However, across a range of nematode species, many laboratories are developing novel vaccination regimens, targeting both human parasites and animal model systems, to induce protective immunity (Adegnika et al., 2021; Diemert et al., 2012; Hewitson & Maizels, 2014; Pompa-Mera et al., 2011).

In order to have an effective vaccine to protect against human nematode infections, the Th2 response which is associated with clearance of the parasite must be boosted without being limited by immunosuppressive mechanisms that are naturally upregulated by the parasite (Hewitson & Maizels, 2014). This caveat makes it very difficult to find a vaccine antigen or epitope(s) from thousands of molecules produced at different life cycle stages which can provide protective immunity without any side effects. It has also been suggested that multiple epitopes in a single vaccine would be a more efficient as a vaccination strategy to prevent escape from the immune response induced by the vaccine (Rick M. Maizels, 2021). It is also possible that a vaccine epitope mixture can be created against homologous helminth antigens to allow protection against multiple species of helminth in a single vaccine (Rick M. Maizels, 2021; Zhan et al., 2014). Protection afforded by vaccines are often dependent on the acquired immune system as it can form memory cells which can be recalled in the future more rapidly than the initial response to antigen. In the case of helminthiases, vaccination would ideally prime the Th cell response to allow faster orchestration of the immune response or the B cell response to allow rapid antibody production which can clear the infection.

While it may be challenging to find a vaccine epitope, many laboratories test similar targets. These targets include whole attenuated worms, ‘hidden’ antigens which the host immune response would usually not be in contact with such as antigens in the gut of the worm, enzymes which are required for survival of the worm and different excretory secretory (ES) products (Coakley et al.,

2017; Drurey, Coakley, & Maizels, 2020; Hewitson et al., 2013; Hewitson, Harcus, et al., 2011).

1.4.1 Vaccination with irradiated helminths

One of the first vaccine studies in helminths administered 40kr X-ray irradiated *Ancyclostoma caninum*, or dog hookworm subcutaneously and saw around a 6 fold decrease in worm numbers compared to their unvaccinated counterparts (Miller, 1964; Schneider *et al.*, 2011). In another irradiated helminth vaccine experiment, the murine nematode *Heligmosomoides polygyrus* L3 larvae were irradiated with cobalt 60 and mice were infected with these irradiated larvae by oral gavage before clearing the infection and challenging with infection using healthy L3 larvae (Hagan, Behnke, & Parish, 1981). This led to a ten-fold reduction in worm recovery at day 35 post challenge when larvae were irradiated with 30kr and significantly lower eggs per gram of faeces at days 10-30 post challenge (Hagan et al., 1981).

1.4.2 Vaccination with helminth excretory secretory products

Helminths excrete and/or secrete thousands of molecules which can have profound effects on the immune response and are thought to be important to the worms' survival by preventing a successful immune response. The first excretory-secretory (ES) product vaccination to be tested gave *Trichinella spiralis* ES subcutaneously in 6 doses every three days (Campbell, 1955). This regime led to stunted female worm growth and significantly lower worm counts and faster clearance of the worm, showing that vaccination with *T spiralis* ES can effectively limit infection (Campbell, 1955).

Among many examples published since the original report, vaccination with 25µg of *H. polygyrus* ES (HES) with alum adjuvant and two 5µg boosts on day 28 and 35 post vaccination was shown to induce sterile immunity and protect mice from *H. polygyrus* infection (Hewitson, Filbey, et al., 2011). However, with the immunomodulatory effects of ES products, the scale of the production needed for commercial batches of HES and potential batch differences, the use of ES products as a vaccination against helminths is likely to be unfeasible.

There are lipid-bound vesicles found within HES that contain proteins and RNA which are protected from enzymes in the environment and from the immune response (Coakley et al., 2017; Drurey et al., 2020). These vesicles have been shown to downregulate the expression of ST2 (IL-33 receptor) on many cells and suppress macrophages which phagocytose the EVs (Buck et al., 2014; Coakley et al., 2017; Drurey et al., 2020). Vaccination with 10µg of these extracellular vesicles (EVs) and alum and 2µg boosts at day 28 and 35 post vaccination led to a strong antibody response and their egg and worm counts decrease by around 80% (Coakley *et al.*, 2017). This increase in expulsion was lost in fully susceptible ST2-deficient mice despite a similar antibody response, suggesting that IL-33 signalling is required for immunity to *H. polygyrus* (Coakley *et al.*, 2017). However, this is also not scaleable to mass production as the EVs are isolated from HES itself, as a result, recombinant protein production of protective EV proteins may be the best route (Drurey et al., 2020).

To overcome the issue of ES product production, molecules found within ES products have been produced as recombinant proteins to use as vaccination targets which can be scaled up to mass production.

1.4.3 Vaccination with recombinant helminth molecules

To overcome the risks of attenuated larvae and the impracticality of upscaling ES production to a commercial level, recombinant helminth proteins and nucleic acids may hold the answer for vaccination to treat helminthiases.

Immunisation with recombinant DNA encoding Ts87, a novel gene found within *T. spirilis* and an amino acid sequence originating from the gp43 glycoprotein of the muscle larval stage of the parasite have been trialled as vaccine candidates for *T. spirilis* (Pompa-Mera et al., 2011; Y. Yang et al., 2010). The gp43 vaccine was delivered using attenuated *Salmonella enterica* which and had a 62% reduction in worm burden when vaccinated mice are infected with *T. spirilis* (Pompa-Mera *et al.*, 2011). Attenuated *Salmonella typhimurium* was used to deliver the Ts87 DNA vaccine and this vaccine leads to a 29.8% reduction in adult *T. spirilis* upon infection (Y. Yang et al., 2010). These results together suggest that using a

recombinant helminth protein or recombinant DNA may be successful in controlling helminthiases (Pompa-Mera et al., 2011; Y. Yang et al., 2010).

Necator americanus is one of the most common hookworms to infect humans and its infection is associated with high morbidity such as anaemia and malnutrition (Hotez *et al.*, 2004, 2013). In 2021, a phase 1 clinical trial was performed in a helminth-endemic region of Gabon. In this trial, two vaccines were given simultaneously, the first targets *Na*-APR-1 which lyses erythrocytes in the worm's blood meal and the second, targeting *Na*-GST-1 which neutralises oxygen radicals produced by the digestion of haemoglobin (Adegnika et al., 2021; Hotez et al., 2013; Hotez, Bethony, Diemert, Pearson, & Loukas, 2010). The inactivation of these molecules would interfere with the feeding pattern of the worms to impact survival and fecundity, minimising transmission to a new host while also minimising blood loss in the host, preventing the development of anaemia (Adegnika et al., 2021; Hotez et al., 2013, 2010). The trial saw vaccination elicit a protective IgG response with high tolerance of the vaccine and mild-to-moderate side effects when both vaccines were given intramuscularly with Alhydrogel adjuvant even at a dose of 100µg of each vaccine (Adegnika *et al.*, 2021). With this success, the dual vaccine is moving forward into phase 2 testing (Adegnika *et al.*, 2021). Only time will tell if this vaccination will be approved for use in humans and if the efficacy is sufficient to justify the higher cost of vaccination versus MDA (Hotez *et al.*, 2013).

Currently, one vaccine has been approved for veterinary use, the Barbervax vaccine for *Haemonchus contortus,* a parasitic worm which infects the abomasum of ruminants and causes severe anaemia (Ehsan *et al.*, 2020). This vaccine is made up of two components, H-gal-GP and H11, which are proteins found in the midgut of the worm. When the worm takes a blood meal from a vaccinated host, the antibodies formed during the vaccine response enter the midgut and bind to these proteins. As a result, the worm is unable to digest its blood meal and will eventually die due to starvation (Ehsan *et al.*, 2012; Smith *et al.*, 2003; Broomfield *et al.*, 2020). The Barbervax vaccination regimen in young lambs has been shown to induce some level of lasting immunity to the worm, showing the effectiveness of targeting the feeding pattern of parasitic helminths as a control measure (Broomfield *at al.*, 2020).

However, not all hookworm vaccine studies have had such a positive outcome. An earlier vaccine targeting ASP-2, an important molecule from the infective larval stage of hookworm infection, was used in a trial in Brazil aiming to control *Necator americanus* infection (Diemert *et al.*, 2012). While the vaccination was effective in laboratory models, when given to volunteers from a hookworm endemic region, it led to allergic-type sensitivity in patients with pre-existing *Na*-ASP-2 IgE from previous exposure to *N. americanus* (Diemert *et al.*, 2012). This shows that while vaccination may be an effective strategy to limit helminth infections, further research is required to assess the safety of these vaccines and prevent unwanted responses.

1.5 The relationship between helminthiases and autoimmune and allergic disorders

While helminthiases can lead to morbidities and a decreased quality of life, there is evidence that areas with the lowest incidence of helminth infection have the highest incidences of autoimmune and allergic diseases. The opposite is also true where the incidence of autoimmune and allergic disorders is lower in areas with endemic helminth infections. This raises the possibility that the absence of helminth infections results in increased autoimmune and type 2 allergic disorders.

1.5.1 The Hygiene Hypothesis

The Hygiene Hypothesis proposes that high levels of hygiene and cleanliness in early life leads to higher incidences of allergy (Strachan, 1989). This increase in allergic disease is thought to be due to the lack of exposure to microbes and parasites in early life or loss of immunosuppression of the mature immune system which leads to immune dysregulation (Strachan, 1989; Okada et al., 2010; Maizels, McSorley and Smyth, 2014). This hypothesis was based initially on the observation that children with multiple older siblings were less likely to develop hay fever (Strachan, 1989). It was postulated that this is due to the increased exposure to microbes and microbial products from older siblings at a young age shaping the immune response (Strachan, 1989).

Since its first formulation, many examples of the hygiene hypothesis have been shown; among the most striking was that exposure to dust from an Amish farm protected mice from allergic airway inflammation while Hutterite dust cannot (Stein *et al.*, 2016). The Hutterite and Amish communities are highly genetically related and have similar heritage, the main difference is the use of modern farming equipment by the Hutterite community while the Amish use traditional farming methods (Stein *et al.*, 2016). This difference in farming method means that the Amish dust had 6.8 times more endotoxin than Hutterite dust, suggesting again that increased exposure to microbes and their products can protect against allergy (Stein *et al.*, 2016).

1.5.2 The Old Friends Hypothesis

In 2005, the Hygiene Hypothesis was extended to create the Old Friends Hypothesis (OFH) (Rook and Brunet, 2005), proposing a mechanism through which lack of exposure to microbes leads to an increase in both allergic and autoimmune disorders (Rook & Brunet, 2005). The OFH postulates that long-lived co-evolution with symbionts and relatively nonpathogenic parasites like certain strains of bacteria and helminths, has led to our immune response operating optimally in their presence, but trending towards autoimmune and allergic disease when absent (Rook, 2010; Rook & Brunet, 2005). Humans have co-evolved with helminths from as far back as the Palaeolithic Era and helminths have been present since the time of the first mammals, meaning we have co-evolved for at least 200 million years (Rook, 2010). As helminths down-regulate their host's immune system, over the course of evolution, the human immune system has evolved a compensatory increase in the intensity of the immune response (Frew, 2019; Rook, 2010). As a result, in the absence of helminths, immune responses are overzealous and dysregulated, leading to type 2 mediated diseases like allergy but also type 1 and type 3 autoimmune disorders (Rook, 2010).

Together, the Hygiene Hypothesis and Old Friends Hypothesis suggest that while helminthiases can lead to morbidity, complete clearance of helminth infection could conversely have deleterious results on the immune system long term.

1.6 Helminth therapy for allergic and autoimmune diseases

In an era where autoimmune and allergic diseases are an increasing burden for modern healthcare, the immunoregulation utilised by helminths has become an alluring potential treatment for these diseases. Many studies have shown that in mouse models, helminth infection can protect against allergic airway inflammation, type 1 diabetes in NOD mice, EAE and food allergy (Bashir, Andersen, Fuss, Shi, & Nagler-Anderson, 2002; Kitagaki et al., 2006; Saunders, Raine, Cooke, & Lawrence, 2007; White, Johnston, et al., 2020; Wilson et al., 2005).

Alongside animal studies, multiple human trials which deliberately infect patients suffering from allergic or autoimmune disorders with helminths have been conducted using the pig whipworm (*Trichuris suis*) or the human hookworm *Necator americanus*. Pig whipworm is a natural parasite of pigs which can infect humans for short lengths of time with very few side effects due, in part, to its inability to fully infect a human host. *Trichuris suis* ova (TSO) are able to be orally administered, making infection simple and more tolerable to the patient. However, since *T. suis* is not a natural human infective parasite, patients have to be repeatedly reinfected as they clear the worm; moreover there is debate as to whether a non-human parasite is as well-adapted to regulate the human immune system. Initial experiments infecting Ulcerative Colitis (UC) and Crohn's Disease (CD) patients with *Trichuris suis* ova showed that treatment was well tolerated, and although infection was cleared within a few weeks, the therapy led to increased remission in the patients (R. Summers, 2003; R. W. Summers, Elliot, Urban, Thompson, & Weinstock, 2005). However, the improvement was temporary and if continuous presence of the parasite is required, patients would have to be repeatedly reinfected (Helmby, 2015; R. Summers, 2003; R. W. Summers et al., 2005). Later trials with *T. suis* ova in Crohn's Disease patients also showed high tolerance of the treatment and a slight improvement in self-reported symptoms of CD (Sandborn *et al.*, 2013).

To overcome the short infection span of *T. suis*, *Necator americanus* may offer a better alternative, and is a parasite fully adapted to the human immune system.

N. americanus is responsible for most of the hookworm-associated morbidity worldwide and can cause anaemia, but is able to sustain infection for years, meaning reinfection is not required as often as in *T. suis* (Maruszewska-Cheruiyot, Donskow-Lysoniewska, & Doligalska, 2018). Trials have been conducted using *N. americanus* controlled infection to treat multiple sclerosis, inflammatory bowel disease (IBD) and coeliac disease with varying results (Bager et al., 2010; Croft, Bager, & Garg, 2012; Daveson et al., 2011; Fleming & Weinstock, 2015; Garg, Croft, & Bager, 2014; Henry J. McSorley et al., 2011). While some trials saw improvement in patients with Chron's Disease, it often did not reach significance (Garg et al., 2014). The same was also seen in *N. americanus* infection of patients with Coeliac Disease where improvements in the response to gluten exposure were only short term and fell short of statistical significance (Daveson et al., 2011; Henry J. McSorley et al., 2011). There has been little efficacy reported for the use of *Necator americanus* or *Trichuris suis* infection in allergic rhinitis (Bager et al., 2010; Croft et al., 2012).

The results of these trials show that helminth therapy is not a blanket treatment for all allergic and autoimmune diseases. There are many potential explanations for why some trials are successful and show protection from disease, others show little effect. First, the experimental infections use fewer *N. americanus* larvae than would be found in natural infection (Evans & Mitre, 2015; Mortimer et al., 2006). For example, Mortimer *et al*. infected their healthy patients with 10 *N. americanus* larvae which resulted in around 50 eggs per gram of faeces (Mortimer *et al.*, 2006). However, in natural infection which protects from allergic wheeze, eggs counts were found to range from 48 to 1458 eggs per gram faeces (Scrivener *et al.*, 2001). It is likely that 10 larvae are too few to affect established autoimmune and allergic diseases, and that protection would occur with higher infection intensity (Evans & Mitre, 2015).

The species and location of the helminths are also likely to be important for protection against immune mediated disorders (Evans & Mitre, 2015). The TSO trials were successful in IBD, where the pathology and *Trichuris suis* are both in the intestinal tract, suggesting that location is important to protection (R. W. Summers et al., 2005). Additionally, different species of helminth may be better equipped to protect against different immune mediated disorders (Evans &

Mitre, 2015). For example, the gut-dwelling *H. polygyrus* was able to protect against established allergic airway inflammation in mice whereas *Nippostrongylus brasiliensis* infection was unable to protect the mice despite its larval lung phase (Jarrett, Mackenzie, & Bennich, 1980; Wilson et al., 2005; Wohlleben et al., 2004). This shows that location of infection is not everything and better understanding of how specific helminths impact immune disorders is required before clinical implementation (Evans and Mitre, 2015).

There is also a genetic component to helminth infection as shown by different mouse strains differing in susceptibility to helminth infection, and similarly the wide range of infection intensity in the human population (Bundy et al., 1987; Evans & Mitre, 2015; Wright, Werkman, Dunn, & Anderson, 2018). Protection from allergic diseases by helminths was also shown to be strain specific, suggesting that the genetics of the host are an important determinant of the success of helminth therapy (Evans & Mitre, 2015; K. J. Turner, Shannahan, & Holt, 1985). With little stratification of patients in the past clinical trials, it is important going forward to divide the patient cohorts who were protected by helminth therapy and those who were not (Evans & Mitre, 2015). This will allow assessment of differences in their genetic, environmental or disease background to begin to build a profile of patients who would benefit from helminth therapy.

1.7 Use of helminth products for inflammatory disease treatment

With the risk of morbidity associated with helminth infection, finding potential drugs within the excretory-secretory products of helminths is a growing area of interest. Treatment with recombinant immunomodulatory proteins found in the ES of helminths may allow safe treatment of patients with a consistent product that has been functionally described, rather than with a mixture of many molecules, which may vary greatly between preparations and within which the effects of many molecules are still unknown.

Many immunomodulatory molecules have been found within the ES of helminths which infect a range of hosts from rodents and dogs to humans (Rick M. Maizels, Smits, & McSorley, 2018; Smallwood et al., 2017; White, McManus, & Maizels,

2020). Amongst the first examples to be described, the rodent infective nematode *Acanthocheilonema viteae* secretes a molecule known as Excretory/Secretory-62 which blocks TLR signalling in immune cells and inhibits both B and T cell responses (M. M. Harnett, Deehan, Williams, & Harnett, 1998; W. Harnett, Worms, Kapil, Grainger, & Parkhousef, 1989). The canine hookworm *Ancyclostoma caninum* produces the glycoprotein Neutrophil Inhibitory Factor (NIF) which blocks neutrophil adhesion and transmigration of neutrophils, minimising the neutrophil response to the helminth (Anbu & Joshi, 2008; Rieu, Ueda, Haruta, Sharma, & Amin Arnaout, 1994). The same parasite also secretes Anti-Inflammatory Protein-2 (AIP-2) which is protective against murine colitis and allergic airway inflammation (Cançado et al., 2011; Ferreira et al., 2013; Riveau et al., 2012; Ruyssers et al., 2009). Many helminth ES products include cystatins which can induce IL-10 production from antigen presenting cells and tolerise the immune response (Dainichi et al., 2001; S. Hartmann, Kyewski, Sonnenburg, & Lucius, 1997; Lustigman, Brotman, Huima, Prince, & McKerrow, 1992; Manoury, Gregory, Maizels, & Watts, 2001). The use of helminth derived immunomodulatory molecules to modulate the host immune response was reviewed in greater detail by Maizels, Smits and McSorley (Rick M. Maizels et al., 2018). These and many more molecules have the potential to be used as drugs for inflammatory disorders although more trials are required to assess their efficacy in protection from immune mediated diseases. Some of the key immunomodulatory proteins found in *H. polygyrus* ES are discussed below in 1.9.

1.8 Mouse models of helminthiases

Studying natural helminth infection of humans is complicated by many factors, including varied histories of infection with multiple species of helminth, the duration of current infection and exposure to other diseases. In addition, volunteers from regions with endemic helminth infections, even if not currently infected are likely to have been previously, and would have been exposed to the molecules the helminths produce to modulate the host immune response. In this case, there is no such thing as a truly ‘naïve’ human. To overcome this, some studies have been performed in which volunteers from countries with low incidence of helminth infection have been experimentally infected with helminths such as *N. americanus* and *A. duodenale* (M. A. Hoogerwerf et al.,

2021; M.-A. Hoogerwerf et al., 2019). While these studies have been carried out and published, it still remains difficult to approve these studies and even more difficult to find volunteers willing to be intentionally infected with a parasite.

As a result of these factors, many helminth studies which require in depth analysis of the immune response and tight control of infection are performed using animal models for human infections. These include *Trichuris muris,* the murine whipworm which can be used to study *Trichuris trichiura,* and *Heligmosomoides polygyrus* and *Nippostrongylus brasiliensis*, which can be used to study hookworms like *A. duodenale* and *N. americanus* in mice (Blaxter, Dorris, Frisse, Vida, & Thomas, 1998). Use of murine models allows more in depth assessment of responses to helminth infection as intervention is easier in the murine system. The effects of different drug regimens, adoptive cell transfer, treatment with blocking monoclonal antibodies and timings of infection are easily carried out in these models. Also, experimental mice are inbred with high genetic similarity which removes genetic variation as a cause of non-responsiveness, and can be genetically manipulated to over- or under-express a gene or completely knock the gene out. With the advent of the Cre-Lox recombination, it is possible to have mouse lines which lack genes in certain cell lineages. Conditional knock-outs are also available including mice with the diphtheria toxin receptor (DTR) gene expressed under a cell-specific promoter, so that diphtheria toxin exposure results in apoptosis in cells expressing DTR. Diphtheria toxin exposure can be chosen for any time point, allowing stage-specific deletion of cells. This allows a fine-tuned investigation of the genes implicated in the balance between resistance and susceptibility to helminths which is not possible with human subjects.

1.8.1 Heligmosomoides polygyrus

Heligmosomoides polygyrus is a natural murine nematode which can, like its human infective counterparts, chronically infect its host following primary infection. *H. polygyrus* and *N. brasiliensis*, another murine nematode model, are both members of the Nematoda clade V along with *A. duodenale* and *N. americanus*, the most prevalent human hookworm species (Hewitson, Harcus, et al., 2011; Montaño, Cue, & Sotillo, 2021; Stoltzfus, Pilgrim, & Herbert, 2017). *H.*

polygyrus infection is also similar to many livestock STHs including *Cooperia oncophora* and *Ostertagia ostertagi,* these parasitic worms have similarities in their GI-restricted life cycle, the type 2 response to infection and ability to modulate the hosts immune response, showing that experiments using *H. polygyrus* are relevant to both human disease and veterinary disease (Kanobana *et al.,* 2003, Kloosterman *et al.,* 1992). This close relationship between the human infective species, livestock infective species and the mouse models allows us to draw conclusions about health-impacting hookworm infection using analyses and interventions that are not possible in human studies.

The experimental life cycle of *H. polygyrus* is easily maintained in the laboratory setting. Infective L3 larvae are orally gavaged into the stomach of the mouse host. The larvae travel to the duodenum of the small intestine, punch through the lamina propria to encyst in the muscularis and undergo two moults before emerging as an adult which coils around the intestinal villi to prevent ejection from the intestine (Johnston *et al.*, 2015). The adult *H. polygyrus* then reproduce and eggs are shed into the faeces of the host. In the wild, the eggs will mature in the soil before hatching the infective L3 larvae to be ingested by another host. In the laboratory, faeces containing the fertilised ova are collected and cultivated in a petri dish with granulated charcoal to mimic the soil stage. L3 larvae are then collected from the petri dish and are ready to be orally gavaged into a new host (Johnston *et al.*, 2015). This life cycle is summarised in Figure 1.1.

H. polygyrus is accomplished in modulating its host's immune response, with many facets that are similar to the immunomodulation seen in hookworm infected patients (Rick M. Maizels et al., 2012). The adult form of the worm is also readily cultured and we can use this technique in the laboratory to collect the molecules the worm produces, known as HES (*H. polygyrus* excretory/secretory products) (Johnston *et al.*, 2015). These molecules and their impact on the immune response of their host species are now being intensively studied.

H. polygyrus infection, like the majority of human helminthiases induces the type 2 immune response including upregulation of Th2 cells, M2 macrophages

and increased IL-4 and IL-13 levels (Figure 1.2). Damage to and clearance of the worm can be mediated by many arms of the type 2 response including antibodies produced by B cells and triggering of goblet cell hyperplasia which lead to the weep and sweep response and produces molecules which can impact worm fitness including RELMß and mucins (Maizels *at al.*, 2012). This anti-helminth response is orchestrated in part by the Th2 cells which produce cytokines and chemokines which come together to mediate mechanisms of clearance (Maizels *et al*. 2012). Early in infection, granulomas form around the L4 larvae encysted in the intestinal submucosa. These granulomas classically contain eosinophils and macrophages which are thought to directly kill the larvae through largely undefined mechanisms, including antibody-dependent cell dependent cytotoxicity, to prevent the emergence of adult worms and subsequent mating and egg production (Esser von Bieren *et al*., 2013; Ariyaratne *et al.*, 2020).

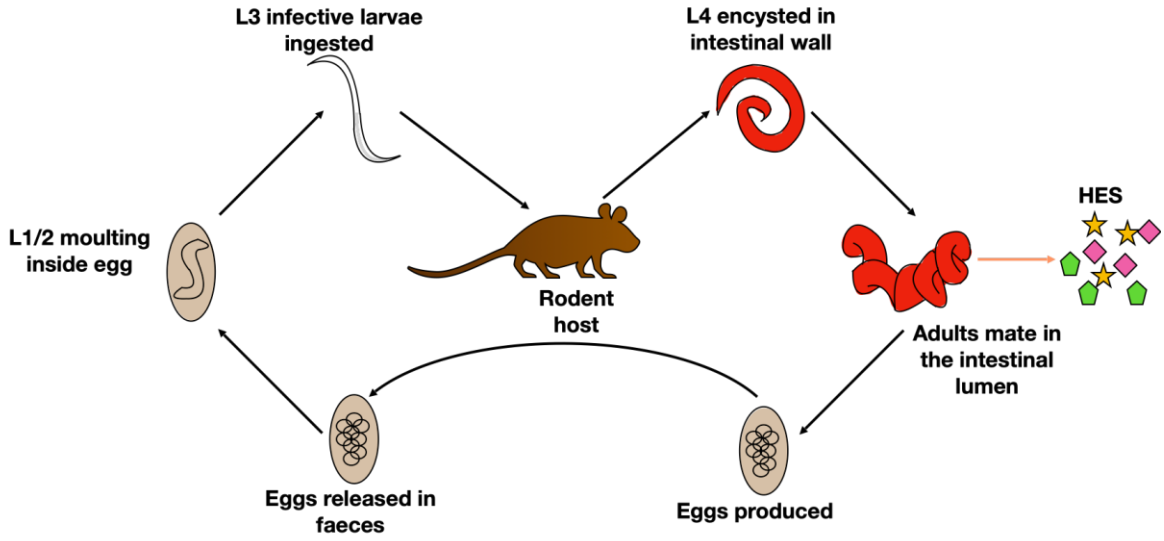

Figure 1.1 Life cycle of Heligmosomoides polygyrus. L3 larvae are ingested from the soil in the wild or gavaged into a murine host in the laboratory setting. The L3 larvae travel to the duodenum of the small intestine and burrow into the muscularis where it encysts and molts twice. The now adult worm burrows out of the muscularis and reenters the lumen where it coils around the intestinal villi and produce eggs that are shed into the faeces. The adult worms can be isolated from the small intestine and cultured in media as described in Johnston *et al.*, 2015 to produce HES. The faeces of infected mice can hatch in the soil in the wild or are cultured in a petri dish with activated charcoal to mimic soil conditions and allow hatching. Once hatching has occurred, L3 larvae can be ingested or collected and gavaged to infect a new host.

1.9 Immune Regulation by H. polygyrus

To survive in the host and reproduce, many helminths, including *H. polygyrus* have evolved sophisticated means of modulating the immune response of the host. Amongst the most well-characterised strategy is that to promote host

immune regulatory pathways, taking advantage of mechanisms to induce tolerance in the host, which are targeted by *H. polygyrus* (White, McManus, et al., 2020).

1.9.1 Tregs

Regulatory T cells or Tregs are a subset of CD4+ T helper cells which regulate the immune response to prevent overzealous or autoimmune responses which can cause damage to the host (Belkaid, 2007; Reynolds et al., 2012; K A Smith et al., 2016). Tregs regulate the T cell response using multiple effector molecules and cytokines. Tregs are known to produce the anti-inflammatory cytokines IL-10 and TGFß which can inhibit Teffector and B cell activation and proliferation while increasing the induction of peripheral (p)Tregs (Shevyrev & Tereshchenko, 2020). There are two subtypes of Tregs; thymic (t)Tregs which originate from the thymus and peripheral Tregs which are induced in the periphery from naïve CD4+ T cells. Thymic Tregs often have TCR specificities against self-antigen and damage markers to maintain homeostasis, pTregs on the other hand can have TCR specificities against foreign antigens found in the periphery (Shevach & Thornton, 2014; Shevyrev & Tereshchenko, 2020). Tregs can also express molecules which suppress CD4+ Teffector cells, including the co-inhibitory receptors CTLA-4 and PD-1 which will be discussed further in Chapter 4.

The importance of Tregs is seen in Scurfy mice which have a missense mutation in the Foxp3 gene that prevents Treg induction (Hadaschik et al., 2015; Sharma, Sung, Fu, & Ju, 2009). These mice develop fatal multi-organ failure and show that Tregs are also required to prevent responses against innocuous antigens, the microbiota and self antigens (Hadaschik et al., 2015; Sharma et al., 2009). In humans, IPEX (Immunodysregulation polyendocrinopathy enteropathy X-linked) syndrome is caused by mutations in the FOXP3 gene which, as in scurfy mice, can lead to the development of autoimmune disorders such as type 1 diabetes, dermatitis and enteropathy (Bacchetta, Barzaghi, & Roncarolo, 2016; Wildin et al., 2000). Tregs are not only essential for steady-state homeostasis and preventing autoimmune diseases, but during infection and inflammation they, are important in balancing the immune response and preventing immunopathology, including during helminth infection (Belkaid, 2007).

Following *H. polygyrus* infection, there is an activation and expansion of the Foxp3+ Treg population between days 3-14 post infection in the mesenteric lymph nodes (MLN) (Finney, Taylor, Wilson, & Maizels, 2007; Rausch et al., 2008). There is also an expansion of Tregs in the Peyer's patches, tertiary lymphoid organs along the intestine that are in close proximity to the parasites (Mosconi *et al.*, 2015). Peyer's patches contain a specialised epithelial cell (M cell) that captures antigen from the intestinal lumen and supplies antigen to APCs in the lamina proporia to initiate an immune response (Jung, Hugot, & Barreau, 2010). The close association between the Peyer's patch and the site of *H. polygyrus* infection may imply that T cells found in Peyer's patches have a different activation status and phenotype than those found in the MLN. However, the majority of data in literature is focused on the MLN.

During infection, Tregs are thought to skew the balance between resistance and susceptibility to *H. polygyrus* by suppressing the Th2 response against the worm and preventing clearance (Finney et al., 2007; Rausch et al., 2008; K A Smith et al., 2016). In addition to their increased number, individual Tregs from *H. polygyrus* infected mice are more suppressive than Tregs from naïve mice (Bowron, Ariyaratne, Luzzi, Szabo, & Finney, 2020; Finney et al., 2007; Rausch et al., 2008). Tregs from *H. polygyrus* infected mice were able to suppress the response of CD4+ T cells to ConA in culture and express high levels of Ki-67, a marker of active proliferation, suggesting that *H. polygyrus* Tregs are active and can suppress Th responses (Filbey et al., 2014; Finney et al., 2007; K A Smith et al., 2016). At the early stages of infection (day 7), C57BL/6 Treg suppression is dependent on CTLA-4 as suppressive ability is lost when CTLA-4 is blocked with a monoclonal antibody (Bowron *et al.*, 2020). However, Tregs from d21 infected mice were unaffected by α-CTLA-4 treatment suggesting this pathway is no longer important for Treg suppression later in infection (Bowron *et al.*, 2020). Interestingly, the expression of CTLA-4 on Tregs has been shown to not be upregulated during *H. polygyrus* infection (Bowron et al., 2020; Finney et al., 2007).

Transferring Th2 cells from *H. polygyrus*-infected mice to naïve donors leads to increased clearance of the worm when the donor mice are subsequently infected (Rausch *et al.*, 2008). When Tregs and Th2 cells from *H. polygyrus* infected mice

are combined and transferred, the recipients also showed a significant increase in worm clearance, suggesting that under the conditions used in this experiment, Treg suppression alone is not enough to dampen the Th2 response (Rausch *et al.*, 2008). However, the T cells that were adoptively transferred were combined from the MLN and spleen, with the majority from the latter; as it is likely that the spleen is not as impacted by *H. polygyrus* infection due to its distal location the *H. polygyrus* induced T cells may have been diluted in this procedure (Rausch *et al.*, 2008).

Clearer evidence of the role of Tregs comes from depletion experiments. For example, when Tregs are depleted *in vivo* using an α-CD25 monoclonal antibody (clone PC61), there is a reduction in Treg numbers alongside increased IL-4 production, as well as an increase in Ki-67 in both the Teffector and Treg compartment suggesting that both cell types were active. Following *H. polygyrus* infection, α-CD25 treated mice showed lower egg counts at d21, and a decrease in worm numbers at day 28 post infection (Smith et al., 2016). Interestingly, the effect of α-CD25 treatment was to reduce Treg frequency to the level observed in naïve mice, suggesting that negating the ability of the parasite to expand Tregs may have been sufficient for a protective Th2 response to develop.

These findings demonstrated that blocking Tregs via CD25 leads to a stronger Th2 response which can increase worm clearance (K A Smith et al., 2016). Complementary studies sought to experimentally expand Treg numbers, which can be achieved in vivo using an IL-2:anti-IL-2 complex (IL-2C) (K. E. Webster et al., 2009). Mice given IL-2C, show an increase in Treg numbers and a decrease in IL-4 and IL-13 and, when challenged with *H. polygyrus*, show increased burdens of adult worms (K A Smith et al., 2016).

Anti-CD25 antibody treatment achieves only a partial depletion of Tregs, and can have confounding effects on activated effector cells which express the same marker. Genetic constructs were therefore developed in which the Foxp3 promoter also drives expression of the human diphtheria toxin receptor (DTR) that is not otherwise present in mice, allowing near-total deletion of the Foxp3+ Treg population by administration of the toxin. Experiments in one such construct, the Foxp3LuciDTR mouse line, showed that the outcome of *H.*

polygyrus infection was different depending on the genetic background of the mouse strain (K A Smith et al., 2016). In BALB/c Foxp3LuciDTR mice, there was increased CD4+ Th activation accompanied by increased IFNγ and IL-6 (K A Smith et al., 2016). Unexpectedly, however, the increase in Teffector activity did not result in clearance of the helminth but increased the worm burden within these Treg-deficient mice, a result which was attributed to high IFNγ levels that may interfere with a type 2 effector response (Smith et al., 2016). In C57BL/6 Foxp3LuciDTR mice, there is an increased Th2 response and IL-4 and IL-13 production, however this again does not lead to increased clearance (K A Smith et al., 2016). Another mouse strain with a deficit in their Treg population are the DEpletion of REGulatory T cells (DEREG) mouse. DEREG mice have a transgenic diphtheria toxin receptor and GFP complex under the control of the Foxp3 reporter, meaning Foxp3+ Tregs specifically express DTR. When diphtheria toxin is administered into the mouse, the Tregs are depleted (Buch *et al.*, 2005). When DEREG mice were infected with *H. polygyrus,* the mice rapidly dropped weight and had to be culled at day 5 post infection, showing that Tregs are required not only to maintain tolerance to *H. polygyrus*, but protect animals against severe pathology during the tissue-penetrating phases of infection when the epithelial barrier is breached (K A Smith et al., 2016).

These differences in the phenotype following Treg depletion may reflect a broader distinction between Treg responses to *H. polygyrus* in the BALB/c and C57BL/6 strains. Firstly, the two strains show differential upregulation of nTregs versus pTregs (K A Smith et al., 2016). BALB/c mice primarily expanding the Helios+ nTregs when infected with *H. polygyrus*, while C57BL/6 mice favour expanding the Helios– pTregs (K A Smith et al., 2016). Secondly, CD103, an integrin which has been implicated in Treg function and surface TGFß are both increased on Tregs from BALB/c mice chronically infected with *H. polygyrus*, suggesting that *H. polygyrus* induced Tregs in BALB/c mice are more suppressive than their naïve counterparts (Finney *et al.*, 2007). Thirdly, the Treg population in *H. polygyrus* infected BALB/c mice also produces IL-10 *in vitro,* however, the effect of this IL-10 on Teffector cells remains unclear (Finney et al., 2007; Rausch et al., 2008; K A Smith et al., 2016). Finally, recent data suggest that although Tregs from *H. polygyrus* infection are suppressive, there is little

difference between naïve Tregs and *H. polygyrus* induced Tregs in C57BL/6 mice (Bowron *et al.*, 2020).

1.9.2 Dendritic cells

Dendritic cells (DCs) are at the centre of the immune response and act as the eyes of the immune system. When DCs encounter a foreign substance or organism, they present antigens from the invader in the form of protease-processed peptides on major histocompatibility complexes (MHC) to T cell receptors, giving rise to the moniker of Antigen Presenting Cells (APCs). DCs are also orchestrators of the response, by delivering different activation signals using a range of co-stimulatory molecules and producing different cytokines and chemokines (Eisenbarth, 2019). Furthermore, DCs are instrumental in maintaining immunological tolerance, through two main strategies: inducing Tregs that will subsequently regulate other effector cells in the immune response; or directly anergising T cells in a contact-dependent manner, rendering them inactive and ineffective (Domogalla, Rostan, Raker, & Steinbrink, 2017; Morante-Palacios, Fondelli, Ballestar, & Martínez-Cáceres, 2021). In the case of *H. polygyrus*, there is evidence that the parasite pursues the strategy of anergising the responsive T cells through tolerogenic DCs (A. M. Blum et al., 2012; Katherine A. Smith et al., 2011).

It is well-established that *H. polygyrus* alters APC functions to limit their ability to activate T cells. There is an increase in $CD11c^{lo}$ $CD103^{-}$ tolerogenic DCs during *H. polygyrus* infection at day 7 and day 28 post-infection, showing that there at alterations to the dendritic cell population in both chronic and acute infection (Katherine A. Smith et al., 2011). When DCs isolated from the intestine of *H. polygyrus* infected mice are transferred into RAG-/- mice subjected to T-cell transfer-mediated colitis, the inflammation score of the mice reduces, alongside subdued levels of IL-17 and IFNγ (A. M. Blum et al., 2012). Moreover, if RAG-/- mice are infected with *H. polygyrus* before the adoptive transfer of colitogenic CD4+ T cells they are protected from colitis and the associated inflammation, suggesting that either the induction or effector phase of inflammatory disease have been altered by infection (Hang et al., 2010a). In fact, if mice are first infected with *H. polygyrus* for 2 weeks, and then drug-cleared of infection, the

now uninfected mice are still protected (using a25iroxicamn induced colitis model), suggesting that the effect of *H. polygyrus* infection on DCs is long lasting and continues after the worm leaves the system of its host (Hang et al., 2010a). This suggests that *H. polygyrus* can modify the DC population in its host to prevent activation of the immune system.

The modulation of DCs by *H. polygyrus* is mediated by factors secreted by the parasite, as it was found that *H. polygyrus* somatic extract does not alter the expression of cytokines, chemokines or co-stimulatory molecules *in vitro*, whereas HES induces tolerised DCs (Segura, Su, Piccirillo, & Stevenson, 2007). When HES and CpG, a TLR agonist, are added to bone marrow dendritic cells (BMDCs) *in vitro*, BMDC production of IL-10, IFNγ, IL-12 and IL-1ß are downregulated and their expression of CD40, CD86 and MHC II is lower than those treated with CpG alone (Segura *et al.*, 2007). This suggests that HES is able to tolerise BMDCs even in the presence of a strong TLR agonist (Segura *et al.*, 2007). *In vivo*, DCs from the intestine of *H. polygyrus* infected mice also show reduced CD86 as well as reduced CD80 (Hang et al., 2010a). These authors hypothesised that when *H.polygyrus*-tolerised DCs interact with CD4+ T cells, they drive several pathways to prevent T cell mediated clearance of the worm, including instructing CD4+ Foxp3- cells to produce IL-10, inducing anergy, or even deletion of the T cell clones that respond to the parasite (Segura et al., 2007; Hang et al., 2010a; Blum et al., 2012). In this way, the worm can prevent its own clearance not only by interfering with the communication between APCs and effector CD4+ T cells, but by subverting that interaction in favour of immunological tolerance.

1.10 Immune regulators from H. polygyrus

Helminths have adapted to produce immunomodulatory molecules which can alter the host immune response to allow chronic infection (Rick M. Maizels et al., 2018; Zakeri, Hansen, Andersen, Williams, & Nejsum, 2018). In recent years, many immunomodulatory products have been found in helminth genomes, secretomes and proteomes which include molecules that interfere with the initiation of the immune response, antigen processing and presentation, effector immune cell function and coagulation (Rick M. Maizels et al., 2018; Zakeri et al.,

2018). These molecules can have effects on the innate and adaptive immune response and can prevent epithelial cell alarmin release (Rick M. Maizels et al., 2018; Zakeri et al., 2018). *H. polygyrus* can produce molecules like cystatins (*Hp*CPI) which induce IL-10 production from macrophages and T cells, as well as extracellular vesicles (eVs) containing proteins and mRNAs which downregulate ST2 expression on macrophages and epithelial cells (Buck et al., 2014; Coakley et al., 2017; Sun et al., 2013). Two molecules found in HES, *Hp*-TGM and *Hp*-ARI will be discussed further in 1.10.1 and 1.10.2 respectively.

1.10.1 TGF-β Mimic

Transforming growth factor-ß or TGFß is a pleiotropic cytokine which has many functions in the immune system including tolerising immune cells. CD8+ T cells exposed to TGFß have reduced cytotoxicity, IFNγ production and migration, while macrophages exposed to TGFß have increased chemotaxis but decreased effector function and antigen presentation (W. Chen & ten Dijke, 2016; Sanjabi, Oh, & Li, 2017). TGFß also causes dendritic cells to reduce their chemotaxis, maturation and antigen presentation, limiting the immune response (W. Chen & ten Dijke, 2016; Sanjabi et al., 2017). Importantly to this project, TGF-ß is also necessary for the differentiation of naïve CD4+ T cells to Foxp3+ pTregs in humans and mice (Figure 1.2)(W. J. Chen et al., 2003).

When studying the effect of *H. polygyrus* on CD4+ T cells, it was found that a component of HES is able to induce Tregs *in vitro* in a manner that required signalling through the TGF-ß pathway (Grainger *et al.*, 2010). Using size and charge-based fractionation, *Hp*-TGM (TGF-ß mimic) was identified to be a functional mimic of TGF-ß which can bind to the two receptor subunits (TßR I and II) to induce Tregs from human and murine naïve CD4+ T cells (Cook et al., 2021; Johnston et al., 2017; Smyth et al., 2018, 2021).

TGF-ß and TGM share no structural homology; active mammalian TGF-ß is made up of two polypeptide sequences of around 110 amino acids, which form a homodimer to bind to to the TßRII receptor. The active domain is produced by furin cleavage of a much larger inactive preprotein, so that physiological activity is tightly controlled. In contrast, *Hp*-TGM requires no post-translational

processing, and is a large polypeptide of around 440 amino acids made up of 5 similar Complement Control Protein (CCP) domains; the parasite protein binds to the TGFβR I and II as a monomer (Johnston *et al.*, 2017; Smyth *et al.*, 2018). Despite the differences in the structure of TGF-β and *Hp*-TGM, their effect on murine CD4+ T cells is conserved in terms of receptor binding and SMAD signalling (White *et al.*, 2021). *Hp*-TGM induced iTregs also show greater stability and suppressive capacity compared to TGF-β induced iTregs (White *et al.*, 2021).

In addition to the original TGM, now renamed TGM-1, nine additional related TGM family members were found in to be secreted by *H. polygyrus*, and have been named TGM-2 through -10. Of the 10 family members, TGM-1, TGM-2 and TGM-3 can induce Tregs and/ or are active in the MFB11 bioassay (Smyth *et al.*, 2018). The MFB11 bioassay utilises embryonic fibroblasts from a TGF-β knock out mouse which cannot produce TGF-β. These fibroblasts were transfected with a secreted alkaline phosphatase (SEAP) reporter gene tagging the SMAD-binding elements of TGF-β. This means that upon stimulation with TGF-β, the fibroblasts secrete SEAP which can be used to quantify TGF-β signalling (Tesseur *et al.*, 2006). TGM-1, TGM-2 and TGM-3 share high structural homology in CCP domains 1, 2 and 3 and vary in domains 4 and 5 (Smyth *et al.*, 2018). By comparing the sequence of the bioactive TGM family members to the non-active members and by testing truncations of TGM lacking particular domains, it has been shown that CCP domains 1-3 are required for the function of TGM (Smyth *et al.*, 2018).

The immunoregulatory effects of TGM have been tested in a number of murine models of disease including allograft rejection, dextran sulphate sodium (DSS)-induced colitis, airway induced hypersensitivity and experimental autoimmune encephalomyelitis (EAE) (Johnston et al., 2017; Smyth et al., 2021; White et al., 2021; White, Johnston, et al., 2020).

In the case of allograft rejection, C57BL/6 mice had osmotic mini pumps, filled with either TGM, whole HES or PBS, implanted in their peritoneal cavity one day before receiving a BALB/c skin transplant (Johnston *et al.*, 2017). The mice treated with TGM had lower Th17 cell numbers, higher Treg numbers and lower rejection scores. This suggests that TGM can induce Tregs which minimise the

Th17 graft rejection response and maintain the graft for longer periods of time (Johnston *et al.*, 2017).

Hp-TGM can be produced using an algal protein expression system which utilises *Chlamydomonas reinhardtii*, an edible algae, to produce bioactive TGM-1 (Smyth *et al.*, 2021). Extracts of TGM-1-producing algae were given to mice in their drinking water. The expression of TGM-1 by these algal organisms protected mice from the development of DSS-induced colitis as shown by reduced weight loss, lower disease score and higher Treg numbers (Smyth *et al.*, 2021).

In EAE, a mouse model of multiple sclerosis, adoptive transfer of iTregs induced *in vitro* with *Hp*-TGM significantly reduces disease score and while the effector Th17 population is not reduced, the production of IL-17A is significantly reduced (White, Johnston, et al., 2020). This shows that *Hp*-TGM induced Tregs are able to reduce the effector function of Th17 cells and attenuate the development of EAE (White, Johnston, et al., 2020). There is also evidence that human Th17 cells are converted to Tregs more efficiently by *Hp*-TGM than TGFß *ex vivo* (Cook *et al.*, 2021). This may imply that during EAE, *Hp*-TGM may be converting Th17 to a Treg-like phenotype, reducing effector function and alleviating disease.

In summary, *Hp*-TGM is a mimic of TGF-ß which can induce human and murine Tregs that are capable of suppressing inflammatory diseases like EAE, colitis and allograft rejection. This molecule is found in the ES of *H. polygyrus* and suggests that the worm has evolved a novel protein structure that upregulates Tregs to control the Th2 response that would otherwise clear the helminth infection.

1.10.2 Hp-ARI

In early studies of the Hygiene Hypothesis, it was found that *H. polygyrus* infection protects against allergic airway inflammation provoked by ovalbumin (OVA) or the house dust mite allergen Der p 1 (Wilson et al., 2005). Further studies showed that HES given i.p. was also able to protect against OVA-induced airway allergic inflammation, showing that active infection was not required for protection (Henry J. McSorley et al., 2012). HES was also evaluated using a murine model of airway induced allergic disease using *Alternaria* allergen, an allergen isolated from the fungus *Alternaria alternata* which is associated with

human asthma (Osbourn *et al.*, 2017). It was then discovered that HES-treated mice undergoing *Alternaria* allergen induced airway allergy had significantly less IL-33 in their bronchoalveolar lavage fluid (H. J. McSorley, Blair, Smith, McKenzie, & Maizels, 2014). *In vitro,* HES was also found to block the release of the alarmin IL-33 from freeze-thawed murine lung cells, showing blocking of the damage response (Osbourn *et al.*, 2017). This *in vitro* read-out of IL-33 production was used to screen for the active molecule within HES which is able to limit IL-33 production (H. J. McSorley et al., 2014; Osbourn et al., 2017). Using a similar method of size and charge fractionation of whole HES, *Hp*-ARI (Alarmin release inhibitor) was found to be the molecule mediating inhibition of IL-33 release (Figure 1.2)(Chauché et al., 2020; Osbourn et al., 2017).

Remarkably, *Hp*-ARI is made up of 3 CCP domains each with distant similarity to Hp-TGM, albeit possessing completely different biological activity. Hp-ARI is able to tether IL-33 produced by necrotic cells to the DNA in the nucleus of the cell, preventing its release and interaction with other immune cells (Osbourn *et al.*, 2017). In mice given *Alternaria* intranasally, the effect of *Hp*-ARI was to reduce eosinophilia, reduce mucus in the lung and diminish ILC2 production of IL-5 and IL-13 (Osbourn *et al.*, 2017). These results show that the type 2 allergic response is dampened in the absence of IL-33 signalling, and that suppression is mediated by *Hp*-ARI. *Hp*-ARI has also been shown to bind to not only murine IL-33 but also human IL-33, meaning *Hp*-ARI may be useful as a treatment for human asthma (Osbourn *et al.*, 2017).

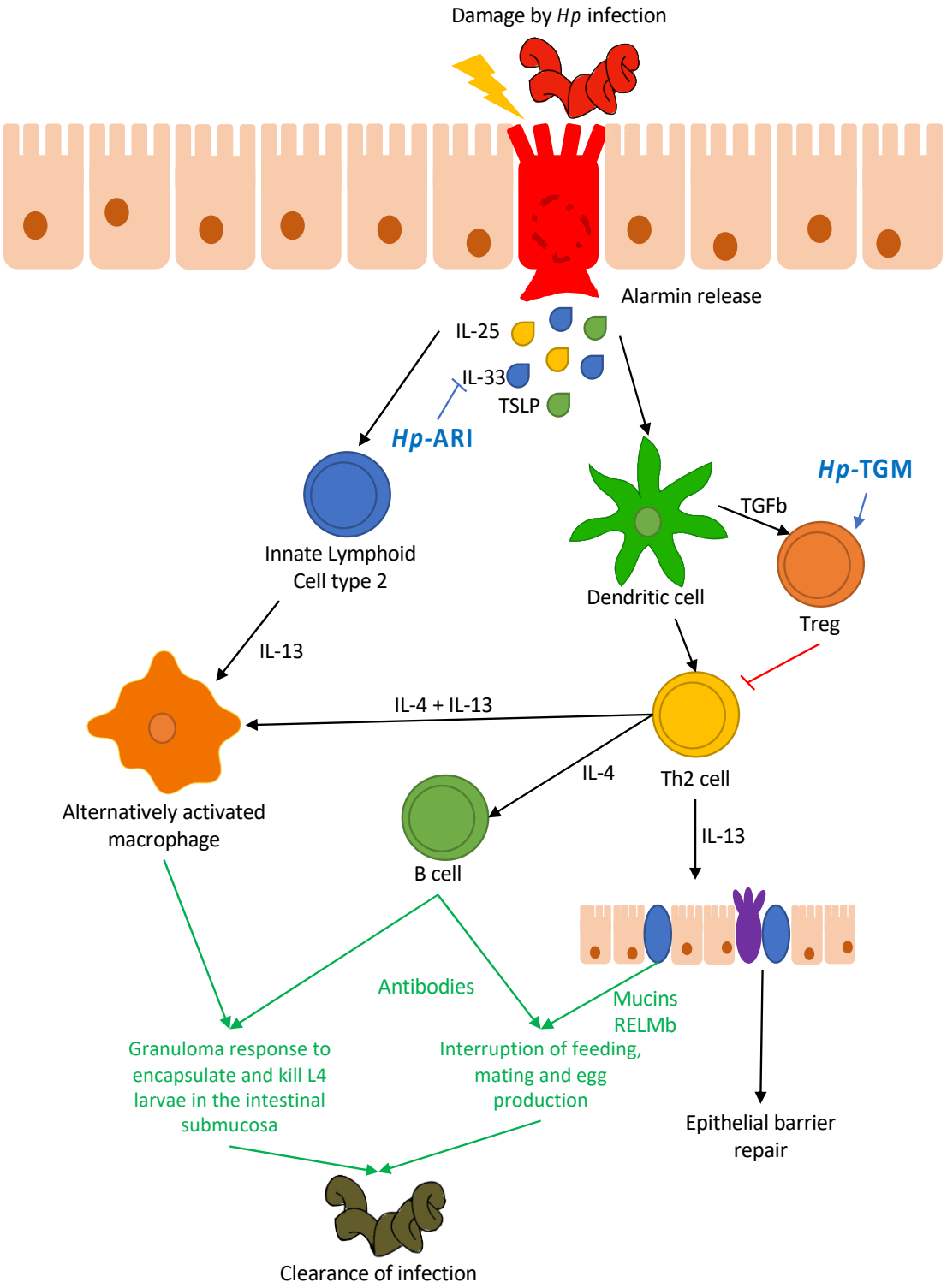

Figure 1.2 The immune response to H. polygyrus and its immunomodulation. Infection with *H. polygyrus* leads to alarmin release from the intestinal epithelium. These alarmins go on to, among other things, activate ILC2s and DCs. ILC2s produce IL-13 which polarizes macrophages to a type 2 phenotype which form part of the granuloma response. DCs are activated and present antigen to and activate CD4+ T cells, resulting in Th2 cells and Tregs. The Th2 cells can orchestrate the immune response and their production of IL-4 and IL-13 lead to B cell maturation and antibody production, polarization of macrophages and goblet cell hyperplasia. The antibodies produced by B cells form part of the granuloma response which can lead to clearance. Antibodies can also interfere with worm feeding and mating alongside mucins and RELMb produced by goblet cells. *Hp*-ARI is able to block alarmin release, *Hp*-TGM is able to increase Treg induction.

1.11 CD4+ T cell activation: from exogenous protein to activation

As seen in section 1.10, helminth parasites are able to interfere with their hosts' innate and adaptive immune responses (Rick M. Maizels et al., 2018; Zakeri et al., 2018). However, when it comes to the balance between resistance and susceptibility to helminths, the adaptive immune response and in particular CD4+ T cell responses are likely key determinants in parasitological outcome of infection. As such, it is important to understand the pathways which lead to active CD4+ Th cell function including antigen processing and presentation.

There are three main steps which are required for CD4+ T cells to become activated: recognition of peptide in MHC II on an APC (Signal 1); ligation of co-stimulatory receptors (Signal 2); and cytokine-dependent T cell specialisation (Signal 3) (J. S. Blum, Wearsch, & Cresswell, 2013; Gfeller & Bassani-Sternberg, 2018; Vyas, van der Veen, & Ploegh, 2008). The quantitative and qualitative nature of each of these signals will determine whether an immune challenge is met with tolerance or responsiveness, and if the latter, what mode of response is mounted.

Before the first step can occur, antigen from the environment must be processed by APCs to allow presentation of T cell epitopes in MHC II. Antigen processing for presentation to CD4+ T cells begins when the APC phagocytoses antigen from the environment into phagosomes (J. S. Blum et al., 2013; Gfeller & Bassani-Sternberg, 2018; Vyas et al., 2008). Antigen-filled phagosomes then mature and begin breaking down the phagocytosed antigen (J. S. Blum et al., 2013; Vyas et al., 2008). The mature phagosome then fuses with lysosomes to form the phagolysosome which contains MHC II molecules (J. S. Blum et al., 2013; Vyas et al., 2008). MHC II molecules found within the phagolysosome carry an invariant peptide known as CLIP (Class II-associated invariant chain peptide) which is removed by H2-DM, an MHC II-like structure, allowing the peptides within the phagolysosome to load onto MHC II (J. S. Blum et al., 2013; Vyas et al., 2008). Once the peptide is bound to the MHC II, the peptide: MHC II complex is trafficked to the cell membrane (J. S. Blum et al., 2013; Vyas et al., 2008).

With antigen processing and presentation complete, the T cells can interact with the APC, and those T cells which recognise the peptide in MHC II receive signal 1 through their TCR (Luckheeram, Zhou, Verma, & Xia, 2012; Schneidman-Duhovny et al., 2019). As discussed in 1.9 and 1.10, there are many ways in which antigen presentation can be affected by helminth infection. For example, *H. polygyrus* can induce tolerogenic DCs which have limited antigen presenting capacity and the production of *Hp*-TGM may inhibit maturation and antigen presentation in the same way as TGFß (W. Chen & ten Dijke, 2016; Sanjabi et al., 2017; Smyth et al., 2018; White et al., 2021).

The peptides which are recognised by the CD4+ T cell population during *H. polygyrus* infection are largely unknown. There is a large pool of potential T cell epitopes during *H. polygyrus* infection including the antigens found in HES, antigens from the worm itself and antigens created by damage caused by infection (Gause, Wynn, & Allen, 2013; Hewitson et al., 2013; Hewitson, Harcus, et al., 2011). The antigen specific Th response to *H. polygyrus* is explored further in Chapter 5.

However, TCR stimulation alone is not enough to activate T cells. To prevent activation of T cells which recognise self-antigen as well as modulating the response to limit damage to the host, a second co-stimulatory signal is required. If no co-stimulation is given to a T cell while receiving TCR stimulation, the T cell becomes anergic or tolerised, limiting responses against self-antigen (Appleman and Boussiotis, 2003; Goronzy and Weyand, 2008). The T cell surface receptor most commonly involved in co-stimulation is CD28 which gives an activating signal to CD4+ T cells when it interacts with its ligands CD80 and CD86 on APCs (Bour-Jordan et al., 2011; Luckheeram et al., 2012; Watanabe et al., 2017).

There are however other molecules capable of providing co-stimulation to CD4+ T cells, including members of the TNFR family such as CD27 and OX40, and ICOS (Inducible co-stimulator) (Luckheeram *et al.*, 2012). ICOS is also a member of the CD28 superfamily and is upregulated upon T cell activation and has a role in the activation of Th1, Th2, Th17 and Tfh cells. ICOS KO mice were found to have impaired germinal centre formation and Th2 responses (Sharpe and Freeman,

2002; Mahajan *et al.*, 2007; Wikenheiser and Stumhofer, 2016). There is also a loss of ICOS expression on Th1 cells over time, whereas the high expression of ICOS is maintained on Th2 cells (Mahajan et al., 2007; Sharpe & Freeman, 2002; Wikenheiser & Stumhofer, 2016). Together these findings suggest that ICOS signalling is more important to Th2 than Th1 responses which brings into question its relevance during helminth infection (Esensten, Helou, Chopra, Weiss, & Bluestone, 2016; Mahajan et al., 2007; Redpath et al., 2013). Once co-stimulated via CD28 or any other co-stimulatory molecule, the cell begins to proliferate and a third signal is then required to direct their specialisation into different Th subsets and further expand the population (Zhu, Yamane and Paul, 2010; Luckheeram *et al.*, 2012).

Signal 3 is mediated by cytokines available in the environment which instruct naïve CD4+ T cells to become Th1 via IFNγ, Th2 via IL-4, Tregs via TGFß and Th17 via IL-6 and TGFß (Luckheeram et al., 2012; Zhu et al., 2010). Once so directed, the differentiated Th cell can leave the lymphoid tissue and enter the tissue site where it is required (Groth, Smith, & Higgins, 2004; Jenkins et al., 2001). As discussed above, during helminth infection there is a dominant shift towards IL-4 responses and Th2 differentiation, but in many cases this is accompanied by expanded Tregs through activation of the TGFß pathway. However, with increasing appreciation of functional subsets of both Th2 and Tregs, and the knowledge that *H. polygyrus* at least intervenes by producing its own ligand to mimic TGFß, much greater detail is required to understand T cell responses and their consequences in helminth infection (Eberl & Pradeu, 2017; Nakajima et al., 2021; Sefik et al., 2016; Shevyrev & Tereshchenko, 2020).

1.12 Thesis Aims

Is the T cell response to *H. polygyrus* important to resistance versus susceptibility to the helminth?

As discussed above, there is a spectrum of infection intensity where the majority of people can maintain a small worm burden with little pathology while a smaller population is overwhelmed with the parasite and suffer more severe pathology. The differences in the immune response of those resistant to

infection versus those with high susceptibility is still unknown. Using infection with the model murine nematode H. polygyrus in partially resistant BALB/c and fully susceptible C57BL/6 mice, it is possible to model this difference in worm burden. By comparing the Th2 and Treg responses in BALB/c and C57BL/6 mice, mechanisms which allow clearance in BALB/c and prevent it in C57BL/6 mice can be discovered and may hold parallels to patients infected with human helminthiases. It is hypothesised that BALB/c mice, with their genetic predisposition toward Th2 responses, mount a stronger Th2 response whereas C57BL/6 mice mount a more regulatory response and thus their Th2 cells are suppressed and unable to clear to worm.

Are Tregs from H. polygyrus infected mice different to Tregs from naïve mice?

It has been postulated that Tregs from H. polygyrus infected mice are more suppressive than Tregs from naïve mice due to their ability to suppress autoimmune and allergic disorders. In recent years, with the discovery of different subtypes of Tregs, further characterisation of the Treg response is required to assess the role and dynamics of these populations is required. Tregs are also able to express a wide range of suppressive molecules, including the co-inhibitory receptors that will be explored further in Chapter 4. It is hypothesised that Tregs from H. polygyrus infected mice are distinct from Tregs from naïve mice due to the presence of immunomodulatory molecules including TGM and the changes in cytokine milieu during infection.

What antigens are recognised by T helper cells during *H. polygyrus* infection?

As discussed previously, the epitopes that are recognised through Th cell TCRs from H. polygyrus-infected mice remain unknown. It is expected that there are immunogenic peptides found within HES which are recognised by the adaptive immune system and in particular by CD4+ T cells. However, it is unknown if the T cell response is induced by recognition of the molecules in HES, recognition of antigen from the parasite (H. polygyrus extract; HEx) or the damage associated with infection (Gause et al., 2013; Hewitson et al., 2013; Hewitson, Filbey, et al., 2011). The discovery of T cell epitopes recognised during H. polygyrus

infection can lead to informed vaccination studies to boost clearance and can be used to generate a transgenic TCR mouse line.

Chapter 2 Materials and Methods

2.1 Methods

2.1.1 Mice

2.1.1.1 Breeding and Husbandry

Inbred BALB/c Foxp3-GFP and C57BL/6 Foxp3-GFP reporter mice were bred in-house and maintained in individually ventilated cages (IVCs) (Fontenot *et al.*, 2005). BALB/cOlaHsd and C57BL/6OlaHsd mice were purchased from Envigo. Foxp3-Tocky and Nr4a3-Tocky Foxp3-GFP mice were obtained from the Masahiro Laboratory at Imperial College London and bred in house. All mice were maintained in IVCs within a barrier unit (Bending, Martín, et al., 2018; Jennings et al., 2020; Bending, Paduraru, et al., 2018).

All animal breeding and experiments were performed under UK Home Office licence and approved by the University of Glasgow Ethical Review Board.

2.1.1.2 Gavage

Each infected mouse was given 200 L3 *H. polygyrus* larvae in 200uL of water using a gavage tube as previously described (Johnston *et al.*, 2015).

2.1.1.3 Intraperitoneal Injection and In Vivo Antibody Depletion

Neutralising monoclonal antibodies and Rat IgG were suspended in 200µL of sterile Dulbecco's Phosphate Buffered Saline (DPBS, Gibco, Catalogue number 14190-094) and injected intraperitoneally using a 26G needle.

200µg of MP5-20F3 (α-IL-6 mAb) produced in house or Rat IgG (Merck, catalogue number I4131-50MG) was given at days 0, 2, 4 and 6 post infection and mice were culled at day 7 or day 14 post infection.

2.1.2 Parasites and Antigens

2.1.2.1 Life cycle

CBA x C57BL/6 F1 mice were infected with 400 L3 *H. polygyrus* larvae by gavage. Faeces from these infected mice was collected 14 days post infection and mixed 1:1 with charcoal to form a paste. This paste is spread thinly on filter paper and placed in the centre of a petri dish and placed in a humid box in a dark drawer for 12-14 days. L3 larvae were collected from the dish from day 7 onwards by rinsing around the edge of the filter paper with 5ml of sterile water per plate as previously described (Johnston *et al.*, 2015).

2.1.2.2 Heligmosomoides polygyrus Excretory-Secretory Products (HES)

Adult *H. polygyrus* were isolated from the duodenum of infected CBAxC57BL/6 F1 mice, washed and treated with antibiotics then cultured in RPMI as described previously (Johnston *et al.*, 2015). Adult *H. polygyrus* were collected from the duodenum of infected mice using a modified Baermann Apparatus filled with HBSS which allows the worms to swim and settle in the bottom of a test tube over the course of 2 hours at 37°C. The adult worms were collected, washed and incubated in RPMI with 10% Gentamycin to remove bacterial contamination. The now clean worms were placed in vented T25 flasks in RPMI1640 supplemented with glucose (1.2% final concentration). The culture supernatant was collected and replaced at twice weekly intervals for 3 weeks before purifying and concentrating HES as described previously (Johnston *et al.*, 2015).

2.1.3 Tissue Processing

2.1.3.1 Mesenteric Lymph Node Cell Isolation

The whole chain of mesenteric lymph nodes was excised from the mouse and either processed together or split into duodenum draining MLN and non-duodenum draining MLN before processing. MLN were pushed through a 70um EasyStrainer (Greiner, catalogue number 542070) with complete RPMI before being counted using the Nexcelom Cellometer 2000 and AOPI or trypan blue and a haemocytometer.

2.1.3.2 Spleen Cell Isolation

The spleen was pushed through a 70µm EasyStrainer with complete RPMI before pelleting the cells by centrifugation (400g, 5 minutes). The supernatant was removed, and the cells resuspended in 2ml of Red Cell Lysis Buffer (Sigma-Aldrich, catalogue number R7757) and incubated for 2 minutes at room temperature before adding 8ml of complete RPMI (Table 2.1) to stop the digestion. The cells were once again pelleted by centrifugation at 400g for 5 minutes before being counted using the Nexcelom Cellometer 2000 and AOPI (Nexcelom, catalogue number CS2-0106-5ML) or trypan blue (Gibco, catalogue number 15250061) and a haemocytometer.

2.1.3.3 Small Intestine Lamina Propria Cell Isolation

The small intestine lamina propria cells were isolated using a Collagenase A digestion optimised by the Mayer Laboratory (Ferrer-Font *et al.*, 2020). The first 10cm of the duodenum was isolated from the mouse, the fat and Peyer's patches removed and cut bilaterally before washing the mucus and worms from the intestine with DPBS. The duodenum was cut into around 1cm pieces before being stored in 10ml of ice cold Collection buffer (Table 2.1). The duodenum was filtered through a small strainer and washed twice with warm HBSS. The tissue was transferred into 10ml of pre-warmed EDTA wash buffer (Table 2.1) before being incubated at 37C in a shaking incubator at 200rpm for 10 minutes to remove remaining mucus. The EDTA digestion was repeated twice, vortexing vigorously for 10 seconds and replacing the EDTA wash buffer between each repeat. The duodenum was washed twice with warm HBSS. The tissue was added to a 50ml falcon tube containing 10ml of Collagenase A digestion buffer (Table 2.1) and incubated for 30 minutes at 37°C in the shaking incubator at 200rpm and shaking vigorously every 5 minutes. 10ml of ice cold FACS buffer (Table 2.1) was then added to stop the digestion. The resulting suspension was pushed through a 100µm (Greiner, catalogue number 542000) then a 40µm EasyStrainer (Greiner, catalogue number 542040) using a serological pipette into a 50ml falcon tube. The single cell suspension was centrifuged at 600g for 6 minutes at 4°C to pellet the cells and was resuspended in FACS buffer containing 20ug/ml DNase I. Cells were then counted using Trypan blue and a haemocytometer. This

protocol was used for 5 samples at a time to maintain a fast pace and ensure high live cell yields.

2.1.3.4 Colon Lamina Propria Cell Isolation

The colon was excised from the mouse and flushed 3 times with cold DPBS before cutting longitudinally and being rinsed in DPBS to remove faecal matter. The colon remains otherwise intact to allow faster work pace to obtain maximum viability. The clean colons are placed in 50ml falcon tubes with 15ml of shake buffer (Table 2.1) warmed to 37°C and shaken vigorously for 30 seconds. The colon was poured over a sieve to remove the shake media and the tissue collected in 15ml of 37°C Mucus removal buffer (Table 2.1) before placing in the shaking incubator at 37°C, 250rpm for 10 minutes. This was repeated once. Colons were then placed in 15ml of shake buffer and shaken vigorously for 30 seconds, collecting the colon in a sieve and discarding the flow through. This step was repeated twice. Colons were washed three times with warm DPBS to remove EDTA from the tissue. The colon tissue was transferred into a gentleMACS C tube (Miltenyi Biotech, Catalogue number 130-093-237) and 1.5ml of 5x colon digestion media (Table 2.1) was added. Complete RPMI (Table 2.1) was added to bring the concentration to 1X. Samples were loaded onto the gentleMACS Octo Dissociator (Miltenyi Biotech, catalogue number 130-095-937) with heating sleeves and the lamina propria isolation program (37C_m_LPDK_1; pre-programmed by the manufacturer) was run. After the program was complete, the C tubes were placed on ice and 10ml of 3% media was added to stop the digestion. The samples were then transferred from the C tubes into 50ml falcon tubes by pushing through a 70µm EasyStrainer using a serological stripette. Colon lamina propria cells were pelleted by centrifugation for 5 minutes at 600g at 4°C. The cell pellet is resuspended in 10ml 3% media (Table 2.1) and pushed through a 40µm EasyStrainer to remove more debris. The cell suspension is pelleted once again before counting using 1:1 trypan blue and a haemocytometer.

2.1.3.5 Peyer's Patch Cell Isolation

The whole small intestine was excised from the mouse and Peyer's patches isolated from the tissue parallel to the mesentery. In *H. polygyrus* infected

mice, only Peyer's patches closely associated with an adult worm were taken for further analysis (Mosconi *et al.*, 2015). Once excised from the tissue, the Peyer's patches were stored in 10ml of ice cold DPBS in a 50ml falcon tube and vortexed for 30 seconds to remove mucus and faecal matter. The tissue was transferred into 20ml of strip buffer (Table 2.1) pre-warmed to 37°C and a 22mm magnetic flea added to each 50ml falcon tube. The tube was placed in a 37°C incubator on a magnetic stirring plate set to 200rpm for 30 minutes. After 30 minutes, 10ml of FACS buffer was added to stop the digestion. The Peyer's patches were then pushed through a 70um EasyStrainer with 20ml of complete RPMI before being washed twice in complete RPMI and counted using the Nexcelom Cellometer 2000 and AOPI or trypan blue and a haemocytometer.

2.1.3.6 Peritoneal Exudate Cell Isolation and Peritoneal Lavage

After sacrificing the mouse, the peritoneal cavity was injected with 2ml of ice cold sterile DPBS using a 26G needle. The cavity was gently massaged to distribute the DPBS. The same needle and syringe were used to recover the DPBS containing the peritoneal exudate cells (PEC) cells from the peritoneal cavity. The peritoneal lavage fluid was then spun at 400g for 5 minutes to pellet the PEC and the supernatant was removed and either disposed of or frozen at -80°C for later cytokine analysis. Cells were then resuspended in complete RPMI and counted using Trypan blue and a haemocytometer or AOPI and the Cellometer Auto 2000 Automated Cell Counter.

2.1.4 Flow cytometry

2.1.4.1 Extracellular Staining

Cells were stained in a round bottom 96 well plate (Corning, Catalog number 3799) at $1*10^6$ cells per well. The cells were washed twice with PBS before staining with eBioscience™ Fixable Viability Dye eFluor™ 506 (Thermo Fischer Scientific, Catalog number: 65-0866-14), diluted 1:1000 (unless otherwise stated) in PBS for 15 minutes at 4°C. The plate was then washed twice with 200uL of FACs buffer. The extracellular antibody mixture containing all extracellular antibodies at their required dilution (Table 2.2) and a 1:50 dilution of Fc block (CD16/CD32 Monoclonal Antibody (93), eBioscience™, Catalog

number 14-0161-82) was added and incubated for 30 minutes at 4°C. Finally, the cells were washed twice in 200uL of FACs buffer and resuspended in 200uL of FACs buffer containing 10U/ml DNase II (Sigma-Aldrich, catalogue number D8764-30KU).

2.1.4.2 Intracellular Staining

Cells were plated and undergo extracellular staining as in 2.1.4.1. After extracellular staining, cells were resuspended in 100µL of IC Fix Buffer (eBiosciences) for 20 minutes at room temperature. The plate was then washed twice with 200µL of Permeabilisation buffer (diluted 1:10 in H_2O). Intracellular antibodies were suspended in Permeabilisation buffer at the required dilution (see Table 2.2) and 50µL of this antibody mixture added to the cells for 30 minutes at 4°C. Finally, the cells were washed twice in 200uL of FACs buffer and resuspended in 200uL of FACs buffer containing 10U/ml DNase II (Sigma-Aldrich, catalogue number D8764-30KU).

2.1.4.3 Intranuclear Staining

Cells were plated and undergo extracellular staining as in 2.1.4.1. After extracellular staining, cells were resuspended in 100µL of Foxp3 Fix Buffer (eBiosciences, catalogue number 00-5523-00) diluted 1:4 in Fixation/Permeabilization Diluent for 40 minutes at room temperature. Cells were then washed twice in Permeabilisation buffer (eBiosciences, catalogue number 00-5523-00). Antibodies against intranuclear targets such as transcription factors are diluted in Permeabilisation buffer at the required dilution (See Table 2.2). 50µL of antibody mixture was added to the cells and incubated at room temperature for 1 hour. Finally, cells were washed and resuspended in FACS Buffer with 10U/ml DNase II (Sigma-Aldrich, catalogue number D8764-30KU).

2.1.5 Cytokine Analysis

2.1.5.1 Cytokine Bead Array (CBA)

CBA Flex Sets from BD Biosciences were used for the beads, antibody and cytokine standards (Mouse IL-4 Flex Set, 558298; IL-13, 558349; IL-5, 558302, IL-10,558300, IL-6, 558301; IL-17A, 560283; IL-9, 558348; IFNg, 558292).

50µL of neat supernatants were defrosted from the -80°C freezer and loaded into a 96 well round bottom plate alongside standard mixes with each cytokine at concentrations ranging from 2500pg/ml to 2.44pg/ml and a blank to allow standard curve generation. The cytokine beads were diluted 1/250 in filtered FACS buffer. 50µL of bead mixture was added to each well and incubated for 1 hour at room temperature in foil. During this incubation, the detection antibody mix was made by diluting each antibody 1/250 in filtered FACS buffer. 50µL of detection antibody mix was added to each well and incubated at room temperature for 1 hour in foil. The plate was then twice washed by adding 100µL of filtered FACS buffer and spinning at 200rpm for 5 minutes. The plate is resuspended in 100µL of filtered FACS buffer and loaded onto the MACS Quant for acquisition or filtered into FACS tubes and acquired on the BD LSR II. The MFI of PE can be used to interpolate the concentration of each sample using the standard curve.

2.1.5.2 Limulus amebocyte lysate (LAL) Assay

After purification, monoclonal antibodies and HES were tested for their endotoxin content to ensure they are safe for *in vivo* use using the Lonza Chromogenic LAL Assay (discontinued). The endotoxin standards (Lonza, discontinued) were prepared at 1U/ml, 0.5U/ml and 0.125U/ml and plated in duplicate in a flat bottom 96 well plate with a blank well containing only LAL reagent water. The sample of interest was diluted to obtain 200µL at a concentration at 10µg/ml which can be diluted to 100µL of 1µg/ml and 0.1µg/ml. The samples can then be plated in duplicate in the same 96 well flat bottom plate. The *Limulus* Amebocyte Lysate (Lonza, discontinued) was reconstituted in LAL reagent water according to the protocol sheet included and lot number and 50µL of this LAL solution was added to each well and incubated

at 37°C for 10 minutes. The chromogenic substrate was reconstituted in LAL reagent water to a concentration of 2mM and 100µL was added to each well. The plate was incubated at 37°C for 6 minutes before stopping the reaction using 25% v/v glacial acetic acid in water. The plate was then read in the plate reader at 405nm and the optical density can be used with the standard curve to interpolate the unknown samples and find the concentration of endotoxin in these samples.

2.1.6 Cell Sorting

2.1.6.1 AutoMACS Pro Separator

MLN or spleens were processed into a single cell suspension as in 2.1.3.1 and 2.1.3.2 then resuspended in AutoMACS Buffer (Table 2.1) at $1*10^7$ cells per 20µL. If the total volume was less than 200µL, the suspension was topped up to this minimum volume. Cells were placed in the Chill 15 Rack (Miltenyi Biotech, catalogue number 130-092-952) and the reagent bottles scanned by the barcode reader on the AutoMACS Pro to set up the protocol. For single cell sequencing of CD3+ T cells, the Pan T Cell Isolation Kit II (Miltenyi Biotech, catalogue number 13-095-130) was used with the depletes program, leaving the CD3+ cells in the negative fraction. For T cell cultures, the Naïve CD4+ T Cell Isolation Kit (Miltenyi Biotech catalogue number 130-104-453) was used with the depletes program, leaving naïve CD4+ T cells in the negative fraction. For BMDC:T cell cocultures and single cell sequencing of CD4+ T cells, the CD4 (L3T4) MicroBeads (Miltenyi Biotech, catalogue number 130-117-043) was used with the Possel program, collecting the CD4+ T cells in the positive fraction.

2.1.7 Cell Culture

2.1.7.1 iTreg Culture

96-well Clear Flat Bottom Polystyrene TC-treated Microplates (Corning, catalogue number 3596) were coated with 50µl/well of 10µg/ml α-CD3 and wrapped in parafilm overnight at 4°C. The following day splenocytes were processed as in 2.1.3.2. The coated plate was washed 3 times with 100µL of sterile DPBS. The splenocytes were counted using 1:1 Trypan Blue and a haemocytometer. Naïve CD4+ T cells were isolated using the AutoMACS Pro

Separator and the Naïve CD4+ T Cell Isolation Kit (Miltenyi Biotech catalogue number 130-104-453) as in 2.1.6.1. The purity of the sort was assessed by flow cytometry with around 95% of cells expressing CD4. The CD4+ cells were counted using Trypan Blue and a haemocytometer. The cells were then resuspended at $2*10^6$ cells/ml in T cell media (TCM, Table 2.1) and 100µl of cell suspension added to each well. 50µL of IL-2 media (TCM, 1600U/ml IL-2) was added to each well and 50µL of TGFß (Gift from Dr Emily Smith, UCB) at 80ng/ml in IL-2 media, TGM at 80ng/ml in IL-2 media (produced in house) or IL-2 media alone for an IL-2 only control. The cells were then incubated at 37°C, 5% CO_2 for 72 hours before staining for flow cytometry. This culture yields on average 75% of the CD4+ T cells expressing Foxp3.

2.1.7.2 Bone Marrow Derived Dendritic Cell Culture

The femur and tibia of mice were collected, and the muscles and tendons removed before storing in ice cold PBS. In the tissue culture hood, the bones were transferred into 70% Ethanol for 3 minutes to sterilise the bone before being washed three times with sterile DPBS. The ends of the bones were cut off with large scissors and 5ml of sterile DPBS pushed through the bone with a 23Ga needle into a sterile petri dish. The bone marrow was suspended in the DPBS by passing it through the needle repeatedly until no more aggregates of tissue remain. The single cell suspension was then be transferred into a 50ml falcon tube and the cells pelleted by centrifugation at 400g for 5 minutes at 4°C. Bone marrow cells were resuspended in 10ml of DPBS and counted using 1:1 Trypan Blue and a haemocytometer. BMDC media was then made up fresh (complete RPMI, 20ng/ml GM-CSF) and 9.8ml added to a bacteriological petri dish. The bone marrow cells were resuspended at $1*10^7$cells/ml and 200µL of cell suspension was added dropwise to the centre of the petri dish. 10ml of freshly prepared DC media was added to the plate on day 3. On day 6 and 8, 9ml of DC media was carefully removed from the edge of the plate before adding 10ml of fresh DC media. BMDCs were harvested on d11 to be used in subsequent experiments by washing the plate gently with the culture suspension and a serological pipette to collect only the non-adherent cells.

2.1.7.3 BMDC:T cell coculture

BMDCs were cultured as in 2.1.7.3. CD4+ T cells were isolated using the CD4 (L3T4) MicroBeads (Miltenyi Biotech, catalogue number 130-117-043) and the AutoMACS Pro Separator as seen in 2.1.6.1. To each well of a 96-well Clear Flat Bottom Polystyrene TC-treated Microplate (Corning, catalogue number 3596), 50µL of TCM containing $2*10^4$ bone marrow derived dendritic cells was added alongside 100µL of TCM containing either 10µg/ml HES, 1µg/ml Hp-VAL-1, 1µg/ml Hp-VAL-2, 1µg/ml Hp-VAL-3, 1µg/ml Hp-VAL-4, 1µg/ml ConA or media alone as a control before incubating for 6 hours to allow BMDC antigen processing and presentation. After this incubation, $1.2*10^5$ CD4+ T cells were added to each well in 50µl of TCM. The BMDC:T cell coculture was incubated for 16h or 72h at 37°C, 5% CO_2 before flow staining as in 2.1.2.4.

2.1.7.4 Hybridoma Culture and mAb Purification

Aliquots of MP5-20F3 (α-IL-6) hybridoma cells (gifted by David Gray, original sorce DNAX) were taken from the liquid nitrogen stores and reconstituted in low IgG RPMI medium (RPMI 1640, 10% low IgG FBS, 10K units Pen/Strep, 200mM L-glutamine and 1X MEM NEAA) and cultured in a T25 flask at 37°C, 5% CO_2. The cells were checked every day under the microscope until a confluent layer of cells was seen. The cells were then moved into a T75 flask using a serological stripette to wash the cells off of the walls of the flask with the current media. The cells were collected in a 50ml falcon tube and centrifuged at 200g for 5 minutes to pellet the hybridoma cells and remove the old media. The pellet was resuspended in 35ml of low IgG RPMI medium and transferred into a T75 flask before incubating at 37°C, 5% CO_2. Once the cells reached confluency in the T75 flask, the cells are again removed from the flask as before, centrifuged at 200g for 5 minutes and resuspended in 10mls of low IgG RPMI medium. This single cell suspension was split in half and 5ml added to 2 new flasks to allow bulking. The cells were then gradually split into more T75 flasks and weaned off of the low IgG RPMI medium and onto Hybridoma Serum Free Media (Gibco, catalogue number 12045-076-1L) until around 7 T75 flasks are in 100% Hybridoma Serum Free Media.

At this stage, the hybridoma cells from all 7 flasks were pooled and transferred into a 1L VectraCell Gas Permeable Bioreactor bag (BioVectra, discontinued) with 500ml total of Hybridoma Serum Free Media. This bag of hybridoma cells was incubated for 4 weeks at 37°C, 5% CO_2.

The supernatant was harvested and spun down to remove the hybridoma cells. The supernatant containing the desired mAbs was sterile filtered and stored at -40°C until purification.

The protein purification, dialysis and concentration were carried out by Patrizia Di Crescenzio. Monoclonal antibodies were purified by using a HiTrap Protein G Column (Cytiva, catalogue number 17040501) and the ÄKTA Pure. The mAbs were then dialysed and concentrated using the Amicon and concentration measured using the Nanodrop. Finally, the LPS concentration in the mAb solution was checked by LAL Assay as in 2.1.5.2 before being used *in vivo* as in 2.1.1.3.

2.1.7.5 MLN Restimulation

MLN of naïve and infected mice were isolated as in 2.1.3.1 taking only the small intestine draining lymph nodes. MLN cells were counted using the Nexcelom Cellometer 2000 and AOPI or trypan blue and a haemocytometer. 100µL of $2*10^6$/ml MLN cells were added to each well of a flat bottom 96 well plate. 100µL of TCM containing either 10µg/ml HES, 1µg/ml Hp-VAL-1, 1µg/ml Hp-VAL-2, 1µg/ml Hp-VAL-3, 1µg/ml Hp-VAL-4, 1µg/ml ConA or media alone as a control was added to each well. The plate was then incubated at 37°C, 5% CO_2 for 16 hours before flow staining as in 2.1.2.4.

2.1.8 Single Cell RNA Sequencing

2.1.8.1 Cell preparation

MLN cells were prepared as shown in 2.1.3.1. CD3+ T cells were isolated using the AutoMACS Pro Separator and the Pan T Cell Isolation Kit II (Miltenyi Biotech, catalogue number 130-095-130) or CD4+ (L3T4) isolation kit (Miltenyi Biotech, catalogue number 130-117-034) as in 2.1.6.1. The purity of the sort was assessed

using flow cytometry showing above 95% purity of sorting in both the CD4 (L3T4) and Pan T Cell Isolation sorted kits.

2.1.8.2 Cell Hashtagging

Cell hashtagging allows multiplexing of multiple samples into one batch for single cell RNA sequencing to minimise batch effects. Cell hashing utilises oligotagged antibodies against a ubiquitously expressed marker, by incubating samples with antibodies tagged with different oligonucleotide sequences before mixing the samples, cells can be separated post-sequencing into their sample of origin (Hicks *et al.*, 2018; Stoeckius *et al.*, 2018). Biolegend TotalSeq A0301 anti-mouse Hashtag 1 (or 2) antibody was diluted to 1µg/100µl in FACS buffer and 100µl added to $1*10^6$ cells. C57BL/6 *H. polygyrus* infected and naïve BALB/c cells were labelled with hashtag 1. Naïve C57BL/6 and *H. polygyrus* infected BALB/c were labelled with Hashtag 2. Cells were incubated at 4°C for 10 minutes before washing twice with complete RPMI (Table 2.1). BALB/c and C57BL/6 naïve mice were pooled into one tube and BALB/c and C57BL/6 *H. polygyrus* infected mice were pooled into a second tube.

2.1.8.3 10X Chromium

$7*10^5$ cells from each tube were loaded onto the 10X Chromium Chip along with gel beads, partitioning gel and amplification master mix by Glasgow Polyomics. The Chromium Chip was loaded onto the 10X Chromium for amplification and library preparation before sequencing on the Illumina. This was also performed by Glasgow Polyomics.

2.1.8.4 Seurat Clustering

All data was loaded into a Seurat object in RStudio before quality control was performed (Butler *et al.*, 2018). The quality of the cells was assessed using the number of unique features, RNA abundance and percentage of mitochondrial genes. Barcodes with more than 4000 unique features and more than 30000 RNA reads were excluded as doublets. Barcodes with more than 10% mitochondrial RNA were excluded as stressed cells. The data was then normalised using the NormalizeData function with a scale factor of 10,000. Next, highly variable

features were selected for downstream analysis and PCA using the FindVariableFeatures function. The data then underwent linear transformation to give equal weight to each gene and prevent highly expressed genes influencing further analyses. Next, principal components analysis was performed using the RunPCA function and the dimensionality of the data assessed using a JackStrawPlot to identify at which principal component significance is lost. The cells were clustered using the FindNeighbours and FindClusters functions of Seurat before visualisation in a UMAP. Clusters were identified using a heat map showing the 25 top expressed genes of each cluster or viewing violin plots of characteristic genes such as *Cd4, Cd8a, Foxp3* etc. Full code can be found in the Appendix.

2.1.8.5 Demuxlet

Demuxlet was used to assign BALB/c or C57BL/6 identities to each cell. To achieve this, the code compares every read of each cell to the reference genomes provided and gives a best prediction of which strain each cell originated from (Kang *et al.*, 2018). The reference genomes provided were the BALB/cJ and C57BL/6NJ genomes from the Welcome Sanger Mouse Genomes Project (Keane *et al.*, 2011). These genomes have high similarity to the BALB/cOlaHsd and C57BL/6OlaHsd strains used in this experiment. The strain predictions from Demuxlet were integrated into the Seurat object using importDemux.

2.1.8.6 Differential Expression

The FindMarkers function of Seurat was used to find the differentially expressed genes between the different subclusters predicted from the Seurat Clustering as well as between the different mouse strains. Full code can be found in the Appendix.

2.1.9 Statistical analysis

2.1.9.1 Normality testing

To test if the data is distributed along a gaussian curve, GraphPad Prism was used to run a Shapiro-Wilk normality test. The Shapiro-Wilk test was used due to

the small sample size and the significance level (α) was set to the standard 0.05.

2.1.9.2 T Tests

T tests were used when there two groups. If both groups passed the normality test, an unpaired T test was used. If one or both groups fail the normality test, a Mann-Whitney test was used. Significance is reached when $p < 0.05$.

2.1.9.3 One-way ANOVA

One-way ANOVAs were used when there were more than two experimental groups to compare. If all groups pass the normality test, an ordinary one-way ANOVA is used to assess the statistical significance of changes between experimental groups. If one or more groups failed the normality test, a Kruksal-Wallis test is used.

2.1.9.4 Multiple comparisons

Multiple comparisons were used to compare individual experimental groups with one another. If all groups pass the normality test, a Holm-Šídák's multiple comparisons test is used to compare pre-determined pairs of groups or a control group to the treated groups. If one or more groups fail normality testing, Dunn’s multiple comparisons test is used. Significance is set at $p < 0.05$.

2.2 Materials

2.2.1 Media table

Buffer	Materials	Supplier	Catalogue Number
FACS Buffer	Dulbeccos Phosphate Buffered Saline	Gibco	14190-094
	5mM Ultrapure EDTA	Invitrogen	15575-038
	1% Sodium Azide	Sigma-Aldrich	199931
	5µg/ml Bovine Serum Albumin	Sigma-Aldrich	A7906-500g
FACS Buffer with DNase I	Dulbeccos Phosphate Buffered Saline	Gibco	14190-094
	5mM Ultrapure EDTA	Invitrogen	15575-038
	1% Sodium Azide	Sigma-Aldrich	199931
	5µg/ml Bovine Serum Albumin	Sigma-Aldrich	A7906-500g
	20µg/ml Deoxyribonuclease I from bovine pancreas	Sigma-Aldrich	DN25-100MG
FACS Buffer with DNase II	Dulbeccos Phosphate Buffered Saline	Gibco	14190-094
	5mM Ultrapure EDTA	Invitrogen	15575-038
	1% Sodium Azide	Sigma-Aldrich	199931
	5µg/ml Bovine Serum Albumin	Sigma-Aldrich	A7906-500g
	10Ug/ml Deoxyribonuclease II from bovine spleen	Sigma-Aldrich	D8764-30KU
AutoMACS Buffer	Dulbeccos Phosphate Buffered Saline	Gibco	14190-094
	5mM Ultrapure EDTA	Invitrogen	15575-038
	5µg/ml Bovine Serum Albumin	Sigma-Aldrich	A7906-500g
Complete RPMI	RPMI Medium 1640	Gibco	31870-025
	10% Heat Inactivated Fetal Bovine Serum	Gibco	10500064
	200mM L-glutamine	Gibco	25030-024
	1X Penicillin/Streptomycin	Gibco	15140-122
Complete HBSS	Hanks Buffered Saline Solution	Gibco	14170-088
	10% Heat Inactivated Fetal Bovine Serum	Gibco	10500064
	200mM L-glutamine	Gibco	25030-024
	1X Penicillin/Streptomycin	Gibco	15140-122
T Cell Media (TCM)	RPMI Medium 1640	Gibco	31870-025
	10% Heat Inactivated Fetal Bovine Serum	Gibco	10500064
	200mM L-glutamine	Gibco	25030-024
	1X Penicillin/Streptomycin	Gibco	15140-122
	1X MEM Non-Essential Amino Acids	Gibco	11140-035
Collection Buffer	Hank's Balanced Saline Solution (1X)	Gibco	14170-088
	2% Heat Inactivated Fetal Bovine Serum	Gibco	10500064
EDTA Wash Buffer	Hank's Balanced Saline Solution (1X)	Gibco	14170-088
	2mM Ultrapure EDTA	Invitrogen	15575-038
Collagenase A Digestion Buffer	RPMI Medium 1640	Gibco	31870-025
	20% Heat Inactivated Fetal Bovine Serum	Gibco	10500064
	1mg/ml Collagenase A	Sigma-Aldrich	1.0104E+10
	0.5 mg/ml Dnase I from bovine pancreas	Sigma-Aldrich	DN25-100MG
Shake Buffer	RPMI Medium 1640	Gibco	31870-025
	10% Heat Inactivated Fetal Bovine Serum	Gibco	10500064
	20mM HEPES Buffer	Gibco	15630056
Mucus Removal Buffer	RPMI Medium 1640	Gibco	31870-025
	3% Heat Inactivated Fetal Bovine Serum	Gibco	10500064
	5mM Ultrapure EDTA	Invitrogen	15575-038
	1mM DTT	Sigma-Aldrich	1.0709E+10

Table 2.1 Media used throughout the project. A table containing the media formulations with the supplier and catalogue number for each material.

Buffer	Materials	Supplier	Catalogue Number
5X Colon Digestion Buffer	RPMI Medium 1640	Gibco	31870-025
	10% Heat Inactivated Fetal Bovine Serum	Gibco	10500064
	20mM HEPES Buffer	Gibco	15630056
	200mM L-glutamine	Gibco	25030-024
	1X Penicillin/Streptomycin	Gibco	15140-122
	0.5mg/ml Liberase TL	Sigma-Aldrich	5401020001
	2.5mg/ml Deoxyribonuclease I from bovine pancreas	Sigma-Aldrich	DN25-100MG
3% Media	RPMI Medium 1640	Gibco	31870-025
	3% Heat Inactivated Fetal Bovine Serum	Gibco	10500064
	20mM HEPES Buffer	Gibco	15630056
Strip Buffer	Hank's Balanced Saline Solution (1X)	Gibco	14170-088
	10% Heat Inactivated Fetal Bovine Serum	Gibco	10500064
	1M DTT	Sigma-Aldrich	1.0709E+10
	1mM Ultrapure EDTA	Invitrogen	15575-038
	200mM L-glutamine	Gibco	25030-024
	1X Penicillin/Streptomycin	Gibco	15140-122
BMDC Media	RPMI Medium 1640	Gibco	31870-025
	10% Heat Inactivated Fetal Bovine Serum	Gibco	10500064
	200mM L-glutamine	Gibco	25030-024
	1X Penicillin/Streptomycin	Gibco	15140-122
	20ng/ml Murine GM-CSF	Peprotech	315-03
Low IgG Media	RPMI Medium 1640	Gibco	31870-025
	1X Penicillin/Streptomycin	Gibco	15140-122
	200mM L-glutamine	Gibco	25030-024
	1X MEM Non-Essential Amino Acids	Gibco	11140-035
Hybridoma Media	Hybridoma Serum Free Media	Gibco	12045-076-1L
	200mM L-glutamine	Gibco	25030-024

Table 2.1 continued.

2.2.2 Antibody table

Target	Fluorophore/Label	Clone	Supplier	Catalogue number	Dilution (10^6 cells)
Bcl2	AF488	BCL110C4	Biolegend	633505	1:100
CD11c	BV421	M1/70	Biolegend	101251	1:100
CD11c	PerCP/Cy5.5	N418	Biolegend	117328	1:100
CD154	PE/Cy7	MR1	Biolegend	106512	1:100
CD25	BV711	PC61	Biolegend	102049	1:100
CD25	BV650	PC61	Biolegend	102038	1:100
CD4	PE/Cy7	GK1.5	Biolegend	100422	1:200
CD4	BV711	GK1.5	Biolegend	100447	1:200
CD4	PerCP/Cy5.5	GK1.5	Biolegend	100434	1:200
CD45	PerCP/Cy5.5	30-F11	Biolegend	103132	1:100
CD69	PE	H1.2F3	Biolegend	104508	1:100
CD69	PE/Cy7	H1.2F3	Biolegend	104511	1:100
CD80	APC	16-10A1	Biolegend	104714	1:100
CD8a	FITC	53-6.7	Biolegend	100706	1:100
CTLA-4	PE	UC10-4B9	Biolegend	106306	1:100
Foxp3	eV450	FJK-165	Invitrogen	48-5773-82	1:100
GATA3	PE/Cy7	L50-823	BD Biosciences	560405	Test size
Helios	APC	22F6	Biolegend	137222	Test size
Helios	APC/Cy7	22F6	Invitrogen	47-9882-42	Test size
Helios	APC	22F6	Miltenyi	103-104-002	Test size
ICOS	AF700	C398.4A	Biolegend	313527	1:100
ICOS (CD278)	PE/Cy7	C3984A	Biolegend	313520	1:100
IL7Rα	APC/Cy7	A7R234	Biolegend	135039	1:100
NK1.1	BV421	PK136	Biolegend	108741	1:100
Nrp-1	APC	3.00E+12	Biolegend	145206	Test size
PD-1	FITC	29F.1A12	Biolegend	135214	1:100
RORγt	PE	AFKJS-9	Invitrogen	12-6988-82	1:100
Sca-1	APC	D7	Biolegend	108111	1:100
TBet	FITC	4B10	Biolegend	644812	1:100
TotalSeq™-A0301 anti-mouse Hashtag 1 Antibody	Oligotag ACCCACCAGTAAGAC	M1/42, 30-F11	Biolegend	155801	1ug
TotalSeq™-A0302 anti-mouse Hashtag 2 Antibody	Oligotag GGTCGAGAGCATTCA	M1/42, 30-F11	Biolegend	155803	1ug

Table 2.2 Antibodies used throughout the project. A table containing the labelled antibodies used throughout the project with the target, label or fluorophore, clone, supplier, catalogue number and dilution used to stain $1*10^6$ cells.

Chapter 3 Single Cell RNA analysis of T cell responses to helminth infection

3.1 Introduction

Helminthiases can lead to morbidity which can severely affect the quality of life of the host in many dimensions (King, 2015). In addition to driving immunopathology, helminth infection may compromise nutrition, lead to lower vaccine responses and can even negatively impact fetal development when the mother is infected with a helminth (Friedman *et al.*, 2007; Mpairwe, Tweyongyere and Elliott, 2014; Hartmann *et al.*, 2019). Thus, although soil transmitted nematode infections are rarely fatal, these are important and complex diseases which require greater understanding. This is especially true in the context of control of helminth infection, where immunological interventions would be preferable to mass drug administration that may flounder in the long term due to anthelminthic resistance (Vercruysse et al., 2012).

3.1.1 Diverse immune responses to the same parasite

As discussed previously, there is a wide spectrum of infection intensity in helminth burden of patients with helminthiases (Bundy *et al.*, 1987; Wright *et al.*, 2018). In many helminth infections, a higher worm burden is associated with high co-morbidities and low burden is associated with asymptomatic infection (Girgis, Mahesh Gundra, & Loke, 2013; Hotez et al., 2010). However, it has also been shown, in a study of African children infected with soil-transmitted helminths, that higher worm burdens correlate with immune regulatory cytokine (IL-10 and TGFß) production, while lower intensity infections associate with IL-4 and T cell proliferative responses (J. D. Turner et al., 2008). Little further detail is known about the immune response of humans with a high worm burden and those who can control infection, particularly at the level of T cell populations. Identifying the critical differences in immune response between patients with a high versus a low worm burden may give insights into optimal mechanisms of immunity, and can allow stratification of patients prior to drug treatment, lowering the odds of anthelminthic resistance developing (Vercruysse et al., 2012).

Studying differential responses to the same parasite in murine models requires a system in which infection outcome is predictably determined by factors such as parasite dose (Bancroft, Else, & Grencis, 1994) or host genetic background (Zhong & Dobson, 1996). In the case of *H. polygyrus* infection, there is the opportunity to compare responses of mouse strains which are either fully susceptible to the worm (C57BL/6) or partially resistant (BALB/c) (Filbey *et al.*, 2014). This allows us to interrogate the differences between those with a high worm burden (modelled by C57BL/6 infection) and low worm burden (modelled by BALB/c infection). Previous work has highlighted a general trend with BALB/c mice predisposed to mounting a Type 2 response associated with parasitic worm clearance, and C57BL/6 mice predisposed to mount a Th1 response, producing higher concentrations of IFN-γ early in infection than BALB/c mice (Filbey *et al.*, 2014). This may indicate that BALB/c mice mount a "purer" type 2 response or develop a type 2 response faster than C57BL/6 mice in order to expel the worms.

Another key difference reported in earlier comparisons relates to Treg populations in the two strains of mice. It is known that while Th2 cells are the effectors required to clear the infection, these cells cannot function optimally when under the control of Treg cells (Belkaid, 2007). While both strains show an expansion in their Tregs during *H. polygyrus* infection, there is a greater increase in Tregs in C57BL/6 mice which may indicate a more profound suppression of the immune system (K A Smith et al., 2016). However, BALB/c mice have a higher baseline frequency of Tregs so the larger Treg expansion in C57BL/6 mice brings the overall number of Tregs to around the same level in both strains (Rick M. Maizels & Smith, 2011; K A Smith et al., 2016). With both strains reaching the same number of Tregs during infection, it is important to investigate the phenotype and genetic profile of Tregs in the two strains to discover the differences in the Treg response of both strains.

3.2 Single cell RNA sequencing

Single cell mRNA sequencing (scRNAseq) is a PCR-based method where the RNA transcriptome of single cells can be individually analysed to allow high resolution cell-by-cell analysis of an immune response (Haque, Engel, Teichmann, &

Lönnberg, 2017; See, Lum, Chen, & Ginhoux, 2018). In earlier years, PCR was developed to give the mRNA levels of a gene of interest within whole tissue or a sorted cell population, but analysed individual genes. Subsequently, bulk RNA sequencing was evolved in which mRNA of all cells from a sample are mixed and the cellular origin of each gene cannot assigned to any sub-population within the sample. In contrast, single cell RNA sequencing allows combinations of genes co-expressed by distinct cell subsets to be used to cluster populations of similar cells, identify novel populations and compare different groups of cells, leading to a transformation in our understanding of the dynamics of the immune response (Haque *et al.*, 2017).

The first step of any single cell RNA sequencing is isolation of cells into a single cell suspension with high viability (Haque *et al.*, 2017; See *et al.*, 2018). The protocol is designed to minimise the number of cells excluded during the quality control process and increase the proportion of cells which can be analysed later in the workflow. At this stage, cells can be pre-sorted by flow cytometric analysis or magnetic bead sorting to allow selection of cells of interest into the sequencing pipeline.

The second step of scRNAseq is to process the samples into single cell compartments to tag mRNA from each cell with an individual oligonucleotide barcode. One scRNAseq platform that is widely employed is 10X Chromium, a droplet-based method (Haque *et al.*, 2017; See *et al.*, 2018). For 10X single cell sequencing, cells are loaded into a well on a Chromium Chip with Master Mix containing the RT reagents and enzymes required for GEM (gel beads in emulsion) generation. Barcoded gel beads which capture the mRNA from lysed cells are added to another well of the chip and partitioning oil, which facilitates capture of droplets containing a single cell and barcoded bead. This chip is loaded into the 10X chromium which uses droplet-based encapsulation to produce GEMs. These GEMs are collected and placed in a thermal cycler and undergo RT-PCR to produce cDNA tagged with the barcode from the gel bead. Now that the RNA is tagged with its cell of origin via the gel bead barcode, the GEMs can be broken down and all RNA pooled into the same suspension. After cleaning up the sample, the cDNA primers are added, and cDNA amplification is performed in a thermocycler. After the cDNA library is amplified, it is loaded

into the Illumina for next generation sequencing. After the sequencing is complete, the cDNA sequences can be aligned to the reference genome of the source organism, allowing identification of different genes.

3.2.1 Cell Hashing

One major concern in single cell RNA sequencing is batch effects which arise when cells from different experimental groups are processed and sequenced separately (Hicks, Townes, Teng, & Irizarry, 2018; Stoeckius et al., 2018). This can generate variability between the samples which is not biologically relevant and can mask true biological differences (Hicks *et al.*, 2018; Stoeckius *et al.*, 2018). Batch effects are especially detrimental to single cell RNA sequencing data as most analyses rely on dimensionality reduction to cluster cells into populations of highly related cells based on their gene expression (Hicks *et al.*, 2018). To overcome these effects, a multiplexing method known as cell hashing has been developed, which utilises antibodies against ubiquitously and highly expressed markers tagged with an oligotag of known sequence (Stoeckius *et al.*, 2018). Cells from different experimental groups are first incubated with antibodies of the same specificity but tagged with different oligotag sequences, and then pooled into a single sample or batch (Stoeckius *et al.*, 2018). This single batch can then be loaded into the single cell RNA sequencing pipeline of your choice and a hashtag oligonucleotide (HTO) library can be built using HTO specific primers for amplification (Stoeckius *et al.*, 2018). After sequencing is complete, the HTO library can be used to assign each cell to the original experimental group using the known hashtag sequence before standard analysis occurs (Stoeckius *et al.*, 2018). This method has been used successfully by many different laboratories and in many different models (Cheng, Liao, Shao, Lu, & Fan, 2021; McFarland et al., 2020; Stuart et al., 2019).

3.2.2 Demuxlet

Another option for multiplexing samples is Demuxlet which does not require the use of any specialist reagents (Kang *et al.*, 2018). However, Demuxlet is best used on different strains of mice with distinct genetics as Demuxlet relies on single nucleotide polymorphisms (SNPs) within the RNA sequencing to identify the animal of origin (Kang *et al.*, 2018). By giving the method reference genomes

of the different mice used, the SNPs can be compared to both genomes and the closest match is assigned as the cell ID (Kang *et al.*, 2018). This method can allow multiplexing of up to 20 samples from genetically distinct backgrounds (Kang *et al.*, 2018).

3.3 Aims

- To characterise the T cell response to *H. polygyrus* infection
- To discover differences in the T cell response of partially resistant BALB/c and fully susceptible C57BL/6 mice
- To discover genes associated with increased clearance of the worm

3.4 Results

3.4.1 Experimental design of single cell RNA sequencing

In order to evaluate the T cell response to early *H. polygyrus* infection, fully susceptible C57BL/6 and partially resistant BALB/c mice were infected with 200 L3 *H. polygyrus* larvae by oral gavage; 7 days post-infection, mice were sacrificed, and their mesenteric lymph nodes collected (Figure 3.1). The day 7 post-infection time point was chosen due to the early expansion of Th2 and initial peak of Treg cells at this time point in both BALB/c and C57BL/6 mice as shown in Chapter 4 (Figure 4.1). Their lymph nodes were made into a single cell suspension as described in the methods chapter before being sorted on the AutoMACS for either CD3+ T cells (3.4.2-3.4.7) or CD4+ T cells (3.4.8-3.4.20) (Figure 3.1). Cells were then stained with cell hashtagging antibodies by incubating 1 million cells with 1µg of antibody in FACS buffer for 30 minutes at 4°C. After washing, the naïve C57BL/6 and naïve BALB/c samples were combined and the *H. polygyrus* infected BALB/c and *H. polygyrus* infected C57BL/6 were combined (Figure 3.1). 7,000 cells from these two samples were then loaded onto the chip for the 10X Chromium and GEM generation completed, halving the batch effect (Figure 3.1). GEMs generated by the 10X Chromium were then amplified into cDNA and the cDNA library sequenced by the Illumina (Figure 3.1). After sequencing is complete, the data can be analysed.

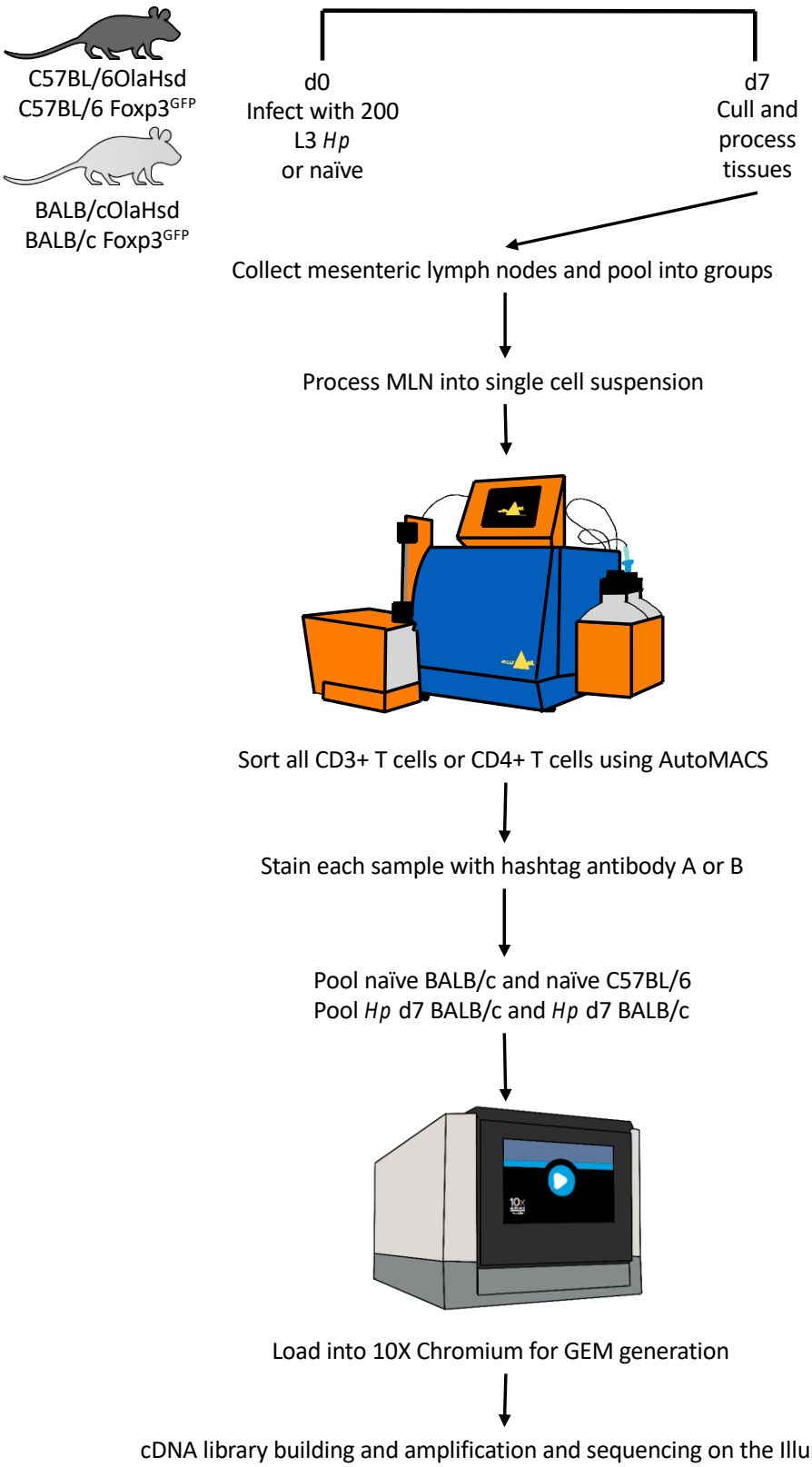

Figure 3.1 Experimental workflow for single cell RNA sequencing. The experimental protocol showing the infection protocol, sample handling, sorting of the MLN cells, hashtag labelling and 10X Chromium run. C57BL/6OlaHsd and BALB/cOlaHsd mice were used for first run of all CD3+ T cells. C57BL/6 Foxp3GFP and BALB/c Foxp3GFP mice were used in the second run of all CD4+ T cells.

3.4.2 Viability and purity of CD3+ T cells sorted for single cell RNA sequencing

After preparing the cells for single cell RNA sequencing, the remaining cells not required for sequencing were stained for flow cytometric analysis to measure viability and expression of CD3, CD4 and CD8. Figure 3.2A shows the high viability (around 91-98%) of all sorted CD3+ T cells from naïve and *H. polygyrus* infected C57BL/6OlaHsd and BALB/cOlaHsd mice. The purity of the sorted population was also high with almost all cells (>98%) expressing CD3 (Figure 3.2B). Since CD3+ T cells contain both CD8+ T cells and CD4+ T cells, the distribution of each of these cell types was assessed. The proportion of CD3+ T cells expressing CD8 decreased by around 10-20% upon infection and the proportion expressing CD4 increased by 10-20% (Figure 3.2C-D). When comparing the proportions of CD4:CD8 T cells, the majority of CD3+ T cells are expressing either CD4 or CD8 (Figure 3.2E). There is a small population of CD3+ CD4- CD8- cells in naïve and infected C57BL/6OlaHsd mice and infected BALB/cOlaHsd mice (Figure 3.2E). There is a higher proportion (21%) of these double negative T cells in naïve BALB/c OlaHsd mice however, the identity of these cells is unknown (Figure 3.2E). Taken together, these data show that the cells analysed by single cell sequencing had a very high viability and included a very high proportion of CD3+ T cells.

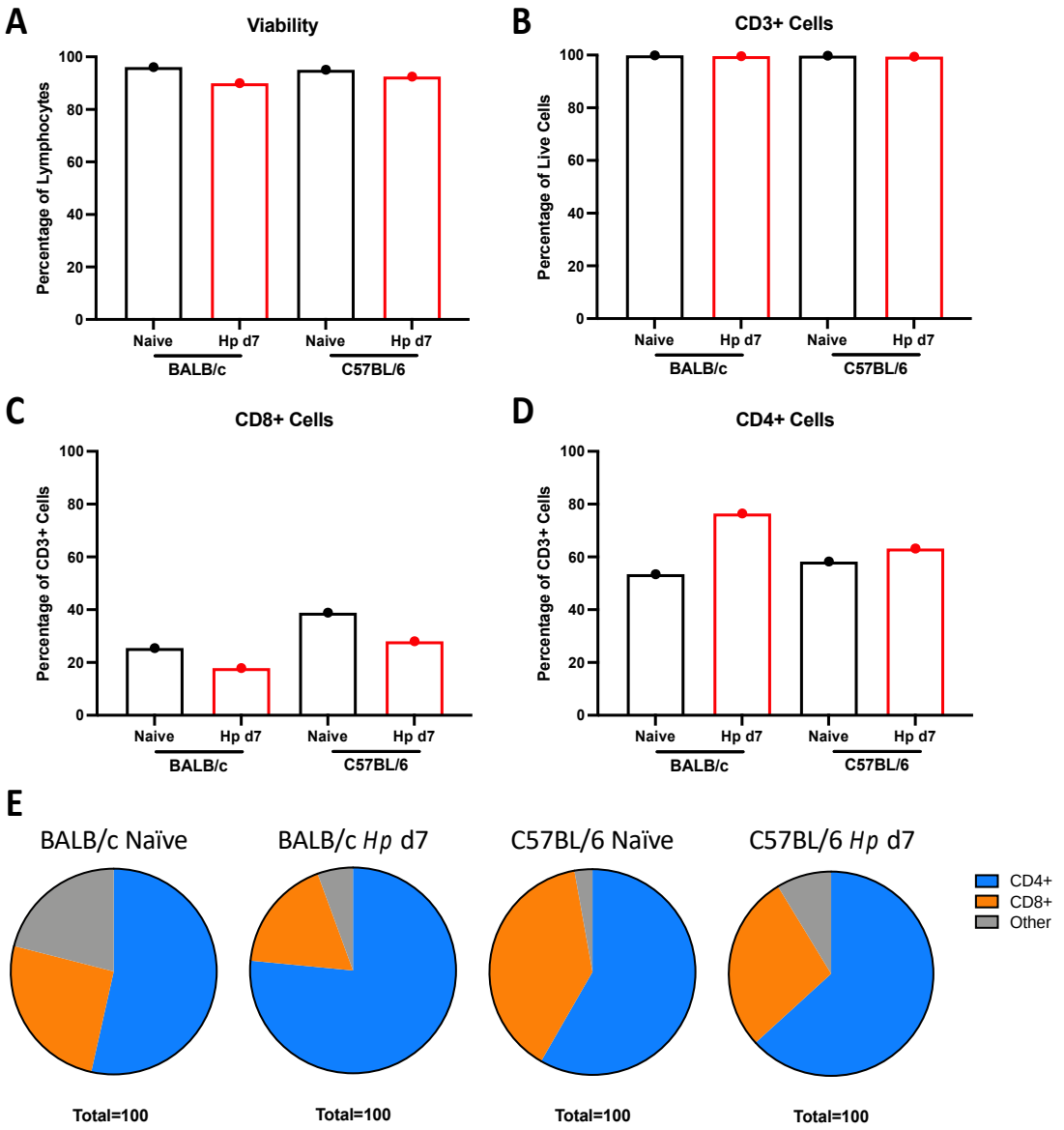

Figure 3.2 Purity and viability of sorted cells for single cell RNA sequencing. (A) The viability of sorted CD3+ T cells from Naïve and *Hp* d7 infected C57BL/6OldHsd and BALB/cOlaHsd mice. (B) The percentage of live cells expressing CD3 in pre-sorted MLN cells from Naïve and *Hp* d7 infected C57BL/6OldHsd and BALB/cOlaHsd mice. (C) The percentage of CD3+ T cells expressing CD8 in pre-sorted cells from Naïve and *Hp* d7 infected C57BL/6OldHsd and BALB/cOlaHsd mice. (D) The percentage of CD3+ T cells expressing CD4 in pre-sorted cells from Naïve and *Hp* d7 infected C57BL/6OldHsd and BALB/cOlaHsd mice. (E) Pie charts showing the proportion of CD4+ (blue), CD8+ (orange) and CD4-CD8- (grey) in pre-sorted MLN cells from Naïve and *Hp* d7 infected C57BL/6OldHsd and BALB/cOlaHsd mice.

Closed circles represent 3 pooled mice. Pie charts represent 3 mice.

3.4.3 Clustering of CD3+ T cells from naïve and *H. polygyrus* d7 infected mice

The initial experiment was designed to identify the genotype of each cell by amplification of the hashtag oligonucleotide corresponding to the anti-CD45 antibody added to the separate samples. Amplification was performed as part of the pipeline by Glasgow Polyomics, but for unknown reasons the amplification was unsuccessful. However, an alternative option remained open, using Demuxlet to separate BALB/cOlaHsd and C57BL/6OlaHsd cells on the basis of strain-specific SNPs (data not shown). This was successfully achieved by the author of this thesis.

After separating the strains, the Seurat program was used to perform clustering which compares the transcriptome of each cell, and then clusters cell subsets which have similar gene expression. Figure 3.3A shows a UMAP plot showing the clusters generated in this manner. Identities were assigned to each cluster using their expression of marker genes such as *Cd3e, Cd4, Cd8* and transcription factors associated with Th cell subtypes (Figure 3.3C-H). For clusters with no obvious identity, identities were assigned by their expression of *Cd4* or *Cd8* and the first relevant gene in their cluster marker, for example, *Ikaros+Cd8+* (Figure 3.3A, data not shown).

The proportion of the total cells belonging to each cluster is shown in Figure 3.3B. Interestingly, there are two separate clusters with a naïve T cell-like profile expressing high levels of *Cd3e, Cd4, Sell, Lef1* and *Tcf7* but differing in their expression of strain-specific genes like *H2,* but also in their *Smc6, Crip1* and *Pdk1* expression; these have been labelled as Naïve(a) and Naïve(b) (Figure 3.3A+C-D). The Naïve(a) population is predominant in both strains, but particularly so in BALB/c mice while Naïve(b) more frequent with C57BL/6 mice (Figure 3.3B) which may suggest that naïve CD4+ T cells from BALB/c and C57BL/6 mice are different even at homeostasis. In addition, while the Naïve(a) population shrinks following infection, the Naïve(b) remains similar in proportion, or even increases as in the C57BL/6 strain.

Two Treg populations (Treg(a) and Treg(b), Figure 3.3A) were identified based on their expression of Foxp3 in addition to *Cd3e* and *Cd4* (Figure 3.3A, C-D+G). In

keeping with our knowledge of Tregs during *H. polygyrus* infection, there is an expansion of the proportion of both clusters in infected mice of either strain. Some cells in each cluster also expressed *Gata3*, but few if any were *Rorc*+ (Figure 3.3 F and H). Notably, there is very little expression of *Il10* in the Treg population (Figure 3.3J). There are also some cells expressing *Foxp3* found in the non-Treg clusters, meaning these *Foxp3* expressing cells are more transcriptomically similar to the other T helper cells than the cells within the Treg clusters. These *Foxp3*+ cells which do not cluster together may represent different Treg subtypes and further analysis is required to describe these cells, for example by using an *in silico* gating strategy to isolate all *Foxp3*+ cells.

The Th2 population in cluster 4 was identified by its expression of both *Gata3* and *Il4* in addition to *Cd3e* and *Cd4,* (Figure 3.3A, C-D,F+I). As with Tregs, there is an expansion of the Th2 subset in both BALB/c and C57BL/6 mice infected with *H. polygyrus* (Figure 3.3B).

Overall, it is also clear from the proportions of the Treg and Th2 clusters that BALB/c and C57BL/6 mice have a differential T cell response to *H. polygyrus* infection, which may explain their difference in worm clearance (Figure 3.3B). Therefore, as described below, the Th2 and Treg populations were further explored.

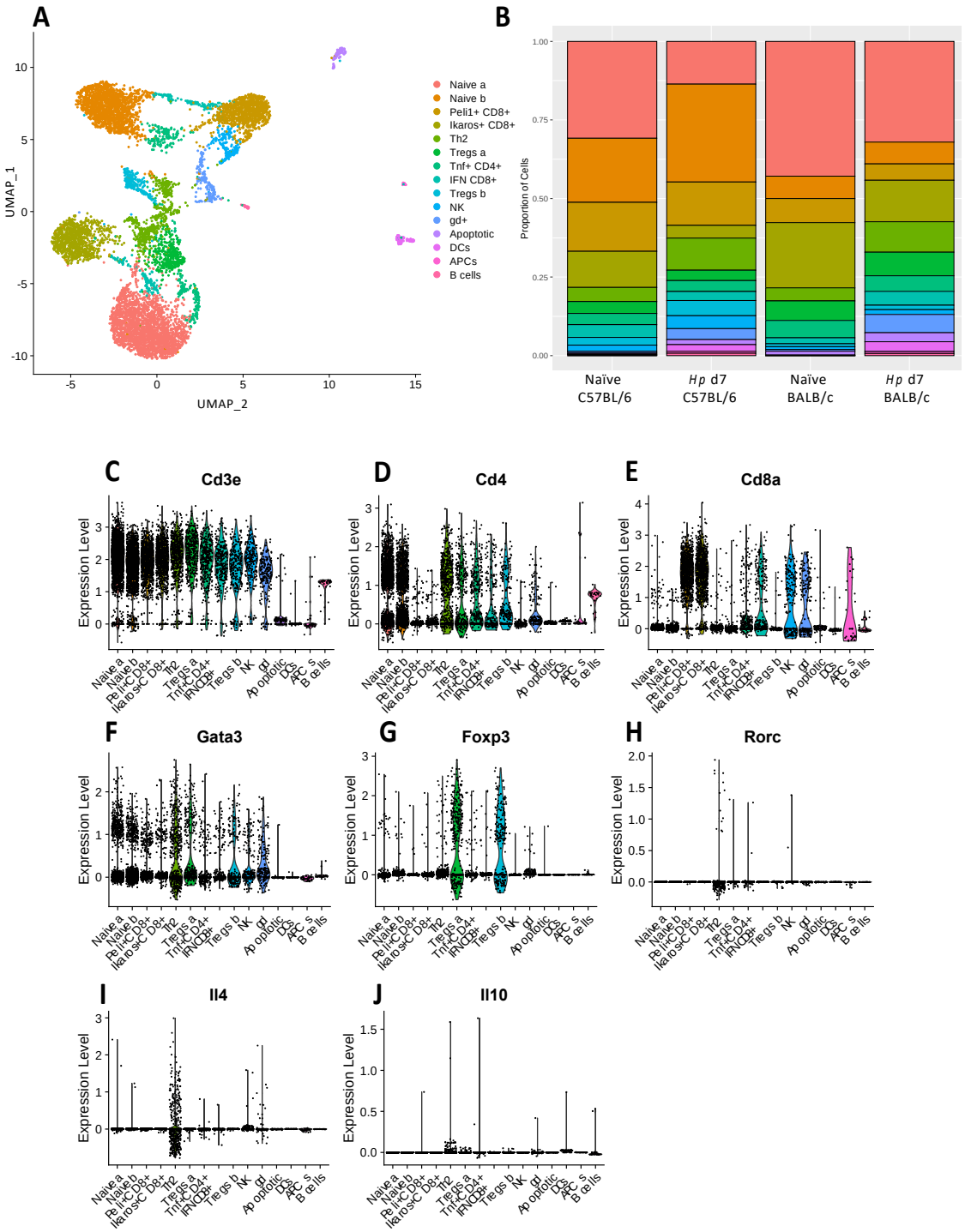

Figure 3.3 Custering of CD3+ T cells from naïve and H. polygyrus infected mice. (A) UMAP showing the clusters of CD3+ T cells as defined by Seurat, labels show cluster identified by their gene expression. (B) A stacked bar graph showing the proportions of each CD3+ T cell cluster in the MLN of Naïve and *H. polygyrus* infected BALB/cOlaHsd and C57BL/6OlsHsd mice. (C-K) Violin plots showing each clusters expression level of (C) *Cd3e* (D) *Cd4* (E) *Cd8a* (F) *Gata3* (G) *Foxp3* (H) *Rorc* (I) *Il4* and (J) *Il10*.

3.4.4 Clustering of Th2 cells from naïve and *H. polygyrus* infected mice

To analyse the Th2 population in more depth, sequence data from cells in the Th2 cluster from Figure 3.3 were selected and re-clustered to identify any clear subtypes of Th2 cells within this population; from this, five subsets were found within the Th2 cell cluster (Figure 3.4A). These clusters were named by their top expressed gene that is known to be important to Th2 cells which gave *Klf2*+, *Maf*+, *Tnfsf8*+, *Icos*+ and *Id2*+ Th2 clusters (Figure 3.4A). In naïve C57BL/6 and BALB/c mice, while the Klf1+ subset represents 40-50% of Th2 cells in both strains, the proportions of the other Th2 clusters are strikingly different, with a major subtype of Maf+ cells in C57BL/6 and Id2+ in BALB/c (Figure 3.4B).

Following infection, however, the dynamics of subset expansion and contraction is very similar in both strains of mice; the *Icos*+ and *Tnfsf8*+ Th2 clusters both expand in response to *H. polygyrus* infection, while the other 3 contract (Figure 3.4B).

Figure 3.4C shows the top 10 genes expressed by each cluster in heatmap form representing gene expression across all 5 Th2 subsets. These data were used to assign cluster names by their top relevant gene (Figure 3.4A-C). Inspection of the heatmap shows that while clusters do overlap in expression of many gene expression, they also have numerous distinct features, suggesting that they may be performing different roles during infection (Figure 3.4C). These clusters were then further scrutinised as described below.

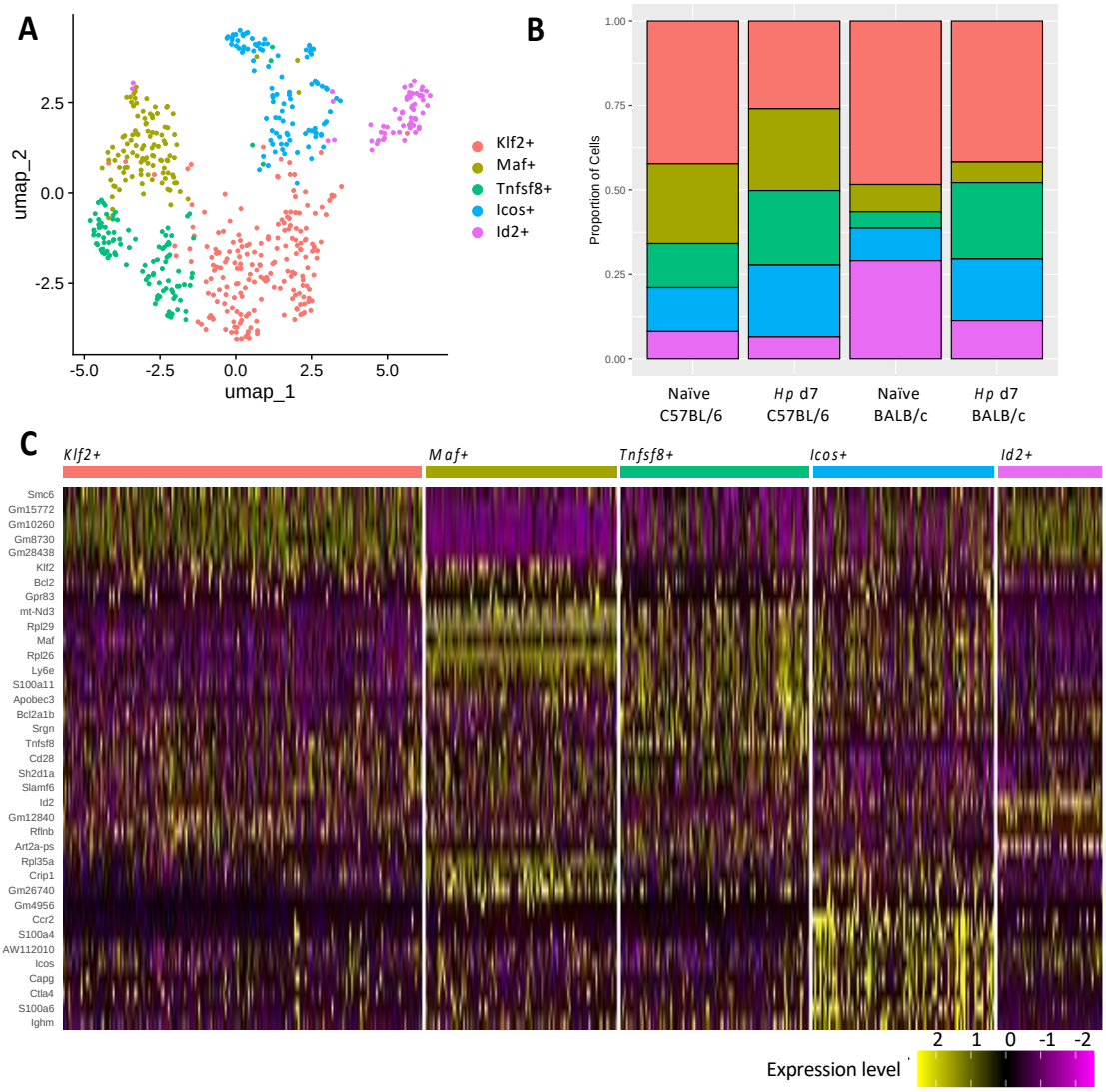

Figure 3.4 Clustering of Th2 cells from naïve and H. polygyrus infected mice. (A) UMAP showing the clusters of cells from the Th2 cluster as defined by Seurat (Figure 3.2), labels show cluster identified by their gene expression. (B) A stacked bar graph showing the proportions of each Th2 cell cluster in the MLN of Naïve and *H. polygyrus* infected BALB/cOlaHsd and C57BL/6OlsHsd mice. (C) A heatmap showing the top 10 expressed genes for each cluster of Th2 cells.

3.4.5 Pathway analysis of Th2 cells from naïve and *H. polygyrus* infected mice

Single cell RNA sequencing yields long lists of thousands of genes which can be overwhelming to analyse. With so many genes to assess, important data can readily be obscured, and it is difficult to evaluate the biological impact of changes in the expression level of individual genes on the pathways in which they are involved (Griss *et al.*, 2020). To resolve this problem, pathway analysis has been introduced, to compare gene expression datasets to known biological pathways, to identify upregulation or downregulation of a group of genes with an associated biological impact.

ReactomeGSA was used to run pathway analysis on the Th2 clusters from 1.3.4 (Griss *et al.*, 2020). ReactomeGSA utilises Seurat to calculate the mean expression of each gene in each cluster then uses gene set enrichment analysis to compare the average gene expression within known biological pathways in different groups of cells with the average expression of the whole experiment (Griss *et al.*, 2020).

3.4.5.1 Pathway analysis of Th2 sub-clusters

Figure 3.5A shows the expression of different biological pathways in the five identified Th2 clusters, with the first parameter being strength of TCR signalling pathway gene expression. The *Icos*+ Th2 cells show the highest levels of both TCR signalling and expand significantly following infection, demonstrating that this subset has been fully activated; however, these cells have high IL-10 signalling which may suggest that they may also be subject to some regulatory suppression (Figure 3.5A).

The small *Id2*+ Th2 cluster also has high levels of TCR signalling and CD28 co-stimulation to suggest these cells are activated, but also show high IL-12 signalling which has been linked to increased proliferation of CD4+ T cells and differentiation into Th1 cells, leading to IFNγ production (Athie-Morales, Smits, Cantrell, & Hilkens, 2004; Culpepper et al., 1995; Yoo, Cho, Lee, & Sung, 2002). *Id2* expression is also implicated in the balance of Th1 and Th2 cells where loss of Id2 leads to an expansion of Th2 cells and reduced expression of IFNγ and IL-

12 (Kusunoki *et al.*, 2003). This may imply that these cells are not an active part of the Th2 response (Figure 3.5A).

A third subset are the *Klf2*+ Th2 cells, which despite having received some degree of TCR signalling, appear to be suppressed by IL-10 signalling and may represent less functional Th2 cells (Figure 3.5A). Another profile is seen in the *Maf*+ cluster, in which TCR signalling or co-stimulation pathways are not activated, and in contrast display higher levels of Treg-associated genes and evidence of receiving IL-33 signalling (Figure 3.5A).

The final cluster is composed of *Tnfsf8*+ Th2 cells, which again do not have high levels of TCR signalling and CD28 signalling which may suggest that they have not been activated through their TCR. However, as their proportions increase following infection, it may be that their activation did not occur recently (Figure 3.5A). Indeed, these Th2 cells are producing chemokines via STAT6 and have undergone IL-33 and IL-10 signalling, suggesting that they are muted or suppressed in a manner that ablates TCR pathway gene expression (Figure 3.5A).

Taken together, these data suggest that the five Th2 clusters represent different activation states or functions which may have resulted from varying levels of regulatory signals such as IL-10 mediated suppression.

3.4.5.2 Pathway analysis of naïve and H. polygyrus infected BALB/c and C57BL/6 mice

To assess the difference in the Th2 response in BALB/c and C57BL/6 mice, pathway analysis was repeated on the Th2 clusters grouped by the infection status of the mouse and its strain. Comparing naïve animals, there were clear differences between the C57BL/6 and BALB/c mice, with steady-state TCR stimulation higher in BALB/c mice while the co-stimulation pathway was stronger in C57BL/6 mice (Figure 3.5B). This suggests that Th2 cells from naïve mice are receiving tonic TCR stimulation and activation, as the animals are maintained in an SPF environment.

There are also striking differences between BALB/c and C57BL/6 Th2 cells following *H. polygyrus* infection that indicate a dichotomy in responsiveness

between the two strains (Figure 3.5B). C57BL/6 mice have very low expression of the signalling pathways associated with TCR stimulation which suggests that these cells are very poorly stimulated (Figure 3.5B). On the other hand, BALB/c Th2 cells from *H. polygyrus* infected mice have high levels of TCR signalling, consistent with a high level of activation (Figure 3.5B). This is in keeping with the differential susceptibility of the two strains when infected with *H. polygyrus* as the BALB/c Th2 response is faster and stronger, leading to more rapid clearance of the worm (Filbey *et al.*, 2014). One factor that may contribute to the different Th2 responses is the increased IL-10 signalling in Th2 cells from C57BL/6 mice compared to BALB/c mice (Figure 3.5B). IL-33 signalling is reduced in both strains of mouse when infected with *H. polygyrus*, which is in keeping with the activity of *Hp*-ARI that tethers IL-33 to the DNA of apoptotic cells, preventing alarmin release and IL-33 signalling through its receptor (Henry J. McSorley et al., 2012; Osbourn et al., 2017).

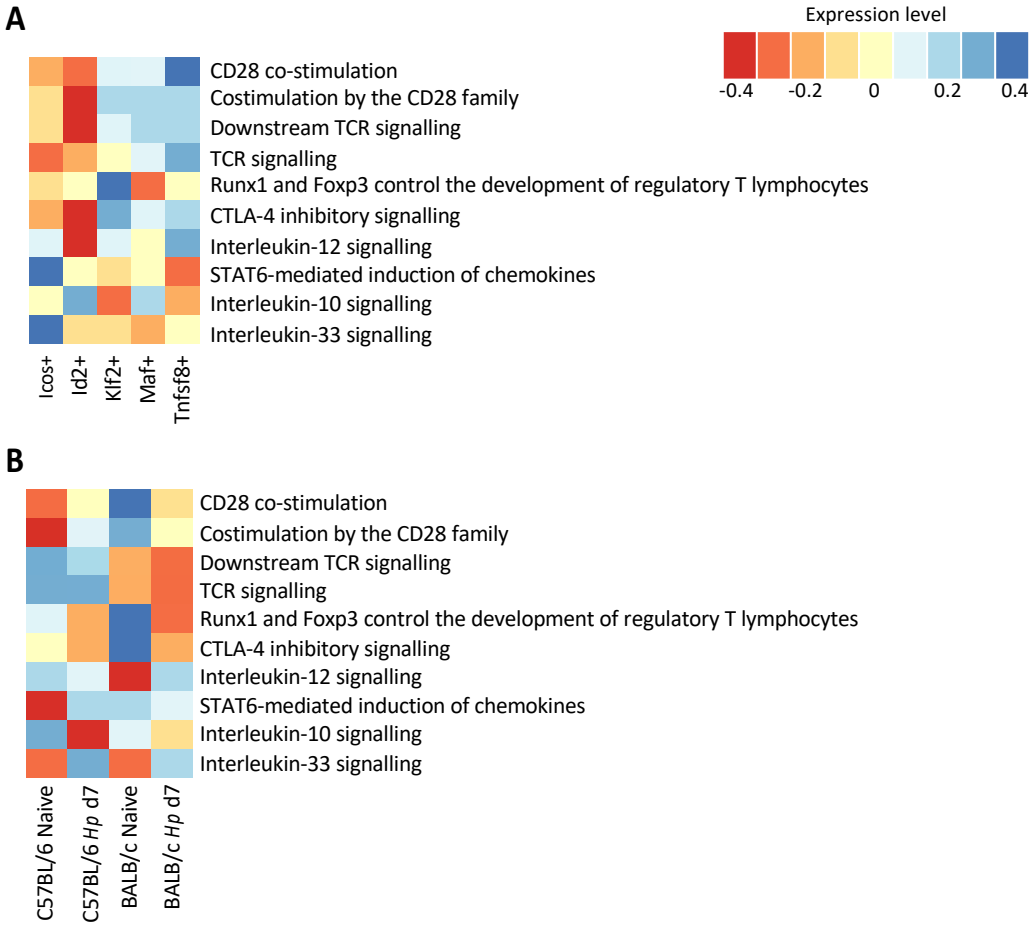

Figure 3.5 Pathway analysis of Th2 cells from naïve and H. polygyrus infected mice. (A) A heat map showing the expression of genes within the pathways on the right in the different clusters of Th2 cells as shown in Figure 3.4. (B) A heat map showing the expression of genes within the pathways on the right in Th2 cells from the MLN of naïve and *H. polygyrus* infected BALB/cOlaHsd and C57BL/6OldHsd mice.
Pathway analysis performed by ReactomeGSA. Heat maps generated using ReactomeGSA.

3.4.6 Clustering of Tregs from naïve and *H. polygyrus* infected mice

The two Treg populations from the CD3+ T cell clustering (3.3.2) were pooled and re-clustered to assess the Treg subtypes found during *H. polygyrus* infection. When these cells were clustered, five populations of Tregs were identified as shown in the UMAP (Figure 3.6A). The 5 clusters were named by the top gene in their cluster that are known to be expressed by Tregs, these were *Bcl2, Cd28, Icos, Ly6e* and *Maf*, two of which had also been highest expressed in Th2 cell clusters.

As seen in Figure 3.6B, naïve C57BL/6 and BALB/c mice have different proportions of these Tregs even at homeostasis, particularly with respect to the Ly6e subset that is more predominant in C57BL/6, and the Bcl2 cluster that is >50% of BALB/c Tregs. Following infection with *H. polygyrus*, there is an expansion of *Maf*+ and *Icos*+ Tregs in both strains, while C57BL/6 mice also expand *Ly6e*+ *and* BALB/c mice expand the, *Cd28*+ Treg cluster (Figure 3.6B). In both strains, it is the *Bcl2* cluster that diminishes in proportion following infection. Bcl-2 is an anti-apoptotic protein which has been shown to be a marker of lymphoid resident Tregs and may represent the proportional loss of lymphoid Tregs as the infection-induced Tregs rapidly expand (Gabriel *et al.*, 2016; Miragaia *et al.*, 2019).

As discussed previously, CD28 which is encoded by *Cd28* is the major co-stimulatory receptor and is required for Teffector suppression by Tregs and maintenance of homeostasis of pTregs (Tang et al., 2003; R. Zhang et al., 2013). When CD28 is knocked out specifically in Treg cells, there is increased Teffector responses despite the proportion of Tregs remaining consistent with wild type counterparts, showing that CD28 signalling is required for Treg suppression (R. Zhang et al., 2013). One interpretation of the preferential expansion of this cluster in *H. polygyrus* infected BALB/c mice is that their Tregs are more active than those from *H. polygyrus* infected C57BL/6 Tregs (Figure 3.6B) (Esensten et al., 2016; Sharpe & Freeman, 2002). However, it has also been reported that strong CD28-mediated costimulation may inhibit Treg function or stability, (Benson, Pino-Lagos, Rosemblatt, & Noelle, 2007; Mikami et al., 2020; Semple et

al., 2011) in which case these data may reflect weaker Treg activity in the BALB/c setting.

Icos or ICOS (Inducible T cell Co-Stimulator) is a co-stimulatory receptor that is upregulated by TCR stimulation and is upregulated on certain subsets such as Tfh cells and Tregs (D. Y. Li & Xiong, 2020; Wikenheiser & Stumhofer, 2016). Although relatively few in number, the *Icos*+ cluster shows the greatest proportional expansion in both C57BL/6 and BALB/c mice (Figure 3.6B). Notably, upregulation of ICOS on Tregs during *H. polygyrus* infection has been reported, and in the absence of ICOS signalling, Tregs are fewer in number and cannot suppress the Th2 response (Redpath *et al.*, 2013).

A particularly conspicuous difference between the strains is seen in the proportions of *Ly6e*+ (Sca-2) Tregs. This is a major subset in C57BL/6 naïve mice, and is further upregulated upon *H. polygyrus* infection (Figure 3.6B), while making up only a small proportion of the BALB/c complement (Figure 3.6B). However, it is important to note that the strains express different alleles of Ly6, BALB/c mice encoding Ly6.1 and C57BL/6 mice Ly6.2 variant. Because the genome alignment was performed using a C57BL/6 genome, the software may underestimate expression in BALB/c cells (Gumly, Mckenzie, & Sandrin, 1995; Lee, Wang, Parisini, Dascher, & Nigrovic, 2013; Rock, Reiser, Bamezai, Mcgrew, & Benacerraf, 1989). There is also known to be higher expression of Ly6 antigens in C57BL/6 mice at homeostasis than in BALB/c mice, which is upregulated upon activation with the mitogen Concanavalin A (ConA) (van de Run, Heimfeld, Spangrude, & Weissman, 1989).

Maf or c-Maf is a transcription factor which is required for RORγt expression in Tregs and c-Maf+ Tregs express higher levels of IL-10 than c-Maf- counterparts (Imbratta, Hussein, Andris, & Verdeil, 2020; Neumann et al., 2019; Wheaton, Yeh, & Ciofani, 2017). While C57BL/6 mice have a higher frequency of Maf+ Tregs, the proportion of this cluster does not change following infection of either strain.

Taken together, the data on these 5 clusters show that the Treg profile is dependent on the genetic background of the host, and that the clusters in

BALB/c and C57BL/6 mice differentially expand when infected with *H. polygyrus*. Analysis of the heatmaps showing the top 10 genes expressed by each cluster, reveals that while each cluster can share gene expression with other clusters, there are also cluster-specific genes, suggesting that each cluster may mediate distinct functions within infection (Figure 3.6C).

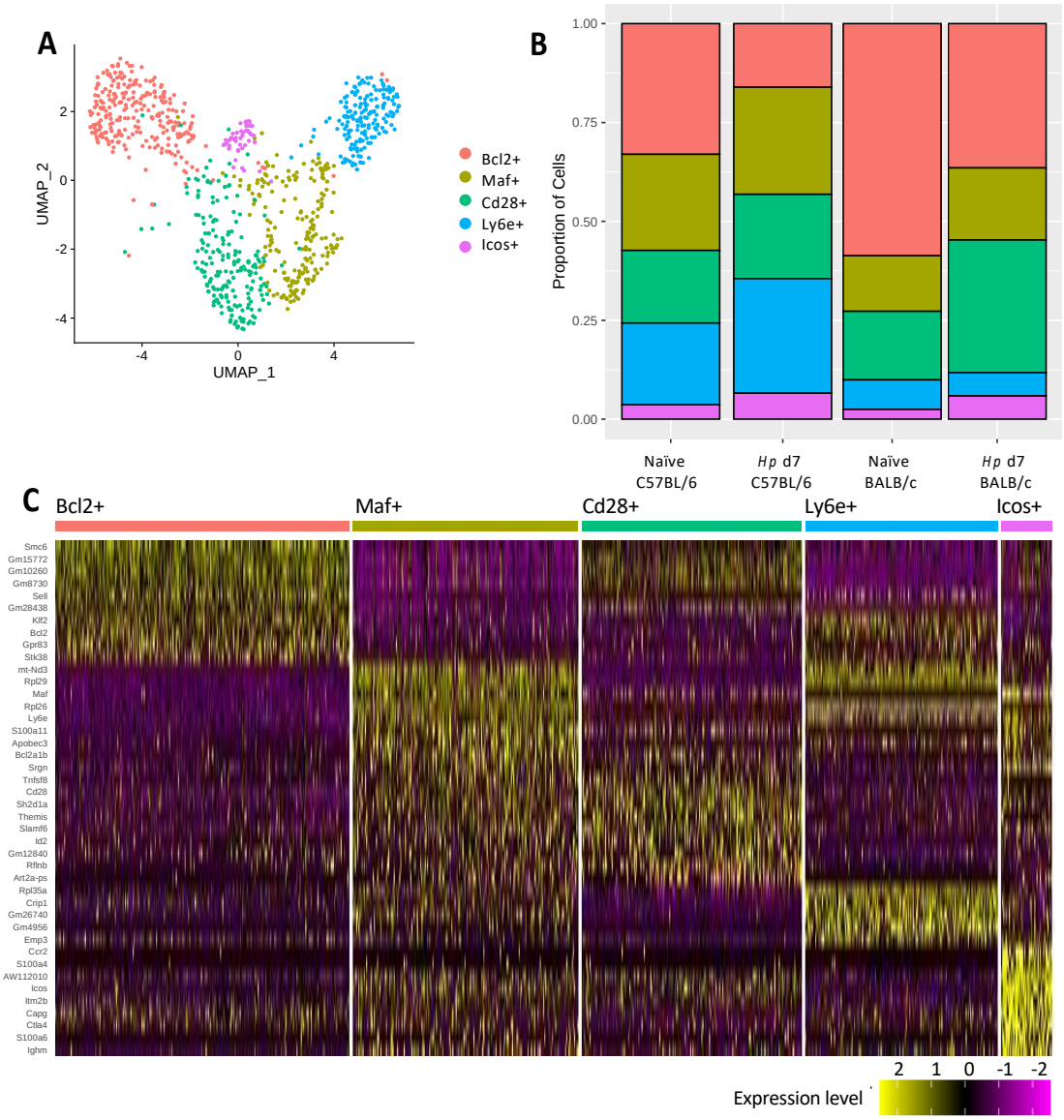

Figure 3.6 Clustering of Tregs from naïve and H. polygyrus infected mice. (A) UMAP showing the clusters of cells from the Treg cluster as defined by Seurat (Figure 3.2), labels show cluster identified by their gene expression. (B) A stacked bar graph showing the proportions of each Treg cluster in the MLN of Naïve and *H. polygyrus* infected BALB/cOlaHsd and C57BL/6OlsHsd mice. (C) A heatmap showing the top 10 expressed genes for each cluster of Tregs.

3.4.7 Pathway analysis of Tregs from naïve and *H. polygyrus* infected mice

As discussed above in 3.3.5, pathway analysis can aid in elucidating the differences between clusters of cells and can be useful in identifying potential functions of different clusters. The 5 Treg clusters were input into ReactomeGSA to undergo pathway analysis (Griss *et al.*, 2020). Figure 3.7A shows the expression level of different immune response pathways within each cluster.

The *Bcl2*+ Tregs have a high level of responsiveness to IL-10 signalling and their gene expression is consistent with having received signal 1 and signal 2 from an APC (Figure 3.7A). *Cd28*+ Tregs are relatively inactive in terms of TCR engagement and co-stimulation but have undergone some IL-33 and IL-12 signalling (Figure 3.7A).

The *Icos*+ cluster, which expands most in relative terms, has received TCR signalling, CD28-mediated co-stimulation and CTLA-4 mediated co-inhibition, suggesting that these are newly-stimulated and antigen-activated Tregs (Figure 3.7A). The *Ly6e*+ Treg population are similarly active with evidence of IL-10 signalling (Figure 3.7A). Finally, *Maf*+ Tregs showed few signs of Signal 1 or Signal 2 delivery, but had been cytokine-stimulated in particular with IL-33 signalling, that has been associated with increased activation, stability and migratory potential of Tregs (Alvarez, Fritz, & Piccirillo, 2019; Pastille et al., 2017).

Pathway analysis was also performed on Tregs subdivided by the strain of mouse and their infection status. In C57BL/6 mice, while naïve Tregs show multiple activated pathways, their *H. polygyrus* infected counterparts show extraordinarily little TCR signalling or co-stimulation from APCs (Figure 3.7B). This profile suggests that Treg activation and function may follow unexpected kinetics, or even not be responsible for the suppression of Th2 cells during *H. polygyrus* infection. In contrast, BALB/c naïve Tregs have generally low-level expression of genes associated with TCR stimulation and Signal 2 co-stimulation suggesting that these cells are not highly activated (Figure 3.7B). Upon infection with *H. polygyrus*, BALB/c Tregs upregulate TCR stimulation pathways, as well as show higher CTLA-4 signalling (Figure 3.7B), which will be returned to in Chapter

4. Hence, in the BALB/c mouse, *H. polygyrus*-induced Tregs are clearly activated through TCRs, indicating that they recognise antigens introduced by infection.

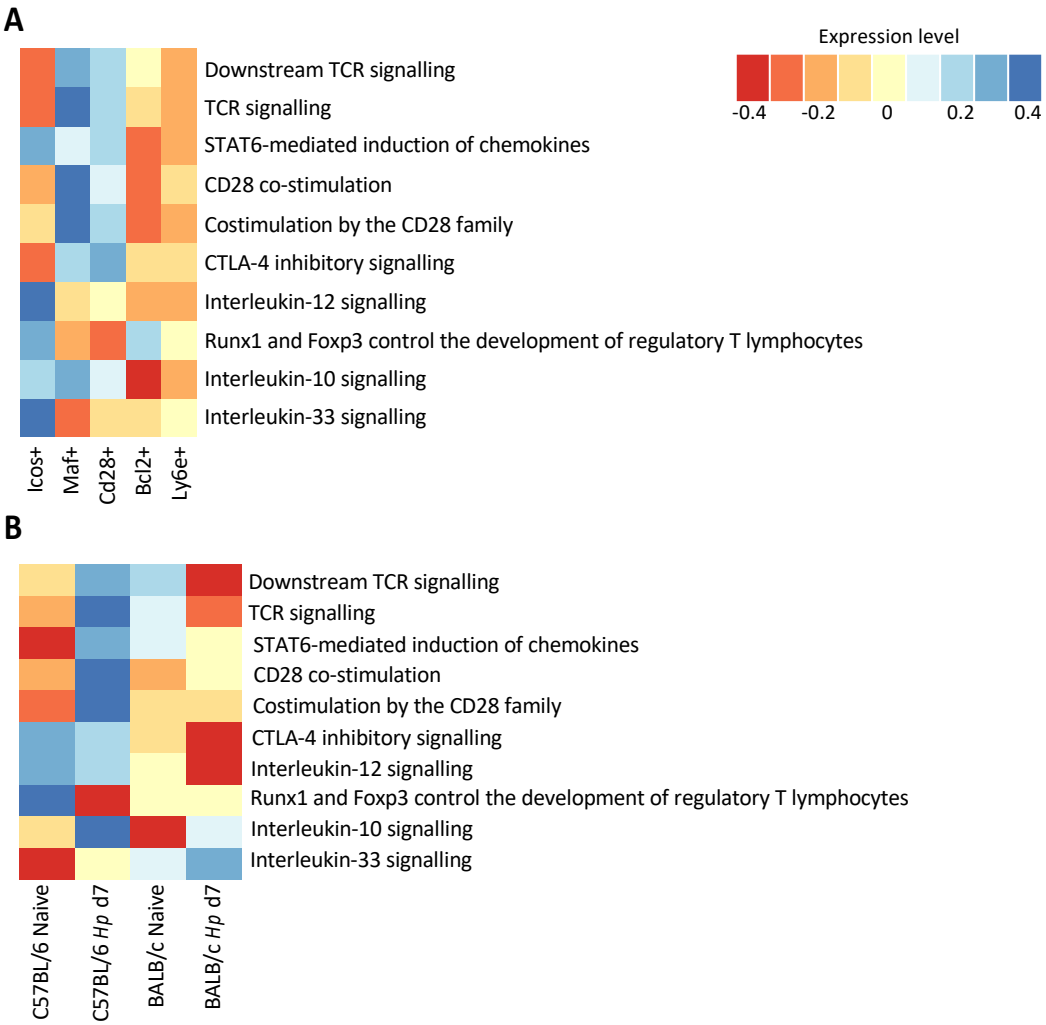

Figure 3.7 Pathway analysis of Tregs from naïve and H. polygyrus infected mice. (A) A heat map showing the expression of genes within the pathways on the right in the different clusters of Tregs as shown in Figure 3.4. (B) A heat map showing the expression of genes within the pathways on the right in Tregs from the MLN of naïve and *H. polygyrus* infected BALB/cOlaHsd and C57BL/6OldHsd mice.
Pathway analysis performed by ReactomeGSA. Heat maps generated using ReactomeGSA.

3.4.8 Purity and viability of CD4+ T cells sorted for single cell RNA sequencing

In planning a repeat single cell RNA sequencing experiment, it was decided to sequence CD4+ T cells in the mesenteric lymph node rather than all CD3+ T cells to increase the number of Th2 and Treg cells being sequenced. The read depth was also increased from 30,000 reads per cell to 50,000 reads per cell, as this would give more robust data and may give more novel insights into the populations found during *H. polygyrus* infection. It is also worth noting that in-house bred Foxp3^{GFP} BALB/c and Foxp3^{GFP} C57BL/6 mice were used for this experiment rather than C57BL/6OlaHsd and BALB/cOlaHsd from Envigo used in the initial experiment.

CD4+ T cells were also sorted using the AutoMACS and labelled with hashtagging antibodies as seen in Figure 3.1. Sorted cells not required for the sequencing sample were stained for viability, CD4 expression, and Foxp3 using the in-cell GFP reporter. The viability of all groups was above 95% showing that sorted cells were healthy and suitable for single cell sequencing (Figure 3.8A). The sort also generated a high purity of CD4+ T cells, with greater than 95% of all cells in all groups expressing CD4 (Figure 3.8B). Foxp3+ Tregs made up around 7.5-9% of CD4+ T cells in all samples, with slightly higher frequencies in those taken from infected mice (Figure 3.8C). On the basis of this analysis showing purified CD4+ T cells with high viability, the cells were submitted for single cell RNA sequencing.

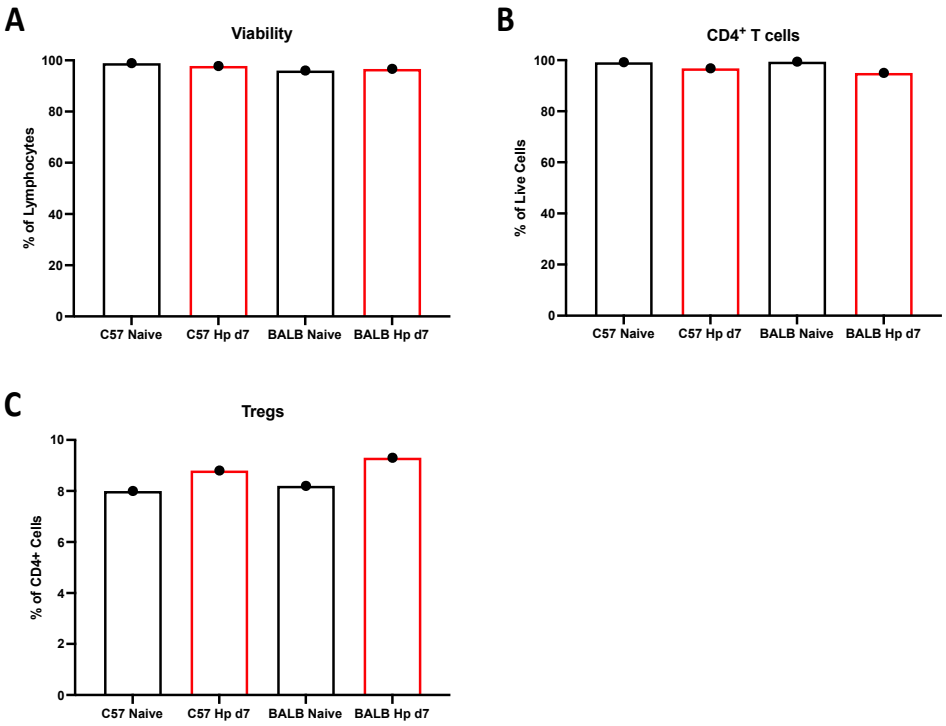

Figure 3.8 Purity and viability of sorted cells for single cell RNA sequencing. (A) The viability of sorted CD4+ T cells from the MLN of Naïve and *Hp* d7 infected Foxp3^{GFP} C57BL/6 and Foxp3^{GFP} BALB/c mice. (B) The percentage of live cells expressing CD4 in pre-sorted cells from Naïve and *Hp* d7 infected Foxp3^{GFP} C57BL/6 and Foxp3^{GFP} BALB/c mice. (C) The percentage of Tregs within the CD4+ T cell population in pre-sorted cells from the MLN of Naïve and *Hp* d7 infected Foxp3^{GFP} C57BL/6 and Foxp3^{GFP} BALB/c mice.
Closed circles represent 2 pooled naïve mice and 3 pooled *H. polygyrus* infected mice.

3.4.9 Assigning cell identities using cell hashing

As discussed previously, cell hashtag oligonucleotide (HTO) binding (also referred to as “hashing”) utilises oligonucleotide-tagged antibodies to allow multiplexing of samples to minimise the batch effects seen in single cell sequencing. Cells were assigned identities based on their expression level of the BALB/c HTO versus the C57BL/6 HTO, where cells expressing the C57BL/6 HTO alone are assigned as C57, those expressing the BALB/c HTO alone are assigned as BALB and those with both BALB/c and C57BL/6 HTO expression were labelled as doublets. Figure 3.9A-D are ridge plots which show the distribution of cells along the spectrum of normalised expression levels of the HTOs associated with BALB/c and C57BL/6 in cells assigned BALB/c (A+C) and C57BL/6 (B+D) naïve and *H. polygyrus* infected samples. The small overlap of cells expressing both C57BL/6 and BALB/c were removed in the next step of quality control as they were assigned as doublets (Figure 3.9A-D). These results show that there is good separation of cells by their expression of the two HTOs, and consequently that cell hashing is able to identify the sample of origin of each cell (Figure 3.9A-D).

Figure 3.9E+F show the clustering of cells based on their HTO expression in a tSNE plot. The majority of cells in both naïve (Figure 3.9E) and *H. polygyrus* infected (Figure 3.9F) are singlets and have been assigned to C57BL/6 or BALB/c. Some doublets were apparent in both samples, but tended to cluster away from their singlet counterparts, and were removed from downstream analysis (Figure 3.9A). Once cells have been assigned an identity and doublets have been excluded, clustering can be performed.

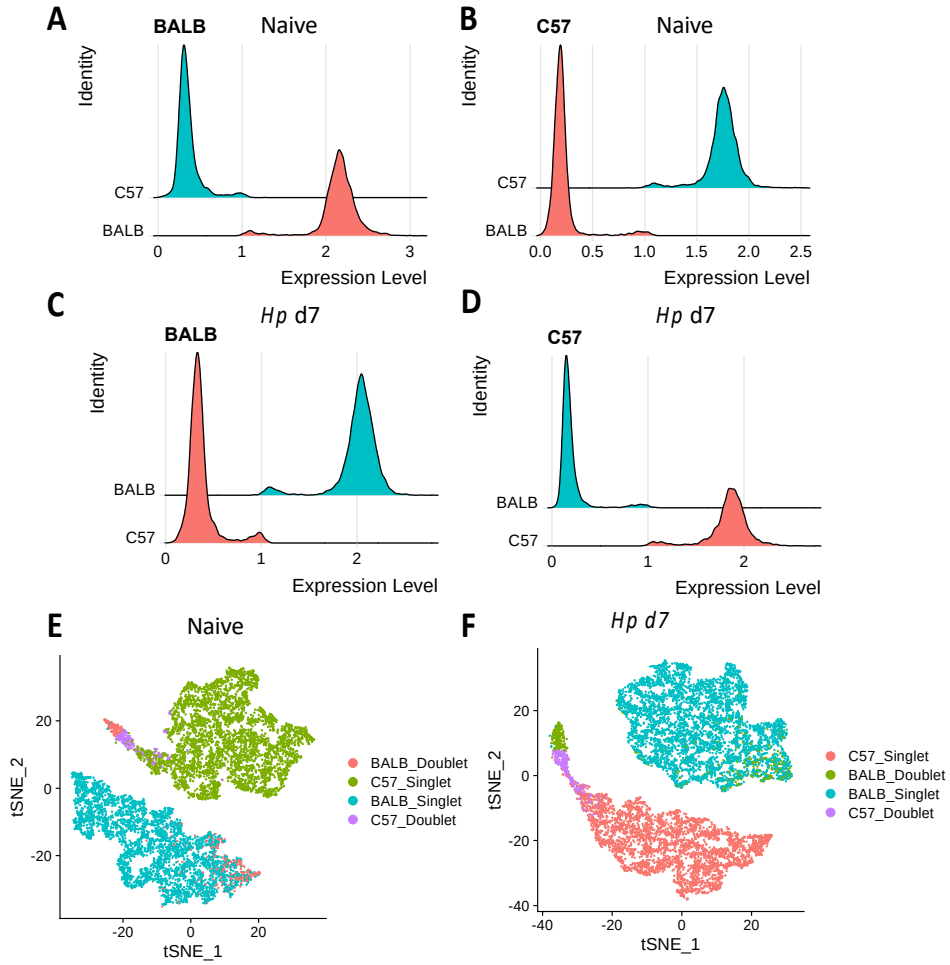

Figure 3.9 Assigning strain IDs to each cell and excluding doublets using Cell hashing. (A-D) Ridge plots showing the expression of the Foxp3^{GFP} BALB/c and Foxp3^{GFP} C57BL/6 HTOs on cells assigned the ID BALB/c (A+C) or C57BL/6 (B+D) in Naïve (A-B) and *H. polygyrus* (C-D) infected samples. (E-F) tSNE plots showing the clustering of the HTO data in naïve (E) or *Hp* infected (F) samples. The tSNE plots are coloured by strain ID and their status as a doublet or singlet.

3.4.10 Clustering of CD4+ T cells in naïve and *H. polygyrus* infected mice

Clustering was performed using the Seurat package and visualised as a UMAP plot. A total of thirteen different clusters were predicted from the sorted CD4+ T cells, of which four were in fact non-T cells. One cluster of CD4+ T cells (stress Th2) was excluded from further analysis as their top 30 genes are all mitochondrial genes and apoptotic factors, which indicates that the cells are reaching the end of their life span and are undergoing apoptosis (Figure 3.10A).

Two clusters of naïve cells were also seen in this experiment and their proportions in C57BL/6 and BALB/c mice show that Naive(a) is associated with the former and Naive(b) is associated with the latter, again suggesting that naïve CD4+ T cells from the two strains are transcriptionally distinct (Figure 3.10A+B).

The Tfh cluster was identified by their high production of IL-4 and expression of *Bcl6* (Figure 3.10A, C-D+I). Two population of Th2 cells (Th2a and Th2b) express high levels of *Gata3* and produce IL-4 (Figure 3.10A, C-D,F+I). Tregs were identified by their expression of *Foxp3*, *Il2ra* and *Il10* production (Figure 3.10A, C-D, G+J). TCR-stimulated CD4+ T cells are identified by their high expression of *Nr4a3* and *Nr4a1*, genes downstream of the TCR (data not shown) (Jennings *et al.*, 2020). The IFN-stimulated cluster was identified by their high expression of interferon stimulated genes (data not shown). The proportion of each of these clusters is similar in naïve BALB/c and C57BL/6 mice except in the case of naïve cells (Naïve(a) and Naive(b)) as mentioned previously (Figure 3.10B). However, upon infection, the proportion of each cell cluster is different in BALB/c and C57BL/6 mice (Figure 3.10B). Both BALB/c and C57BL/6 mice increase the proportion of Th2 cells upon infection with *H. polygyrus* however, the Treg cluster did not increase in proportion upon infection in either strain, which is unexpected (Figure 3.10B). Further analysis is required to discover the role of these different cell clusters during *H. polygyrus* infection.

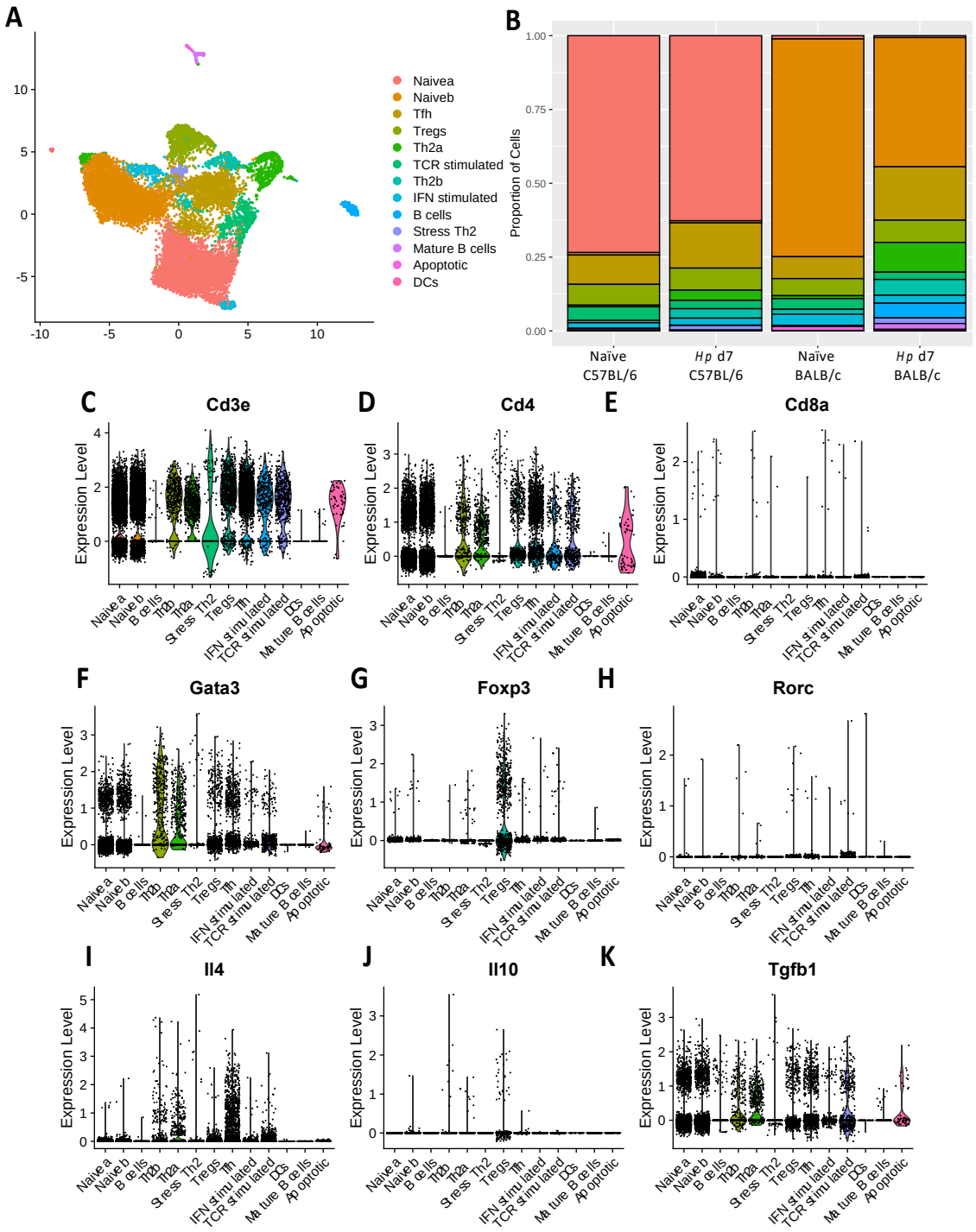

Figure 3.10 Clustering of CD4+ T cells from naïve and H. polygyrus infected mice. (A) UMAP showing the clusters of CD4+ T cells as defined by Seurat, labels show cluster identified by their gene expression. (B) A stacked bar graph showing the proportions of each CD4+ T cell cluster in the MLN of Naïve and *H. polygyrus* infected Foxp3^{GFP} C57BL/6 and Foxp3^{GFP} BALB/c mice. (C-K) Violin plots showing each clusters expression level of (C) *Cd3e* (D) *Cd4* (E) *Cd8a* (F) *Gata3* (G) *Foxp3* (H) *Rorc* (I) *Il4* (J) *Il10* and (K) *Tgfb1*.

3.4.11 Pathway analysis of CD4+ T cells from naïve and *H. polygyrus* infected mice

As with previous datasets, pathway analysis was run using ReactomeGSA (Griss *et al.*, 2020) to assess the activation status and cytokine signalling within the CD4+ T cells. The analysis was first applied to the different CD4+ T cell clusters, and it was immediately obvious that the most active CD4+ T cells are the Th2a cells, with the highest levels TCR signalling and co-stimulation, however, they also have high levels of IL-10 signalling may be counteracting the activation signals (Figure 3.11A). The second Th2 cluster, Th2b, is markedly lower in every pathway measured, including IL-10 signalling, indicating both a weaker activation signal and less likelihood of tolerization (Figure 3.11A).

The pathway analysis of Tregs indicated surprisingly little expression of any of the pathways except IL-33 signalling, which may suggest that Tregs during *H. polygyrus* infection are not receiving ongoing TCR stimulation and co-stimulation (Figure 3.11A); however, the dynamics of Treg activation *in vivo* are poorly characterised and it is possible that this cluster retains functional regulatory activity.

The two naïve clusters show very similar TCR and co-stimulation pathway profiles to each other, and also only differ from the Th2b cluster by a higher level of regulatory signalling, indicating that these cells are perhaps held in an anergic state (Figure 3.11A). In fact, the Tfh cluster shows even lower TCR signalling, with only higher IL-33 and IL-10 signalling being apparent (Figure 3.11A). Finally, the IFN-stimulated cell cluster differs in having the highest ratio of IL-12 to STAT6 signalling, as well as TCR and IL-33 (Figure 3.11A). While these data are only indicative of the functional properties of each cluster, it is clear that each population of CD4+ T cells is in a different stage and combination of activation pathways, and that among them all the Th2a cluster is clearly the most highly activated.

Next, pathway analysis was performed on the CD4+ T cell population subdivided by the infection status and strain of the mouse. Focusing first on BALB/c mice, naïve BALB/c CD4+ T cells show a mixed profile with high expression of IL-33 signalling and low TCR stimulation consistent with resting tissue cells (Figure

3.11B). However, following infection, BALB/c CD4+ T cells show striking changes with high levels of TCR signalling, CD28 co-stimulation and cytokine signalling, representing a broad pattern of T cell activation of T cells within infected BALB/c mice (Figure 3.11B). Most notably, C57BL/6 mice do not follow the same pattern. Naïve C57BL/6 mice show higher expression of genes associated with cytokine signalling and the development of Tregs (Figure 3.11B). But upon infection with *H. polygyrus*, levels of TCR signalling do not change much among CD4+ T cells, and CD28 family costimulation actually declines; in contrast, CTLA4 inhibitory signalling is upregulated in C57BL/6 mice, resulting in a greatly inferior CD28:CTLA4 balance compared to BALB/c mice (Figure 3.11B). This difference may reflect a fundamental dichotomy in the activation of CD4+ T cells in the two strains of mice in response to *H. polygyrus* which could underpin their differential susceptibility to infection.

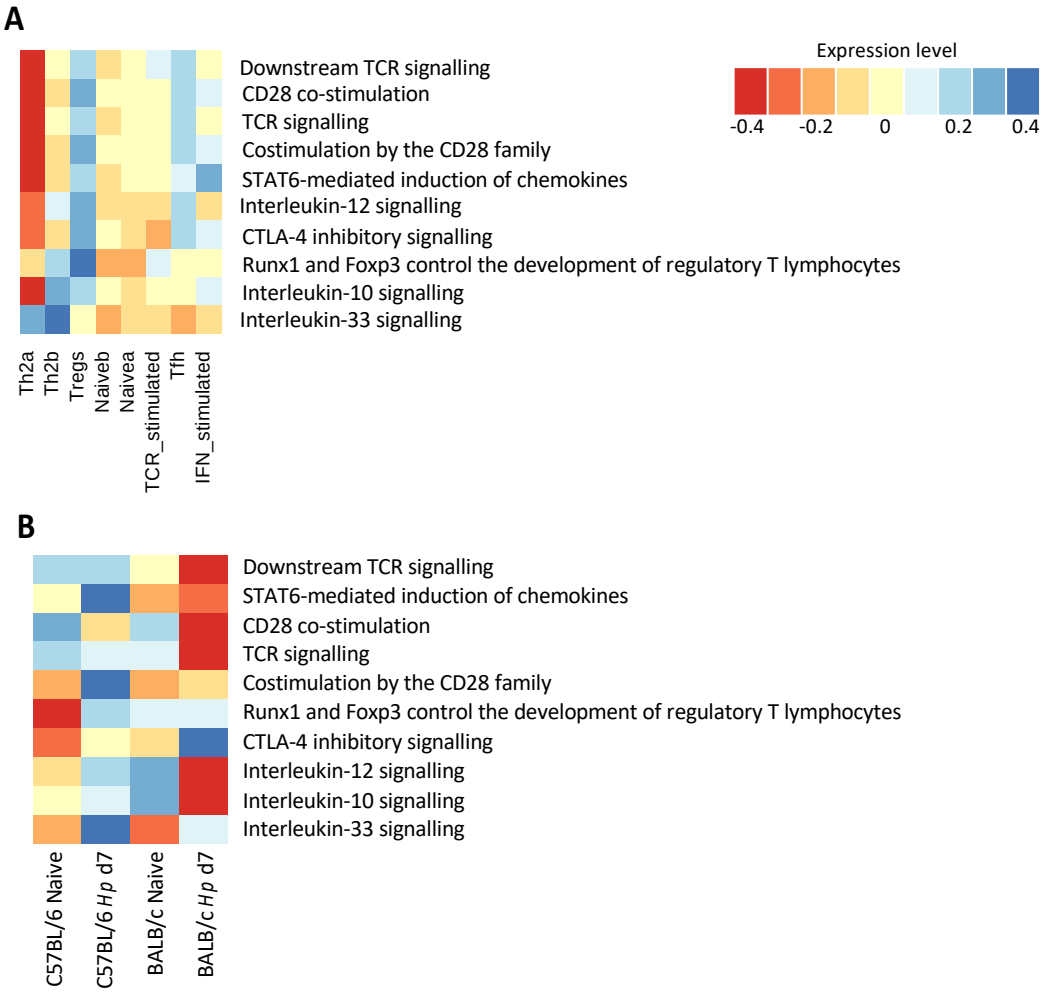

Figure 3.11 Pathway analysis of CD4+ T cells from naïve and H. polygyrus infected mice. (A) A heat map showing the expression of genes within the pathways on the right in the different clusters of CD4+ T cells as shown in Figure 3.4. (B) A heat map showing the expression of genes within the pathways on the right in CD4+ T cells from the MLN of naïve and *H. polygyrus* infected Foxp3^{GFP} C57BL/6 and Foxp3^{GFP} BALB/c mice.
Pathway analysis performed by ReactomeGSA. Heat maps generated using ReactomeGSA.

3.4.12 Clustering of Th2 cells from naïve and *H. polygyrus* infected mice

To further examine the Th2 response to *H. polygyrus*, sequence data from the two Th2 clusters from 3.4.10 were selected and pooled for separate analysis. Figure 3.12A shows the 5 clusters of Th2 cells predicted from these data by Seurat, as well as one small population that identified as infiltrating B cells and were removed from further analysis (Figure 3.12A-C). As before, the Th2 clusters were assigned identities by their most highly-expressed distinguishing genes, which were different from those assigned in the previous single cell dataset. Further analysis is required to compare the Th2 sub-clusters from the initial experiment and this experiment. It is likely that there is overlap between the clusters from the initial experiment and this experiment as they both separate into 5 distinct clusters. Integration of the two experiments and comparison of the Th2 (and Treg) response from the two experiments will give insights into genes consistently upregulated in response to *H. polygyrus* infection.

The 5 clusters showed varying patterns of contraction or expansion following infection. One which decreased upon infection in both strains of mice was the *Ccl5*+ cluster (Figure 3.12A-C); the product of this gene, CCL5 or RANTES has been seen at higher expression levels in human patients with IBD, suggesting this chemokine is important in intestinal immune responses (Figure 3.12A-C) (Ajuebor, Hogaboam, Kunkel, Proudfoot, & Wallace, 2001).

Two clusters with differing dynamics in the two strains are *Plac8* and *Ran*; *Plac8* expands only in the C57BL/6 and is slightly reduced in BALB/c; interestingly, Th2 cells during allergic airway inflammation were found to express *Plac8*, but it is now known if *Plac8* expressing Th2 cells may contribute to the protection from allergy endowed by helminth infection (Kitagaki et al., 2006; Tibbitt et al., 2019; Wilson et al., 2005). Conversely, *Ran*+ Th2 cells are downregulated in C57BL/6 mice upon infection but upregulated in infected BALB/c (Figure 3.12A-C). The GTPase Ran, or Ras-related nuclear protein, regulates DNA replication and cell cycle progression and overexpression of this enzyme has been shown to attenuate T cell responses which may suggest that these Th2 cells are suppressed (Qiao, Pham, Luo, & Wu, 2010)

In addition, two clusters expand in response to *H. polygyrus* infection in both strains. One is the *Mki67*+ cluster, Ki-67 is encoded by *Mki67* and is a marker of proliferation which suggests these Th2 cells are actively proliferating (Figure 3.12A-C). Finally, *Bcl2*+ Th2 cells are increased in response to *H. polygyrus* infection, Bcl-2 is an inhibitor of apoptosis and is important for CD4+ T cell survival. This suggests that these cells are protected from undergoing apoptosis (Figure 3.12A-C) (Hata, Engelman, & Faber, 2015; Rogers, Song, Gramaglia, Killeen, & Croft, 2001). Taken together, these data identify distinct populations of Th2 cells, with specific gene expression profiles; their differential dynamics following infection in susceptible and resistant mice suggest that they may be performing unique functions in the anti-parasite immune response.

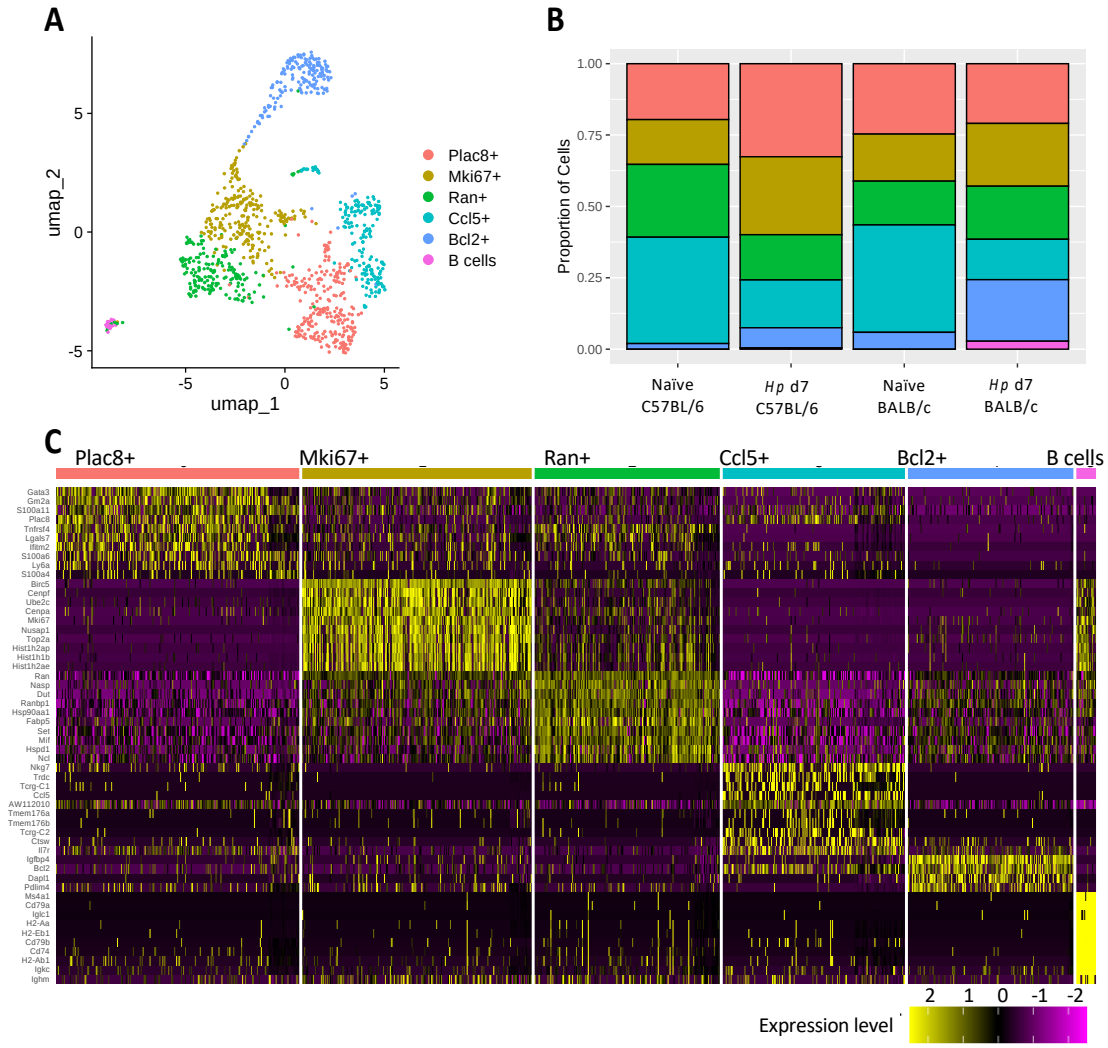

Figure 3.12 Clustering of Th2 cells from naïve and H. polygyrus infected mice. (A) UMAP showing the clusters of cells from the Th2 cell cluster as defined by Seurat (Figure 3.2), labels show cluster identified by their gene expression. (B) A stacked bar graph showing the proportions of each Th2 cluster in the MLN of Naïve and *H. polygyrus* infected Foxp3^{GFP} C57BL/6 and Foxp3^{GFP} BALB/c mice. (C) A heatmap showing the top 10 expressed genes for each cluster of Th2 cells.

3.4.13 Pathway analysis of Th2 cells from naïve and *H. polygyrus* infected mice

Pathway analysis was then performed on the Th2 populations from naïve and *H. polygyrus*-infected mice using ReactomeGSA (Griss *et al.*, 2020). First, the analysis was undertaken on the different clusters of Th2 cells found in 3.4.10, and the results presented in Figure 3.13A. The strongest TCR activation signatures were within the *Ran*+ *and* Bcl2 Th2, with the former cluster showing higher levels of CD28 costimulation. Interestingly, the *Ran*+ Th2 subset expanded only in the partially resistant BALB/c strain (Figure 3.12). The Th2 cluster expressing *Bcl2* are also highly activated, and more abundant in the BALB/c mice, but in this case show evidence of Runx1 and Foxp3 pathway expression, and so may be generating Tregs. This observation may suggest that, unexpectedly, there are Tregs which arise from Th2-like cells, but more studies will be required to elucidate any relationship between Bcl-2+ Th2 cells and the Treg compartment (Figure 3.13A).

The *Mki67*+ Th2 cell cluster, which expands in both strains of mice following *H.* polygyrus infection, shows intermediate expression of TCR engagement and co-stimulation pathway genes, suggesting that these cells have had antigen presented to them, and constitute part of the mainstream Th2 response (Figure 3.13A). While these cells appear to have escaped CTLA-4 inhibition, they do show a pattern of IL-10 signalling, an interesting dichotomy that would be worth exploring in functional terms (Figure 3.13A).

The final two Th2 clusters show, in contrast, relatively little evidence of activation. The *Ccl5*+ Th2 cell expression profile reveals an IL-33 response, but in the absence of TCR or CD28 signalling, these cells would appear to be inactive during *H. polygyrus* infection (Figure 3.13A). Even more quiescent are the *Plac8*+ Th2, which is in line with their downregulation during *H. polygyrus* infection as shown in Figure 3.12 (Figure 3.13A). Together these findings reiterate that the different clusters of Th2 cells within *H. polygyrus* infection represent functionally different effector subsets.

The pathway analysis was then re-run with datasets divided by infection status and strain of mouse to assess any differences in Th2 cell populations between

C57BL/6 and BALB/c mice. As shown in Figure 3.13B, Th2 cells in naïve and infected C57BL/6 and BALB/c mice express highly divergent levels of each of the pathways analysed (Figure 3.13B). However, as found in the first experiment (Figure 3.7), Th2 cells from C57BL/6 mice show little sign of activation following infection, and indeed they appear to be more activated in naïve mice than *H. polygyrus* infected mice, particularly with respect to CD28 co-stimulation and downstream TCR signalling (Figure 3.13B). The only pathway upregulated in C57BL/6 *H. polygyrus* infected mice compared to C57BL/6 naïve mice is IL-10 signalling, which would be consistent with a model IL-10 mediated suppression blocks Th2 responses in this strain of mouse (Figure 3.13B).

In contrast to the C57BL/6 genotype, BALB/c naïve mice have low levels of TCR stimulation and co-stimulation suggesting these cells are broadly quiescent (Figure 3.13B). When BALB/c mice are infected with *H. polygyrus*, however, their Th2 cells receive strong TCR stimulation and CD28 mediated co-stimulation suggesting that these cells recognise and respond well to antigens introduced by *H. polygyrus* infection (Figure 3.13B). In addition, IL-12 signalling is subdued following infection. Together, this analysis recapitulates earlier findings that BALB/c Th2 cells are more responsive during *H. polygyrus* infection, and raises the new suggestion that Th2 cells in *H. polygyrus* infected C57BL/6 mice are actually less active than their naïve counterparts.

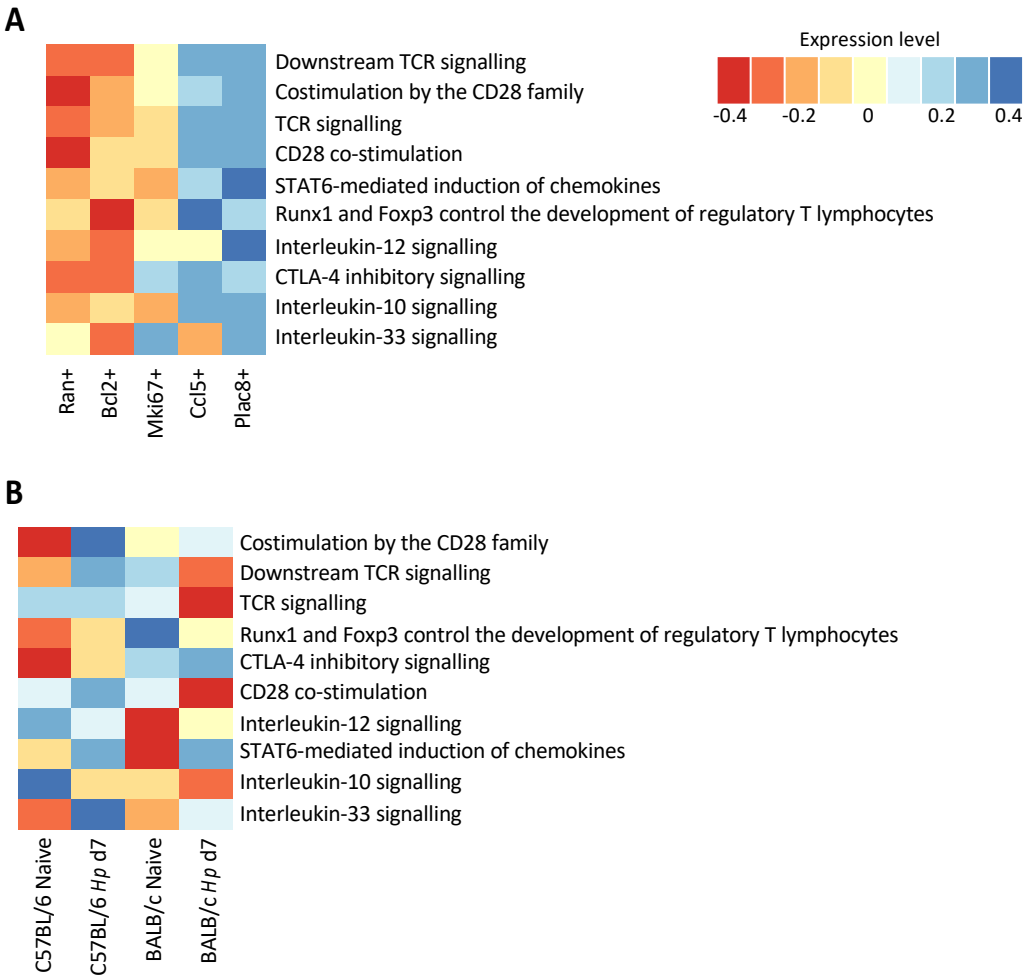

Figure 3.13 Pathway analysis of Th2 cells from naïve and H. polygyrus infected mice. (A) A heat map showing the expression of genes within the pathways on the right in the different clusters of Th2 cells as shown in Figure 3.4. (B) A heat map showing the expression of genes within the pathways on the right in Th2 cells from the MLN of naïve and *H. polygyrus* infected Foxp3^{GFP} C57BL/6 and Foxp3^{GFP} BALB/c mice.
Pathway analysis performed by ReactomeGSA. Heat maps generated using ReactomeGSA.

3.4.14 Differential expression of genes in Th2 cells from naïve and *H. polygyrus* infected mice

In addition to pathway analysis of gene expression patterns, it can be very informative to examine regulation of individual genes that are most significantly up- or down-regulated between different subsets of cells. Such changes were identified in comparisons between cells in the Th2 cluster of Figure 3.10 from naïve and infected C57BL/6 and BALB/c mice (Figure 3.14). Differential expression was used which compares the average expression of each gene within one cluster to the average expression of the gene within another cluster, giving a fold change and p value.

Figure 3.14A shows genes upregulated in C57BL/6 Th2 cells from *H. polygyrus*-infected mice compared to those from naïve animals of the same strain. Surprisingly few Th2 genes show up-regulation following *H. polygyrus* infection (Figure 3.14A). Equally unexpectedly, Th2 cells from infected mice have significantly lower expression of the *Il4* gene, indicating that these cells have their IL-4 capacity reduced (Figure 3.14B). However, when looking at the distribution of cells along the spectrum of *Il4* expression levels using a ridge plot, there is a sub-population of Th2 cells in *H. polygyrus* experienced Th2 cells which express higher (>1) expression of *Il4* than any naïve Th2 cells (Supplementary Figure 3.1). Among the very few genes showing raised expression following infection, is *Mcm3ap* or germinal centre–associated nuclear protein (GANP) which has been shown to be upregulated in activated CD4+ T cells, but only in the setting of HIV-1 infection (Maeda *et al.*, 2013). *Erbin* has a broadly inhibitory role in many cell types, and suppresses the TGFß signalling pathway via STAT3; in T cells loss of Erbin leads to increased IL-4Rα expression and greater Th2 responses (Lyons et al., 2017); this might suggest that in infection, Erbin is involved in suppression of the Th2 response in C57BL/6 mice. Whether or not this latter point is true, the overall gene expression analysis presents a picture of muted, if not suppressed C57BL/6 Th2 cells during *H. polygyrus* infection.

A similar comparison between naïve and *H. polygyrus*-infected BALB/c Th2 cells was also conducted at the gene level. *Trdc* is the TCR receptor delta common

chain and is upregulated in *H. polygyrus* Th2, suggesting there are infiltrating γδ T cells within the Th2 cluster (Figure 3.14B).

As with the C57BL/6 mice, global *Il4* is also downregulated in infected BALB/c mice, suggesting again that *H. polygyrus*-responsive Th2 cells may be suppressed to some degree (Figure 3.14B). *Nkg7* is upregulated in Th2 cells during *H. polygyrus* infection, Nkg7 is often associated with NK cells, but Nkg7 can also be expressed by CD4+ T cells and is associated with increased inflammation (Figure 3.14B) (Malarkannan, 2020; Ng *et al.*, 2020). RANTES (Ccl5) expression is also upregulated 2-fold in Th2 cells from *H. polygyrus* infected BALB/c mice, despite the *Ccl5*+ Th2 subcluster contracting (Figure 3.14B, Figure 3.12B). Taken together, these data show that while BALB/c mice are also reduce *Il4* expression, their cells may be more active than C57BL/6 *H. polygyrus*-induced Th2 cells.

The Th2 clusters from C57BL/6 and BALB/c mice were then compared to identify any differentially regulated genes (Figure 3.14C). There is higher expression of *Ly6a* or Sca-1 on Th2 cells from C57BL/6 which may well be due to strain differences, as BALB/c mice express lower levels of the Ly6.1 variant than do C57BL/6 mice of the Ly6.2 variant (Figure 3.14C) (Gumly et al., 1995; Lee et al., 2013; Rock et al., 1989; van de Run et al., 1989). *Crip1* was also upregulated in C57BL/6 Th2 cells; it is known that when CRIP (cysteine-rich intestinal protein) is overexpressed, type 1 cytokine responses are diminished which may be due to a favouring of the type 2 response (Figure 3.14C) (Lanningham-Foster et al., 2002). There were no genes upregulated in BALB/c Th2 cells which hold significant function to Th2 cells (Figure 3.14C). Overall, very few significant differences were found in the Th2 response to *H. polygyrus* infection in C57BL/6 and BALB/c mice at a single gene level.

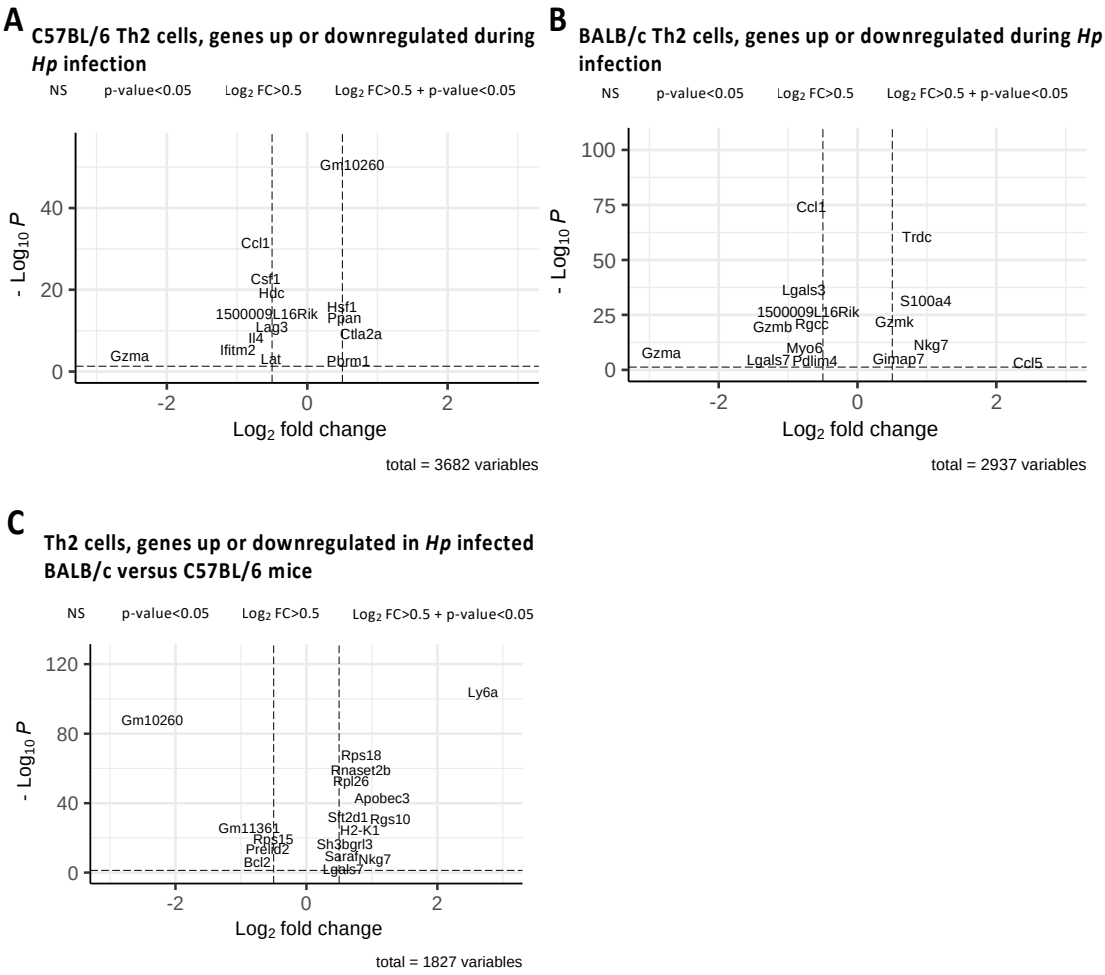

Figure 3.14 Differentially expressed genes in the Th2 cell cluster during H. polygyrus infection. (A-B) Volcano plots showing the genes upregulated in the Th2 cell cluster upon infection on the right and downregulated on the left in Foxp3^{GFP} C57BL/6 (A) and Foxp3^{GFP} BALB/c (B) mice. (C) A volcano plot showing genes upregulated in the MLN of *Hp* infected Foxp3^{GFP} C57BL/6 mice compared to *Hp* infected BALB/c and genes on the right and genes downregulated on the left. Differential expression performed using Seurats FindMarkers function. Volcano plot generated using EnhancedVolcano.

3.4.15 Clustering of Tregs from naïve and *H. polygyrus* infected mice

To compare the Treg response to *H. polygyrus* in BALB/c and C57BL/6 mice, the Treg cluster from 3.4.10 was isolated and re-clustered. Figure 3.15A shows the 4 subclusters of Tregs predicted by Seurat. Clusters are named after the top Treg relevant gene in their cluster markers (Figure 3.15A-C). As in the first experiment, *Maf*+ Tregs were upregulated in *H. polygyrus* infected mice regardless of their strain, which is interesting in view of reports that these are IL-10 producing Tregs with the capacity to express RORγt (Figure 3.15B) (Neumann et al., 2019; Wheaton et al., 2017).

Ly6e+ Tregs are again higher in the C57BL/6 samples, however, in this experiment, their proportion did not increase during *H. polygyrus* infection (Figure 3.15B) (Gumly et al., 1995; Lee et al., 2013; Rock et al., 1989). This implies that these cells may not be reproducibly induced by *H. polygyrus* infection and may not play a key role in setting the balance between clearance and susceptibility response.

In this experiment *Bcl2*+ Tregs were massively upregulated in response to *H. polygyrus* in BALB/c mice and to a lesser extent in C57BL/6 mice (Figure 3.15B), although this contradicts the findings of the first experiment. Bcl2 KO mice have impaired Teffector responses and expanded Treg responses and Bcl2 expression has been linked to reduced efficacy of Tregs during colitis (Gabriel et al., 2016; Tischner et al., 2012). More studies are required to ascertain if this population is dysfunctional, and if it is generally upregulated, by *H. polygyrus* infection.

Interestingly, the cluster identified as CD25+ (*Il2ra*) Tregs decreases upon *H. polygyrus* infection (Figure 3.15B). CD25 (IL-2Rα) is essential to the development and function of Tregs as IL-2 is a key factor in the survival and responses of Tregs; the loss of CD25 may indicate abated IL-2 signalling and thus again lowered efficiency (Sakaguchi, Yamaguchi, Nomura, & Ono, 2008). Taken together, these analyses reveal several intriguing differences in the Treg response to *H. polygyrus* between BALB/c and C57BL/6 mice, suggesting that either or both the frequency and regulatory function of specific Treg subsets may underpin the different genetically-determined outcomes of infection.

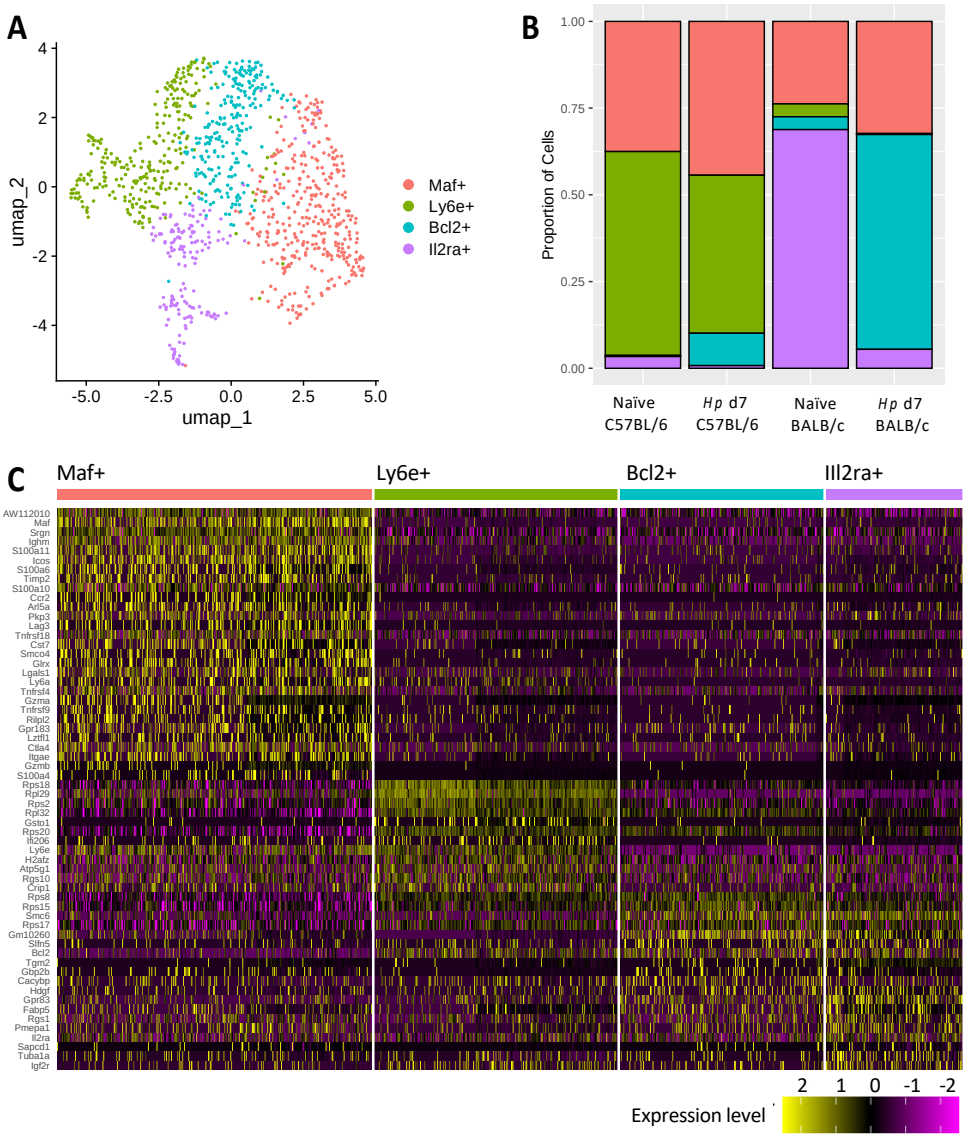

Figure 3.15 Clustering of Tregs from naïve and H. polygyrus infected mice. (A) UMAP showing the clusters of cells from the Treg cluster as defined by Seurat (Figure 3.2), labels show cluster identified by their gene expression. (B) A stacked bar graph showing the proportions of each Treg cluster in the MLN of Naïve and *H. polygyrus* infected Foxp3^{GFP} C57BL/6 and Foxp3^{GFP} BALB/c mice. (C) A heatmap showing the top 10 expressed genes for each cluster of Tregs.

3.4.16 Pathway analysis of Tregs from naïve and *H. polygyrus* infected mice

Pathway analysis was next performed on the Treg cluster from Figure 3.10 comparing the expression of T cell activation and stimulation pathway genes in different subsets of cells. First, the dataset was separated into each of the 4 Treg subclusters with the pathway analysis results as presented in Figure 3.16A.

The *Maf*+ Treg population, which shows marginal expansion in both strains following infection, expresses high levels of CD28 co-stimulation but paradoxically low expression of TCR signalling (Figure 3.16A); this profile could indicate that they have been activated through their TCR but at an earlier time point. Notably, this subcluster also shows high TGF-ß signalling, although that is not accompanied by significant Runx- and Foxp3-pathway activation.

In contrast, the *Ly6e*+ Treg population has received a broad range of activation signals through most of the pathways under analysis, including TCR activation and IL-4/IL-13, TGFß family member, IL-10 and IL-33 signalling, with only the costimulatory/coinhibitory pathways (both CD28 and CTLA4) being relatively weak (Figure 3.16A).

Cells from the *Bcl2*+ Treg cluster have received TCR signalling to a similar degree to the Ly6e+ subset, and similarly little co-stimulation; they differ however in displaying weak cytokine responses of both Type 2 and TGFß pathways, while also showing high IL-12 signalling (Figure 3.16A). IL-12 has been shown to induce IFNγ expression in Tregs (Verma et al., 2014; Zhao, Zhao, & Perlman, 2012). However, the impact of IL-12 signalling in Tregs from *H. polygyrus* infection has not been explored.

Finally, *Il2ra*+ Tregs are found to express high levels of genes associated with co-stimulation and co-inhibition by CTLA-4 as well as producing chemokines via STAT6, and yet like the Maf+ Tregs, seem not to have recently seen antigen through their TCR (Figure 3.16A). Together this analysis shows that the four distinct populations of Tregs found within the MLN show extensive differences in expression of genes related to activation and cytokine signalling.

To assess the difference in the Treg response to *H. polygyrus* between the C57BL/6 and BALB/c strains, a further pathway analysis was performed with the dataset divided according to mouse strain and infection status. Figure 3.16B presents the relative expression level of genes associated with the indicated pathways in Tregs from naïve and *H. polygyrus* infected mice of each strain. In naïve C57BL/6 mice, as in the first experiment, Tregs appear to be more active in terms of cytokine signalling than following *H. polygyrus* infection (Figure 3.16B). Overall, Tregs from *H. polygyrus* infected C57BL/6 mice have very low levels of TCR signalling and intermediate expression of genes associated with CD28 co-stimulation, suggesting these cells are in a relatively low activation state (Figure 3.16B). BALB/c Tregs, in contrast, present higher levels of overall activation; naïve BALB/c Tregs show high levels of IL-10 and IL-33 signalling but little TCR signalling and co-stimulation, suggesting that they are quiescent (Figure 3.16B). Upon infection with *H. polygyrus*, however, Tregs from BALB/c mice upregulate multiple genes associated with co-stimulation and TCR signalling, a profile compatible with antigen-mediated activation (Figure 3.16B). The results reiterate findings from the first experiment in which Tregs from BALB/c mice, but not from C57BL/6 mice, show signs of activation by infection. This disparity may explain the difference in outcome of infection in these two mouse strains.

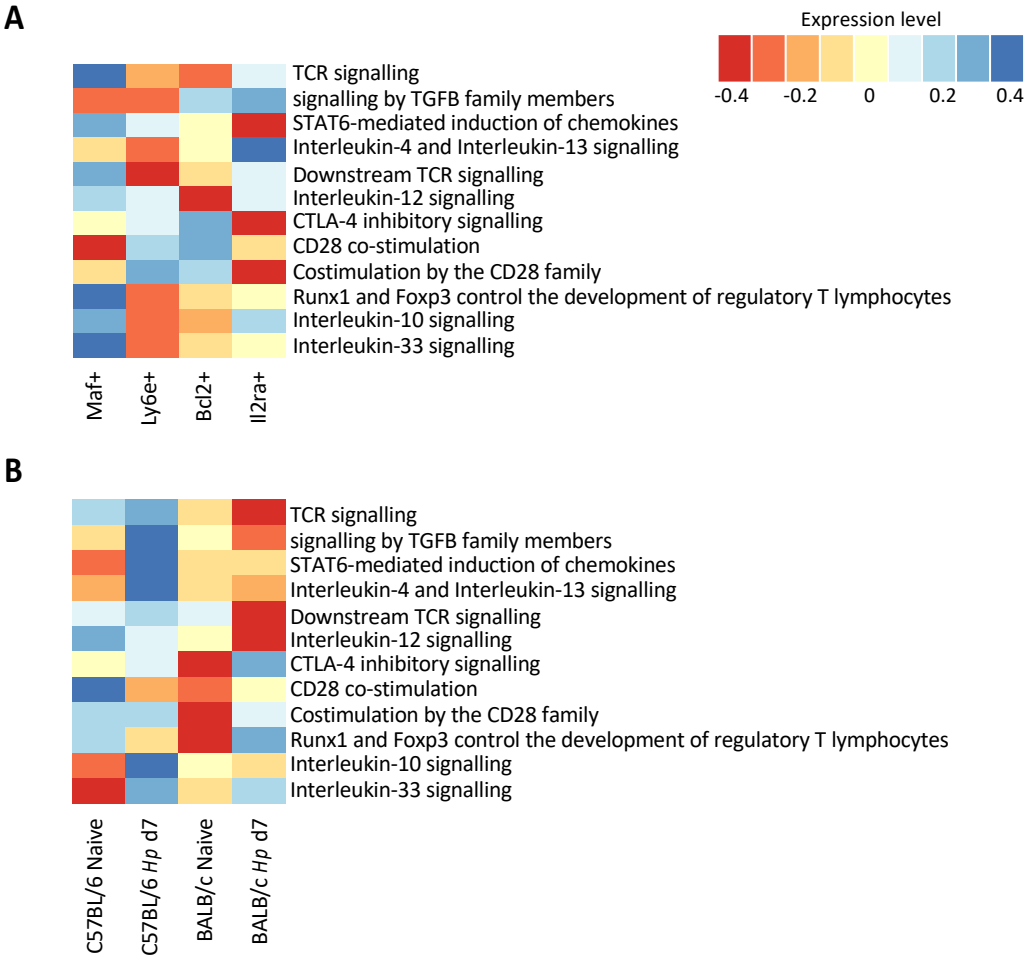

Figure 3.16 Pathway analysis of Tregs from naïve and H. polygyrus infected mice. (A) A heat map showing the expression of genes within the pathways on the right in the different clusters of Tregs as shown in Figure **3.4**. (B) A heat map showing the expression of genes within the pathways on the right in Tregs from the MLN of naïve and *H. polygyrus* infected Foxp3^{GFP} C57BL/6 and Foxp3^{GFP} BALB/c mice.
Pathway analysis performed by ReactomeGSA. Heat maps generated using ReactomeGSA.

3.4.17 Differential expression of genes in Tregs from naïve and *H. polygyrus* infected mice

To assess difference in the Treg response to *H. polygyrus* in C57BL/6 and BALB/c mice at the gene level, differential expression was used to compare the Treg clusters from these mice. Figure 3.17A shows the differential expression of genes in Tregs from naïve and *H. polygyrus* infected C57BL/6 mice. There are no genes significantly upregulated in Tregs upon *H. polygyrus* infection of C57BL/6 mice and a loss of Granzyme A (*Gzma*) and Granzyme B (*Gzmb*) expression when compared to their naïve counterparts (Figure 3.17B). Granzyme B has been shown to be important to tumour and viral responses and Granzyme A expression by Tregs is required to prevent graft versus host disease, suggesting that these Treg effector molecules are important in type 1 immune responses and the tumour response but may be dispensable during helminth infection (Cao *et al.*, 2007; Loebbermann *et al.*, 2012; Velaga *et al.*, 2015). When comparing Tregs from naïve and *H. polygyrus* infected BALB/c mice, the same lack of gene upregulation is seen and *Gzma* and *Gzmb* are once again downregulated, recapitulating that these Treg effector genes are downregulated during *H. polygyrus* infection (Figure 3.17A+B). To assess whether there are differences in the Treg response to *H. polygyrus*, the Treg clusters from infected BALB/c and C57BL/6 mice were compared using differential expression (Figure 3.17). There are more differences in the gene expression of Tregs from *H. polygyrus* infected BALB/c versus C57BL/6 mice (Figure 3.17C). However, the majority of these genes, *Ly6a, Ly6e* and *H2* genes are differential between the strains and their differential expression is independent of *H. polygyrus* infection (Figure 3.17C) (Gumly et al., 1995; Lee et al., 2013; Rock et al., 1989; van de Run et al., 1989). Other genes which vary between the strains response to *H. polygyrus* include many ribosomal genes (beginning with *Rp*) which give little insight into the response of these cells (Figure 3.17C). The remaining genes including Cathepsin E (*Cste*), cysteine rich protein 1 (*Crip1*) and regulatory of G protein signalling (*Rgs10*) have limited information on their role in the Treg population. Together, this shows that naïve and *H. polygyrus* induced Tregs are similar in C57BL/6 and BALB/c mice on a single gene level.

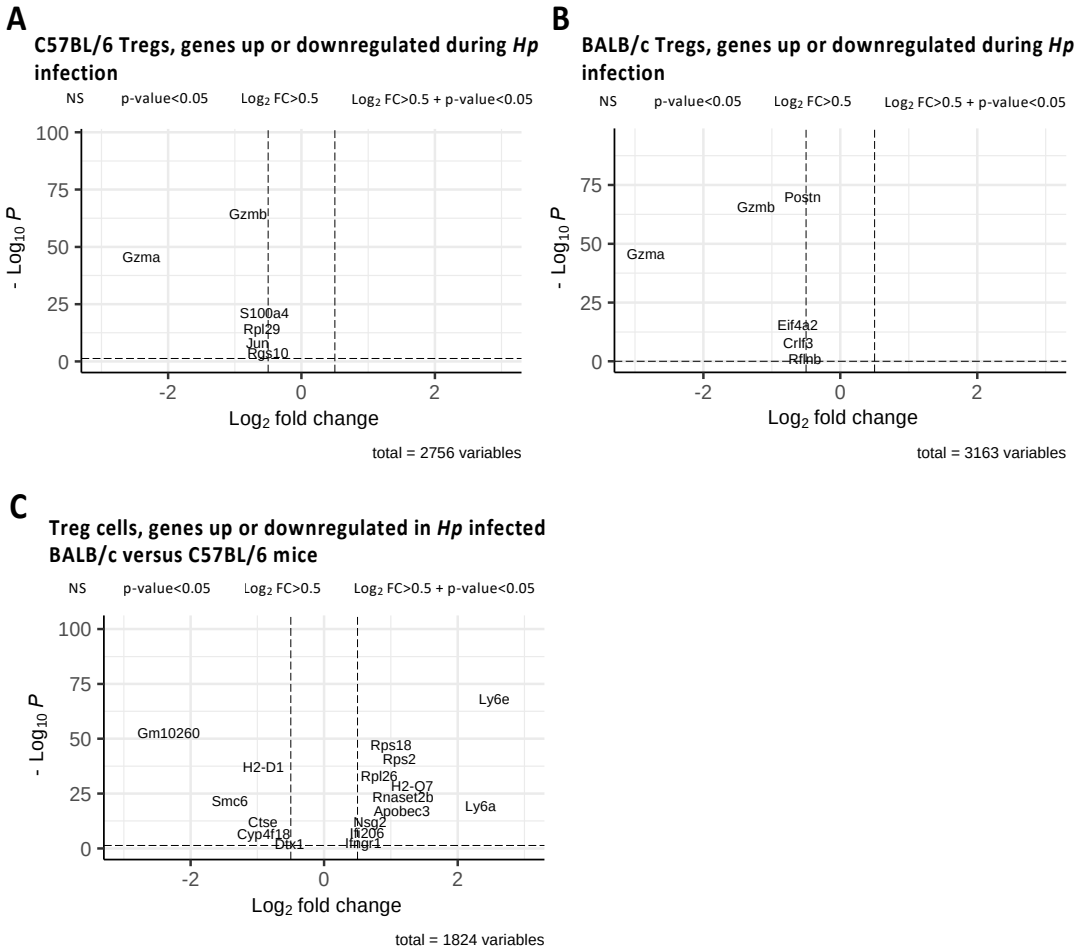

Figure 3.17 Differentially expressed genes in the Treg cluster during H. polygyrus infection. (A-B) Volcano plots showing the genes upregulated in the Treg cluster upon infection on the right and downregulated on the left in the MLN of Foxp3^{GFP} C57BL/6 (A) and Foxp3^{GFP} BALB/c (B) mice. (C) A volcano plot showing genes upregulated in *Hp* infected Foxp3^{GFP} BALB/c mice on the left and upregulated in *Hp* infected Foxp3^{GFP} C57BL/6 mice on the right.
Differential expression performed using Seurats FindMarkers function. Volcano plot generated using EnhancedVolcano.

3.4.18 Validation of Treg gene hits from single cell RNA sequencing at the protein level

Changes at the mRNA level may not lead to changes at the functional protein level, and require different techniques to evaluate protein expression. To address this question, flow cytometric analysis was performed by staining for the proteins encoded by the genes associated with each of the 4 Treg clusters, namely c-Maf, Ly6E, ICOS and Bcl2 (Figure 3.18). *Il2ra* (CD25) was not used to distinguish clusters as CD25 is used as a marker of the Treg population, meaning almost all Tregs express CD25.

Ly6E follows the same pattern at the protein level as at the mRNA level whereby BALB/c mice have lower proportions of Ly6E+ Tregs whereas C57BL/6 mice have significantly more of this subtype of Tregs (Figure 3.18A).

At the protein level, Bcl2+ Tregs are not significantly different in naïve and *H. polygyrus* infected BALB/c mice and are significantly but not greatly increased in Tregs from *H. polygyrus* infected C57BL/6 mice (Figure 3.18B). However, *Bcl2* expression was found within many clusters, not only the Bcl2+ cluster. Further analysis is required to find a panel of markers which can identify the *Bcl2*+ Treg population alone and not every Bcl2 expressing Treg.

ICOS was also assessed and is reduced in Treg C57BL/6 mice and increased in BALB/c Tregs upon infection with *H. polygyrus* (Figure 3.18C). This may suggest that ICOS mediated co-stimulation is an important component of the Treg response to *H. polygyrus* in BALB/c but not C57BL/6 mice.

Maf encoded c-Maf is associated with higher IL-10 production in Tregs, Tregs from *H. polygyrus* infected C57BL/6 mice decrease the proportion of their Tregs expressing c-Maf at day 7 post infection whereas BALB/c increase their proportion of c-Maf+ Tregs during *H. polygyrus* infection (Figure 3.18D) (Imbratta et al., 2020; Neumann et al., 2019; Wheaton et al., 2017). This may imply that Tregs from BALB/c mice are more capable of IL-10 expression upon infection with *H. polygyrus* than C57BL/6 mice, however, this requires further study (Figure 3.18D).

Together this shows that changes in the mRNA level do not always match up with changes on the functional protein level and that Tregs from *H. polygyrus* infected BALB/c and C57BL/6 mice are expressing different Treg suppressive molecules.

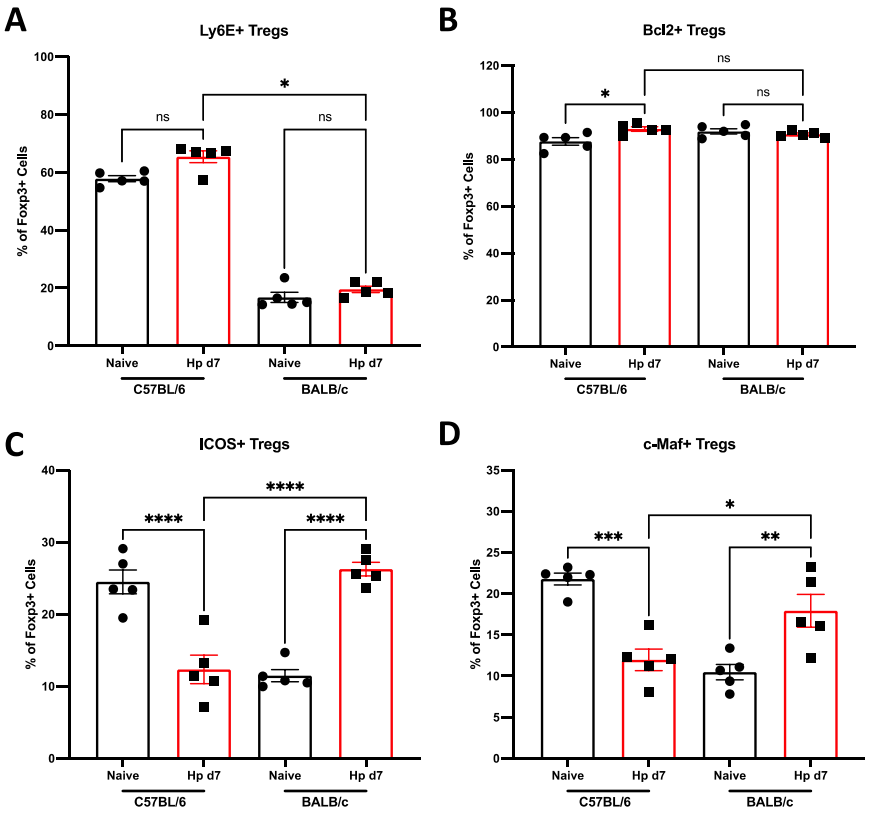

Figure 3.18 Confirmation of gene hits at the protein level. (A-E) Bar graphs showing the percentage of Foxp3+ Tregs expressing Ly6E (A), Bcl2 (B), ICOS (C) and cMaf (D) in the MLN of naïve and *H. polygyrus* infected Foxp3^{GFP} C57BL/6 and Foxp3^{GFP} BALB/c mice.
Closed circles are representative of one naïve mouse, square symbols are representative of one *Hp* d7 mouse. Error bars represent the SEM. Graphs representative of 2 experiments. Normality tested using a Shapiro-Wilk normality test. Significance tested using an ordinary one-way ANOVA and Holm-Šídák's multiple comparisons test. ns P>0.05, * P<0.05, ** P<0.01, ** P<0.001, **** P<0.0001

3.5 Discussion

H. polygyrus infection induces an expansion of Th2 cells and Tregs in C57BL/6 and BALB/c mice. However, despite superficially similar responses, C57BL/6 mice are unable to clear infection whereas BALB/c mice do slowly clear the worm (Filbey *et al.*, 2014). Single cell RNA sequencing was used as a new tool to elucidate differences in the adaptive immune response to *H. polygyrus* in these two strains of mice.

Th2 cells, the Teffector cells associated with clearance of the worm, are the most active CD4+ T cell subtype in terms of TCR signalling, co-stimulation and cytokine signalling (Figure 3.11B). This recapitulates published work that the main CD4+ T cell which is stimulated by *H. polygyrus* infection has the Th2 phenotype and is important in the anti-helminth response (Mohrs, Harris, Lund, & Mohrs, 2005). Within the Th2 population, sub clusters of Th2 cells can now be discerned, which may represent different subpopulations of Th2 cells with distinct functions during infection. Certain Th2 subsets appear to be induced by infection as their expression of genes associated with TCR signalling and co-stimulation are increased, suggesting these cells have seen antigen recently. There is also evidence of IL-10 mediated suppression of some Th2 subtypes which implies a modified function of these cells. To further understand the roles these Th2 cells are performing during *H. polygyrus* infection, further phenotyping is required including their expression of marker genes at the protein level and sorting to allow functional assessments such as IL-4 production.

In BALB/c mice, Th2 cells become more activated in terms of TCR signalling and co-stimulation when infected with *H. polygyrus*. However, when C57BL/6 mice are infected with *H. polygyrus*, their Th2 cells have lower levels of co-stimulation and TCR signalling compared to their naïve counterparts. This suggests not only that Th2 cells from BALB/c mice are more active, but that in the C57BL/6 mouse there is more potent suppression of the Th2 response. This is in keeping with their parasitology where BALB/c mice are better able to clear the infection due to their increased Th2 activation.

Analysis at the single gene level revealed very few significant differences between Th2 cells from *H. polygyrus* infected BALB/c versus C57BL/6 mice, with the majority of differentially expressed genes being strain specific alleles such as MHC products and Ly6 antigens (Gumly et al., 1995; Lee et al., 2013; Rock et al., 1989; van de Run et al., 1989). Globally, the average expression of *Il4* decreased following *H. polygyrus* infection in mice of both C57BL/6 and BALB/c background. However, a finer-grained analysis showed that a sub-population of Th2 cells expressing high levels of *Il4* emerges in *H. polygyrus* infected BALB/c and C57BL/6 mice. This demonstrates the importance of analysing single cell RNA sequencing data at multiple levels from the single gene and single cell levels through to pathway analysis to obtain a full picture of the changes which occur during helminth infection.

Other genes upregulated by *H. polygyrus* in a subpopulation of Th2 cells include *Gata3, Icos, Gzma* (Granzyme A), *Cd69* and *Plac8*. GATA3 is the transcription factor associated with Th2 cells and the increase of GATA3 expression in Th2 cells from *H. polygyrus* infected mice is consistent with known activation of this subset in infection (Zhu, Yamane, Cote-Sierra, Guo, & Paul, 2006). The higher expression of ICOS is a trademark of Th2 cells, as it has been shown to be important to Th2 cell migration and enhances IL-4/IL-4R signalling (Tesciuba et al., 2008; M. Watanabe et al., 2005).

Granzymes are proteases which play a role in activation induced cell death and are well-characterized effector molecules of NK cells and CD8+ T cells (W. Hartmann et al., 2011; Loebbermann et al., 2012; Velaga et al., 2015). During infection with the filarial nematode *Litomosoides sigmodontis*, Granzyme A expression is associated with increased Th2 responses and clearance of the worm whereas Granzyme B expression contributes to susceptibility to helminth infection (W. Hartmann et al., 2011). This may suggest that Th2 cells increasing their *Gzma* expression during *H. polygyrus* infection are better equipped to clear the helminth than Th2 cells from naïve counterparts.

CD69 is a transmembrane C-type lectin which is rapidly upregulated upon TCR stimulation (Cibrián & Sánchez-madrid, 2017). The population of Th2 cells with high expression of CD69 may represent newly-activated antigen-specific Th2

cells recognising *H. polygyrus* antigens. The dynamics of CD69 and antigen specificity of CD4+ T cells during *H. polygyrus* infection will be further discussed in Chapter 5.

Placenta-specific 8 (Plac8), encoded by *Plac8*, is a cysteine-rich protein which has been implicated in tumour progression in mammals (Cabreira-Cagliari *et al.*, 2018). Plac8 has been shown to be an enriched in Th2 cells from HDM induced airway allergy in mice, although further work is necessary to test the importance of Plac8 in Th2 cells during type 2 inflammation (Tibbitt *et al.*, 2019). At least, it is known that expression of Plac8 limits IFNγ production by influenza-specific Th1 cells, suggesting that this gene product may favour Th2 responses by suppressing Th1 cytokine production during *H. polygyrus* infection (Slade, Reagin, Lakshmanan, Klonowski, & Watford, 2020).

Taken together, these data suggest that despite IL-10 signalling within Th2 cells from *H. polygyrus* infected mice, these Th2 cells show high activation and have sub populations of cells expressing high levels of many effector molecules. Differential expression of these genes and different expansion of the different subpopulations of Th2 cells may explain the difference in parasitological outcome in these two strains of mice.

As discussed above, Th2 cells from *H. polygyrus*-infected BALB/c and C57BL/6 receive IL-10 signalling which is an indicator of suppression or modulation of the Th2 population. The main suppressors of Teffector cells are T regulatory cells which can produce IL-10. Tregs are also upregulated by *H. polygyrus* infection and are important to prevent damage associated with overzealous immune responses and have been implicated in the balance between resistance and susceptibility for infection (Belkaid, 2007; Reynolds et al., 2012; K A Smith et al., 2016).

Single cell RNA sequencing revealed multiple clusters of Tregs which have different marker genes and may play different roles during infection. There are populations of Tregs which have received TCR stimulation and others which show no TCR signalling, which may represent cells responding to *H. polygyrus*-specific and non- specific antigens respectively. Better characterisation of the antigenic

nature of *H. polygyrus*, particularly at the T cell level, would assist in future dissection of Treg antigen specificity in helminth infection.

The different clusters of Tregs were shown to express different levels of gene transcripts associated with TCR stimulation, co-stimulation and cytokine signalling. It has been demonstrated that TCR signalling strength controls the phenotype and function of Tregs (Shevyrev & Tereshchenko, 2020; Zemmour et al., 2018), and it would be very interesting to test the hypothesis that TCR signalling strength may be a determinant of Treg function during *H. polygyrus* infection. A further observation is that not all subclusters showed recent TCR ligation, which may reflect the changing nature of the parasite as it migrates and develops through successive life cycle stages in the 7 days prior to analysis of the T cell population. A broader time course of T cell responses may in future provide more insight into this question.

The different Treg populations were also found to have different levels of IL-33 signalling. IL-33 is an alarmin cytokine which is released from necrotic epithelial cells and acts as signal that there is damage to the body. IL-33 signalling through its receptor ST2 in Tregs induces IL-13 secretion during lung injuries which dampens the immune response and leads to increased fibrosis, showing that IL-33 signalling is important during the wound healing response (Q. Liu et al., 2019; Schiering et al., 2014). There is also evidence that IL-33 can activate Tregs in response to lung injury that can suppress γδ T cells during the innate phase of the immune response (Faustino *et al.*, 2020).

In the colon, ST2+ Tregs are highly activated, show an increased migration compared to ST2- counterparts (Pastille et al., 2019), often co-express GATA3 and can produce Th2 cytokines in response to IL-33, showing that ST2+ Tregs are similar in phenotype to Th2 cells (Siede *et al.*, 2016). ST2+ Tregs are also able to suppress T helper cell proliferation more efficiently than ST2- counterparts in a manner partially dependent on IL-10 and TGFß (Siede et al., 2016). These reports may imply that Tregs which receive IL-33 signalling are more active and suppressive. However, in the *H. polygyrus* model, Tregs are not aberrant in ST2-deficient mice, which are highly susceptible to infection (Coakley *et al.*, 2017) . Taken together, these data show that there are different subtypes of Tregs in

naïve and *H. polygyrus* infected BALB/c and C57BL/6 mice which have distinct transcriptomes and may be performing distinct functions during infection.

To explore whether differential expansion or gene expression in Treg subpopulations in BALB/c and C57BL/6 mice may explain the difference in parasitology of these two mouse strains, their Treg clusters were compared in these two strains. Pathway analysis showed that in general, *H. polygyrus* infection of BALB/c mice causes an upregulation of pathways associated with TCR signalling and co-stimulation, suggesting these cells have seen antigen and received co-stimulation recently; one further interpretation is that BALB/c mice can induce *H. polygyrus* antigen-specific Tregs. However, in C57BL/6 mice, naïve Tregs have higher levels of TCR signalling, co-stimulation and cytokine signalling than Tregs from *H. polygyrus* infected mice. This suggests that C57BL/6 Tregs are not significantly activated in *H. polygyrus* infection and that the suppression of Th2 cells in C57BL/6 mice may not be mediated by Tregs alone.

When evaluating single genes upregulated by Tregs during infection, remarkably few genes showed major shifts upon infection in either BALB/c or C57BL/6 mice. However, granzyme A (*Gzma*) and granzyme B (*Gzmb*) are both downregulated upon infection in BALB/c and C57BL/6 mice, suggesting that this is a conserved response. The expression of granzymes by Tregs can directly suppress both B and T cells in a contact-dependent manner, such that for example reconstitution of DEREG mice with *Gzmb* KO Tregs leads to increased immune infiltrate in the lung of RSV-infected mice (Cao et al., 2007; Efimova & Kelley, 2009; Loebbermann et al., 2012). Notably, granzymes have been shown to be important during infection with the filarial nematode L*itomosoides sigmodontis* whereby Granzyme A is associated with parasite clearance and Granzyme B with susceptibility to infection (Hartmann et al., 2011).

CTLA-4 is a co-inhibitory receptor which can be used as a suppressive molecule by Tregs by preventing APC co-stimulation and inducing anergy in Teffector cells (Ovcinnikovs et al., 2019; L. Walker, 2013; Wing et al., 2008). During early *H. polygyrus* infection, Treg suppression of Teffector cells can be blocked using and α-CTLA-4 antibody, showing that this is an important suppressive strategy used by *H. polygyrus* experienced Tregs (Bowron *et al.*, 2020). Our data showing

upregulation at day 7 post infection further reinforces the importance of CTLA-4 during *H. polygyrus* infection.

The differences in the microbiota of the BALB/c and C57BL/6 mice may also impact the dynamics of the immune response. It has been shown previously that BALB/c and C57BL/6 mice housed in the same cage do not have identical microbiota, which may be due in part to their difference in IgA levels (Fransen *et al.*, 2015). The differences in microbiota between the strains may change the immune response and subsequent outcome of infection as it has been shown that the presence of the helminth alters the composition of the microbiota and the composition of the microbiota affects the helminths ability to colonise and maintain chronic infection (Reynolds, Finlay, Maizels 2015). Further studies on the microbiota composition of the two strains in this experiment are required to fully understand the difference in the responses between the mice including faecal transplants, infection of germ free mice and microbial diversity profiles.

The comparison of gene expression by Tregs from *H. polygyrus*-infected BALB/c and C57BL/6 mice showed, as found for Th2 cells, remarkably few differences other than those corresponding to allelic variation. However, changes in the average expression levels may hide important differences in subpopulations. On top of this, pathway analysis showed variation between the two strains responses that were hidden at the single gene level, showing the importance of scrutinising the data at multiple biological levels.

3.6 Summary

- Th2 cells are the most active CD4+ T cells within *H. polygyrus* infected mice

- Th2 cells from *H. polygyrus* infected BALB/c and C57BL/6 mice show signs of suppression via IL-10 signalling

- Tregs and Th2 cells from *H. polygyrus* infected BALB/c and C57BL/6 mice have similar average gene expression at a single gene level but differ in

their expression of genes associated with TCR stimulation, co-stimulation and cytokine signalling

- Tregs and Th2 cells from BALB/c mice appear to be more transcriptionally active during *H. polygyrus* infection when compared to Tregs from infected C57BL/6 mice

- Differences in the Th2 and Treg populations in BALB/c and C57BL/6 mice may explain the difference in parasitology seen during *H. polygyrus* infection

Chapter 4 Treg Characterisation

4.1 Introduction

In recent years the dogma of one factor, one fate in terms of T helper cell subtypes has proven to be overly simplistic (Eberl & Pradeu, 2017; White, McManus, et al., 2020). Tregs are commonly described as CD4+ CD25+ Foxp3+ T cells which patrol the body controlling the immune system to prevent inappropriate responses such as recognising self-antigen, immune responses to the microbiota or overzealous responses to infection which can cause major damage to the host (Belkaid, 2007; Rick M. Maizels & Smith, 2011; Sakaguchi et al., 2008; White, McManus, et al., 2020). However, it is increasingly clear that there are many different types of Tregs which express a plethora of different transcription factors, as well as suppressive molecules like coinhibitory molecules and a range of different cytokines (White, McManus, et al., 2020). This suggests a level of specialisation of the Treg compartment which may lead to more efficient suppression of Teffector cells.

4.1.1 Treg subtypes

Classically, three main types of regulatory T cell have been recognised: nTregs (natural) which originate from the thymus and are often selected for recognition of self-antigen and antigens from the microbiome; pTregs (peripheral) which are induced in the periphery from naïve Th0 cells and are dependent on TGFß; and finally Tr1 cells which do not express Foxp3 but produce high levels of IL-10 (Shevach & Thornton, 2014; Shevyrev & Tereshchenko, 2020). However, the functional borderlines between nTregs and pTregs are not clear, and a number of other types of regulatory T cells are found in the immune system. Understanding which Tregs impact which part of the immune system is imperative to be able to understand the immune landscape and work towards treatments of inflammatory diseases and chronic infections.

4.1.2 Co-expression of transcription factors

There have been many examples of Foxp3+ Tregs expressing transcription factors more commonly associated with Teffector subtypes. These include T-bet+ Tregs

(Koch *et al.*, 2009; Levine *et al.*, 2017; Sprouse *et al.*, 2018), GATA3+ Tregs (Schiering et al., 2014; Wohlfert et al., 2011) and RORγt+ Tregs (Eberl & Pradeu, 2017; Ohnmacht et al., 2015; Sefik et al., 2016). The stability of these subsets is often debated with some being long-lived and others reverting to Foxp3- Teffector cells or to the conventional Treg phenotype; hence these subtypes may represent an intermediate and bipotential population between Tregs and Teffector cells (Koch et al., 2009; Levine et al., 2017; Ohnmacht et al., 2015).

The exact role of these transcription factor-positive Tregs has not been fully elucidated but many hypothesise that they are more capable of suppressing their corresponding Th subset (Koch et al., 2009; Levine et al., 2017; Ohnmacht et al., 2015). This may be due to shared trafficking via common chemokine receptors which localise the Tregs to the same environment or tissue as the Th subtype sharing the same transcription factor (Koch et al., 2009; Levine et al., 2017; Ohnmacht et al., 2015). The relationship between such specialised Tregs and their corresponding Th subtype during *H. polygyrus* infection is largely unknown, and dissecting the Treg signature of infected mice may lead to greater understanding of the immune response against human helminthiases.

4.1.2.1 T-bet+ Tregs

T-bet is the transcription factor commonly associated with Th1 cells which primarily recognise and respond to intracellular viruses and bacteria mounting a type 1 response (Luckheeram *et al.*, 2012). It is thought that Th1 cells and Th2 cells are mutually exclusive and so the more GATA3+ Th2 cells there are, the fewer T-bet+ Th1 cells there will be. Since *H. polygyrus* infection is a strong inducer of the Th2 response, it may be expected that there would be little expression of T-bet in *H. polygyru*s-infected mice. However, at day 7 post-infection of C57BL/6 mice, there is a significant increase in IFNγ+ CD8+ T cells and IFNγ production when the MLN is restimulated *in vitro* with α-CD3 (Filbey *et al.*, 2014). Loss of IFNγ signalling in enteric glial cells during *H. polygyrus* infection leads to increased granuloma sizes and significantly higher number of innate immune cells in the granuloma (Progatzky *et al.*, 2021). IFNγ production is also able to revert the intestine to a fetal-like structure during *H. polygyrus* infection with hyper-proliferation of the crypts of the intestine which is lost in

IFNγ KO mice (Nusse *et al.*, 2018). The impact of losing IFNγ signalling during infection with *H. polygyrus* shows the requirement for type 1 responses to control the immune response to infection which may imply a role of Th1 cells.

Tregs are also able to co-express T-bet and Foxp3, although this population has been primarily associated with type 1 inflammation (Koch *et al.*, 2009). For example, infection of T-bet$^{fl/fl}$Foxp3^{Cre} mice with *Toxoplasma gondii*, a parasite which induces a Th1 response, leads to death due to increased pathology associated with infection (Warunek *et al.*, 2021). This shows that T-bet+ Tregs are required to control the Th1 response and prevent overzealous immune responses to infection (Warunek *et al.*, 2021). There is also an increase in the number of T-bet+ Tregs during infection with *Mycobacterium* and these Tregs expressed CXCR3, a homing receptor usually found on Th1 cells, suggesting shared migration with their Th1 counterparts (Koch *et al.*, 2009). T-bet+ Tregs which can produce IFNγ are increased in the lamina propria of ulcerative colitis and Crohn's disease patients and are thought to exacerbate the disease rather than suppress the Th1 response (di Giovangiulio *et al.*, 2019). Multiple studies also show IFNγ production from Th1-like Tregs which suggests that T-bet expression in Foxp3+ Tregs can mark both Tregs which suppress Th1 cells and Th1-like Tregs which act more like Th1 cells and contribute to immunopathological diseases (di Giovangiulio et al., 2019; Feng, Cao, Weaver, Elson, & Cong, 2011; Kitz et al., 2016; Koch et al., 2009; Oldenhove et al., 2009; Warunek et al., 2021).

4.1.2.2 GATA3+ Tregs

GATA3 is the transcription factor associated with Th2 cells which are central to the anti-helminth immune response (Luckheeram *et al.*, 2012; Nutman, 2015). GATA3 is also required for thymic selection of T cells and was also found to be crucial to Treg stability, plasticity and effector function at barrier sites such as small intestine, colon and dermis (Wan, 2014; Wohlfert et al., 2011; Xu et al., 2018). As newly emerging Tregs do not express GATA3, its expression in Tregs is believed to be induced by TCR engagement and IL-2 (Wohlfert *et al.*, 2011). Initial studies showed that while GATA3$^{fl/fl}$ Foxp3$^{GFP\text{-}Cre}$ mice survived into adulthood, at around 16 weeks of age they developed a lymphoproliferative

disease which manifested as enlarged lymph nodes and spleen with lymphocyte infiltration of various tissues like the lung and pancreas (Y. Wang, Su, & Wan, 2011). Foxp3^{Cre} GATA3$^{fl/fl}$ mice also show limited Treg accumulation at barrier sites and transferring Tregs from Foxp3^{Cre} GATA3$^{fl/fl}$ mice is not sufficient to protect against T cell transfer colitis (Wohlfert *et al.*, 2011). GATA3+ Tregs are also elevated in asthmatic human samples and produce IL-4, potentially exacerbating the disease (T. Chen et al., 2018). Together this suggests that GATA3+ Tregs are important for the maintenance of tolerance at barrier sites and play a particularly important role in type 2 immune responses, even in humans. Since *H. polygyrus* resides in the intestine and induces a highly-skewed Th2 response, it is possible that GATA3+ Tregs are involved in either dampening or heightening the immune response against the helminth.

4.1.2.3 RORγt+ Tregs

RORγt is the transcription factor associated with Th17 cells which classically respond to extracellular bacteria and fungal infection (Luckheeram *et al.*, 2012). The expression of RORγt with Foxp3 is associated with increased expression of many Treg suppressive molecules such as CTLA-4, IRF4, GITR and ICOS which can be seen at an RNA and protein level which suggests these specialised Tregs are more suppressive than conventional Tregs (Ohnmacht et al., 2015; B. Yang et al., 2016).

RORγt+ Tregs have been found to be dependent on vitamin A metabolism, as their numbers are reduced when mice are given RARi, an inhibitor of the retinoic acid receptor (Ohnmacht *et al.*, 2015). Numbers are also reduced in germ-free mice, but can be restored by recolonisation of the gut by bacterial commensals, implicating the microbiota as a driver of RORγt+ Tregs (Ohnmacht *et al.*, 2015).

RORγt+ Tregs have also been implicated as major players in the balance between resistance and susceptibility to *H. polygyrus,* as Foxp3^{Cre} RORγt$^{fl/fl}$ mice are able to clear *H. polygyrus* infection to around $0.5*10^4$ eggs per gram of faeces (EPG) at day 31 post infection, whereas their wild type counterparts had an average of around $3.5*10^4$ EPG at day 31 post infection (Ohnmacht *et al.*, 2015). This suggests that RORγt+ Tregs are involved in suppressing the type 2

response against helminths, so that removal of this suppression leads to increased Th2 cell activity and worm expulsion (Ohnmacht *et al.*, 2015). The involvement of RORγt+ Tregs in suppressing the type 2 immune response is thought to be driven by the mutual suppression of the different immune response types (Eberl & Pradeu, 2017; Ohnmacht et al., 2015). For example, in Foxp3 ^{Cre} RORγt$^{fl/fl}$ mice, the loss of RORγt expression in Tregs leads to a 2-fold increase in both GATA3+ Th2 cells and GATA3+ Tregs and the associated cytokines IL-4, IL-5 and IL-13 (Ohnmacht *et al.*, 2015). The opposite is also true for Foxp3^{Cre} GATA3$^{fl/fl}$ mice which have a lost GATA3 expression in Tregs and leads to a 2-fold expansion of RORγt+ Tregs and a 3-fold increase in IL-17A expression in Tregs (Wohlfert *et al.*, 2011).

The interactions between RORγt+ Tregs and the type 2 immune response are both cell-intrinsic and -extrinsic and are independent of IL-10 production (Ohnmacht *et al.*, 2015). RORγt+ Tregs express high levels of CTLA-4 which can limit the availability of CD80 and CD86 on antigen-presenting DCs and in this way can limit their ability to induce Th2 effector cells (Ohnmacht *et al.*, 2015). This pro-tolerization effect is lost in Foxp3^{Cre} RORγt$^{fl/fl}$ mice in which DCs express significantly more CD80 and CD86 and are thus more capable of inducing Teffector cells (Ohnmacht *et al.*, 2015). There also appears to be a mutual exclusion of GATA3 and RORγt in Tregs which is dependent on STAT3, as loss of STAT3 in Tregs leads to co-expression of GATA3 and RORγt (Ohnmacht *et al.*, 2015). This mutual exclusion is thought to be due to STAT3 signalling, due to cytokines such as IL-6, IL-27, allowing RORγt expression but inhibiting expression of GATA3 (Wohlfert *et al.*, 2011). In human renal cell carcinoma, overexpression of GATA3 inhibits STAT3 signalling through IL-6, showing that GATA3 can also inhibit STAT3 phosphorylation and prevent RORγt expression (Shi *et al.*, 2020). Together these observations imply that RORγt+ Tregs control the type 2 response by limiting the number of GATA3+ cells at tissue sites, in part by tolerization of APCs.

4.1.3 The importance of IL-6 during *H. polygyrus* infection

Traditionally, IL-6 is involved in the balance between Tregs and Th17 effector cells in a paradigm in which cells receiving TGFß alone become Foxp3+ Tregs and

those which receive TGFß and IL-6 become Th17 cells (Dienz & Rincon, 2009; Luckheeram et al., 2012). However, it has also been shown that overexpression of IL-6 leads to both increased Th17 and Treg cells and lower peripheral Tregs (Fujimoto *et al.*, 2011). In mice deficient for IL-6, clearance of *H. polygyrus* is accelerated alongside increased Th2 responses and cytokine production (Katherine A. Smith & Maizels, 2014). Notably, monoclonal antibody blockade of IL-17 had no effect on worm burden, suggesting that the phenotype of increased helminth immunity is not dependent on Th17 cell dysregulation (Katherine A. Smith & Maizels, 2014). However, one cell subset that was impacted in mice lacking IL-6 was the Treg compartment, which comprised fewer Helios+ natural Tregs and expressed lower levels of GATA3 (Katherine A. Smith & Maizels, 2014). Taken together these findings suggest that IL-6 does not convert Tregs, at least under the conditions of a *H. polygyrus* infection, but that its presence or absence qualitatively modifies the Treg population and their suppressive capacity.

4.1.4 Expression of co-inhibitory molecules by Tregs

Another aspect of Treg specialisation is the expression of different suppressive molecules which can inhibit specific pathways and cell types. One family of suppressive molecules that are commonly expressed by Tregs are co-inhibitory receptors. These molecules are used to give inhibitory signals to immune effector cells at the co-stimulation step of T cell activation to prevent their activation and induce tolerance (L. Chen & Flies, 2013; Lucca & Dominguez-Villar, 2020). Co-inhibitory receptors and their ligands are involved in many Treg processes from Treg selection in the thymus to suppression of Th cells (Kumar, Bhattacharya, & Prabhakar, 2018; Lucca & Dominguez-Villar, 2020). As detailed below, these molecules are also commonly upregulated in Tregs from multiple helminth infections (Ahn, Kang, Kim, & Yu, 2016; Finney et al., 2007; Henry J. McSorley, Harcus, Murray, Taylor, & Maizels, 2008; Redpath et al., 2013; Taylor et al., 2007; Walsh, Smith, & Fallon, 2007; K. Watanabe et al., 2007; White, McManus, et al., 2020).

4.1.4.1 CTLA-4

CTLA-4 (cytotoxic T-lymphocyte-associated protein 4, CD154) is a member of the CD28 superfamily and shares CD80 and CD86 as its ligands (Kumar et al., 2018; Lucca & Dominguez-Villar, 2020; L. S. K. Walker & Sansom, 2015). CTLA-4 binds CD80 and CD86 with higher affinity than CD28 and competes with CD28 for binding to their receptors and can remove CD80/86 from the surface of the APC, resulting in reduced co-stimulation and reduced T cell activation (Hou et al., 2015; Linsley et al., 1991; Ovcinnikovs et al., 2019; Qureshi et al., 2011; Walunas et al., 1994). As discussed previously, co-stimulation is required for activation of CD4+ T cells and is usually delivered by CD28 binding to either CD80 or CD86, leading to T cell activation and proliferation (Kumar et al., 2018; Lucca & Dominguez-Villar, 2020; Wing et al., 2008). CTLA-4 acts in opposition to CD28, where CD28 engagement with CD80/86 activates the T cell and CTLA-4 binding to CD80/86 gives the T cell an inhibitory signal which prevents activation and proliferation (Kumar et al., 2018; Lucca & Dominguez-Villar, 2020). CTLA-4 is found at very low levels in naïve T cells and is upregulated on activated T cells (Kumar et al., 2018; Lucca & Dominguez-Villar, 2020; L. Walker, 2013; L. S. K. Walker & Sansom, 2015).

There are conflicting reports of the role of CTLA-4 in Treg cells and how loss of CTLA-4 affects their suppressive function (Kumar et al., 2018; Lucca & Dominguez-Villar, 2020; L. Walker, 2013; L. S. K. Walker & Sansom, 2015). In thymic Tregs but not Foxp3- T cells, stable CpG hypomethylation was seen in not only the *Foxp3* locus but also *Il2ra* (CD25) and *Ctla4,* suggesting that CTLA-4 expression is stably high in tTregs (Ohkura & Sakaguchi, 2020). The phenotype of CTLA-4 KO mice is very similar to that of Scurfy (Foxp3 mutant) mice which are deficient in Tregs altogether (L. S. K. Walker & Sansom, 2015). This suggested that CTLA-4 and Tregs act in the same way to prevent T cell activation (L. Walker, 2013; L. S. K. Walker & Sansom, 2015). $Foxp3^{Cre}$ $CTLA\text{-}3^{fl/fl}$ mice die at around 7 weeks of age and show dysregulation of T cell responses associated with a lack of thymic Tregs, demonstrating an essential role of CTLA-4 in the development of tolerogenic Tregs (Lucca & Dominguez-Villar, 2020; Wing et al., 2008). However, studies blocking or interfering with CTLA-4 in the intact adult immune system showed very little difference in Treg suppressive capacity,

suggesting once thymic Tregs are established, there are compensatory pathways which can act in the absence of CTLA-4 (L. Walker, 2013).

One major role of Tregs expressing CTLA-4 during inflammation is inhibition of DCs and other cells which express CD80 and CD86 (Hou *et al.*, 2015; Ovcinnikovs *et al.*, 2019). When CTLA4+ Tregs are cultured with DCs *in vitro*, a phenomenon known as trans-endocytosis or trogocytosis removes CD80 and CD86 from the dendritic cell surface and internalises it within the Treg, in a process that is dependent on the TCR (Hou et al., 2015; Ovcinnikovs et al., 2019; Qureshi et al., 2011). This prevents the DC from activating more T cells by limiting their capacity to provide co-stimulation (Hou et al., 2015; Ovcinnikovs et al., 2019; Qureshi et al., 2011). A similar phenomenon has also been reported, to a lesser extent, in Foxp3- Teffector cells (Lucca & Dominguez-Villar, 2020; Ovcinnikovs et al., 2019). During *H. polygyrus* infection, there is a tolerization of dendritic cells which leads to lower expression of CD80 and CD86 (Katherine A. Smith et al., 2011), which may be due in part to the action of CTLA-4+ Tregs.

It has also been shown that CTLA-4+ Tregs induce APCs to express indoleamine 2,3-dioxygenase (IDO), an enzyme involved in tryptophan catabolism (Fallarino et al., 2003; Mellor & Munn, 2004). The kynurenine products of this reaction are able to induce Tregs, suggesting an amplification loop for Treg expansion through CTLA-4 and APCs (Fallarino *et al.*, 2003).

CTLA-4 has now been shown to be upregulated on Tregs in many different helminth infections including *Brugia malayi, Litomosoides sigmodontis, Schistosoma mansoni* and *Trichinella spiralis* (Ahn et al., 2016; Finney et al., 2007; Henry J. McSorley et al., 2008; Walsh et al., 2007; White, McManus, et al., 2020). In the case of *H. polygyrus*, it was recently shown that Tregs isolated from the mice 7 days post-infection are unable to suppress CD4+ T cell responses to ConA in the presence of a CTLA-4 blocking antibody (Bowron *et al.*, 2020). This finding suggests that the suppression of Th2 cells by Tregs early in infection is mediated by CTLA-4 (Bowron *et al.*, 2020). However, the surface expression of CTLA-4 was shown to decrease on CD25+ CD4+ 'Tregs' at day 28 post-*H. polygyrus* infection (Finney *et al.*, 2007). The dependence on CTLA-4 for Treg-mediated suppression during early *H. polygyrus* infection while downregulating

its expression on Tregs at 28 days post-infection shows that the expression of CTLA-4 requires further investigation during *H. polygyrus* infection.

4.1.4.2 PD-1

PD-1 (programmed cell death 1, CD279) is another member of the CD28 superfamily which, like CTLA-4, gives an inhibitory signal to T cells when it engages with its ligands PD-L1/PD-L2 (programmed cell death ligand 1/2) and leads to cell cycle arrest (Kumar et al., 2018; Lucca & Dominguez-Villar, 2020). PD-L1 and PD-L2 are expressed on many cells in the immune system including but not limited to T cells, B cells, DCs and macrophages (Kumar et al., 2018; Lucca & Dominguez-Villar, 2020). Unlike CTLA-4 which is rapidly endocytosed and degraded, PD-1 is stably expressed on the surface of activated T cells (Kumar et al., 2018).

Tregs express high levels of both PD-1 and PD-L1 and the axis between these two partners has been implicated in the expansion and maintenance of Tregs as PD-1 KO naïve T cells have reduced iTreg induction *in vitro* and iTregs induced in the presence of TGFß and PD-L1 there is 2 fold increase in iTregs (Francisco *et al.*, 2009). iTregs induced in the presence of PD-L1 were also able to suppress CD4+ T cell proliferation significantly more than iTregs induced without PD-L1 (Francisco *et al.*, 2009; Tan *et al.*, 2021). PD-1 deficient Tregs show increased Ki-67 and increased expression of other coinhibitory receptors CTLA-4, GITR and TIGIT, suggesting higher activation (Tan *et al.*, 2021). Foxp3^{Cre} PD-1$^{fl/fl}$ Tregs are also able to suppress Teffector cell proliferation more efficiently than wild type counterparts, showing that PD-1 expression in Tregs limits their suppressive capacity (Tan *et al.*, 2021).

In effector cells, PD-1 signalling is also inhibitory, for example downregulating casein kinase 2 (CK2) to restrict T cell growth and survival through inhibition of TCR signalling (Patsoukis, Li, Sari, Petkova, & Boussiotis, 2013). PD-1 signalling in CD8+ T cells downregulates the expression of the TCR by increasing its internalisation, and the same process is thought to be found in CD4+ T cells (Karwacz *et al.*, 2011). PD-1 blockade has been used to reverse suppression in the tumour microenvironment and allows Teffector cells to escape exhaustion,

become activated and destroy the tumour (Iwai *et al.*, 2002; Topalian *et al.*, 2012). PD-1 blockade is being trialled as a cancer immunotherapy in human patients (Iwai *et al.*, 2002; Topalian *et al.*, 2012).

There is also upregulation of PD-1 on Tregs from helminth-infected hosts including those with *S. mansoni* and *L. sigmodontis* (Redpath et al., 2013; Taylor et al., 2007; Walsh et al., 2007; K. Watanabe et al., 2007; White, McManus, et al., 2020). The potential role of PD-1 expression on Tregs from *H. polygyrus*-infected mice has not been explored and will be discussed in this chapter.

4.1.4.3 TIGIT

TIGIT (T-cell immunoreceptor with Ig and ITIM domains) is a co-inhibitory receptor which does not belong to the CD28 superfamily; instead TIGIT is part of the PVR (polio virus receptor) family and competes with the co-activating molecule CD226 for their shared ligands CD155 and CD112 (L. Chen & Flies, 2013; Lucca & Dominguez-Villar, 2020). TIGIT expression has been seen on Tregs, Tfh cells and NK cells. TIGIT, like CTLA-4 and PD-1, is expressed at low levels on naïve T cells and is upregulated after TCR engagement (Lucca & Dominguez-Villar, 2020).

A potential role for TIGIT in the response against *H. polygyrus* lies in TIGIT's ability to attenuate Th1 and Th17 induction, allowing the Th2 response to flourish (Joller *et al.*, 2014). Evidence has also emerged that while TIGIT is known as an inhibitory molecule, TIGIT is able to increase the Th2 response (Kourepini *et al.*, 2016). When Th2 cells are cultured *in vitro* with TIGIT blocking antibody, there is significant reduction of IL-4, IL-13, IL-5 and IL-10 production and a reduction in *Gata3* mRNA (Kourepini *et al.*, 2016).

When TIGIT is expressed on Tregs, the interaction between TIGIT and its ligands on APCs induces DC production of IL-10 and TGF-β and inhibits IL-12 production which in turn suppresses the Teffector response (Joller et al., 2014; X. Yu et al., 2009). TIGIT+ Tregs have also been shown to express higher levels of other Treg suppressive molecules and other coinhibitory receptors including PD-1, CD103, and CD39 than TIGIT− counterparts, suggesting that they have enhanced suppressive capacity (Joller et al., 2014; Lucca & Dominguez-Villar, 2020). TIGIT

mRNA also been seen to increase in Th2 cells from *Litomosoides sigmodontis* infected mice (Knipper, Ivens, & Taylor, 2019). However, at the protein level, upregulation of TIGIT was not seen in CD4+ T cells from *Litomosoides sigmodontis* infected mice (W. Hartmann et al., 2019). In the broader Th2 context, the expression of TIGIT increases during airway allergy in BALB/c mice, while T cells from children with asthma show hypomethylation of the TIGIT locus, again implicating TIGIT as a central player in the type 2 immune response (Kourepini et al., 2016; I. v. Yang et al., 2015).

To summarise, TIGIT is a co-inhibitory receptor which favours the Th2 response by limiting the induction of Th1 and Th17 cells, and its expression on Tregs is associated with suppression of those modes of immunity. Despite its importance to the type 2 immune response, the dynamics of TIGIT have not been assessed during *H. polygyrus* infection and will be explored further in this chapter.

4.2 Aims

- To investigate the locations where Tregs are induced by *H. polygyrus* infection

- To assess the co-expression of different transcription factors in Tregs during *H. polygyrus* infection

- To investigate the role of IL-6 and RORγt+ Tregs during *H. polygyrus* infection

- To assess the expression of key Treg suppressive molecules during *H. polygyrus* infection

4.3 Results

4.3.1 Dynamics of Treg expansion at d7 and d14 post *H. polygyrus* infection

The expansion of Tregs during *H. polygyrus* infection has been observed in different strains of mice, most often in BALB/c and C57BL/6. To assess the dynamics of these cells in these two strains, mice were infected for 7 or 14 days and their MLN assessed for changes in the CD4+ T cell population. As seen in Figure 4.1A, BALB/c mice exhibit an increase in the proportion of Tregs within the CD4+ compartment at d7 post *H. polygyrus* infection. In terms of percentage, this expansion returns to near homeostatic levels at d14 post-*H. polygyrus* infection (Figure 4.1A). Similarly, in C57BL/6 mice, the proportion of Tregs within the CD4+ T cell compartment expands at d7 post-*H. polygyrus* infection and returns to pre-infection percentages at d14 post-*H. polygyrus* infection (Figure 4.1B).

It is important to note, however, that during *H. polygyrus* infection there is a large expansion in the number of cells in the MLN, so that even if the proportion of the CD4+ T cells which express Foxp3 may not have changed, the total number of Tregs found in the MLN is much greater. This indeed is observed, as can be seen in Figure 4.1C, there is an increase in MLN Tregs at d7 post *H. polygyrus* infection in BALB/c mice (although not reaching statistical significance), and a further substantial (and highly significant) increase by day 14 post-infection (Figure 4.1C). In the case of C57BL/6 mice, the increase in the number of Tregs at day 7 post-infection is more marked and significant than in BALB/c, and continues to grow by day 14 (Figure 4.1D). Interestingly, while the C57BL/6 strain therefore appears to expand Tregs more rapidly, the absolute number of Tregs by day 14 of infection does not reach the same level as in their BALB/c counterparts (Figure 4.1C-D). These data suggest that the dynamics of Treg induction during *H. polygyrus* infection differ between fully-susceptible C57BL/6 mice and partially-resistant BALB/c mice.

It has been suggested that Tregs with higher expression of Foxp3 have an increased suppressive capacity, in which case the quantitative level of Foxp3 may reflect the functional potential of each cell (Chauhan, Saban, Lee, & Dana,

2009; Venken et al., 2008). The mean fluorescence intensity (MFI) of Foxp3 was therefore evaluated in the different populations from naïve and infected mice of each strain. Figure 4.1E shows that Foxp3 expression in BALB/c Tregs is significantly increased at d7 post *H. polygyrus* infection but declines to below steady-state expression levels at d14. In the case of C57BL/6 mice, baseline MFI values are much higher than in BALB/c mice, and the expression level of Foxp3 does not change when mice are infected with *H. polygyrus* (Figure 4.1F). It remains to be ascertained if Foxp3 levels in *H. polygyrus* induced Tregs are predictive of suppressive function, but if so then the dynamics of C57BL/6 and BALB/c Tregs during *H. polygyrus* infection show different patterns likely to impinge on the different outcome of *H. polygyrus* infection in the two strains.

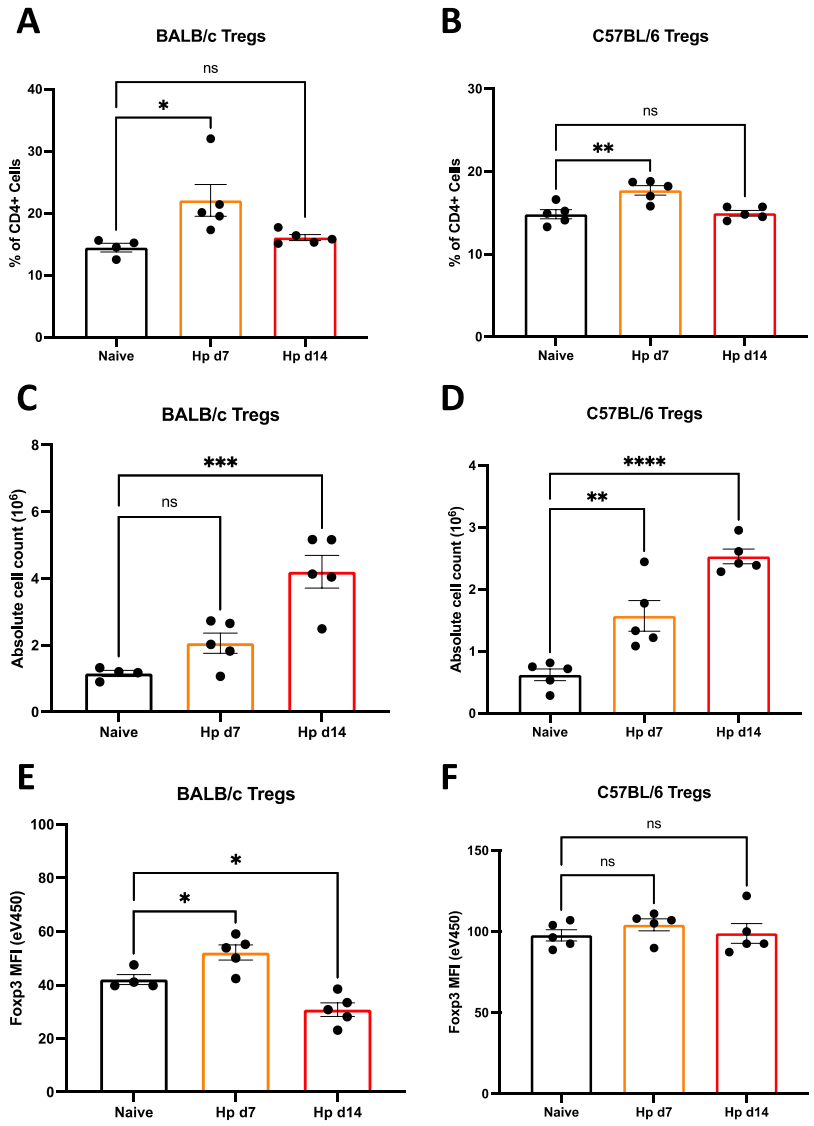

Figure 4.1 The dynamics of Treg expansion at d7 and d14 H. polygyrus infection.
(A-B) The proportion of Tregs within the CD4+ T cell population in the MLN of naïve (black), *Hp* d7 (orange) and *Hp* d14 (Red) in BALB/c (A) and C57BL/6 (B) mice. (C-D) The absolute number of Tregs in the MLN of naïve (black), *Hp* d7 (orange) and *Hp* d14 (Red) in BALB/c (C) and C57BL/6 (D) mice. (E-F) The MFI of Foxp3 (eV450) in Tregs from the MLN of BALB/c (E) and C57BL/6 (F).
Graphs representative of 3 experiments. Each point represents a single mouse, error bars represent the standard error of the mean. In each group n=5, except BALB/c naïve where n=4. Normality tested using a Shapiro-Wilk normality test. Significance tested using an ordinary one-way ANOVA and Holm-Šídák's multiple comparisons test. ns P>0.05, * P<0.05, ** P<0.01, ** P<0.001, **** P<0.0001

4.3.2 Dynamics of Th2 cells at d7 and d14 post *H. polygyrus* infection

On the opposite side of the equation to Tregs, Teffector cells are required to drive the immune response and expedite clearance of the worm, primarily through the expansion of Th2 cells. To understand the dynamics of the worm clearance response, CD4+ Foxp3- GATA3+ Th2 cells from BALB/c and C57BL/6 *H. polygyrus* infected mice were compared. As seen in Figure 4.2A and Figure 4.2B, there are similar increases in the percentage of Th2 cells in each strain at d7 post infection, and a degree of contraction at d14, although the frequencies are still significantly above naïve Th2 levels. A more striking difference in the Th2 response to *H. polygyrus* in BALB/c and C57BL/6 mice can be seen, however, in the absolute number of MLN Th2 cells during different stages of *H. polygyrus* infection. As shown in Figure 4.2C and D, the number of Th2 cells expands at d7 post infection in both strains, but of note C57BL/6 Th2 numbers are around 10-fold lower than those in BALB/c mice; in both strains, numbers contract by d14 post infection but remain higher in absolute terms in BALB/c mice. It is likely that the ratio of Tregs to Th2 cells is a determining factor for the outcome of infection. Comparing the absolute cell counts of Tregs versus Th2 cells, BALB/c mice have more Tregs than Th2 cells in naïve conditions, at day 7 post infection BALB/c Th2 cells outnumber Tregs and then contract to below Treg numbers by day 14 (Figure 4.2E). In C57BL/6 mice, Tregs outnumber Th2 cells in naïve and *H. polygyrus* infected mice at day 7 and day 14 post-infection (Figure 4.2F). When comparing the proportion of Tregs to Th2 cells in both strains, it is clear that by day 14, the ratio of Tregs to Th2 cells is higher in C57BL/6 mice than in BALB/c mice at the same time point (Figure 4.2E-F), which further shows that C57BL/6 mice have a Treg dominated response. With more Tregs than Th2 cells in C57BL/6 mice during infection, it is likely that Th2 cells from these mice are receiving more suppression than Th2 cells from the Th2 dominating BALB/c mice and may this explain their difference in infection outcome.

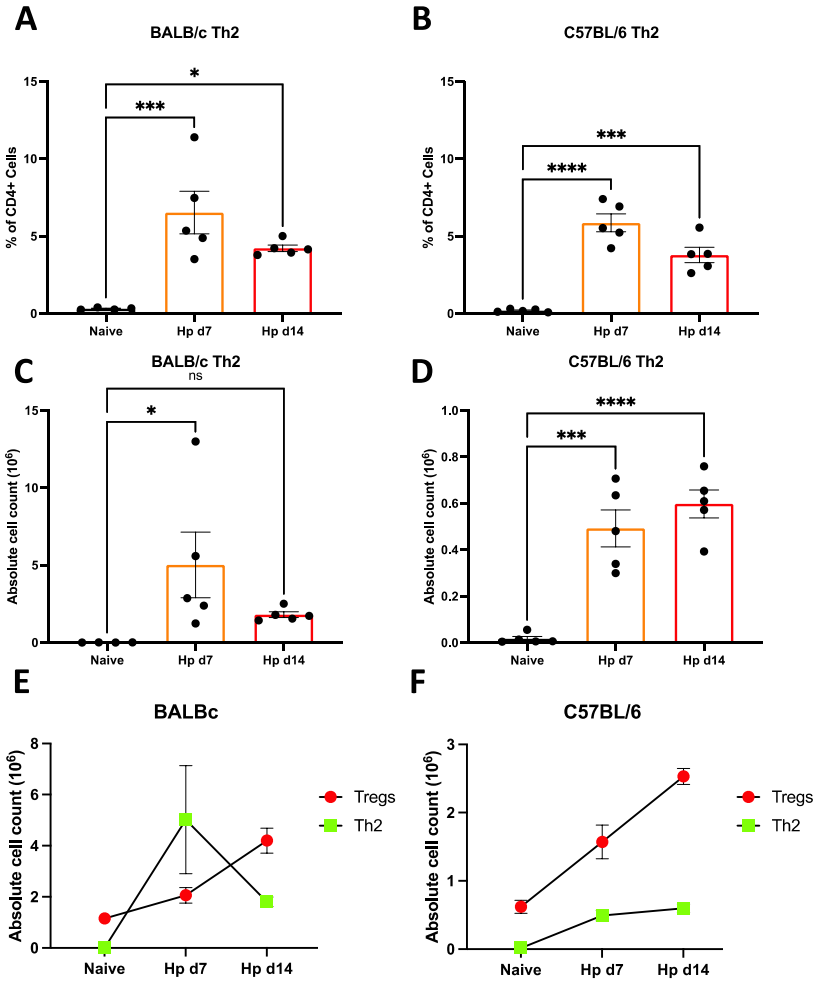

Figure 4.2 The dynamics of Th2 expansion at d7 and d14 H. polygyrus infection. (A-B) The proportion of Th2 cells within the CD4+ T cell population in naïve (black), *Hp* d7 (orange) and *Hp* d14 (Red) in the MLN of BALB/c (A) and C57BL/6 (B) mice. (C-D) The absolute number of Th2 cells in the MLN of naïve (black), *Hp* d7 (orange) and *Hp* d14 (Red) in BALB/c (C) and C57BL/6 (D) mice. (E-F) Line graphs showing the mean absolute number of Tregs and Th2 cells in the MLN of naïve, *Hp* d7 and *Hp* d14 in (E) BALB/c and (F) C57BL/6 mice.
Graphs representative of 3 experiments. Each black point represents a single mouse, error bars represent the standard error of the mean. In each group n=5, except BALB/c naïve where n=4.Normality tested using a Shapiro-Wilk normality test. Significance tested using an ordinary one-way ANOVA and Holm-Šídák's multiple comparisons test. ns P>0.05, * P<0.05, ** P<0.01, ** P<0.001, **** P<0.0001

4.3.3 Location of Treg expansion during *H. polygyrus* infection

H. polygyrus adult parasites reside in the duodenum of the small intestine (Figure 4.3A). However, effects of infection have been seen on a systemic level and *H. polygyrus* can attenuate the development of EAE in the central nervous system and allergic asthma in the airways (Kitagaki et al., 2006; Saunders et al., 2007; White, Johnston, et al., 2020; Wilson et al., 2005). To evaluate the systemic effects of *H. polygyrus* on Tregs, multiple tissues both proximal and distal to the site of infection we evaluated for Treg levels.

Figure 4.3A shows in schematic form the organs and structures found within the peritoneal cavity, including the worm in the duodenum of the intestine together with the mesenteric lymph nodes and their respective draining regions. Examining first the small intestine lamina propria (SILP) from the duodenum of C57BL/6, there is an uplift in the proportion of Foxp3+CD4+ T cells, although quite variable and not attaining statistical reach significance (Figure 4.3B). One factor in the variability is that SILP cells from *H. polygyrus* infected mice rapidly lose viability after removing from the mouse, and the degree to which this affects different cell type is not known.

Peyer's patches are tertiary lymphoid organs that are found embedded in the epithelium of the small intestine, and which capture and respond to luminal antigens. There is a highly significant increase in Tregs in the Peyer's patches by day 7 of *H. polygyrus* infection, rising from a mean of 11.8% to 18.42% of CD4+ cells (Figure 4.3C), confirming that the gut associated lymphoid tissue (GALT) is responding to the helminth infection.

There is also a trend towards an increase in Tregs in the colonic lamina propria which suggests either that helminths or their products can exert effects downstream into the colon, or that the colon is responding to systemic signals (Figure 4.3D). The peritoneal cavity was also assessed by analysis of PBS-flushed peritoneal exudate cells (PEC) to determine the proportion of Tregs found with or without *H. polygyrus* infection. Surprisingly, despite the close association between the PEC and the intestine, there was only slight expansion of Tregs in this cavity during *H. polygyrus* infection, which did not reach significance (Figure

4.3E). A similar result was obtained by analysis of BALB/c mice, in parallel with the data from C57BL/6 strain.

More distal tissues were also examined, but no expansion of Tregs was seen in either the spleen (Figure 4.3F) or the inguinal lymph nodes (iLN, Figure 4.3G) which drain the limbs of the mouse, and in the latter case the same outcome was found with BALB/c mice. Taken together, these results suggest that *H. polygyrus* drives an expansion of Tregs which is apparent in the small intestine Peyer's patches and MLN which are all in close association with the infection site, but by day 7 of infection at least, is not significantly reproduced in in the peritoneal cavity or more peripheral sites like the spleen and iLN.

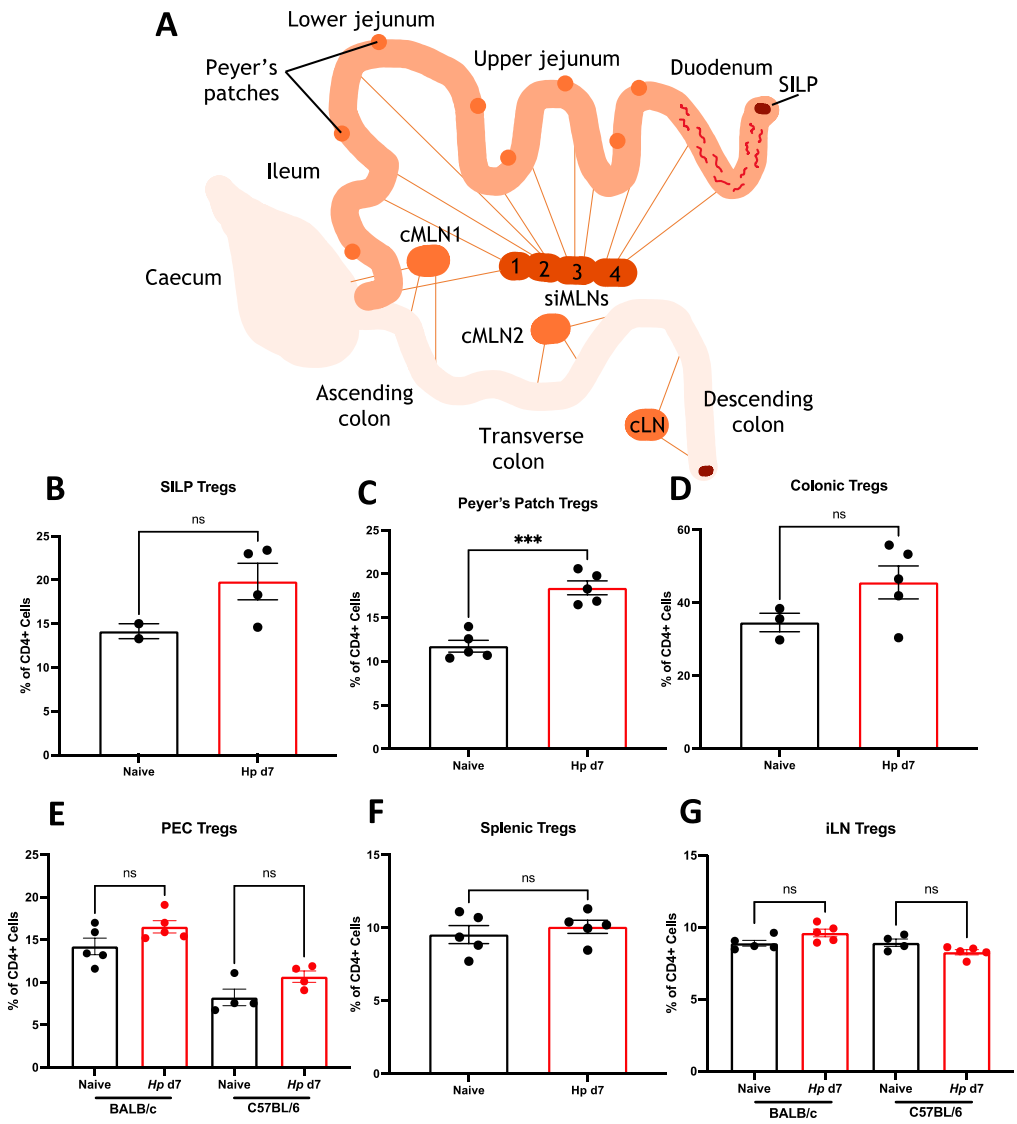

Figure 4.3 The locations of Treg expansion during H. polygyrus infection. (A) A schematic showing the major organs within the peritoneal cavity as well as the location of *H. polygyrus* and the areas each lymph node drains. (B) The proportion of Tregs within the small intestine lamina propria (SILP) of naïve (black, n=2) and *Hp* d7 (red, n=4) of C57BL/6 mice. (C) The proportion of Tregs within the Peyer's patches of naïve (black) and *Hp* d7 (red) of C57BL/6 mice (n=5). (D) The proportion of Tregs within the colon lamina propria of naïve (black, n=3) and *Hp* d7 (red, n=5) of C57BL/6 mice. (E) The proportion of Tregs within the peritoneal excaudate cells (PEC) of naïve (black) and *Hp* d7 (red) of C57BL/6 mice (BALB/c n=5, C57BL/6 n=4). (F) The proportion of Tregs within the spleen of naïve (black) and *Hp* d7 (red) of C57BL/6 mice (n=5). (G) The proportion of Tregs within the inguinal lymph node (iLN) of naïve (black) and *Hp* d7 (red) of BALB/c (n=5) C57BL/6 mice (n=4-5).
Graphs representative of 2 or 3 experiments. Each point represents a single mouse, error bars represent the standard error of the mean. Normality tested using a Shapiro-Wilk normality test. Significance tested using an ordinary one-way ANOVA and Holm-Šídák's multiple comparisons test. ns P>0.05, * P<0.05, ** P<0.01, ** P<0.001, **** P<0.0001

4.3.4 Dynamics of T-bet+ T cells during *H. polygyrus* infection

As discussed above, there are Tregs which can co-express Foxp3 with other transcription factors more often associated with effector Th subtypes, such as T-bet, the transcription factor commonly associated with Th1 cells (Koch *et al.*, 2009; Levine *et al.*, 2017). Since Th1 cells exist in opposition to the Th2 cells which promote *H. polygyrus* clearance, it may be expected that expression of T-bet is low in *H. polygyrus* infected MLN. Hence, expression of T-bet was measured in MLN T cells, both Foxp3– effectors (Th1) and Foxp3+ Tregs.

It has been shown previously that C57BL/6 mice express higher IFNγ levels than BALB/c mice at d7 of *H. polygyrus* infection (Filbey *et al.*, 2014) and this profile was found to be repeated when CD4+ Foxp3– T-bet+ Th1 cells were analysed, with their percentage of Th1 Teffector cells is elevated nearly 3-fold at d7 post infection in C57BL/6 mice but not significantly increased by infection in BALB/c mice (Figure 4.4A). Similarly, in terms of absolute numbers, the Th1 cohort is sharply elevated in *H. polygyrus* infected C57BL/6 mice, but not significantly so in BALB/c mice (Figure 4.4B). In terms of the expression level of T-bet within CD4+ cells, no difference in T-bet MFI was observed during *H. polygyrus* infection in either BALB/c and C57BL/6 CD4+ T cells (Figure 4.4C).

A similar overall picture was seen of T-bet expression within the Foxp3+ Treg population. Overall, few Tregs co-expressed T-bet in the MLN of *H. polygyrus* infected mice of either strain, although the proportion of T-bet+ Tregs was elevated to a varying degree in infected C57BL/6 mice (Figure 4.4D). Absolute numbers of T-bet+ Tregs were also evaluated (Figure 4.4E), showing little change in BALB/c mice; However, there was a substantial increase in T-bet+ Treg numbers in infected C57BL/6 mice during *H. polygyrus* infection (Figure 4.4E). As with the Th1 subset, there was no increase in T-bet MFI within Tregs following infection (Figure 4.4F).

There is clear variation in the level of T-bet induction amongst both Th1 and Treg subsets in C57BL/6 mice, suggesting induction is not a consistent feature of *H. polygyrus* infection. Interestingly, the individual mice with the highest number of Th1 cells (*Hp* d7 C57BL/6 mice # 2, 3 and 4) also have the highest

percentage and number of T-bet+ Tregs (Figure 4.4 B, D, E). These indications of a positive correlation need to be substantiated with additional experiments, but at the early time point of d7 post infection, T-bet induction may be due to exposure to microbiota translocating into the lamina propria during larvae invasion of the submucosa at around 24 hours after infection (Reynolds et al., 2012).

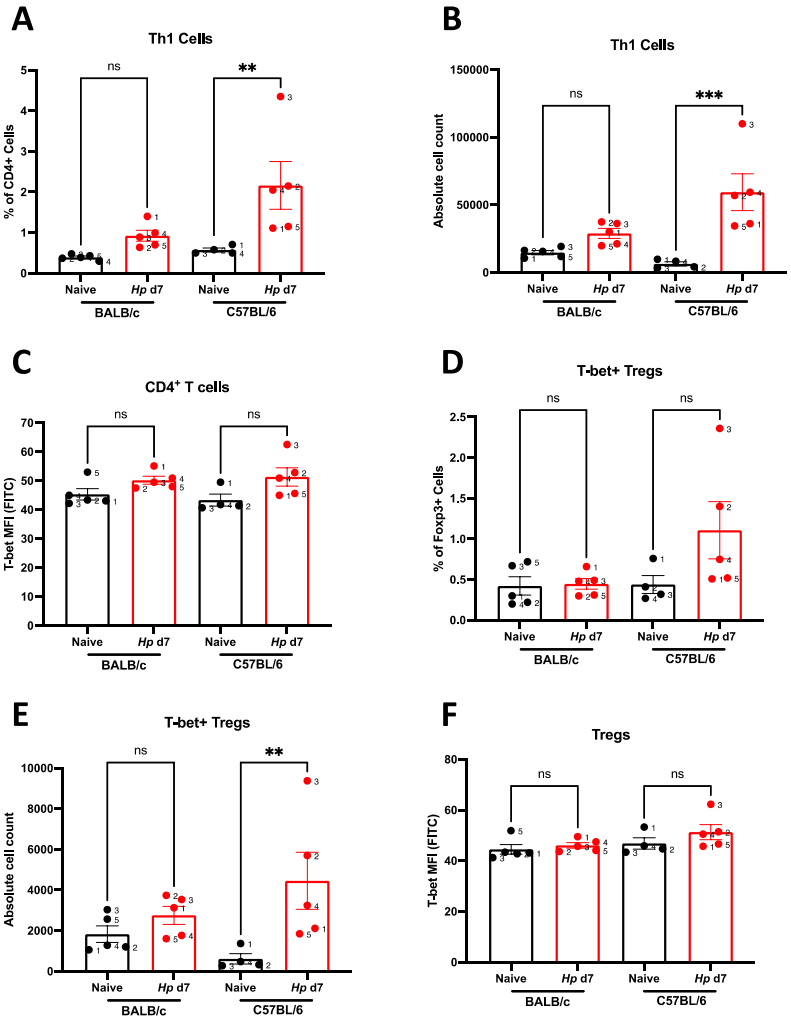

Figure 4.4 The dynamics of T-bet expansion at d7 and d14 H. polygyrus infection.
(A) The proportion of T-bet+ Tregs within the Treg population in the MLN of naïve (black) and *Hp* d7 (Red) in BALB/c and C57BL/6 mice. (B) The proportion of Th1 cells within the Treg population in the MLN of naïve, *Hp* d7 in BALB/c and C57BL/6 mice (C-D) The absolute number of T-bet+ Tregs (C) and Th1 cells (D) in the MLN of naïve, and *Hp* d7 in BALB/c and C57BL/6 mice. (E-F) The MFI of T-bet in Tregs (E) and CD4+ T cells (E) in the MLN of naïve and *Hp* d7 in BALB/c and C57BL/6 mice.
Graphs representative of 3 experiments. Each point represents a single mouse, error bars represent the standard error of the mean. In each group n=5. Normality tested using a Shapiro-Wilk normality test. Significance tested using an ordinary one-way ANOVA and Holm-Šídák's multiple comparisons test. ns P>0.05, * P<0.05, ** P<0.01, ** P<0.001, **** P<0.0001

4.3.5 Dynamics of GATA3+ CD4+ T cells during *H. polygyrus* infection

In the case of *H. polygyrus,* the Th2 response is central to clearing the infection and the expression of GATA3, the Th2 transcription factor, is increased during infection. GATA3 is also known to regulate the plasticity and stability of Tregs and is required by all CD4 T cells to mature and leave the thymus (Wan, 2014; Wohlfert et al., 2011; Xu et al., 2018). With this in mind, the dynamics of GATA3 expression by Tregs and Teffector cells was assessed during *H. polygyrus* infection.

As expected from previous published work, the expression of GATA3 within the effector T cell populations rises dramatically following *H. polygyrus* infection (Figure 4.5A). There is a similar expansion of CD4+ Foxp3- GATA3+ Th2 effector cells in both strains of mice, reaching between 5.4 and 17.3% of all CD4+ cells (Figure 4.5A-B), although no significant increase was seen in MFI levels between the groups (Figure 4.5C).

The Foxp3+Treg compartment following *H. polygyrus* infection presents a similar picture. There is an increase in the proportion of Tregs expressing GATA3 during *H. polygyrus* infection in both BALB/c and C57BL/6 mice, with means of 9.3% and rising to as much as 16.6% in individual mice (Figure 4.5D). Likewise, with respect to the total number of GATA3+ Tregs, there are substantial increases in all mice of both strains after infection with *H. polygyrus* (Figure 4.5E). However, as for the Th1 subset, no change was noted in GATA3 MFI following infection (Figure 4.5F).

It was noted that as for T-bet expression, the increases in GATA3 in Tregs and Th2 cells are proportional in individual mice (Figure 4.5A-D). For example, *H. polygyrus*-infected mice #2 and 3 had the highest proportion of both GATA3+ Th2 and GATA3+ Tregs (Figure 4.5A-D). This suggests either that the development of one subset is dependent on the action of the other, or that both phenotypes are induced by a common factor or cell type.

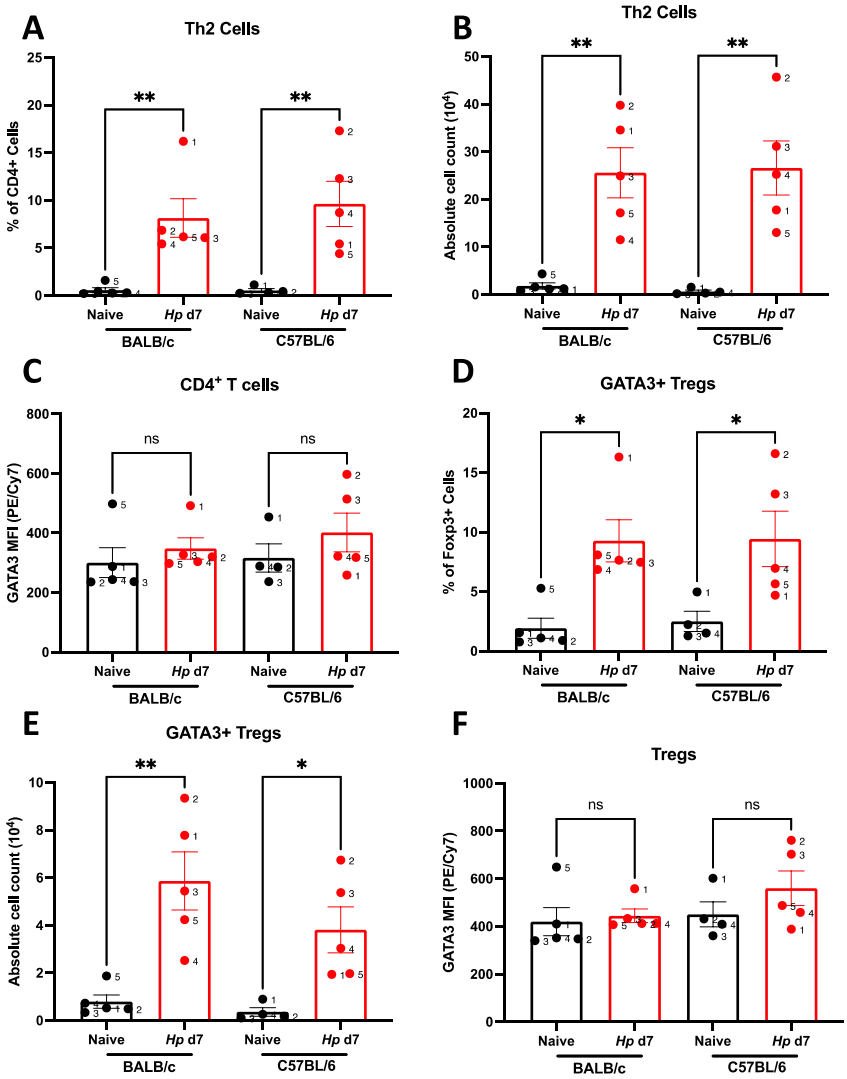

Figure 4.5 The dynamics of GATA3 expansion at d7 and d14 H. polygyrus infection. (A) The proportion of GATA3+ Tregs within the Treg population in the MLN of naïve (black) and *Hp* d7 (Red) in BALB/c and C57BL/6 mice. (B) The proportion of Th2 cells within the Treg population in the MLN of naïve, *Hp* d7 in BALB/c and C57BL/6 mice (C-D) The absolute number of GATA3+ Tregs (C) and Th2 cells (D) in the MLN of naïve, and *Hp* d7 in BALB/c and C57BL/6 mice. (E-F) The MFI of GATA3 in Tregs (E) and CD4+ T cells (E) in the MLN of naïve and *Hp* d7 in BALB/c and C57BL/6 mice.
Graphs representative of 3 experiments. Each point represents a single mouse, error bars represent the standard error of the mean. In each group n=5. Normality tested using a Shapiro-Wilk normality test. Significance tested using an ordinary one-way ANOVA and Holm-Šídák's multiple comparisons test. ns P>0.05, * P<0.05, ** P<0.01, ** P<0.001, **** P<0.0001

4.3.6 Dynamics of RORγt+ CD4+ T cells during *H. polygyrus* infection

As discussed earlier, when RORγt is selectively depleted from Tregs through the Foxp3^{Cre}RORγt$^{fl/fl}$ mouse model, there is increased clearance of *H. polygyrus* infection (Ohnmacht *et al.*, 2015). However, there is no published information on the dynamics of the Foxp3+RORγt+ population in *H. polygyrus*-infected mice (Ohnmacht *et al.*, 2015). Hence, data were collected on the expression of the RORγt transcription factor in BALB/c and C57BL/6 mice within the total CD4+ population and the Foxp3+ subset.

At day 7 post-*H. polygyrus* infection there are substantial (2-3 fold) increases in the proportion of RORγt+ Th17 cells, which attained statistical significance in the C57BL/6 cohort (Figure 4.6A). The absolute numbers of Th17 cells also increased in both strains, reaching significance in both cases (Figure 4.6B), although no change was observed in MFI (Figure 4.6C). These data very clearly demonstrate that *H. polygyrus* infection also induces Th17 cells.

In contrast to the Th17 profile, relatively little expansion in the proportion of RORγt+ Tregs was observed at day 7 of infection in either strain (Figure 4.6D). In terms of the absolute number of RORγt+ Tregs, an increase was seen in infected C57BL/6 mice but not to a significant degree in BALB/c mice (Figure 4.6E), and again no change in MFI occurred (Figure 4.6F).

In a similar pattern to that observed for T-bet+ and GATA3+ Tregs, the proportion of Tregs expressing RORγt correlates with the proportion of Th17 cells (Figure 5.6A-D). For example, mice # 2-4 of the C57BL/6 *H. polygyrus* infected group have the highest numbers of both Th17 numbers and RORγt+ Tregs (Figure 5.6A-D). As there is no increase in the proportion of Tregs expressing RORγt at this stage of *H. polygyrus* infection, it is not clear whether this Treg subtype has a major influence on the outcome of *H. polygyrus* infection.

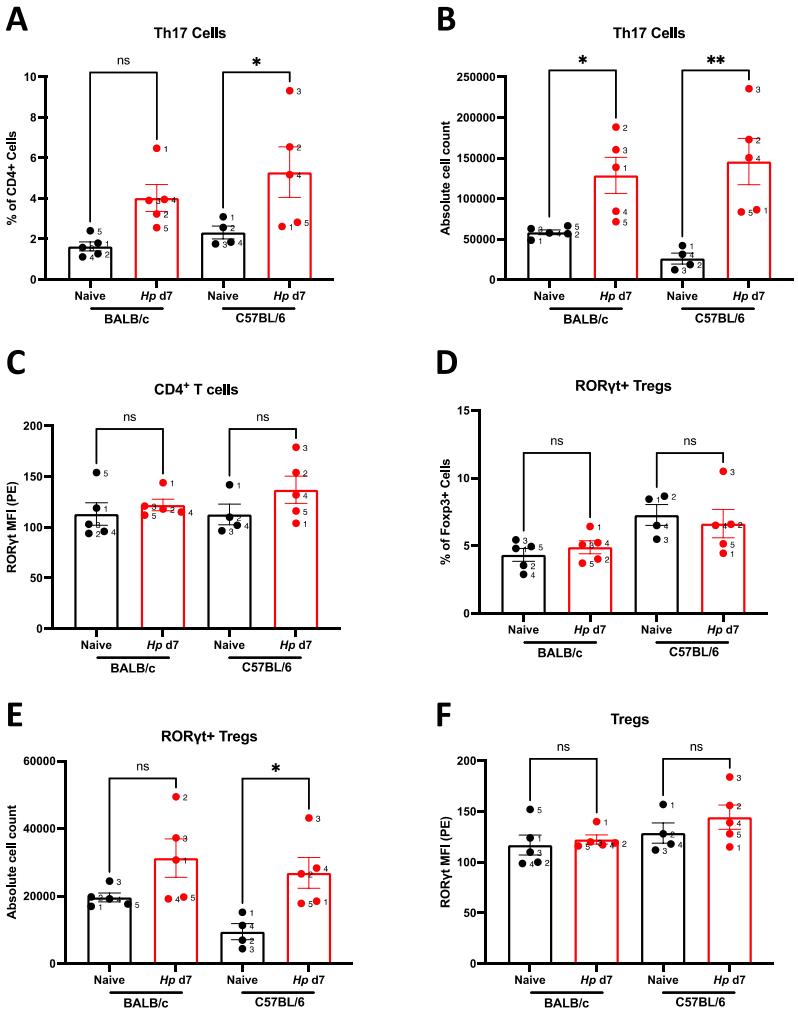

Figure 4.6 The dynamics of RORγt expansion at d7 and d14 H. polygyrus infection. (A) The proportion of RORγt+ Tregs within the Treg population in the MLN of naïve (black) and *Hp* d7 (Red) in BALB/c and C57BL/6 mice. (B) The proportion of Th17 cells within the Treg population in the MLN of naïve, *Hp* d7 in BALB/c and C57BL/6 mice (C-D) The absolute number of RORγt + Tregs (C) and Th17 cells (D) in the MLN of naïve, and *Hp* d7 in BALB/c and C57BL/6 mice. (E-F) The MFI of RORγt in Tregs (E) and CD4+ T cells (E) in the MLN of naïve and *Hp* d7 in BALB/c and C57BL/6 mice. Graphs representative of 3 experiments. Each point represents a single mouse, error bars represent the standard error of the mean. In each group n=5. Normality tested using a Shapiro-Wilk normality test. Significance tested using an ordinary one-way ANOVA and Holm-Šídák's multiple comparisons test. ns P>0.05, * P<0.05, ** P<0.01, ** P<0.001, **** P<0.0001

4.3.7 IL-6 antibody blockade effect on H. polygyrus infection

As discussed previously, RORγt expression can be induced in Th17 cells by IL-6, a cytokine with known pleiotropic effects on both immune and non-immune cells

(Dienz & Rincon, 2009; Luckheeram et al., 2012; Puel & Casanova, 2019; Katherine A. Smith & Maizels, 2014). There has also been a link made between IL-6 and Treg function during *H. polygyrus* infection, as depletion of IL-6 leads to a decrease in worm burden (Katherine A. Smith & Maizels, 2014). Experiments were undertaken to test whether RORγt+ Tregs are affected by anti-IL-6 antibody blockade, and whether this could explain the matching parasitology between mice with the Foxp3^{Cre}RORγt$^{fl/fl}$ genotype, and those lacking IL-6 (Ohnmacht et al., 2015; Katherine A. Smith & Maizels, 2014).

Figure 4.7A shows the experimental set up used to block IL-6 using the α-IL-6 monoclonal antibody 20F3. Mice were infected or left naïve and given either 200 µg of 20F3 or 200 µg of rat IgG control i.p. on d0, 2, 4 and 6 post infection before culling on d7 (Figure 4.7A). Interestingly, in this experiment no Treg expansion was found in the MLN of *H. polygyrus*-infected mice regardless of antibody treatment (Figure 4.7B). However, in mice given α-IL-6 i.p., the expansion of Th2 cells is higher than the expansion of Th2 cells in the mice given the control antibody (Figure 4.7C). This suggests that IL-6 availability is a limiting factor for Th2 cell expansion during H. polygyrus infection.

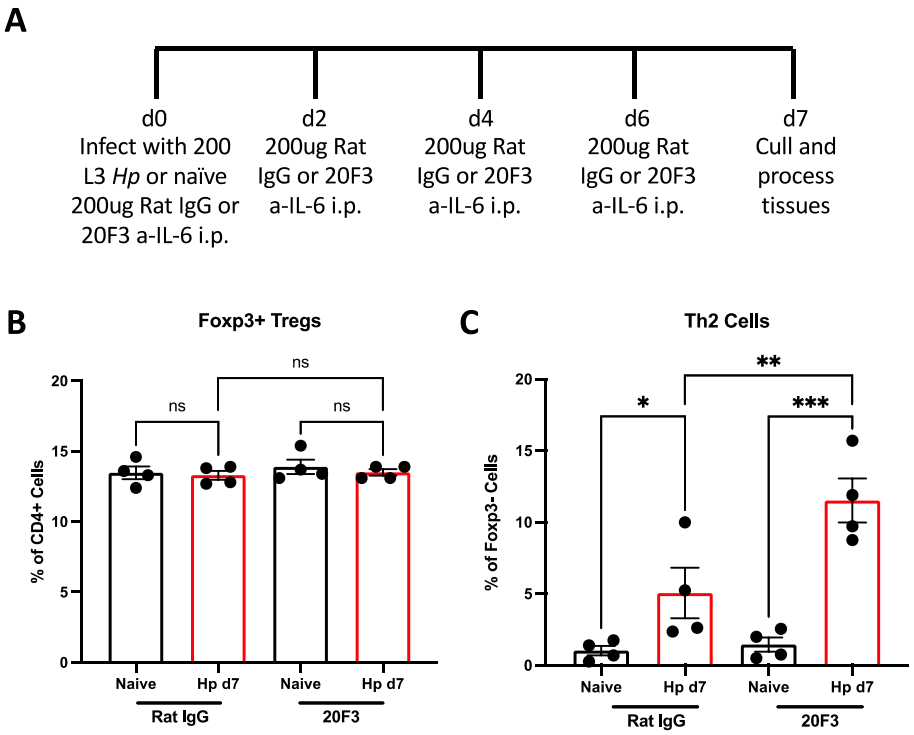

Figure 4.7 Th2 cells induced by H. polygyrus are further expanded in IL-6 blockade. (A) A schematic showing the experimental procedure showing the days of infection and i.p. monoclonal antibody injection. (B) The proportion of Tregs within the total CD4+ T cell population in the MLN of naïve (black) and *Hp* d7 infected mice (red) given 20F3 (anti-IL-6) or control antibody (Rat IgG) i.p. (C) The proportion of Th2 cells in the Foxp3- T cell compartment in the MLN of *Hp* d7 infected (red) or naïve (black) mice treated with 20F3 or Rat IgG i.p.
Graphs representative of 1 experiment. Each point represents a single mouse, error bars represent the standard error of the mean. In each group n=4. Normality tested using a Shapiro-Wilk normality test. Significance tested using an ordinary one-way ANOVA and Holm-Šídák's multiple comparisons test. ns P>0.05, * P<0.05, ** P<0.01, ** P<0.001, **** P<0.0001.

4.3.8 The effect of IL-6 blockade on RORγt+ CD4+ T cells during *H. polygyrus* infection

As stated previously, RORγt can be co-expressed by Tregs and in its absence worm clearance has been reported to be enhanced (Ohnmacht *et al.*, 2015). Since IL-6 is required for expression of RORγt in Th17 cells, it may also be necessary for the expression of RORγt in Tregs. Mice treated with the α-IL-6 monoclonal antibody clone 20F3 were therefore assessed for the proportion of Tregs co-expressing RORγt (Figure 4.8A). While there is a trend towards a decrease in the proportion of RORγt+ Tregs in α-IL-6 treated mice, this does not reach significance. Moreover, there was a significant reduction in RORγt+ Tregs in animals given the control Rat IgG antibody, which may suggest that i.p. injection alone affects the proportions of RORγt+ Tregs (Figure 4.8A).

Unexpectedly, there is no effect on the proportion of RORγt+ Th17 cells when IL-6 is blocked with 20F3 versus the control antibody group (Figure 4.8B). The absolute number of RORγt+ Tregs and RORγt+ Th17 cells are also unaffected by blocking IL-6 antibody (Figure 4.8C-D). To assess whether IL-6 blockade affects the expression level of RORγt, the MFI of RORγt was assessed in Tregs and Th17 cells. However, there is no difference in the MFI of RORγt in Tregs or Th17 cells when IL-6 is blocked by 20F3 (Figure 4.8E-F)

One observation is that the expansion of RORγt cells when given i.p. antibody is limited compared to the RORγt expression in CD4+ T cells in previous experiments with *H. polygyrus* infected mice (Figure 4.6A). Taken together, these findings suggest that the availability of IL-6 does not significantly impact the expression of RORγt, but i.p. injection of antibody does partially prevent the expansion of Th17 cells during *H. polygyrus* infection.

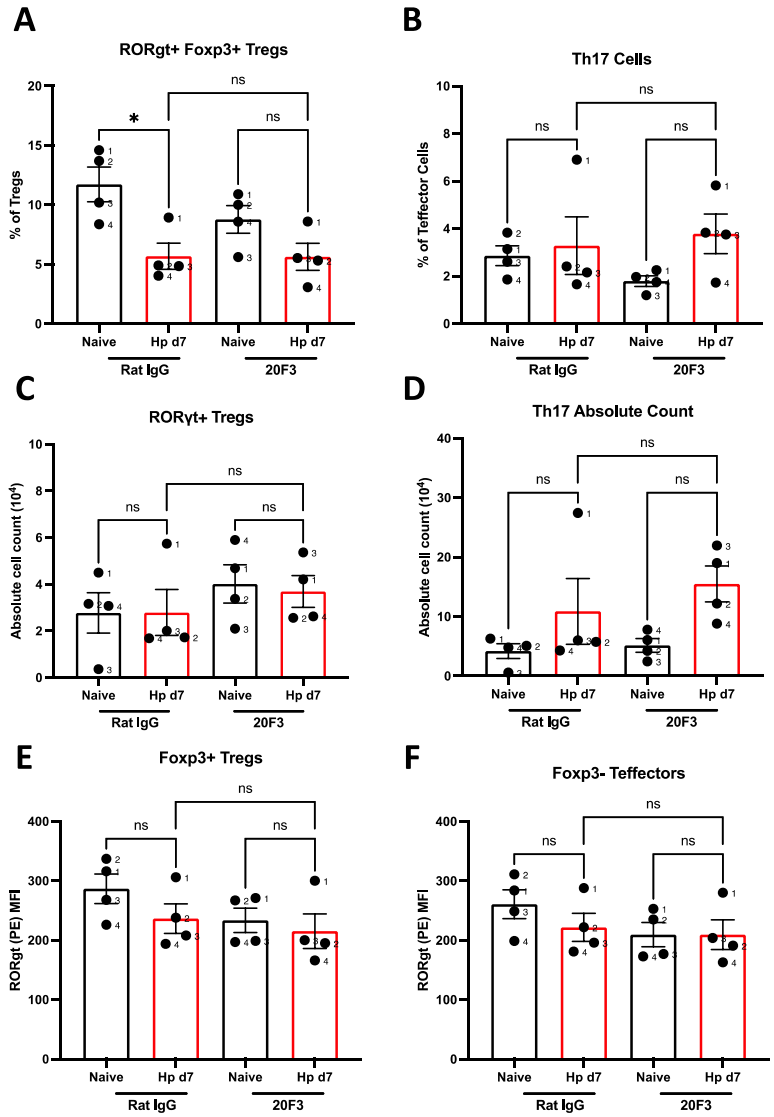

Figure 4.8 Dynamics of RORγt during H. polygyrus infection during IL-6 blockade.
(A-B) The proportion of RORγt+ Tregs within the total CD4+ T cell population (A) and Th17 cells within the Teffector population (B) in the MLN of naïve (black) and *Hp* d7 infected mice (red) given 20F3 (anti-IL-6) or control antibody (Rat IgG) i.p. (C-D) The absolute number of RORγt+ Tregs (C) and Th17 cells (D) in the MLN of naïve (black) and *Hp* d7 infected mice (red) given 20F3 (anti-IL-6) or control antibody (Rat IgG) i.p. (E-F) The MFI of RORγt in the Treg (E) and Teffector (F) populations in the MLN of naïve (black) and *Hp* d7 infected mice (red) given 20F3 (anti-IL-6) or control antibody (Rat IgG) i.p.
Graphs representative of 1 experiment. Each point represents a single mouse, error bars represent the standard error of the mean. In each group n=4. Normality tested using a Shapiro-Wilk normality test. Significance tested using an ordinary one-way ANOVA and Holm-Šídák's multiple comparisons test. ns P>0.05, * P<0.05, ** P<0.01, ** P<0.001, **** P<0.0001.

4.3.9 The effect of IL-6 blockade on GATA3 expression in Tregs during *H. polygyrus* infection

Although little effect of IL-6 blockade was seen on the RORγt+ T cell compartment (4.3.8), the increase in Th2 cell numbers (4.3.7) during *H. polygyrus* infection was noted, and the GATA3 Treg compartment was assessed. In certain settings, RORγt+ Tregs are GATA3hi Tregs appear to oppose each other, and Ohnmacht and colleagues found that loss of Treg RORγt expression led to an upregulation of GATA3+ Tregs (Ohnmacht *et al.*, 2015). It was found that the proportion of GATA3hi Foxp3+ Tregs was unaffected by IL-6 antibody mediated blockade (Figure 4.9A). In terms of absolute number of GATA3hi Tregs, there is a trend towards higher numbers of GATA3hi Tregs in α-IL-6 treated mice versus Rat IgG control mice, however, this does not reach significance (Figure 4.9B). In terms of average expression, there is no difference in the MFI of GATA3 in Tregs from α-IL-6 treated mice (Figure 4.9C). Altogether these data suggest that IL-6 blockade has minimal effects on the expression GATA3 in the Treg population and does not impact the number of GATA3hi Tregs.

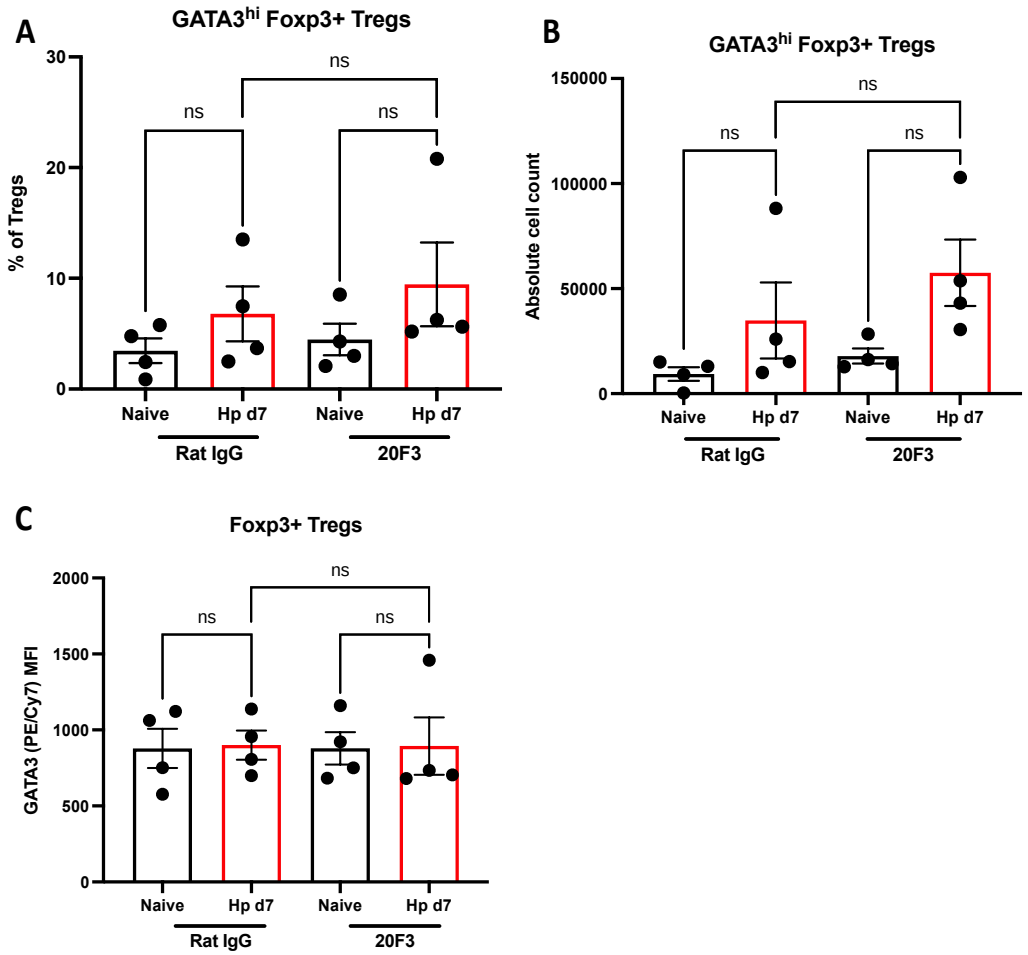

Figure 4.9 Dynamics of GATA3+ Tregs during H. polygyrus infection during IL-6 blockade. (A) The proportion of GATA3+ Tregs within the total Treg population in the MLN of naïve (black) and *Hp* d7 infected mice (red) given 20F3 (anti-IL-6) or control antibody (Rat IgG) i.p. (B) The absolute number of GATA3+ Tregs in the MLN of naïve (black) and *Hp* d7 infected mice (red) given 20F3 (anti-IL-6) or control antibody (Rat IgG) i.p. (C) The MFI of GATA3 in the Treg population in naïve (black) and *Hp* d7 infected mice (red) given 20F3 (anti-IL-6) or control antibody (Rat IgG) i.p. Graphs representative of 1 experiment. Each point represents a single mouse, error bars represent the standard error of the mean. In each group n=4. Normality tested using a Shapiro-Wilk normality test. Significance tested using an ordinary one-way ANOVA and Holm-Šídák's multiple comparisons test. ns P>0.05, * P<0.05, ** P<0.01, ** P<0.001, **** P<0.0001.

4.3.10 The effect of IL-6 blockade on T cell activation during *H. polygyrus* infection

To analyse T cell activation, a useful marker is CD44, a transmembrane glycoprotein which is upregulated upon TCR ligation and plays roles in migration and memory T cell formation (Baaten, Li, & Bradley, 2010; Lesley, Howes, Perschl, & Hyman, 1994; T. Liu, Soong, Liu, König, & Chopra, 2009). To assess whether blocking IL-6 affects the activation of T cells during *H. polygyrus* infection, the expression of CD44 on Tregs and Teffector cells was explored.

CD44 expression was measured following IL-6 is blockade with monoclonal antibody. In the context of *H. polygyrus* infection, there is a reduction of CD44hi Tregs in antibody-treated mice, which suggests that the activation of Tregs is impacted by the loss of IL-6 (Figure 4.10A). However, among Foxp3- Teffector cells, there is an increase in the proportion of cells expressing high levels of CD44 (Figure 4.10B). These results suggest that IL-6 blockade impairs Treg activation, thereby leading to more activated Teffector cells. The expression of CD44, shown as MFI of CD44, is significantly downregulated in both Tregs (Figure 4.10C) and Teffector cells (Figure 4.10D). Hence, IL-6 is clearly required for the optimal activation of Treg cells during *H. polygyrus* infection and ablation of IL-6 leads to lower CD44 expression on T cells, especially in the Treg compartment.

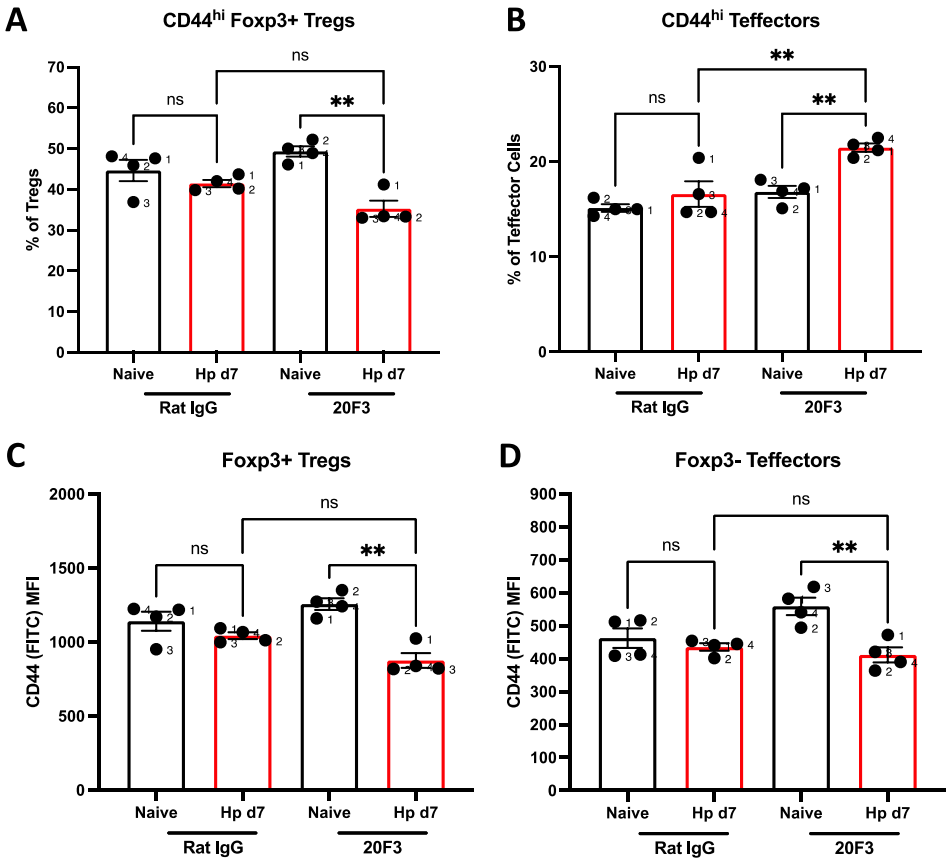

Figure 4.10 Dynamics of CD44 expression on Tregs in H. polygyrus infection during IL-6 blockade. (A-B) The proportion of CD44+ Tregs within the total Treg population (A) and CD44^{hi} Teffectors within the total Teffector population (B) in the MLN of naïve (black) and *Hp* d7 infected mice (red) given 20F3 (anti-IL-6) or control antibody (Rat IgG) i.p. (C-D) The MFI of CD44 in the Treg population (C) and Teffector population (D) in the MLN of naïve (black) and *Hp* d7 infected mice (red) given 20F3 (anti-IL-6) or control antibody (Rat IgG) i.p.
Graphs representative of 1 experiment. Each point represents a single mouse, error bars represent the standard error of the mean. In each group n=4. Normality tested using a Shapiro-Wilk normality test. Significance tested using an ordinary one-way ANOVA and Holm-Šídák's multiple comparisons test. ns P>0.05, * P<0.05, ** P<0.01, ** P<0.001, **** P<0.0001.

4.3.11 The expression of CD44 on Teffector cells from *H. polygyrus* infected mice after IL-6 blockade

One interpretation of the increase in CD44hi Foxp3- cells observed after IL-6 blockade is that they are highly activated Th cells which have escaped Treg suppression. To identify which Th cells are more strongly activated during IL-6 blockade, expression of CD44 in Th2 and Th17 cells was scrutinised, to establish whether CD44hi Teffectors correspond to the Th2 population required to clear the helminth infection. If so, the increased worm clearance in IL-6 KO mice would be explained by increased activation of Th2 cells in the absence of suppression.

However, in mice receiving IL-6 blocking antibody, there is no increase of CD44hi GATA3+ Foxp3- Th2 cells compared to controls, and in fact show a non-significant decrease (Figure 4.11A). The mean expression of CD44 also trends lower in the IL-6-blocked *H. polygyrus*-infected mice compared to controls (Figure 4.11B), indicating that the activated CD44hi cells from *H. polygyrus* infected mice do not belong to the Th2 subset.

CD44 expression on Th17 cells was also examined, to establish if it is negatively impacted by limited IL-6. Indeed, there is a significant decrease in CD44hi Th17 cells following α-IL-6 treatment (Figure 4.11C) as well as a decrease in CD44 MFI (Figure 4.11D) when comparing infected and naïve mice both treated with α-IL-6. Together this suggests that there is a population of CD44hi CD4+ Foxp3- cells which are significantly increased after α-IL-6 treatment but these cells are not Th2 or Th17 cells.

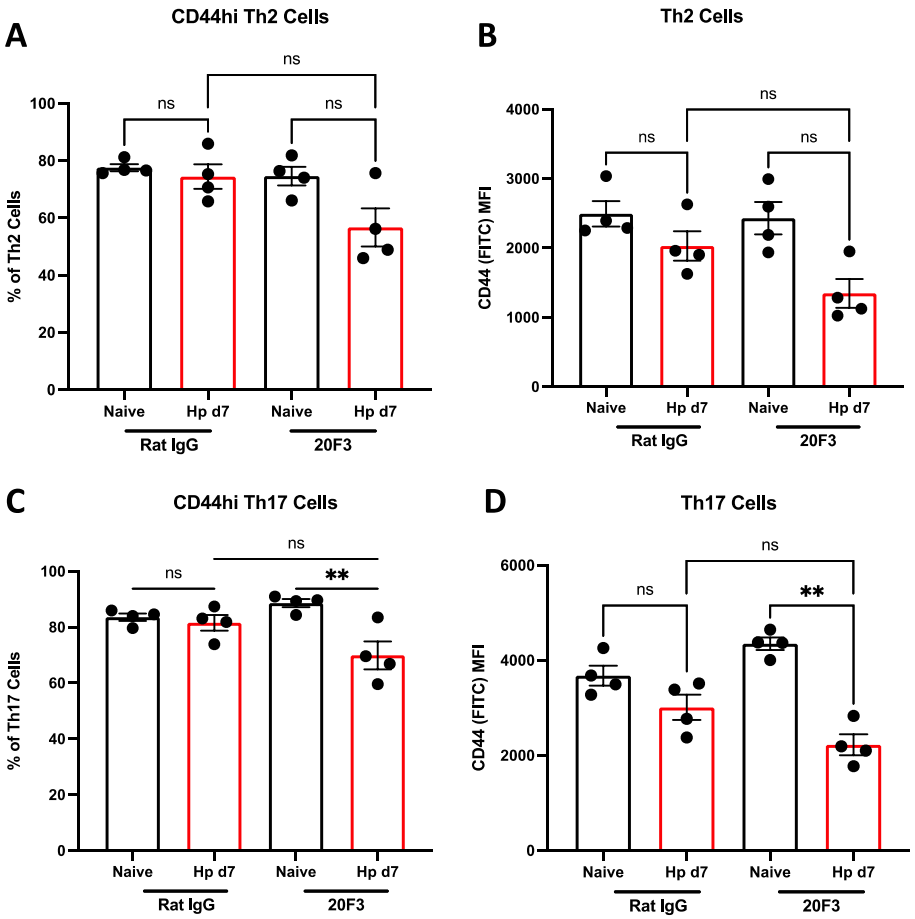

Figure 4.11 Dynamics CD44 on different Teffector populations during H. polygyrus infection during IL-6 blockade. (A) The proportion of CD44+ Th2 within the total Th2 population in the MLN of naïve (black) and *Hp* d7 infected mice (red) given 20F3 (anti-IL-6) or control antibody (Rat IgG) i.p. (B) The MFI of CD44 in the Th2 population in the MLN of naïve (black) and *Hp* d7 infected mice (red) given 20F3 (anti-IL-6) or control antibody (Rat IgG) i.p. (C) The proportion of CD44+ Th17 within the total Th17 population in the MLN of naïve (black) and *Hp* d7 infected mice (red) given 20F3 (anti-IL-6) or control antibody (Rat IgG) i.p. (B) The MFI of CD44 in the Th17 population in the MLN of naïve (black) and *Hp* d7 infected mice (red) given 20F3 (anti-IL-6) or control antibody (Rat IgG) i.p.
Graphs representative of 1 experiment. Each point represents a single mouse, error bars represent the standard error of the mean. In each group n=4. Normality tested using a Shapiro-Wilk normality test. Significance tested using an ordinary one-way ANOVA and Holm-Šídák's multiple comparisons test. ns P>0.05, * P<0.05, ** P<0.01, ** P<0.001, **** P<0.0001.

4.3.12 The effect of IL-6 blockade on the cytokine production of MLN T cells

IL-6 is a pleiotropic cytokine and its presence or absence can change the cytokine output of T cells. To assess whether IL-6 blockade during *H. polygyrus* infection affects the T cell response in terms of their cytokine production, 1 million MLN cells were restimulated with α-CD3 for 3 days and their supernatants analysed for cytokine concentration using cytometric bead array. In line with the increase in Th2 cells, there is also an increase in IL-4 production from the MLN when *H. polygyrus* mice are treated with α-IL-6 antibody, suggesting a more robust Th2 response (Figure 4.7C, Figure 4.12A). The IL-13 concentration was unaffected by IL-6 blockade which suggests that there was selective upregulation of IL-4 without also raising other Th2 cytokines like IL-13 (Figure 4.12B). Another Th2 cytokine is IL-5 which recruits eosinophils to the site of infection and mediates class switching of antibody towards IgA (Harriman, Kunimoto, Elliott, & Paetkau, 1988). Interestingly, the rise in concentration of IL-5 during *H. polygyrus* infection is blocked by IL-6 blockade with monoclonal antibody (Figure 4.12C). IL-10 is increased upon infection with *H. polygyrus* and upon IL-6 blocking, IL-10 is further increased which may suggest that the Tregs are more active (Figure 4.12D). Figure 4.12E shows the concentration of IL-6 in MLN culture supernatants incubated for 3 days, it appears that the IL-6 blockade leads to an increase in IL-6 production by T cells, this may indicate that the cells are compensating for the blocking antibody. There is a non-significant increase in IL-17A although there is a trend for an increase when IL-6 is blocked (Figure 4.12F). IL-9 is also increased during *H. polygyrus* infection and is further increased when IL-6 is blocked *in vivo* (Figure 4.12G). There is little difference in the IFNγ production when IL-6 is blocked in *H. polygyrus* infected mice but there is an increase in IFNγ in naïve mice when IL-6 is blocked (Figure 4.12H). Together, this shows that blocking IL-6 during *H. polygyrus* infection leads to increased IL-4, IL-6, IL-9 and IL-10 production by MLN T cells. This suggests that loss of IL-6 leads to dysregulation of the cytokine response to *H. polygyrus*.

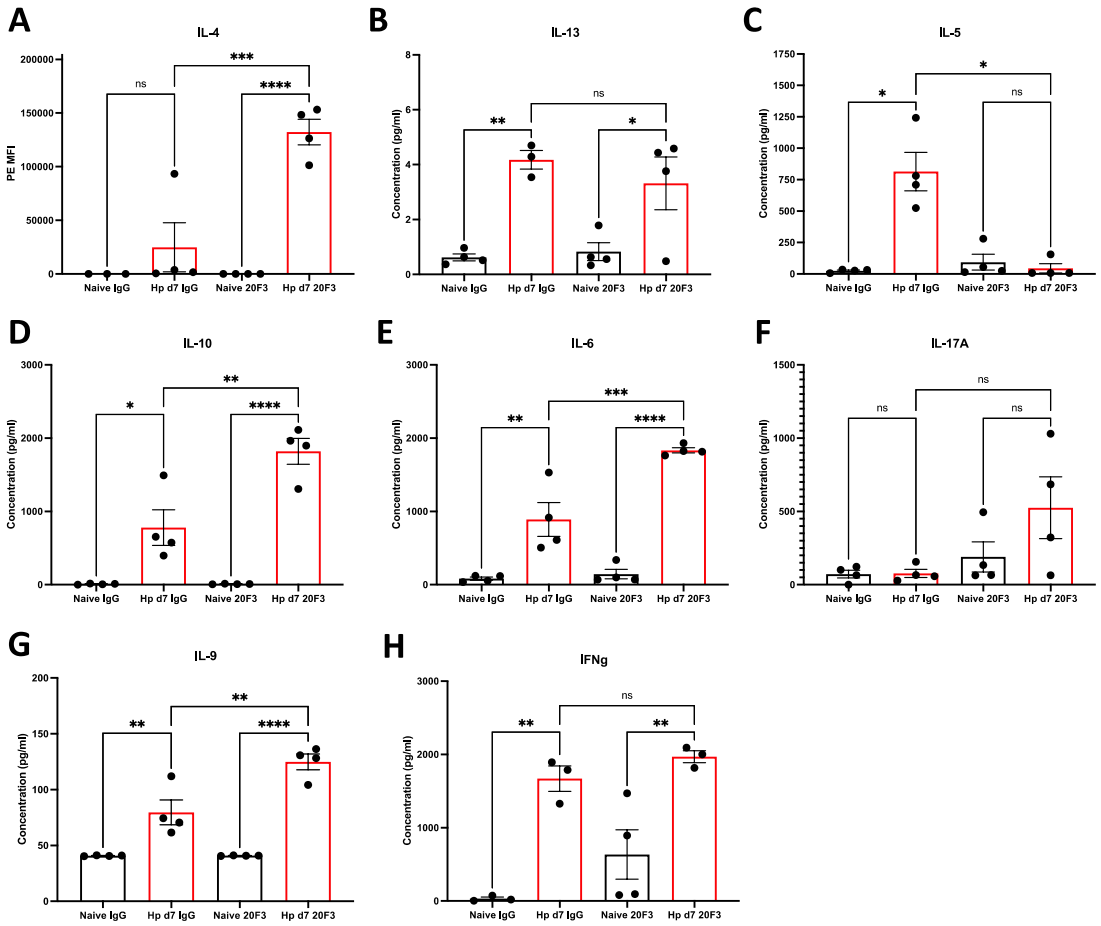

Figure 4.12 Cytokine output from anti-CD3 treated whole MLN is affected by IL-6 blockade during infection. (A-H) The concentration of (A) IL-4 (n=3-4), (B) IL-13 (n=3-4), (C) IL-5 (n=4), (D) IL-10 (n=4), (E) IL-6 (n=4), (F) IL-17A (n=4), (G) IL-9 (n=4) and (H) IFNg (n=3-4) in the supernatant of MLN cells from naïve (black) and *Hp* d7 infected mice (red) given 20F3 (anti-IL-6) or control antibody (Rat IgG) i.p. cultured with anti-CD3 for 3 days before running a cytometric bead array.
Graphs representative of 1 experiment. Each point represents cells from a single mouse, error bars represent the standard error of the mean. Normality tested using a Shapiro-Wilk normality test. Significance tested using an ordinary one-way ANOVA and Holm-Šídák's multiple comparisons test. ns P>0.05, * P<0.05, ** P<0.01, ** P<0.001, **** P<0.0001.

4.3.13 The expression of CTLA-4 on T cells from *H. polygyrus* infected mice

As discussed previously, during early *H. polygyrus* infection, the Treg population requires CTLA-4 for their suppressive action (Bowron *et al.*, 2020). However, it has also been shown that Tregs from *H. polygyrus* mice express less CTLA-4 on their surface than naïve Tregs (Finney *et al.*, 2007). To assess the dynamics of CTLA-4 expression on Tregs, C57BL/6 mice were infected for 7 or 14 days with *H. polygyrus* before their MLN cells were recovered and stained for CTLA-4. In this analysis, shown in Figure 4.13A, the percentage of Tregs expressing CTLA-4 on their surface increases in both infected BALB/c and C57BL/6 mice. This is in opposition to what was found by Finney and colleagues (Finney *et al.*, 2007).

CTLA-4 was also stained intracellularly as CTLA-4 is rapidly up taken by endocytosis and degraded within the cell, resulting in around 90% of CTLA-4 being found intracellularly (L. S. K. Walker & Sansom, 2015). Intracellular CTLA-4 is found in the great majority of Tregs from naïve and *H. polygyrus* infected mice (Figure 4.13B), in direct contrast to Foxp3- Teffector cells which have around 10% of Teffectors expressing intracellular CTLA-4; moreover, there is an expansion in the Foxp3– CTLA-4+ population at day 7 post-*H. polygyrus* infection (Figure 4.13C). The proportion of CTLA-4+ Teffectors peaks at day 7 post infection and contracts by d14, but does not return to naïve level at that time (Figure 4.13C). These results confirm that the CTLA-4 pathway is a significant part of the T cell response to *H. polygyrus* as indicated by the earlier single cell sequencing data which shows Teffector cell expression of the genes associated with CTLA-4 mediated inhibition.

While both Tregs and effector cells can be found expressing CTLA4, there is a sharp contrast in their levels of expression, as can be seen by staining for intracellular expression at day 7 of infection (Figure 4.13D). Moreover, while nearly all Tregs express CTLA-4 intracellularly, the levels are upregulated during *H. polygyrus* infection (Figure 4.1E), suggesting that these Tregs may be more reliant on CTLA-4 mediated suppression. The intracellular expression level of CTLA-4 in Teffector cells remains much lower in both naïve and infected mice (Figure 4.13E-F).

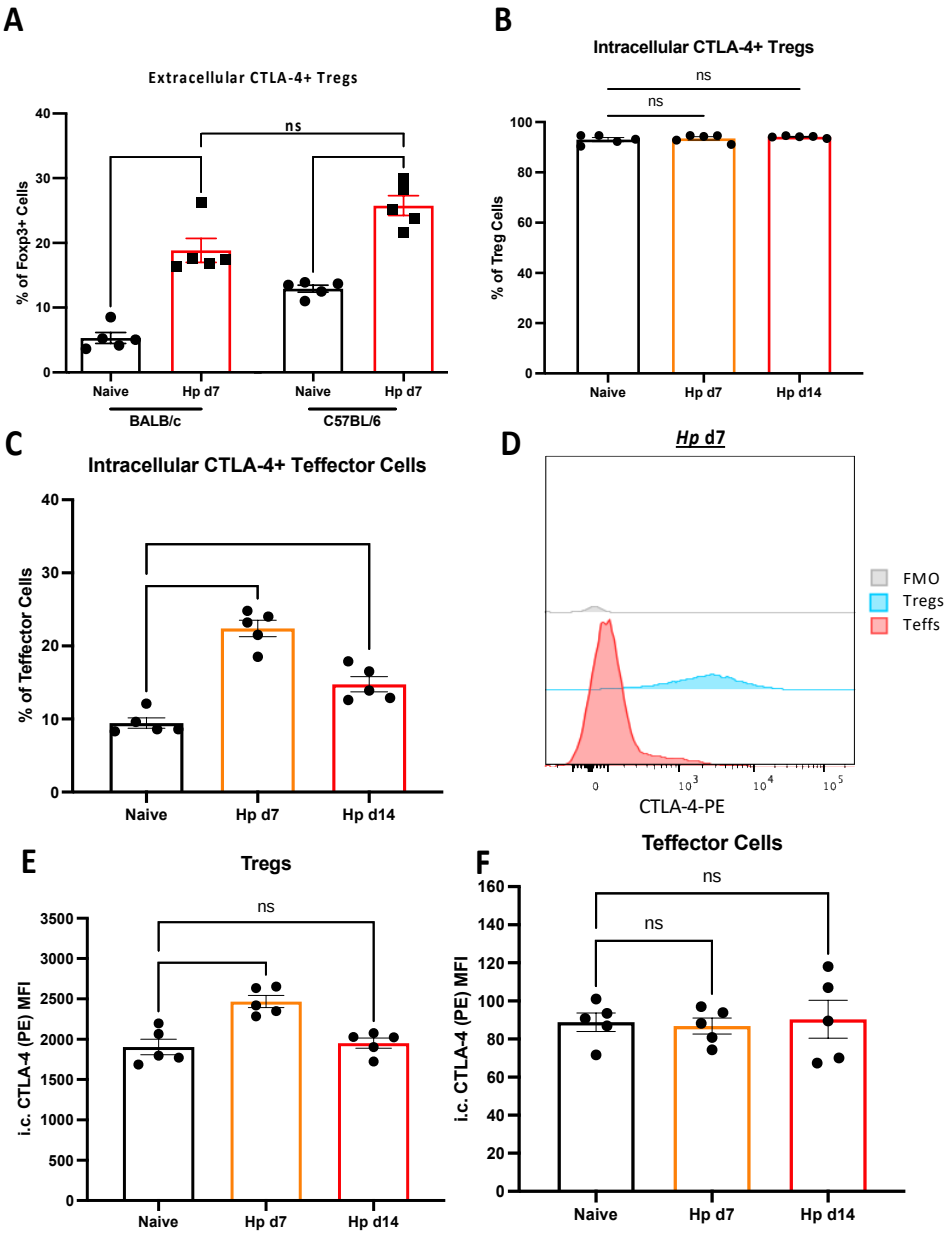

Figure 4.13 The expression of CTLA-4 on Tregs and Teffectors cells from H. polygyrus infected mice. (A) The proportion of Tregs expressing extracellular CTLA-4 within the total Treg population in the MLN of naïve (black) and *Hp* d7 (red) BALB/c and C57BL/6 mice (B) The proportion of Tregs expressing intracellular CTLA-4 within the total Treg population in the MLN of naïve (black), *Hp* d7 (orange) and *Hp* d14 infected mice (red) (C) The proportion of CTLA-4+ Teffectors within the total Teffector population in the MLN of naïve (black), *Hp* d7 (orange) and *Hp* d14 infected mice (red) (D) The MFI of CTLA-4 in Tregs (blue) and Teffectors (red) from an *Hp* d7 infected mouse with an FMO control in grey. (E-F) The MFI of intracellular CTLA-4 in (E) Tregs and (E) Teffector cells from naïve (black), *Hp* d7 (orange) or *Hp* d14 (red) infected mice.
Graphs representative of 1 experiment. Each point represents a single mouse, error bars represent the standard error of the mean. In each group n=5. Normality tested using a Shapiro-Wilk normality test. Significance tested using an ordinary one-way ANOVA and Holm-Šídák's multiple comparisons test, ns P>0.05, * P<0.05, ** P<0.01, ** P<0.001, **** P<0.0001

4.3.14 The expression of PD-1 on CD4+ T cells during *H. polygyrus* infection

PD-1 is another co-inhibitory molecule which can limit T cell activation (L. Chen & Flies, 2013; Lucca & Dominguez-Villar, 2020). As discussed previously, the expression of PD-1 on Tregs can tolerise dendritic cells and upregulate their expression of IL-10 while inhibiting IL-12 which leads to less Th cell activation. With the proposed role of Tregs during *H. polygyrus* infection being control of the Th2 response, PD-1 may be a key molecule used to suppress the Th2 response. However, as seen in Figure 4.14A, there is no expansion of PD-1 expressing Tregs when infected with *H. polygyrus*. There was also no increase in the average expression of PD-1 within the Treg compartment, showing that PD-1 is also not upregulated on a cell by cell basis (Figure 4.14B). However, there is an increase of PD-1+ Teffector cells at both day 7 and day 14 post infection (Figure 4.14C). There is a contraction of the response at day 14 post infection but the proportion of PD-1+ cells does not return to naïve levels (Figure 4.14C). This suggests that PD-1 is upregulated by *H. polygyrus* infection but this expansion is limited to Teffector cells (Figure 4.14C). There is also an increase in the MFI of PD-1 in Teffector cells at d7 which again diminishes by d14 but not to naïve levels (Figure 4.14D). This suggests that PD-1 is important for the dynamics of Teffector cells during *H. polygyrus* infection but not for the Treg population.

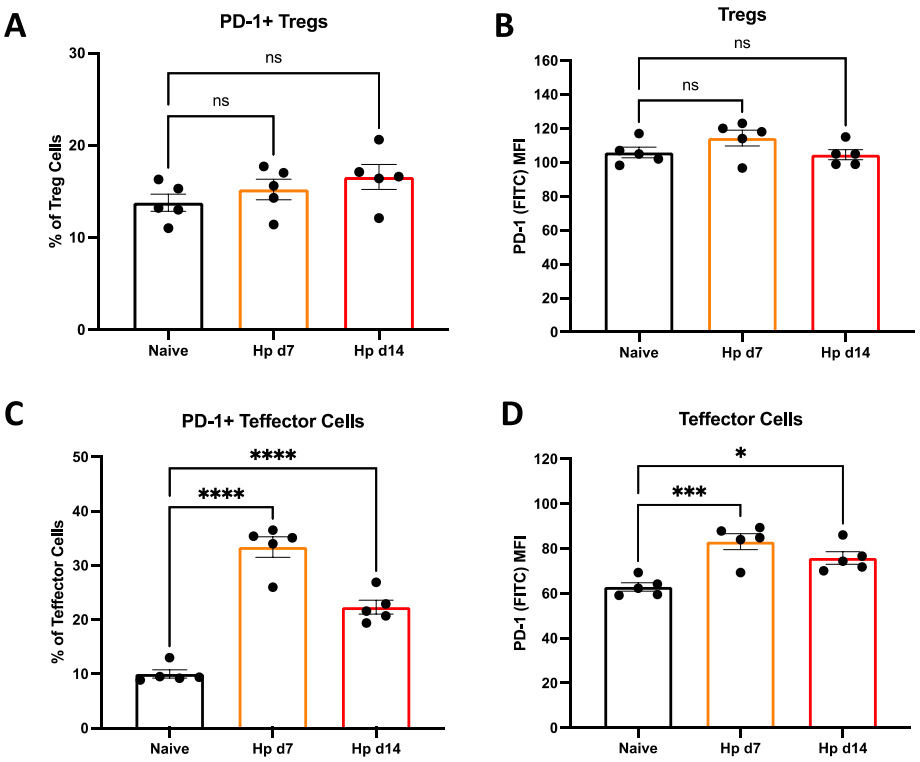

Figure 4.14 The expression of PD-1 on Tregs and Teffector cells from H. polygyrus infected mice. (A) The proportion of PD-1+ Tregs within the total Treg population in the MLN of naïve (black), *Hp* d7 (orange) and *Hp* d14 infected mice (red) (B) The MFI of PD-1 in the Treg population in the MLN of naïve (black), *Hp* d7 (orange) and *Hp* d14 infected mice (red) (C) The proportion of PD-1+ Teffectors within the total Teffector population in the MLN of naïve (black), *Hp* d7 (orange) and *Hp* d14 infected mice (red) (D) The MFI of PD-1 in the Teffector population in naïve (black), *Hp* d7 (orange) and *Hp* d14 infected mice (red).
Graphs representative of 1 experiment. Each point represents a single mouse, error bars represent the standard error of the mean. In each group n=5. Normality tested using a Shapiro-Wilk normality test. Significance tested using an ordinary one-way ANOVA and Holm-Šídák's multiple comparisons test. ns $P>0.05$, * $P<0.05$, ** $P<0.01$, ** $P<0.001$, **** $P<0.0001$.

4.3.15 The expression of TIGIT on CD4+ T cells during *H. polygyrus* infection

TIGIT is another co-inhibitory receptor which belongs to the PVR family and as discussed previously, preferentially activates the Th2 response while suppressing the Th1 and Th17 populations. During *H. polygyrus* infection, the percentage of Tregs expressing TIGIT does not increase, although around 12% of the Tregs in both naïve and *H. polygyrus* infected mice express TIGIT (Figure 4.15A). This suggests that in C57BL/6 mice, TIGIT is expressed at some level in a proportion of Tregs but the TIGIT+ Treg population is not upregulated by helminth infection. In terms of the average expression of TIGIT in Tregs, there is very low expression and this expression does not change upon infection with *H. polygyrus* (Figure 4.15B). Together this suggests that TIGIT is not an important Treg effector molecule during H. polygyrus infection. However, there is an expansion in TIGIT+ Teffector cells during *H. polygyrus* infection which is highest at d7 post infection and contracts to near-naïve levels by d14 post infection (Figure 4.15C). There is also an increase in the average expression of TIGIT in Teffector cells 7 days post *H. polygyrus* infection but not at d14 post infection (Figure 4.15D). This suggests that, like PD-1, the expression of TIGIT is involved in the Teffector response to *H. polygyrus* but not in the Treg response.

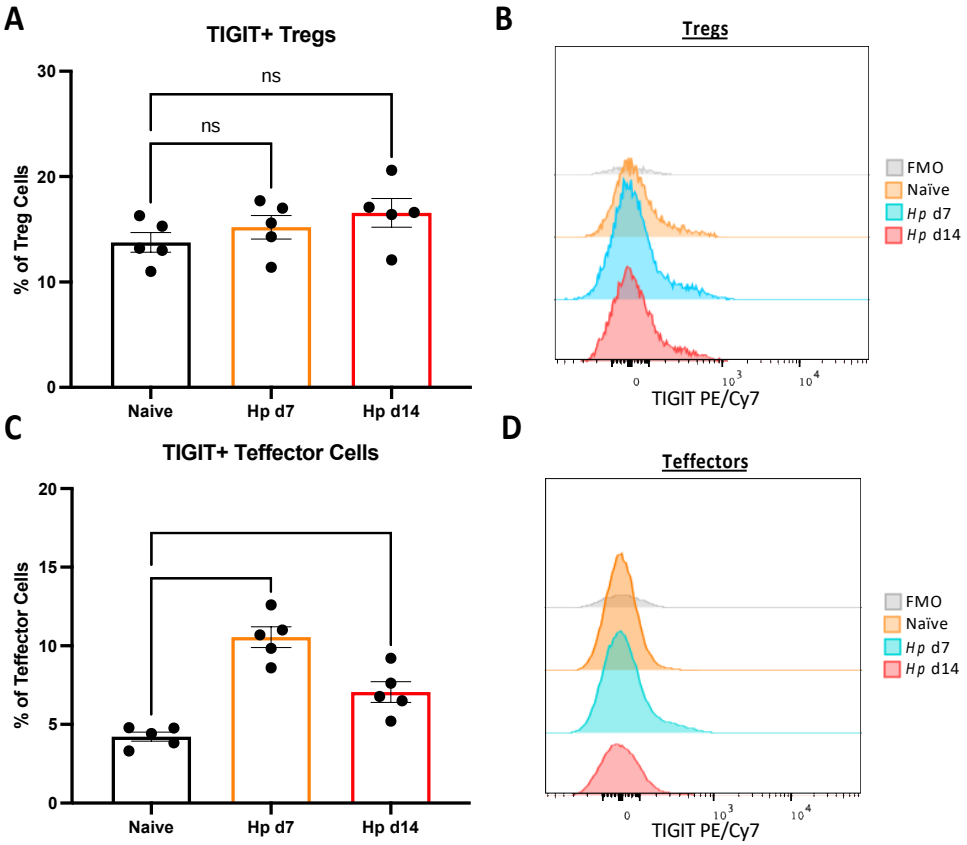

Figure 4.15 The expression of TIGIT on Tregs and Teffector cells from H. polygyrus infected mice. (A) The proportion of TIGIT+ Tregs within the total Treg population in the MLN of naïve (black), *Hp* d7 (orange) and *Hp* d14 infected mice (red) (B) The MFI of TIGIT in the Treg population in the MLN of naïve (black), *Hp* d7 (orange) and *Hp* d14 infected mice (red) (C) The proportion of TIGIT+ Teffectors within the total Teffector population in the MLN of naïve (black), *Hp* d7 (orange) and *Hp* d14 infected mice (red) (B) The MFI of TIGIT in the Teffector population in the MLN of naïve (black), *Hp* d7 (orange) and *Hp* d14 infected mice (red).
Graphs representative of 1 experiment. Each point represents a single mouse, error bars represent the standard error of the mean. In each group n=5. Normality tested using a Shapiro-Wilk normality test. Significance tested using an ordinary one-way ANOVA and Holm-Šídák's multiple comparisons test. ns P>0.05, * P<0.05, ** P<0.01, ** P<0.001, **** P<0.0001.

4.4 Discussion

Tregs from *H. polygyrus*-infected mice show a specialist phenotype in early infection which is associated with the Th2 transcription factor GATA3 and the co-inhibitory molecule CTLA-4. However, the exact role of these Tregs and the part they play in infection remains a mystery.

Tregs are expanded in many tissues within the intestinal milieu despite *H. polygyrus* infection being limited to the duodenum (White, Johnston, et al., 2020). The expansion of Tregs in the small intestine lamina propria and the mesenteric lymph nodes which drain lymph from this region was expected, as the cells in these regions will be in direct contact with the worm and its ES products. The same is true of the Peyer's patches as those isolated for these experiments were all in close proximity to an *H. polygyrus* helminth, as also in keeping with work from the Harris Laboratory (Mosconi *et al.*, 2015). Peyer's patches are an important part of the gut-associated lymphoid tissues (GALT) and contain specialised epithelial M (microfold) cells which can capture antigen from the lumen of the intestine and deliver this antigen to immune cells within the Peyer's patch (Jung et al., 2010). In this way, Peyer's patches act as a tissue embedded lymphoid organ and are an important source of *H. polygyrus* responsive immune cells (Mosconi *et al.*, 2015).

Notably, Tregs increase in the Peyer's patches during *H. polygyrus* infection, showing that these tertiary lymphoid organs are responding to *H. polygyrus* in the same way as in the MLN and SILP. This is especially helpful with the difficulties in isolating viable cells from the SILP (Ferrer-Font et al., 2020; H. C. Webster, Andrusaite, Shergold, Milling, & Perona-Wright, 2020). There is also an expansion of Tregs in the colonic lamina propria which may explain the protection against colitis that is seen in *H. polygyrus* infected mice (Elliott et al., 2004; Hang et al., 2010b). This expansion may be due to responses against worms being expelled out of the gastrointestinal tract travelling through the colon or the presence of HES in the colon. The expansion of Tregs at a distal sites during *H. polygyrus* infection may also explain the protection against allergic and autoimmune diseases in many different tissues in the body (Bashir et

al., 2002; Kitagaki et al., 2006; Saunders et al., 2007; White, Johnston, et al., 2020; Wilson et al., 2005).

However, no Treg expansion was observed in the spleen and inguinal lymph node, at least at the time points sampled, showing that while *H. polygyrus* infection can affect gut-associated tissues, this effect is not necessarily seen in peripheral organs. It has been previously shown that *H. polygyrus* infection can protect against the development of EAE, allergic airway inflammation, food allergy and type 1 diabetes (Bashir et al., 2002; Kitagaki et al., 2006; Saunders et al., 2007; White, Johnston, et al., 2020; Wilson et al., 2005). With the lack of Treg expansion in the spleen and iLN during infection, the effects of *H. polygyrus* infection on peripheral organs are likely not straightforward global expansion of Tregs in all tissues of infected mice.

During *H. polygyrus* infection, there is a change in the Treg population which allows co-expression of transcription factors which are associated with the classical T helper subsets. There are very few T-bet expressing Tregs found in the MLN of C57BL/6 and BALB/c mice, although this small population does expand in C57BL/6 mice after 7 days of *H. polygyrus* infection. These T-bet+ Tregs are potentially functioning to maintain tolerance to the antigens introduced by *H. polygyrus* damaging the gut throughout its life cycle. However, such cells make up a small proportion of T cells within the MLN and may have limited impact on infection. Notably, the expansion of these T-bet+ Tregs is proportional to the increase in Th1 cells seen in *H. polygyrus* infected C57BL/6 mice, suggesting that the role of these T-bet+ Tregs is to control the Th1 response. Further work is needed to confirm this phenomenon and study the dynamics of T-bet+ Tregs throughout the course of chronic helminth infection. Understanding the role of not only the T-bet+ Tregs but also the expanded Th1 cells may give more insight into the role of type 1 immunity throughout the course of *H. polygyrus* infection.

Expansion of GATA3hi Tregs is seen during *H. polygyrus* infection in both BALB/c and C57BL/6 mice which suggests these Tregs are important in the immune response against the helminth. There was also a relationship between the proportion of Th2 cells and the proportion of GATA3hi Tregs where those with

the highest proportion of Th2 cells had the highest proportion of Tregs expressing GATA3. These shared dynamics suggest that GATA3hi Tregs are induced proportionally to their Teffector counterparts to allow effective suppression of these Teffectors and prevent Th2 mediated damage to the host. This is an important part of any immune response as uncontrolled Th responses can lead to immunopathology and even autoimmune responses (Belkaid, 2007; Rick M. Maizels & Smith, 2011; Sakaguchi et al., 2008; White, McManus, et al., 2020).

However, we do not know what role these Tregs are playing during infection and additional work is required to discover the role of this subtype of Treg. First, their expression of Th2-associated chemokine receptors like CCR3 and CCR8 can be compared to the receptor expression in Th2 cells, this would give an indication about whether these Tregs are migrating along the same chemokine gradients as Th2 cells and thus are being trafficked together. Another assay that would elucidate the role of these Tregs would be sorting the GATA3hi Tregs and culturing with α-CD3 to assess the cytokine output of these cells. If these Tregs are producing type 2 cytokines like IL-4, IL-5 and IL-13, this may imply that they are playing a role in the anti-helminth response rather than suppressing that response. This is a feasible possibility as T-bet+ Tregs which produce IFNγ and behave more like a Teffector cell have been previously described in the gut of Ulcerative Colitis and Crohn's Disease patients (di Giovangiulio *et al.*, 2019). On the other hand, if these Tregs are producing higher levels of tolerogenic cytokines like IL-10, this indicates that the cells are performing a regulatory function and are not contributing to the Th2 response. To assess whether these Tregs are active and capable of suppressing Th2 responses, a GATA3 Foxp3 dual reporter mouse is required to allow sorting of this specialised population. After sorting, GATA3hi Tregs can be used in a T cell suppression assay and their ability to suppress different Th subtypes can be used to assess whether these Tregs are in fact better at suppressing Th2 responses rather than Th1 or Th17. If these Tregs do suppress the Th2 response, targeting this population may increase clearance of the worm by removing the suppression of Th2 cells.

The role of RORγt+ Tregs during *H. polygyrus* infection is complex and their dynamics during infection makes it difficult to assess their exact function and

impact on Th2 cells. While the number of RORγt+ Tregs increases during *H. polygyrus* infection, the proportion of Tregs expressing this transcription factor does not increase upon infection. Of note is that during *H. polygyrus* infection, there is an expansion of the total cell number within the MLN when compared to their naive counterparts and this alone may be the reason for the increased numbers of RORγt+ Tregs rather than an active upregulation of this population. To further understand the roles of these cells during helminth infection, a RORγt Foxp3 dual reporter mouse line is required to allow sorting of RORγt+ Tregs without fixing the cells for intranuclear staining. After sorting RORγt+ Tregs, the cells can be cultured with α-CD3 to induce cytokine production. Like with GATA3hi Tregs, if the cells produce high levels of IL-10, they are likely performing a role in regulation of the immune response and if they produce IL-17, they are likely performing effector functions associated with the type 3 (Th17) response. Sorted RORγt+ Tregs can also be used in T cell suppression assays with different Th cells to assess their ability to suppress Th17 cells and the Th2 cells associated with helminth clearance.

Ohnmacht and colleagues found that loss of RORγt in the Treg population alone led to higher GATA3+ Tregs and Th2 cells along with increase type 2 cytokines IL-4, IL-5 and IL-13 (Ohnmacht *et al.*, 2015). When RORγtfl/fl Foxp3Cre mice are infected with *H. polygyrus*, there is decreased eggs in their faeces at days 14, 24 and 31 post infection compared to wild type control mice (Ohnmacht *et al.*, 2015). This suggests that the RORγt+ Tregs are limiting the expansion of both GATA3+ Tregs and Th2 cells. With the mutual suppression between RORγt+ Tregs and GATA3+ Tregs, it is possible that the RORγt+ Tregs are suppressing the type 2 response indirectly by filling a niche so that GATA3+ cells are limited. More studies are required to elucidate the exact role of RORγt+ Tregs during *H. polygyrus* infection.

With the parasitological outcome of RORγtfl/fl Foxp3Cre and IL-6KO mice being very similar, it was decided to assess whether the deficit in Tregs when IL-6 is blocked is due to loss of RORγt+ Tregs. Since IL-6 signals through STAT3 and the STAT3fl/fl Foxp3Cre mice had a loss of RORγt expression in Tregs, this solidified our hypothesis. However, when α-IL-6 monoclonal antibody was given i.p. to block IL-6 signalling during infection, there is no change in the percentage of

Tregs expressing RORγt nor the percentage of Th17 cells compared to the rat IgG control. This suggests that IL-6 blockade using monoclonal antibody does not significantly impact RORγt expression in either Tregs or Th17 cells when compared to the rat IgG control. This may be due to compensatory IL-6 production seen in Figure 4.13 and 20F3 has been used in other studies where there was also no impact on the RORγt+ Treg population (Bhaumik, Mickael, Moran, Spell, & Basu, 2021). It was also suggested by this study that RORγt+ Tregs are suppressing the type 1 immune response by limiting T-bet expression and IFNγ production (Bhaumik *et al.*, 2021). Together this shows that limiting IL-6 availability does not significantly impact the co-expression of RORγt and Foxp3 and the reduced Treg suppression in IL-6 KO mice is likely not due to loss of RORγt+ Tregs.

The expression of CD44 is altered by IL-6 blockade during *H. polygyrus* infection. The ability of IL-6 to alter CD44 expression is seen in human myeloma and macrophages isolated from atherosclerosis where higher levels of IL-6 lead to higher expression of CD44 at the protein and RNA level (Vincent 2004, Hagg 2007). In this experiment, there is a loss of CD44 on Tregs and Foxp3- CD4+ Teffector cells increase the percentage of CD4+ T cells expressing CD44. This suggests that the Tregs are less active and a population in the Foxp3- population is more active as a result. The most logical hypothesis is that the loss of Treg suppression allows increased expansion and activation of Th2 cells, however, the CD44 expression on GATA3+ Foxp3- CD4+ T cells was also reduced, suggesting that these cells are also tolerised by the IL-6 blockade. The increase in CD44hi Teffectors is also not due to RORγt+ Foxp3- CD4+ Th17 cells. It is worth noting that the proportion of Th2 cells is increased when treated with α-IL-6, showing that suppression by Tregs has been lowered, allowing a further expansion than in untreated mice.

IL-6 is a pleiotropic cytokine which can at as both a pro-inflammatory and an anti-inflammatory factor and impacts many arms of the immune response as well as non-immune cells (C. A. Hunter & Jones, 2015; Puel & Casanova, 2019). This makes it difficult to untangle the response and see cause and effect on the immune system. IL-6 is required in some capacity for the polarisation and maintenance of Th17 cells, Tregs, Th1 cells and Tfh cells (Dienz & Rincon, 2009).

Classically, it is thought that IL-6 expands the Th17 cell population while inhibiting the expansion of Tregs by mutual exclusion of the two cell types (Luckheeram *et al.*, 2012). With this dogma in mind, IL-6 blockade should increase the number of Tregs by decreasing the number of Th17 cells. However, this was not seen in *H. polygyrus* infection when IL-6 is inhibited by a monoclonal antibody.

The interaction between IL-6 and T follicular helper (Tfh) cells may hold the answer to the altered T cell response when IL-6 is blocked. IL-6 alongside IL-21 is required for the differentiation of Tfh cells and signals via STAT1 and STAT3 (Choi, Eto, Yang, Lao, & Crotty, 2013; Dienz & Rincon, 2009; Eto et al., 2011). Tfh cells are central to the B cell response and give survival signals to B cells which recognise an antigen with high affinity (Crotty, 2014, 2015a). After getting survival signals from the Tfh cells in the germinal centre, activated B cells proliferate and undergo somatic hypermutation to produce high affinity antibody (Crotty, 2014, 2015a). The newly mutated B cell can then interact again with the Tfh cells and clones with a high affinity receptors are given survival signals and leave the lymph node to produce antibody in the periphery (Crotty, 2014, 2015a). IL-6 blockade may change the differentiation of Tfh cells and this could impact the whole B cell response which could explain the difference in parasitological outcome. Tfh cells are also important players in the immune response against *H. polygyrus* as they are the biggest producers of IL-4 during *H. polygyrus* and produce significantly more IL-4 than Th2 cells (I. L. King & Mohrs, 2009). There is also evidence that Th2 cells can become Tfh-like cells during *H. polygyrus* infection and produce IL-4 within the B cell follicle of the lymph node (Zaretsky *et al.*, 2009). It is possible that this switch of Th2 cells to Tfh-like cells is affected by the lack of IL-6 and this impacts both the B cell response and increases the number of true Th2 cells.

In a repeat of this experiment, a Tfh cell staining panel was added but the CD44 phenomenon was not as pronounced in this experiment despite following the same protocol and using the same batch of monoclonal antibody. With the role the microbiota plays in the type 3 RORγt and IL-6 associated response being dependent on the microbiome, there is a possibility that the difference in

microbiome from the two batches of mice impacted the outcome of the blockade.

Further work is required to assess what type of CD4+ T cell is more activated and expressing high levels of CD44 and whether their role in the immune response against *H. polygyrus* impacts the outcome of infection.

There is an expansion of extracellular CTLA-4+ Tregs during early *H. polygyrus* infection and an increase in the MFI of intracellular CTLA-4 within Tregs. This confirms earlier findings that Tregs *H. polygyrus* infected C57BL/6 mice lose their suppressive capacity in the presence of α-CTLA-4 blocking monoclonal antibody (Bowron *et al.*, 2020). However, the mechanism through which CTLA-4 is mediating this suppression is unknown. One potential mechanism, as discussed previously, is tolerization of DCs which involves trans-endocytosis of CD80 and CD86 which lowers the DCs ability to activate more Teffector cells (Hou *et al.*, 2015; Ovcinnikovs *et al.*, 2019). To assess whether this mechanism is being used by Tregs from *H. polygyrus* infection, Tregs from *H. polygyrus* infected mice can be sorted and cultured with DCs expressing CD80 and CD86. After culturing together, the cells can be stained for Treg markers as well as CTLA-4, CD80 and CD86. The samples can then be run on the ImageStream cytometer which performs fluorescence microscopy alongside flow cytometric analysis, this will allow us to see not only if Tregs have CD80 and CD86 expression but also where these molecules localise within the cell. This can be used to assess whether there is CD80 and CD86 found within CTLA-4+ Tregs, showing whether *H. polygyrus*-induced Tregs are capable of performing trans-endocytosis.

There is also an increase of intracellular CTLA-4+ Th2 effector cells during *H. polygyrus* infection. The expression of CTLA-4 by Teffector cells is often associated with anergy which may imply that Teffectors from *H. polygyrus* infected mice are in an anergic state. This is in keeping with findings during infection with the filarial nematode *Litomosoides sigmodontis,* During the late phases of infection, the helminth responsive Th2 cells become dysfunctional which is mediated by CTLA-4 and their responsiveness can be restored using an α-CTLA-4 monoclonal antibody (Taylor *et al.*, 2007). However, there is also evidence that Foxp3- CTLA-4+ Teffector cells can suppress other Teffectors *in*

vitro, this might suggest that these CTLA-4+ Teffector cells are acting as a Foxp3- regulatory T cell (Tai *et al.*, 2012).

To establish the role of CTLA-4 during *H. polygyrus* infection, Foxp3Cre CTLA-4fl/fl and CD4Cre CTLA-4fl/fl mice are required to untangle the role of CTLA-4 on Tregs versus CTLA-4 on Teffectors. This would allow us to assess whether CTLA-4 is required for tolerance and if loss of this molecule on all CD4+ T cells or Tregs leads to increased parasite clearance.

PD-1 is not increased on Tregs during early *H. polygyrus* infection. This is somewhat surprising with the upregulation of CTLA-4 in the Treg compartment alongside the increase in PD-1 on Tregs during *L. sigmodontis* and *S. mansoni* infection (Taylor et al., 2007; Walsh et al., 2007; K. Watanabe et al., 2007; White, McManus, et al., 2020). These experiments looked at an early time point during infection but did not look in chronically infected animals. It is possible that PD-1 on Tregs may be important when infection reaches chronicity as seen in *L. sigmodontis* and schistosomiasis (Taylor et al., 2007; Walsh et al., 2007; K. Watanabe et al., 2007; White, McManus, et al., 2020). However, PD-1 was upregulated on Th2 cells. PD-1 is another marker of anergic and dysfunctional T cells and has been shown to limit clonal expansion of T cells, again inducing tolerance (Knipper et al., 2019; Konkel et al., 2010; Redpath et al., 2013; Taylor et al., 2007; van der Werf, Redpath, Azuma, Yagita, & Taylor, 2013). In fact, in chronic *L. sigmodontis* dysregulated and hyporesponsive T cells are able to be rescued when blocking PD-1 and its interaction with PDL2, which shows that PD-1 is a marker of helminth dysregulated T cells (Knipper et al., 2019; van der Werf et al., 2013). When EAE is induced in *H. polygyrus* infected mice, there is an upregulation of PD-1+ CD4+ T cells (White, Johnston, et al., 2020). However, this PD-1 expression is not associated with protection from EAE (White, Johnston, et al., 2020). This may suggest that PD-1+ Teffector cells are not performing a suppressive function.

As discussed preciously, TIGIT is another co-inhibitory receptor which preferentially suppresses Th1 and Th17 cells (Joller *et al.*, 2014). During *H. polygyrus* infection, there is no differential expression of TIGIT on Tregs compared to naïve counterparts. TIGIT+ Tregs have been shown to be more

efficient at suppressing Th1 and Th17 cells, this could explain why this population does not expand during *H. polygyrus* infection where the active Th cells that require suppression are Th2 cells (Joller *et al.*, 2014). However, TIGIT is upregulated on Foxp3- Teffector cells. TIGIT has been shown to preferentially induce Th2 cells and is also upregulated in *L. sigmodontis* (Joller et al., 2014; Knipper et al., 2019). This suggests that TIGIT is also an important receptor for Th2 responses in early infection with *H. polygyrus*. Of note is that Knipper *et al.* found that TIGIT is a marker of dysregulated Th2 responses during chronic *L. sigmodontis* infection, this means that TIGIT may be marking Th2 cells which will go on to become dysfunctional in chronic infection (Knipper et al., 2019). More studies are required to elucidate the role of TIGIT expression by Teffector cells during *H. polygyrus* infection.

Overall, it seems that co-inhibitory receptors, with the exception of CTLA-4, are not used as a method of suppression during the early stages of *H. polygyrus* infection. However, there is an increase in co-inhibitory molecules on the Teffector cells from early *H. polygyrus* infection, this may be evidence of dysregulation of the Th2 response or evidence that Th2 expansion and function is limited by their expression of co-inhibitory receptors.

4.4.1 Summary

- Tregs are expanded in many tissues in the peritoneal cavity during *H. polygyrus* infection

- GATA3hi Tregs are expanded during *H. polygyrus* infection in the same proportions as the Th2 cells

- RORγt+ Tregs are not increased in proportion during *H. polygyrus* infection but are increased in number. Their role in the suppression of the type 2 response against *H. polygyrus* infection is still largely unknown

- Blocking IL-6 causes a deficiency in the Treg compartment but does not affect RORγt+ Tregs

- CTLA-4 is increased on Tregs and Teffector cells during *H. polygyrus* infection

- Tregs do not upregulate the co-inhibitory receptors TIGIT and PD-1 during early *H. polygyrus* infection

- TIGIT and PD-1 are upregulated on Teffector cells during early *H. polygyrus* infection

Chapter 5 T Cell antigen specificity during H. polygyrus infection

5.1 Introduction

5.1.1 Potential T cell epitopes during H. polygyrus infection

During *H. polygyrus* infection, there is an expansion of CD4+ T cells, including Tregs and Th2 cells which together control the outcome of infection (K A Smith et al., 2016). However, very little is known about which antigens these T cells are recognising through their TCR, and whether they are shared or distinct between the regulatory and effector populations. Identification of either would shed light on how the parasite escapes immune attack, and which epitopes might be most suitable to induce protective immunity.

When considering the range of antigens available for T cell recognition, *H. polygyrus* infection contains a vast array of potential epitopes. Unlike single molecule substances, viruses and bacteria, common subjects of transgenic TCR mouse lines, *H. polygyrus* is a macroparasite of with a length of around 4-12mm depending on its sex and life cycle stage (Pritchett-Corning & Clifford, 2012). Soluble somatic *H. polygyrus* extract (HEx), is obtained by homogenising adult *H. polygyrus* in PBS and collecting the supernatant. Despite omitting membrane proteins and other poorly soluble components, this extract contains many hundreds of different proteins (Hewitson et al., 2013; Hewitson, Harcus, et al., 2011). Some investigators have focussed on the *H. polygyrus* excretory-secretory products (HES), although there are again several hundred proteins, some of which are shared with HEx (Hewitson et al., 2013; Hewitson, Harcus, et al., 2011). These antigen preparations are vastly different from simple molecules or viruses made up of RNA or DNA sequences surrounded by a capsid and envelope made up of repeating lipids and proteins (Louten, 2016).

With this many potential epitopes, the generation of a TgTCR mouse against a natural *H. polygyrus* epitope found in normal infection of its host must start with a large peptide screening process. Transgenic TCR (TgTCR) mice have an altered T cell repertoire in which the majority of their repertoire is monoclonal and recognises an epitope of interest (Bettini, Bettini, & Vignali, 2012; Cho, Lee,

Joo, Hong, & Seo, 2020; C. Li et al., 2018). TgTCR mice have been generated with many different antigen specificities such as ovalbumin (an inert antigen from the white of chicken eggs), *Salmonella spp*, herpes simplex virus (HSV), *Plasmodium chabaudi* and *Plasmodium berghei* and work is being done to produce a TgTCR mouse against an allergen (Barnden, Allison, Heath, & Carbone, 1998; Cho et al., 2020; Fernandez-Ruiz et al., 2017; S. J. McSorley, Asch, Costalonga, Reinhardt, & Jenkins, 2002; Stephens et al., 2005; Vanheerswynghels et al., 2018). These transgenic mice can be used to study the antigen specific response of mice to the substance or organism of choice. The antigen specific T cell response can be tracked from TCR:MHC II ligation to activation to specialisation into Teffector cells versus Treg cells and migration, among other things (Barnden et al., 1998; Cho et al., 2020; S. J. McSorley et al., 2002; Vanheerswynghels et al., 2018). However, there are few TgTCR mice currently available which recognise epitopes from more complex organisms like *H. polygyrus* (Stephens *et al.*, 2005).

Within the complexity of *H. polygyrus* antigenicity, some indication of the most immunogenic proteins can be gained from their relative abundance and the strength of the host antibody response that is mounted during infection. In particular, the venom allergen-like (VAL) proteins are found in great abundance in both HES and Hex, and in both immature larval and adult worm stages (Hewitson, Harcus, *et al.*, 2011). These proteins induce strong humoral responses in mice which in the case of combined *Hp*-VAL-1/-2/-3 immunisation, induces protective immunity (Hewitson *et al.*, 2015). However VAL proteins are frequently glycosylated, and a non-protective antibody response has been seen against the glycans of VAL proteins, with IgM response directed against glycans found in *Hp*-VAL-1, *Hp*-VAL-2 and *Hp*-VAL-5 and an IgG1 response against glycans in *Hp*-VAL-3 and *Hp*-VAL-4 (Hewitson, Filbey, *et al.*, 2011). These data suggest that there are CD4+ Th cells giving very effective help to VAL-specific B cells which go on to produce antibody against the VALs (Crotty, 2015a). With this in mind, the VAL protein family will be screened for T cell recognition, using both bioinformatic and experimental approaches.

5.1.2 MHC II Epitope Prediction Methods

As discussed in Chapter 1, binding of a peptide representing a T cell epitope to MHC class II is required for CD4+ T cell recognition through the T cell receptor (TCR) and activation of the cell. The peptides have a MHC II-binding core of around 9 amino acids which are required for epitopes to be presented to CD4+ T cells and unlike MHC class I, MHC II has no physical size restriction for the peptides it binds, most epitopes which bind to MHC II are between 13 and 25 amino acids long (Nielsen, Lund, Buus, & Lundegaard, 2010; P. Wang et al., 2008; L. Zhang, Udaka, Mamitsuka, & Zhu, 2012). There are 5 residues within the 9 residue binding core which are thought to be paramount for the binding of peptide to MHC II. These anchor residues are at positions 1, 4, 6, 7 and 9 of the binding core (Nielsen et al., 2010; L. Zhang et al., 2012). Utilising the known structure of MHC II and the locations of the binding residues along with databases of known MHC II binding peptides, it is possible to predict presentable peptides from full protein sequences (Nielsen et al., 2010; L. Zhang et al., 2012).

MHC I epitope prediction has always been more straightforward than MHC II prediction due to the binding pocket of MHC I being size restricted (L. Zhang et al., 2012). This means that all peptides which bind to MHC I must be a maximum of 11 amino acids long which allows restriction of epitope predictions (L. Zhang et al., 2012). For MHC II however, the binding pocket is open ended and peptides can range in length, rendering size based exclusion more complex (Nielsen et al., 2010; P. Wang et al., 2008; L. Zhang et al., 2012). As a result, the prediction of MHC II epitopes is less accurate than prediction of MHC I epitopes (L. Zhang et al., 2012).

MHC II epitope prediction has been greatly improved in recent years with increasing sizes of peptide libraries and more advanced algorithms and neural networks (Wang et al., 2008; Nielsen and Lund, 2009; Nielsen et al., 2010; Zhang et al., 2012; Graham et al., 2018; Jensen et al., 2018; Reynisson et al., 2020). Where previously epitope predictions were made based on anchor points within the binding groove of MHC II, new methods utilise libraries of known MHC II peptides to predict areas in the protein which have similarity to known peptides

(Jensen et al., 2018; Nielsen & Lund, 2009; Nielsen et al., 2010; Reynisson et al., 2020; P. Wang et al., 2008).

NetMHCII is a well-known MHC II epitope prediction method which utilises a trained artificial neural network (ANN) and a database containing around 100,000 known MHC II peptides, to predict potential T cell epitopes (Jensen *et al.*, 2018). The neural network is trained to predict the sequence of the peptides binding core while also predicting the strength of the affinity with which it binds to MHC II (Jensen et al., 2018; Nielsen et al., 2010; P. Wang et al., 2008; L. Zhang et al., 2012). The IEDB MHC II Prediction method on the other hand uses a consensus method where multiple MHC II epitope prediction methods (including NetMHCII) are run and the mean of the top performing prediction methods is given (Nielsen, Lundegaard and Lund, 2007; Wang et al., 2008, 2010; Nielsen and Lund, 2009; Jensen et al., 2018). This considers different methods of prediction and ensures the methods with the best predictions are taken into account (Wang et al., 2008, 2010). The NetMHCII ANN method and IEDB consensus methods will be compared to test the accuracy of the prediction and avoid missing epitopes which may be important during *H. polygyrus* infection.

5.1.3 Experimental Markers of TCR engagement

To screen for peptides which are recognised by and induce T cell activation, CD4+ T cells can be isolated from the MLN of *H. polygyrus* infected and naïve mice and restimulated *in vitro* with different proteins from HES and HEx to test for engagement of the TCR and thus recognition. A number of surface markers have been utilised as measures of TCR engagement with the most common being CD69, CD154 and CD25 as summarised below; in addition, a recently devised intracellular signalling approach will be described which resolves the issue of whether T cells taken from infected mice may be expressing surface markers of activation due to stimulation *in vivo* rather than through antigen presentation *in vitro*.

5.1.3.1 CD69

CD69 is a C-type lectin which is found on the surface membrane of CD4+ T cells as early as 4 hours post-TCR engagement (Antas et al., 2002; Cibrián & Sánchez-madrid, 2017). It is one of the earliest known markers of T cell activation and is thought to be involved in the differentiation process which directs a naïve CD4+ T cell towards a Teffector or Treg phenotype as well as the migration or retention of these cells (Antas et al., 2002; Cibrián & Sánchez-madrid, 2017; Peixoto et al., 2019; Radulovic et al., 2013b; L. Yu et al., 2018). CD69 deficient T cells have reduced *in vitro* induction of Tregs and significantly lower Treg numbers in many tissues, showing that the balance between Tregs and other CD4+ T cell subtypes is affected by the loss of CD69 (Radulovic *et al.*, 2012). CD69 is also downregulated beginning around 24 hours post-TCR engagement and returns to near homeostatic level at 120 hours post-engagement (Antas *et al.*, 2002). These properties give a window between 4-24 hours post TCR engagement to evaluate restimulation.

5.1.3.2 CD154 (CD40L)

Another surface marker of T cell activation following *in vitro* restimulation of CD4+ T cells is CD40L or CD154 (Chattopadhyay, Yu, & Roederer, 2006; Elgueta et al., 2009). CD154 is the ligand for CD40, a costimulatory molecule which directs the humoral and cellular immune response (Chattopadhyay et al., 2006; Elgueta et al., 2009). The interaction between CD40L on T cells and CD40 on B cells and APCs leads to increased B cell survival, proliferation and production of antibody (Elgueta *et al.*, 2009). CD40:CD40L signalling is also central to germinal centre formation which is essential for B cell memory and somatic mutation of the BCR and resulting class-switched antibody (Elgueta et al., 2009; Crotty, 2015a; Watanabe et al., 2017). CD154 is upregulated as quickly as 4 hours and can maintained beyond 24 hours post TCR engagement (Chattopadhyay et al., 2006). However, CD154 is quickly internalised and degraded, limiting its accumulation at the cell surface and its instability as a complex with labelled antibody may limit its usefulness as a marker to identify activated T cells (Chattopadhyay et al., 2006). However, in terms of recent restimulation, the fast degradation of CD154 starting 6 hours post-stimulation may show more

accurately which cells have been very recently stimulated (Chattopadhyay et al., 2006).

5.1.3.3 CD25 (IL-2Rα)

The IL2Rα or CD25 is another marker of activation which could be used for identification of newly activated T cells. CD25 is upregulated by the influx of calcium ions into the cell in response to TCR engagement with MHC II (Komada, Nakabayashi, Hara, & Izutsu, 1996). However, while CD25 is a good marker of TCR engagement in Teffector cells, Tregs are often identified based on their constitutive expression of CD4, CD25 and Foxp3. In the case of Tregs, CD25 would not therefore be a clear marker of early T cell activation and thus CD25 was not used as a primary activation marker in this study.

5.1.3.4 Nr4a3-Tocky mice

While there are multiple early activation markers, the expression of these markers can be relatively long lived and poorly discriminatory in the case of CD25 and CD69, or be too short-lived as in the case of CD40L. To overcome these limitations, a novel transgenic mouse model has been developed, termed the Nr4a3-Tocky mouse. This system can be used to distinguish which cells were activated *in vivo* prior to *in vitro* culture with antigen.

The model exploits Nr4a3, a gene upregulated by calcineurin and NFAT downstream of TCR:MHC II engagement. Within around 30 minutes of TCR signalling, responding T cells upregulate Nr4a3 (Bending, Martín, et al., 2018; Jennings et al., 2020). In the Nr4a3-Tocky mouse, the Nr4a3 gene is tagged with a timer protein which is a modified mCherry (Bending, Martín, et al., 2018; Bending, Paduraru, et al., 2018; Jennings et al., 2020). In normal circumstances, mCherry has a very short-lived phase where it emits a blue light before maturing into its red form (Bending, Martín, et al., 2018; Bending, Paduraru, et al., 2018; Jennings et al., 2020). Timer protein mCherry has been mutated to extend the blue phase of mCherry (timer blue) and delay its maturation into red mCherry (timer red) to around 7 hours (Bending, Martín, et al., 2018; Bending, Paduraru, et al., 2018; Jennings et al., 2020). After maturation into the red timer protein,

there is a decay of the mCherry until its signal is lost around 20 hours after maturation (Figure 5.1A).

The cyclical maturation of mCherry in response to the upregulation of Nr4a3 allows the time of TCR engagement to be estimated by flow cytometry from the intensity of the mCherry protein and the relative intensity of timer red and timer blue expression (Bending, Martín, et al., 2018; Bending, Paduraru, et al., 2018; Jennings et al., 2020). This allows identification of cells that have been previously activated in the mouse, and those restimulated *in vitro* which are recognising the proteins given in the culture. Figure 5.1B shows a mock scatter plot of timer-red versus timer-blue and shows the different fluorescent phenotypes of cells from the Nr4a3-Tocky mice. For the purposes of measuring TCR engagement in response to HES, the New and Persistent populations are both expressing the blue variant of the protein, indicating cells (re-)stimulated within the last 7 hours.

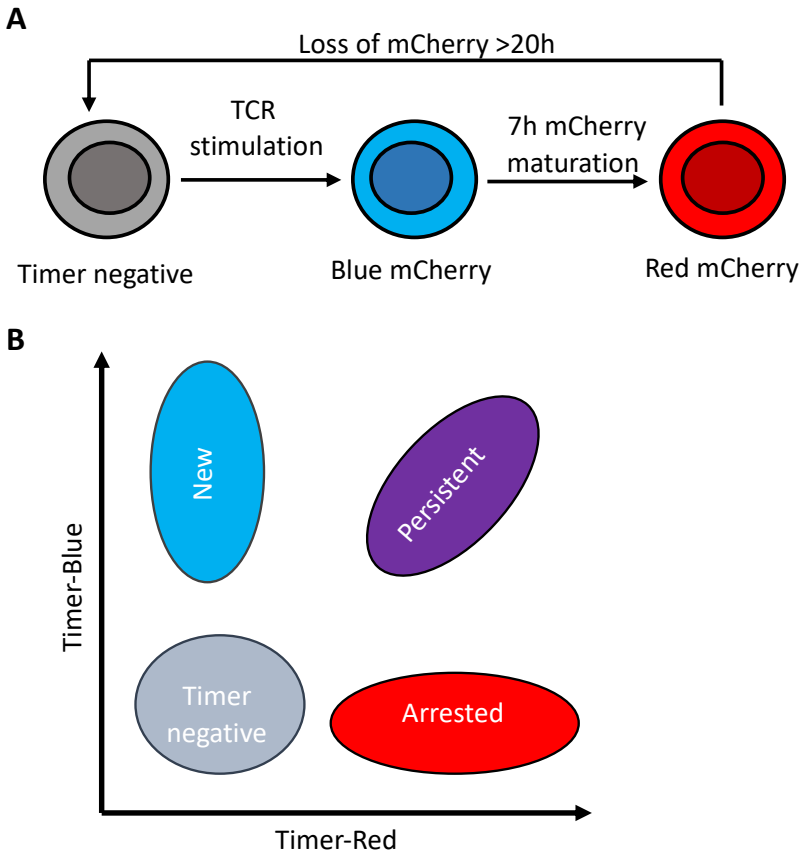

Figure 5.1 Dynamics of Nr4a3-tocky mice after TCR stimulation. (A) A flow chart showing the maturation of the timer protein (mutated mCherry) after TCR stimulation. (B) A representative scatter plot showing the position of the new (blue), persistent (purple), arrested (red) and timer- (grey). Figures adapted from (Bending *et al.*, 2018).

5.2 Aims

- To understand the antigen-specific T cell response to *Heligmosomoides polygyrus* in the mesenteric lymph nodes

- To identify T cell epitope(s) within HES that are recognised in a natural murine *H. polygyrus* infection

- To explore the dynamics of early activation markers in CD4+ T cells

5.3 Results

5.3.1 Hp-VAL-1.1 epitope predictions for C57BL/6 and BALB/c mice

Hp-VAL-1 is an abundant secreted protein of adult *H. polygyrus;* transcriptomics and proteomics identified at least 4 minor sequence variants, of which the most common is designated VAL-1.1 (Hewitson, Harcus, *et al.*, 2011). The sequence of VAL-1.1 was input into the NetMHCII and IEDB MHC II epitope prediction methods. Figure 5.2 shows the formatted alignment of *Hp*-VAL-1.1 and 3 variants also found in HES, *Hp*-VAL-1.2, -1.3, and 1.4, with the NetMHCII and IEDB predictions overlaid for BALB/c (H2-IA^{d}) and C57BL/6 (H2-IA^{b}) mice, which are respectively good and poor responders to *H. polygyrus*. Table 5.1 summarises the epitope prediction outputs for C57BL/6 and BALB/c, showing the peptide sequence, IC50 (half maximal inhibitory concentration) which represents the binding affinity using the concentration of a peptide needed to replace 50% of a high affinity molecule bound to MHC II and the strength of the affinity as suggested by NetMHCII or IEDB.

In the case of BALB/c mice and one of their MHC II haplotypes, H2-IA^{d}, both NetMHCII and IEDB predict aa 26-42 of Hp-VAL-1.1 to be an MHC II epitope (Figure 5.2A). IEDB predicts that this epitope is an intermediate binder of H2-IA^{d} while NetMHCII predicts that the epitope could be a weaker binder or a stronger binder of H2-IA^{d} depending on the flanking regions of the peptide (Table 5.1). This is in line with data which has shown differential binding affinity to MHC II depending on the interactions between the flanking regions of the epitope and the plasma membrane of the presenting APC or other cells (Nielsen *et al.*, 2010). The IEDB consensus method predicts aa 98-115 as a C57BL/6 T cell epitope (Figure 5.2B) that binds with intermediate strength (Table 5.1) and also contains multiple amino acid substitutions in the *Hp*-VAL-1 variants. IEDB (yellow) and NetMHCII (blue) both predict that aa 125-144 of *Hp*-VAL-1.1 is an epitope for C57BL/6 mice (Figure 5.2C). This epitope is predicted to be a strong binder to H2-IAb by NetMHCII and an intermediate binder by IEDB (Table 5.1). Notably, this epitope and lies along a stretch of peptides that are highly polymorphic

between the 4 variants of *Hp*-VAL-1, suggesting that sequence diversity may have been driven to escape T cell recognition.

IEDB also predicts aa 174-190 of *Hp*-VAL-1.1 as an intermediate binder of H2-IA^d whereas NetMHCII does not have this epitope in its top 10 predicted BALB/c epitopes (Figure 5.2D, Table 5.1). NetMHCII predicted aa 236-246 as an epitope which strongly binds to C57BL/6 MHC II (Figure 5.2E, Table 5.1). NetMHCII also predicts aa 335-358 as a strong binder of H2-IA^d which is not predicted by the IEDB consensus method (Figure 5.2F, Table 5.1).

Interestingly, the regions of *Hp*-VAL-1.1 which are predicted to bind to H2-IA^d are mostly conserved between the variants of *Hp*-VAL-1.1 which is in direct contrast to the predicted binders of H2-IA^b which show high levels of polymorphism. This suggests that the worm has evolved variants which may escape recognition of the C57BL/6 immune system but the same is not true of the BALB/c immune system. Together, this suggests that there are multiple potential T cell epitopes in *Hp*-VAL-1.1 which have different predicted binding strengths and differ between C57BL/6 and BALB/c mice.

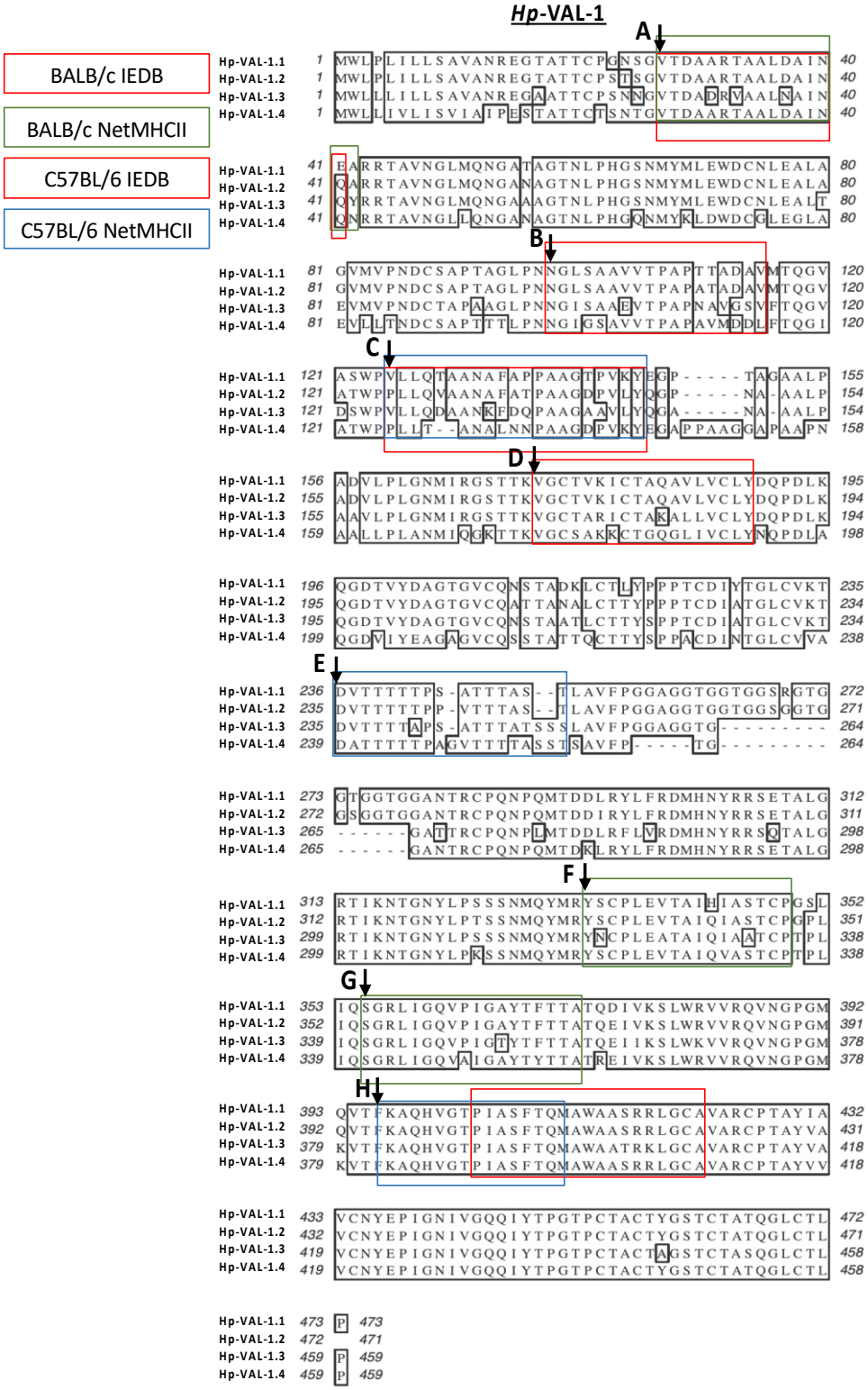

Figure 5.2 Peptide predictions from NetMHCII and IEDB for Hp-VAL-1.1. The epitopes predicted to be T cell immunogenic in *Hp*-VAL-1.1 superimposed on the formatted alignment of *Hp*-VAL-1.1 and its variants *Hp*-VAL-1.2, *Hp*-VAL-1.3 and *Hp*-VAL-1.4. NetMHCII predictions for C57BL/6 are shown in blue and BALB/c prediction is shown in green. IEDB predictions for C57BL/6 are shown in yellow and for BALB in pink.

Hp-VAL-1.1	Allele	a.a. position	Peptide Sequence	ic50 (nM)	Bind Level
IEDB	H2-IAd	403-417	ASFTQMAWAASRRLG	283.7	Intermediate
	H2-IAd	402-416	IASFTQMAWAASRRL	298.6	Intermediate
	H2-IAd	172-186	GCTVKICTAQAVLVC	296.6	Intermediate
	H2-IAd	404-418	SFTQMAWAASRRLGC	341.1	Intermediate
	H2-IAd	171-185	VGCTVKICTAQAVLV	288.2	Intermediate
	H2-IAd	173-187	CTVKICTAQAVLVCL	324.5	Intermediate
	H2-IAd	27-41	VTDAARTAALDAINE	191.7	Intermediate
	H2-IAd	401-415	PIASFTQMAWAASRR	449.7	Intermediate
	H2-IAd	405-419	FTQMAWAASRRLGCA	446.7	Intermediate
	H2-IAd	174-188	TVKICTAQAVLVCLY	421.9	Intermediate
	H2-IAb	128-142	QTAANAFAPPAAGTP	35.3	Strong
	H2-IAb	126-140	LLQTAANAFAPPAAG	34.9	Strong
	H2-IAb	127-141	LQTAANAFAPPAAGT	37.3	Strong
	H2-IAb	129-143	TAANAFAPPAAGTPV	38.1	Strong
	H2-IAb	125-139	VLLQTAANAFAPPAA	40.4	Strong
	H2-IAb	130-144	AANAFAPPAAGTPVK	45.3	Strong
	H2-IAb	131-145	ANAFAPPAAGTPVKY	64.3	Intermediate
	H2-IAb	98-112	NGLSAAVVTPAPTTA	117.8	Intermediate
	H2-IAb	99-113	GLSAAVVTPAPTTAD	130.1	Intermediate
	H2-IAb	100-114	LSAAVVTPAPTTADA	135.2	Intermediate
NetMHCII	H-2-IAd	357-372	GRLIGQVPIGAYTFT	112.2	Strong
	H-2-IAd	356-371	SGRLIGQVPIGAYTF	128.9	Strong
	H-2-IAd	358-373	RLIGQVPIGAYTFTA	130.5	Strong
	H-2-IAd	332-347	SCPLEVTAIHIASTC	147.5	Strong
	H-2-IAd	333-348	CPLEVTAIHIASTCP	151.6	Strong
	H-2-IAd	331-346	YSCPLEVTAIHIAST	161.8	Strong
	H-2-IAd	28-42	TDAARTAALDAINEA	178.4	Strong
	H-2-IAd	355-370	QSGRLIGQVPIGAYT	188.7	Weak
	H-2-IAd	27-41	VTDAARTAALDAINE	191.7	Weak
	H-2-IAd	347-362	ATTTASTLAVFPGGA	192.9	Weak
	H2-IAb	126-140	LLQTAANAFAPPAAG	34.9	Strong
	H2-IAb	128-142	QTAANAFAPPAAGTP	35.3	Strong
	H2-IAb	127-141	LQTAANAFAPPAAGT	37.3	Strong
	H2-IAb	129-143	TAANAFAPPAAGTPV	38.1	Strong
	H2-IAb	125-139	VLLQTAANAFAPPAA	40.4	Strong
	H2-IAb	130-144	AANAFAPPAAGTPVK	45.3	Strong
	H2-IAb	131-145	ANAFAPPAAGTPVKY	64.3	Strong
	H2-IAb	393-407	FKAQHVGTPIASFTQ	100	Strong
	H2-IAb	236-250	DVTTTTTPSATTTAS	111.7	Strong
	H2-IAb	237-251	VTTTTTPSATTTAST	115.2	Strong

Table 5.1 Peptide predictions from NetMHCII and IEDB for Hp-VAL-1.1. H2-IA^{d} represent predictions for BALB/c mice and H2-Ia^{b} represent predictions for C57BL/6 mice. For IEDB, weak binding is classified as an ic50 <5000nM, intermediate as an ic50 <500nM , strong as an ic50<50nM. For NetMHCII, an ic50 <50nM is classified as a strong bond and ic50 >50nM is classified as a weak bond.

5.3.2 Hp-VAL-2.1 epitope predictions for C57BL/6 and BALB/c mice

Hp-VAL-2 is, like VAL-1, a highly expressed secreted protein from the adult stage of *H. polygyrus*, and is found with several microvariants (Hewitson, Harcus, *et al.*, 2011). The sequence of the most abundant variant, *Hp*-VAL-2.1 was also input into both the NetMHCII method and the IEDB consensus method for MHC II epitope prediction. In contrast to *Hp*-VAL-1.1, *Hp*-VAL-2.1 has both strain-restricted epitopes, and others that are predicted to be shared between C57BL/6 mice and BALB/c mice.

IEDB predicts a weak binding epitope for I-A^d between aa 62-79 and an intermediate binding epitope at aa 92-109 (Figure 5.3A+B, Table 5.2). IEDB predicted an I-A^b epitope at aa 112-131 overlaps with an I-A^d epitope predicted by NetMHCII (Figure 5.3C, Table 5.2). It is predicted that the I-A^b binding to this epitope with intermediate affinity and binds to I-A^d with varying affinities depending on the flanking regions (Table 5.2). There is also an I-A^b epitope predicted by IEDB at aa 149-165 with intermediate binding strength (Figure 5.3D, Table 5.2). The peptide sequence between aa 226-275 has been predicted to contain epitopes for I-A^b (C57BL/6) by IEDB and NetMHCII as well as an epitope for I-A^d (BALB/c) as predicted by IEDB (Figure 5.3E, Table 5.2). However, this sequence is within the hinge region of the protein and is unlikely to be immunogenic. Finally, there is an I-A^d epitope predicted by IEDB at aa 403-420 which has an intermediate predicted affinity for MHC II (Figure 5.3F, Table 5.2).

Of note, despite the lower degree of polymorphism in the *Hp*-VAL-2 variants, the predicted epitopes are positioned in regions with amino acid substitutions and deletions, again giving rise to the suggestion that VAL proteins may be evolving to escape T cell recognition.

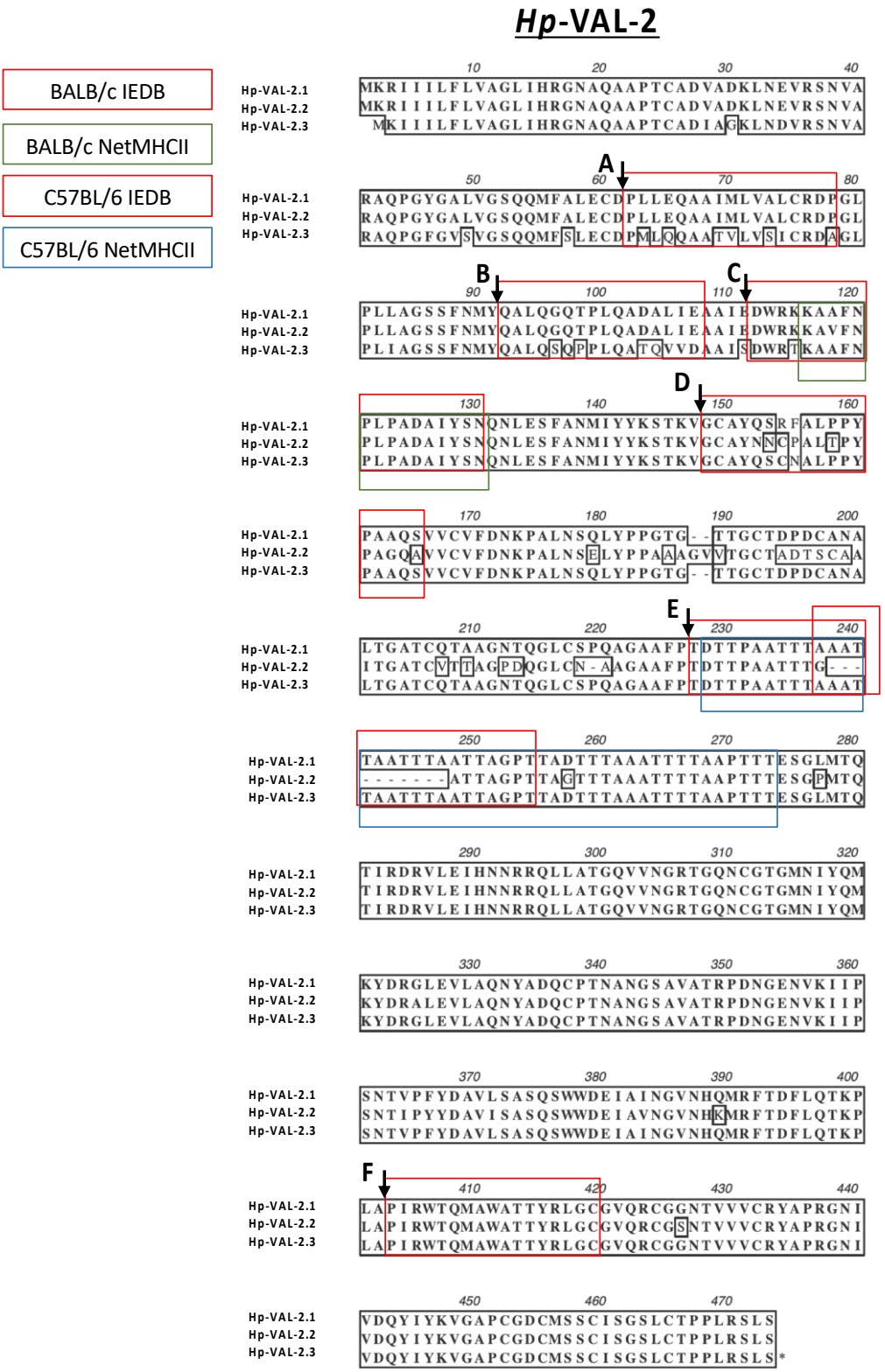

Figure 5.3 Peptide predictions from NetMHCII and IEDB for Hp-VAL-2.1. The epitopes predicted to be T cell immunogenic in *Hp*-VAL-2.1 superimposed on the formatted alignment of *Hp*-VAL-2.1 and its variants *Hp*-VAL-2.2 and *Hp*-VAL-2.3. NetMHCII predictions for C57BL/6 are shown in blue and BALB/c prediction is shown in green. IEDB predictions for C57BL/6 are shown in yellow and for BALB in pink.

Hp-VAL-2.1	Allele	a.a. position	Peptide Sequence	ic50 (nM)	Bind Level
IEDB	H2-IAd	401-415	PIRWTQMAWATTYRL	440.9	Intermediate
	H2-IAd	402-416	IRWTQMAWATTYRLG	421.5	Intermediate
	H2-IAd	403-417	RWTQMAWATTYRLGC	489.2	Intermediate
	H2-IAd	227-241	TTPAATTTAAATTAA	301.9	Intermediate
	H2-IAd	228-242	TPAATTTAAATTAAT	318.6	Intermediate
	H2-IAd	92-106	QALQGQTPLQADALI	208.6	Intermediate
	H2-IAd	230-244	AATTTAAATTAATTT	355.1	Intermediate
	H2-IAd	229-243	PAATTTAAATTAATT	362.1	Intermediate
	H2-IAd	231-245	ATTTAAATTAATTTA	361.5	Intermediate
	H2-IAd	61-75	DPLLEQAAIMLVALC	767.1	Weak
	H2-IAb	113-127	WRKKAAFNPLPADAI	147.7	Intermediate
	H2-IAb	114-128	RKKAAFNPLPADAIY	167.7	Intermediate
	H2-IAb	115-129	KKAAFNPLPADAIYS	193.6	Intermediate
	H2-IAb	152-166	QSRFALPPYPAAQSV	123	Intermediate
	H2-IAb	153-167	SRFALPPYPAAQSVV	96.7	Intermediate
	H2-IAb	150-164	AYQSRFALPPYPAAQ	143.5	Intermediate
	H2-IAb	151-165	YQSRFALPPYPAAQS	144.7	Intermediate
	H2-IAb	240-254	AATTTAATTAGPTTA	97.7	Intermediate
	H2-IAb	116-130	KAAFNPLPADAIYSN	260.5	Intermediate
	H2-IAb	241-255	ATTTAATTAGPTTAD	113.9	Intermediate
NetMHCII	H-2-IAd	116-130	KAAFNPLPADAIYSN	187.4	Strong
	H-2-IAd	117-129	KKAAFNPLPADAIYS	192.9	Weak
	H-2-IAd	92-106	QALQGQTPLQADALI	208.6	Weak
	H-2-IAd	93-107	ALQGQTPLQADALIE	240.1	Weak
	H-2-IAd	151-165	YQSRFALPPYPAAQS	250.4	Weak
	H-2-IAd	152-166	QSRFALPPYPAAQSV	264.6	Weak
	H-2-IAd	91-105	LQGQTPLQADALIEA	266.1	Weak
	H-2-IAd	88-102	YQALQGQTPLQADAL	300.1	Weak
	H-2-IAd	227-241	TTPAATTTAAATTAA	301.9	Weak
	H-2-IAd	113-127	WRKKAAFNPLPADAI	313.5	Weak
	H2-IAb	233-247	TTTAAATTAATTTAA	36.3	Strong
	H2-IAb	234-248	TTAAATTAATTTAAT	39.1	Strong
	H2-IAb	228-242	TPAATTTAAATTAAT	42.6	Strong
	H2-IAb	227-241	TTPAATTTAAATTAA	45.7	Strong
	H2-IAb	229-243	PAATTTAAATTAATT	46.2	Strong
	H2-IAb	231-245	ATTTAAATTAATTTA	47	Strong
	H2-IAb	230-244	AATTTAAATTAATTT	47.8	Strong
	H2-IAb	237-251	TAAATTAATTTAATT	49.4	Strong
	H2-IAb	238-252	AAATTAATTTAATTA	52.6	Strong
	H2-IAb	236-250	TTAAATTTTAAPTTT	57.6	Strong

Table 5.2 Peptide predictions from NetMHCII and IEDB for Hp-VAL-2.1. H2-IA^{d} represent predictions for BALB/c mice and H2-Ia^{b} represent predictions for C57BL/6 mice. For IEDB, weak binding is classified as an ic50 <5000nM, intermediate as an ic50 <500nM , strong as an ic50<50nM. For NetMHCII, an ic50 <50nM is classified as a strong bond and ic50 >50nM is classified as a weak bond.

5.3.3 Hp-VAL-3 epitope predictions for C57BL/6 and BALB/c mice

Hp-VAL-3 is another member of the venom allergen-like protein family found in abundance in HES, although from transcriptomics it appears to be monomorphic.

As with the previous VAL proteins, the sequence of this protein was fed into IEDB and NetMHCII for MHC II epitope prediction (Hewitson, Harcus, *et al.*, 2011). Figure 5.3 shows the sequence of *Hp*-VAL-3 with the epitope predictions overlaid. The prediction for *Hp*-VAL-3 stands out from the predictions for *Hp*-VAL-1.1 and *Hp*-VAL-2.1 firstly as there are relatively few predicted epitopes, and secondly as they for the most part overlap not only between the different mouse strains but also the different prediction methods (Figure 5.4).

There are several shared epitopes between aa 87-120 whereby the I-A^d is predicted to bind aa 100-120 with weak affinity and I-A^b bind to aa 87-107 with strong to intermediate affinity (Figure 5.4A, Table 5.3). There is also a predicted strongly binding I-A^b epitope from aa 125-142 (Figure 5.4B, Table 5.3). There is a third predicted set of epitopes at aa 263-288 which contains weak binding I-A^d epitopes and intermediate to strong binding I-A^b epitopes (Figure 5.4C. Table 5.3). In the case of *Hp*-VAL-3, it appears that C57BL/6 mice may have a broader range of epitopes targeted by the immune response.

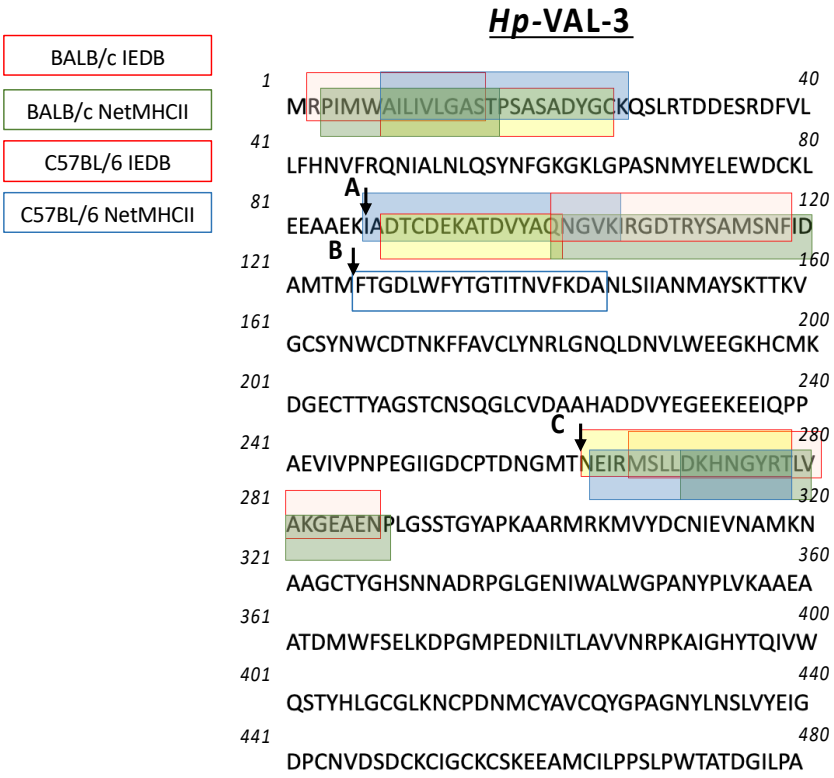

Figure 5.4 Peptide predictions from NetMHCII and IEDB for Hp-VAL-3. The epitopes predicted to be T cell immunogenic in *Hp*-VAL-3 superimposed on the peptide sequence of *Hp*-VAL-3. NetMHCII predictions for C57BL/6 are shown in blue and BALB/c prediction is shown in green. IEDB predictions for C57BL/6 are shown in yellow and for BALB in pink.

G

Hp-VAL-3	Allele	a.a. position	Peptide Sequence	ic50 (nM)	Bind Level
IEDB	H2-IAd	2-16	RPIMWAILIVLGAST	955.8	Weak
	H2-IAd	3-17	PIMWAILIVLGASTP	918.7	Weak
	H2-IAd	341-355	ANYPLVKAAEAATDM	364.4	Intermediate
	H2-IAd	4-18	IMWAILIVLGASTPS	791.3	Weak
	H2-IAd	5-19	MWAILIVLGASTPSA	681.9	Weak
	H2-IAd	140-154	KDANLSIIANMAYSK	543.5	Weak
	H2-IAd	1-15	MRPIMWAILIVLGAS	1153.5	Weak
	H2-IAd	141-155	DANLSIIANMAYSKT	470.9	Intermediate
	H2-IAd	340-354	PANYPLVKAAEAATD	384	Intermediate
	H2-IAd	142-156	ANLSIIANMAYSKTT	438.1	Intermediate
	H2-IAb	8-22	ILIVLGASTPSASAD	90.3	Intermediate
	H2-IAb	9-23	LIVLGASTPSASADY	94.7	Intermediate
	H2-IAb	7-21	AILIVLGASTPSASA	96.8	Intermediate
	H2-IAb	10-24	IVLGASTPSASADYG	122.3	Intermediate
	H2-IAb	6-20	WAILIVLGASTPSAS	144.2	Intermediate
	H2-IAb	125-139	TGDLWFYTGTITNVF	83.4	Intermediate
	H2-IAb	126-140	GDLWFYTGTITNVFK	90.9	Intermediate
	H2-IAb	335-349	WALWGPANYPLVKAA	202.3	Intermediate
	H2-IAb	127-141	DLWFYTGTITNVFKD	102.7	Intermediate
	H2-IAb	11-25	VLGASTPSASADYGC	200.2	Intermediate
NetMHCII	H-2-IAd	341-355	ANYPLVKAAEAATDM	364.4	Weak
	H-2-IAd	340-354	PANYPLVKAAEAATD	384	Weak
	H-2-IAd	142-156	ANLSIIANMAYSKTT	438.1	Weak
	H-2-IAd	141-155	DANLSIIANMAYSKT	470.9	Weak
	H-2-IAd	342-356	NYPLVKAAEAATDMW	505.1	Weak
	H-2-IAd	143-147	NLSIIANMAYSKTTK	517.6	Weak
	H-2-IAd	140-153	KDANLSIIANMAYSK	543.5	Weak
	H-2-IAd	339-353	GPANYPLVKAAEAAT	568.4	Weak
	H-2-IAd	142-146	LSIIANMAYSKTTKV	580.4	Weak
	H-2-IAd	343-357	YPLVKAAEAATDMWF	664.3	Weak
	H2-IAb	125-139	TGDLWFYTGTITNVF	83.4	Strong
	H2-IAb	8-22	ILIVLGASTPSASAD	90.3	Strong
	H2-IAb	126-140	GDLWFYTGTITNVFK	90.9	Strong
	H2-IAb	9-23	LIVLGASTPSASADY	94.7	Strong
	H2-IAb	7-21	AILIVLGASTPSASA	96.8	Strong
	H2-IAb	127-141	DLWFYTGTITNVFKD	102.7	Strong
	H2-IAb	124-138	FTGDLWFYTGTITNV	105.4	Strong
	H2-IAb	129-143	LWFYTGTITNVFKDA	122	Strong
	H2-IAb	10-24	IVLGASTPSASADYG	122.3	Strong
	H2-IAb	6-20	WAILIVLGASTPSAS	144.2	Strong

Table 5.3 Peptide predictions from NetMHCII and IEDB for Hp-VAL-3. H2-IA^{d} represent predictions for BALB/c mice and H2-Ia^{b} represent predictions for C57BL/6 mice. For IEDB, weak binding is classified as an ic50 <5000nM, intermediate as an ic50 <500nM , strong as an ic50<50nM. For NetMHCII, an ic50 <50nM is classified as a strong bond and ic50 >50nM is classified as a weak bond.

5.3.4 Hp-VAL-4 epitope predictions for C57BL/6 and BALB/c mice

Hp-VAL-4 is the most abundant VAL protein in L4 larval ES, the products produced by larvae early in infection and is likely to be one of the first *H. polygyrus* proteins seen by the host immune system (Hewitson *et al.*, 2013). While VAL-1 through -3 are comprised of 2 SCP (sperm coating protein) domains, *Hp*-VAL-4 is made up of a single SCP domain and so is around half the length of its relatives (Hewitson et al., 2013; Hewitson, Harcus, et al., 2011). Despite this difference, there are still multiple potential T cell epitopes found within the sequence. There are 3 regions which contain epitopes of both I-A^b and I-A^d MHC Class II molecules (Figure 5.5). The first is between aa 39-58, within which a weak I-A^d epitope is predicted between aa 39-56, and a similarly weak I-A^b epitope between aa 42-58 (Figure 5.5A, Table 5.4). The second I-A^d epitope predicted by the IEDB consensus method is found at aa 91-109 and has weak binding affinity (Figure 5.5B, Table 5.4). The third region is found between aa 114-148 with a weak I-A^d epitope between 114-132 and an I-A^b epitope predicted between aa 126-148 with a binding affinity being classed as intermediate by IEDB and strong by NetMHCII (Figure 5.5C, Table 5.4).

As was the case with *Hp*-VAL-3, *Hp*-VAL-4 is monomorphic and its epitopes are predicted to bind more strongly to I-A^b, again suggesting that C57BL/6 mice may mount a stronger adaptive immune response against these proteins (Figure 5.5, Table 5.4).

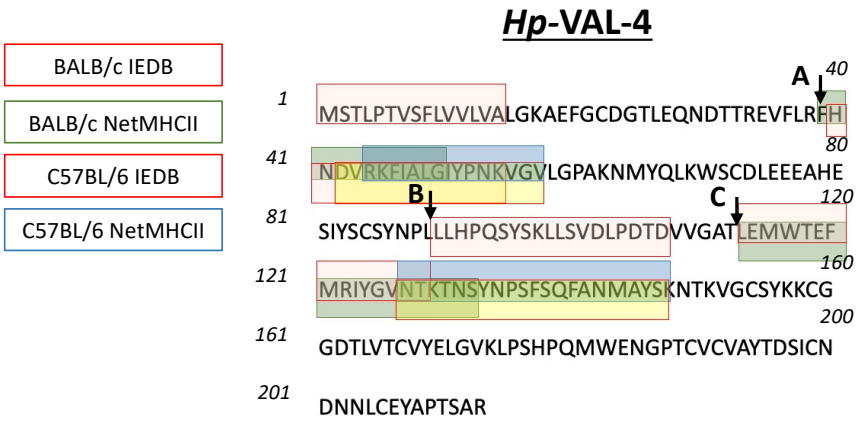

Figure 5.5 Peptide predictions from NetMHCII and IEDB for Hp-VAL-4. The epitopes predicted to be T cell immunogenic in *Hp*-VAL-4 superimposed on the peptide sequence of *Hp*-VAL-4. NetMHCII predictions for C57BL/6 are shown in blue and BALB/c prediction is shown in green. IEDB predictions for C57BL/6 are shown in yellow and for BALB in pink.

Hp-VAL-4	Allele	a.a. position	Peptide Sequence	ic50 (nM)	Bind Level
IEDB	H2-IAd	93-107	LHPQSYSKLLSVDLP	899	Weak
	H2-IAd	94-108	HPQSYSKLLSVDLPD	937.5	Weak
	H2-IAd	92-106	LLHPQSYSKLLSVDL	1265.1	Weak
	H2-IAd	1-15	MSTLPTVSFLVVLVA	1518.3	Weak
	H2-IAd	95-109	PQSYSKLLSVDLPDT	985.4	Weak
	H2-IAd	41-55	HNDVRKFIALGIYPN	504.8	Weak
	H2-IAd	42-56	NDVRKFIALGIYPNK	445.3	Intermediate
	H2-IAd	96-110	QSYSKLLSVDLPDTD	1287	Weak
	H2-IAd	40-54	FHNDVRKFIALGIYP	739.2	Weak
	H2-IAd	116-130	LEMWTEFMRIYGVNT	729.6	Weak
	H2-IAb	129-143	NTKTNSYNPSFSQFA	104	Intermediate
	H2-IAb	130-144	TKTNSYNPSFSQFAN	117.3	Intermediate
	H2-IAb	131-145	KTNSYNPSFSQFANM	124.6	Intermediate
	H2-IAb	132-146	TNSYNPSFSQFANMA	131.4	Intermediate
	H2-IAb	133-147	NSYNPSFSQFANMAY	204	Intermediate
	H2-IAb	134-148	SYNPSFSQFANMAYS	349.9	Intermediate
	H2-IAb	135-149	YNPSFSQFANMAYSK	712	Weak
	H2-IAb	44-58	VRKFIALGIYPNKVG	1637.3	Weak
	H2-IAb	45-59	RKFIALGIYPNKVGV	1745.5	Weak
	H2-IAb	43-57	DVRKFIALGIYPNKV	1754.3	Weak
NetMHCII	H-2-IAd	43-57	DVRKFIALGIYPNKV	415.8	Weak
	H-2-IAd	119-133	MWTEFMRIYGVNTKT	426.5	Weak
	H-2-IAd	42-56	NDVRKFIALGIYPNK	445.3	Weak
	H-2-IAd	117-131	EMWTEFMRIYGVNTK	450.1	Weak
	H-2-IAd	120-134	WTEFMRIYGVNTKTN	487.7	Weak
	H-2-IAd	41-55	HNDVRKFIALGIYPN	504.8	Weak
	H-2-IAd	44-58	VRKFIALGIYPNKVG	519	Weak
	H-2-IAd	121-135	TEFMRIYGVNTKTNS	586.5	Weak
	H-2-IAd	116-130	LEMWTEFMRIYGVNT	729.6	Weak
	H-2-IAd	40-54	FHNDVRKFIALGIYP	739.2	Weak
	H2-IAb	129-143	NTKTNSYNPSFSQFA	104	Strong
	H2-IAb	130-144	TKTNSYNPSFSQFAN	117.3	Strong
	H2-IAb	131-145	KTNSYNPSFSQFANM	124.6	Strong
	H2-IAb	132-146	TNSYNPSFSQFANMA	131.4	Strong
	H2-IAb	133-147	NSYNPSFSQFANMAY	204	Strong
	H2-IAb	134-148	SYNPSFSQFANMAYS	349.9	Weak
	H2-IAb	135-149	YNPSFSQFANMAYSK	712	Weak
	H2-IAb	128-142	VNTKTNSYNPSFSQF	1183.8	Weak
	H2-IAb	44-58	VRKFIALGIYPNKVG	1637.3	Weak
	H2-IAb	45-59	RKFIALGIYPNKVGV	1745.5	Weak

Table 5.4 Peptide predictions from NetMHCII and IEDB for Hp-VAL-4. The epitopes predicted to be T cell immunogenic in *Hp*-VAL-1.1 superimposed on the formatted alignment of *Hp*-VAL-1.1 and its variants *Hp*-VAL-1.2 and *Hp*-VAL-1.3. NetMHCII predictions for C57BL/6 are shown in blue and BALB/c prediction is shown in green. IEDB predictions for C57BL/6 are shown in yellow and for BALB in pink.

5.3.5 Comparison of BMDC:CD4+ T cell cocultures versus whole MLN restimulation of T cells in vitro

Restimulation of T cells *in vitro* with a protein of interest is a central technique to identify and characterise antigen-specific T cells, as well as to purify them by cell sorting where possible. For T cells to 'see' antigenic peptides, proteins must must be processed and presented by antigen-presenting cells (APCs). To mimic this *in vitro*, APCs can be provided as antigen-pulsed bone marrow-derived dendritic cells (BMDC), or can be found within the MLN cell population together with CD4+ T cells to be tested. We first compared these two sources of APCs for stimulation of antigen-specific T cell recall responses.

The experimental set up is summarised in Figure 5.6A. Mice were infected with 200 L3 *H. polygyrus* larvae for 14 days, alongside naïve control animals. Four days later, BMDC cultures were initiated, with GM-CSF media changed on d7, d10 and d12 post infection, to generate mature DCs by day 14. The mice were then culled, with one fraction of the MLN cultured directly with HES, and the other fraction used to purify CD4+ T cells by AutoMACS sorting, and cultured at a 10:1 ratio with BMDCs and HES. Both sets of cultures included controls with media alone, and all were incubated for 16 hours before their levels of CD69 and CD154 were assessed using flow cytometry.

As stated previously, when a CD4+ T cell recognises an epitope loaded onto MHC II, the cell becomes activated and upregulates many molecules including CD69 and CD154. Figure 5.6B and Figure 5.6C show the percentage of Teffector cells expressing CD69 and CD154 when cultured with HES and native MLN APCs or HES and BMDCs versus resting overnight in media alone. There is little difference between the whole MLN versus BMDC:T cell coculture in terms of CD69 upregulation on T cells as there is no upregulation of CD69 in response to culturing with HES overnight (Figures 5.6B and C). There is also an upregulation of naïve CD4 T cells expressing CD69 when exposed to HES in whole MLN cultures, suggesting there are epitopes in HES that can be recognised by naïve cells (Figure 5.6B). The naïve T cells within the BMDC:T cell coculture did not respond to HES in this experiment but did respond in previous experiments where BMDC:T cell cocultures were used (Figure 5.6C, data not shown). In terms

of CD154 expression, there is no response to HES in the naïve or infected mice regardless of the type of culture (Figure 5.6D+E). This suggests that BMDC:T cell cocultures are no more reliable in terms of reducing background signal and the consistent lack of response may suggest that this culture type is unsuitable for restimulation assays. As a result, whole MLN cultures are used from this point onwards.

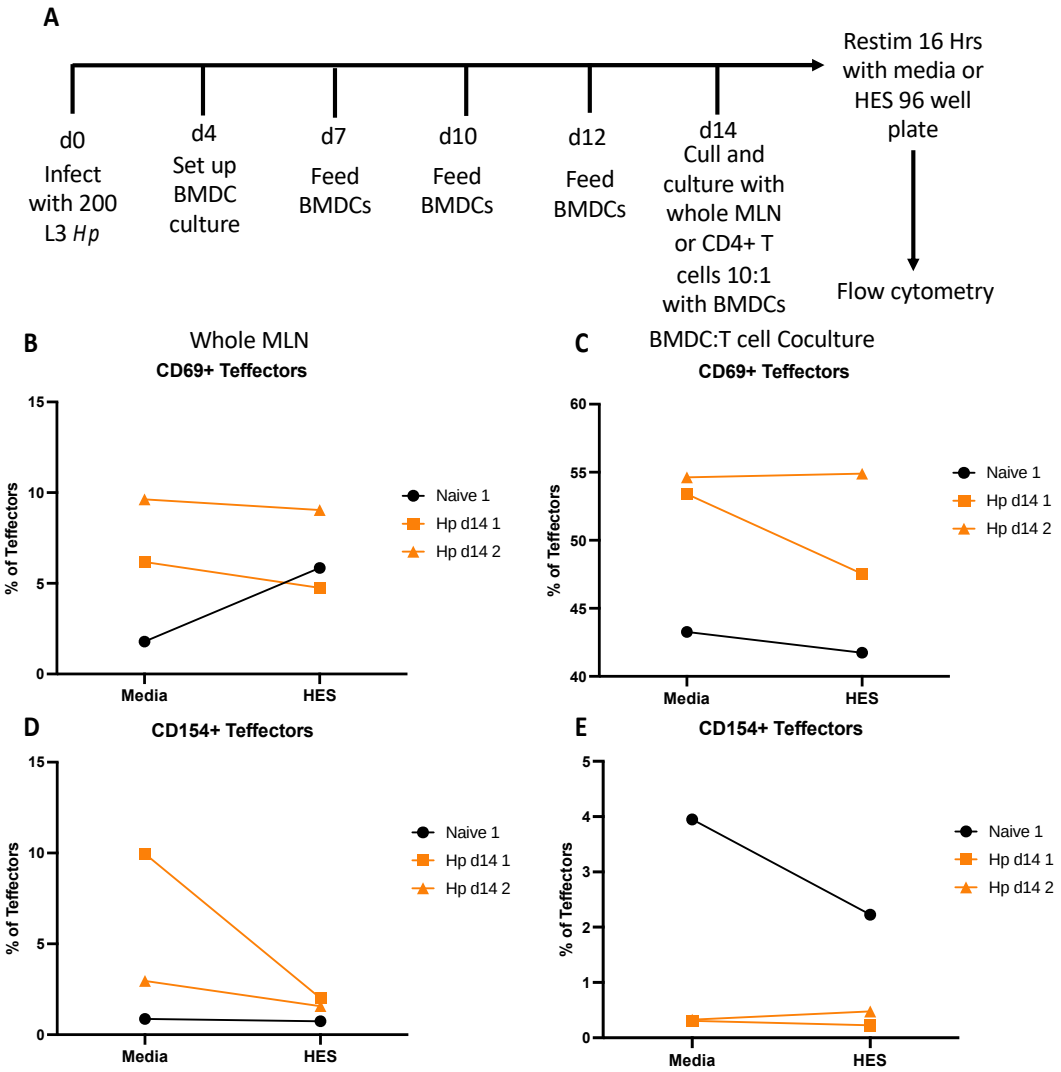

Figure 5.6 In vitro restimulation of Teffector (Foxp3-) cells using whole MLN culture versus BMDC:T cell coculture. C57BL/6 mice were infected with 200 L3 *H. polygyrus* for 14 days before *in vitro* restimulation for 16 hours. (A) The experimental procedure followed in this experiment including the growing of BMDCs. (B) The proportion of CD4+ T cells expressing CD69 after 16 hours in whole MLN culture with media alone or 10ug/ml HES in naïve (black circles) and two d14 *H. polygyrus* infected mice (orange squares and triangles. (C) The proportion of cells expressing CD69 after 16 hours of BMDC:T cell coculture with media alone or HES in naïve (black circles) and *H. polygyrus* d14 (orange squares and triangles). (D) The proportion of Teffector (Foxp3-) cells expressing CD154 after 16 hours in whole MLN culture with media alone or HES in naïve (black circles) and two d14 *H. polygyrus* infected mice (orange squares and triangles. (E) The proportion of cells expressing CD69 after 16 hours of BMDC:T cell coculture with media alone or HES in naïve (black circles) and *H. polygyrus* d14 (orange squares and triangles). Data is representative of two experiments.

5.3.6 CD69 as a marker of in vitro TCR stimulation in Teffector cells

As discussed previously CD69 is the one of the earliest known markers of TCR engagement which appears on the cell surface as early as 4 hours post-TCR engagement. We postulated that Teffectors from *H. polygyrus* infected mice should respond more rapidly than those from a naïve mouse that has not been exposed to the parasite. However, as seen in Figure 5.6B-C, the percentage of Teffectors from the naïve mice expressing CD69 increases when comparing those cultured in media alone versus those cultured with HES and *Hp* d14 mice did not have an increase in CD69+ Teffector cells in response to HES after 16 hours in culture. This may be due to the cells which have seen HES *in vivo* still expressing some level of CD69 when cultured in media alone. To further validate the use of CD69 as a marker of *in vitro* restimulation in response to HES, we cultured whole MLN with HES or media alone for 16 hours to examine T cells responding to HES antigens.

To assess whether the average expression level of CD69 was a more effective marker of T cell activation, the mean fluorescence intensity (MFI) of CD69 was also evaluated. However there also does not appear to be an upregulation of CD69 on either the naïve cells or the cells from *H. polygyrus* infected mice when cultured with HES versus media alone (Figure 5.7A). In fact, the MFI of CD69 on Teffectors from infected mice was downregulated when cultured with HES versus media alone (Figure 5.7A). When looking at the expression level of CD69 on Teffectors from *H. polygyrus* infected mice, the expression between cells cultured in media alone (orange) versus HES (blue) are indistinguishable (Figure 5.7B). Those cultured with ConA (Concanavalin A, red), the positive control, upregulate their expression of CD69 compared to media alone, showing that CD69 expression can be upregulated in response to T cell stimulation (Figure 5.7B).

In this experiment, the response to *in vitro* challenge with purified recombinant VAL proteins was also tested. However, there was no expansion of *H. polygyrus* experienced CD69+ T cells in response to 16 hour culture with *Hp*-VAL-1, *Hp*-VAL-2, *Hp*-VAL-3 or *Hp*-VAL-4 (Figure 5.7C). In contrast, there was a substantial

increase in CD69 expression by T cells stimulated with ConA, again showing that CD69 is upregulated upon T cell activation but not in response to HES (Figure 5.7C). Together, this shows that while CD69 is a marker of T cell activation and can be upregulated by Teffector cells in response to a strong stimulus like ConA, it is not sensitive enough to use as a marker of restimulation on Teffector cells.

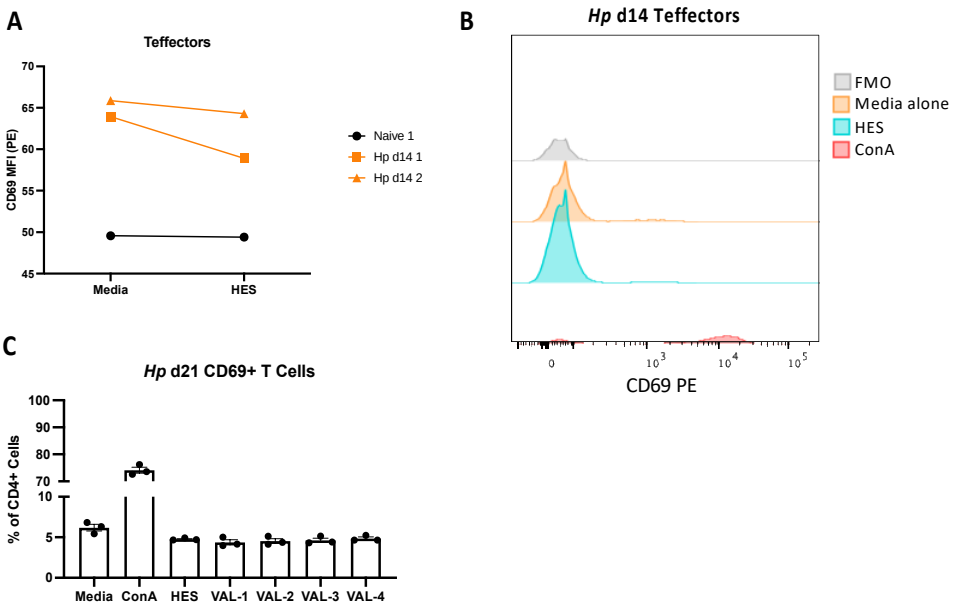

Figure 5.7 The expression of CD69 on Teffector cells after 16 hours restimulation with HES and some components. C57BL/6 mice were infected with 200 L3 *H. polygyrus* for 14 days before *in vitro* restimulation for 16 hours. (A) The average expression of CD69 on Teffector cells after 16 hours *in vitro* in Teffector cells from naïve mice (black circles) or *H. polygyrus* d14 mice (orange squares and triangles). (B) Histogram showing representative CD69 expression on Teffector cells from *H. polygyrus d14* infected mice in response to 10ug/ml of HES (blue), 1ug/ml of ConA (red), media alone (orange) and the FMO control (grey). (C) Bar graph showing the proportion of Teffector cells from *H. polygyrus* d14 mice expressing CD69 in response to 16 hour restimulation with media alone, 1ug/ml ConA, 10ug/ml HES, 1ug/ml VAL-1, 1ug/ml VAL-2, 1ug/ml VAL-3 and 1ug/ml VAL-4. Data representative of 3 experiments. Each point represents a replicate well from the same mouse. Error bars represent the standard error of the mean.

5.3.7 CD69 as a marker of in vitro TCR stimulation in Tregs

Next, the expression of CD69 on CD4+ Foxp3+ Tregs isolated from naïve or *H. polygyrus* infected mice when stimulated *in vitro* was assessed. The baseline percentage of Tregs expressing CD69 is higher than on Teffectors from naïve mice (Figure 5.6 B-C, Figure 5.8A). Much like the Teffector cells, there is around a 10% expansion of naïve CD69+ Tregs 16 hours after culture with HES (Figure 5.8A), again suggesting that there are antigens within HES that are recognised by T cells that have not encountered that antigen before. Among Tregs isolated *H. polygyrus* infected mice, however, the baseline percentage expressing CD69 is lower than that of Tregs from naïve mice (Figure 5.8A). When cultured with HES versus media alone, Tregs from one *H. polygyrus* infected mouse expanded its CD69+ Treg population by around 1%, markedly lower than the response in its naïve counterpart while the Tregs from the second infected mouse did not respond at all to HES (Figure 5.8B). In parallel with the increased percentage of CD69+ Tregs, there is also an increase in the MFI of CD69 on Tregs from naïve mice when cultured with HES (Figure 5.8B), while MFI of Tregs from the *H. polygyrus* infected mice only increased in the population which had shown an increased percentage (Figure 5.8A, Figure 5.8B). Tregs from *H. polygyrus* infected mice also showed no upregulation of CD69 when cultured with *Hp*-VAL-1, *Hp*-VAL-2, *Hp*-VAL-3 or *Hp*-VAL-4 but did upregulate CD69 in response to the ConA control (Figure 5.8D). These results are similar to the dynamics of CD69 on Teffector cells and shows once again that CD69 is a good marker of strong TCR stimulation as seen in the cultures with mitogen and TCR crosslinker ConA but is not sensitive enough to mark restimulation of T cells from infected mice.

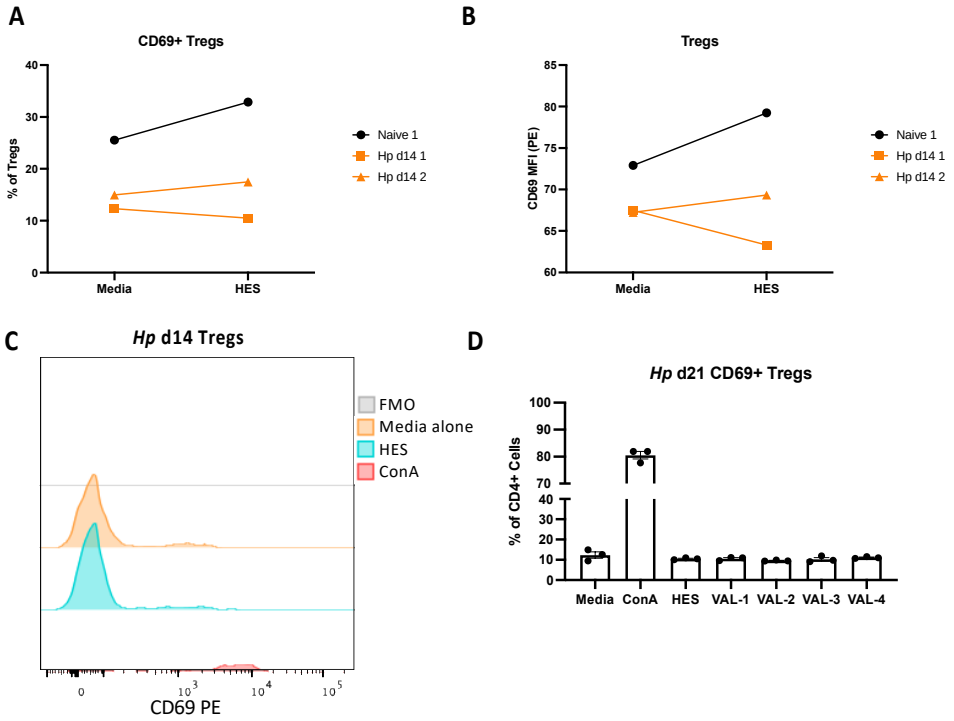

Figure 5.8 The expression of CD69 on Foxp3+ Treg cells after 16 hours restimulation with HES and some components. C57BL/6 mice were infected with 200 L3 *H. polygyrus* for 14 days before *in vitro* restimulation for 16 hours. (A) The proportion of Tregs expressing CD69 after 16 hours in whole MLN culture with media alone or HES in naïve (black circles) and two d14 *H. polygyrus* infected mice (orange squares and triangles). (B) The average expression of CD69 on Tregs cells after 16 hours *in vitro* in CD4+ T cells from naïve mice (black circles) or *H. polygyrus* d14 mice (orange squares and triangles). (C) Histogram showing representative CD69 expression on Tregs from *H. polygyrus d14* infected mice in response to HES (blue), ConA (red), media alone (orange) and the FMO control (grey). (D) Bar graph showing the proportion of Tregs from *H. polygyrus* d14 mice expressing CD69 in response to 16 hour restimulation with media alone, 1ug/ml ConA, 10ug/ml HES, 1ug/ml VAL-1, 1ug/ml VAL-2, 1ug/ml VAL-3 and 1ug/ml VAL-4. Data representative of 3 experiments. Each point represents a replicate well from the same mouse. Error bars represent the standard error of the mean.

5.3.8 CD154 as a marker of in vitro TCR stimulation in Teffector cells

CD40L or CD154 is another marker of TCR engagement which could be used as a readout for T cell restimulation *in vitro*. As discussed previously, CD154 is readily degraded in the lysosome and most protocols use monensin to stabilise the internalised antibody CD154 complexes to maintain the fluorescent signal (Chattopadhyay et al., 2006). However, for our uses, this degradation can allow a snapshot of those cells which have very recently received TCR stimulation and negate background expression from TCR stimulation received *in vivo*.

Following *in vitro* restimulation and flow cytometry, very few cells were found to express CD154 (Figure 5.6D-E). Indeed, while Teffector cells from naïve mice have unchanged CD154 expression, Teffectors from *H. polygyrus* infected mice actually lose CD154 when cultured with HES for 16 hours versus media alone (Figure 5.6D-E).

To further assess whether the dynamics of CD154 expression can be used as a marker of recent TCR stimulation, further analysis of CD154+ T cells from restimulation assays were compared. Similarly to the proportion of CD154+ Teffectors (Figure 5.6D-E), the MFI of CD154 on Teffectors, did not change when cultured with HES versus media and again was reduced when cultured with HES (Figure 5.9A, Figure 5.9B). In contrast to the increased CD69 discussed above, there is also no upregulation of CD154 in terms of MFI and percentage of Teffectors expressing CD154 in response to ConA (Figure 5.9A, Figure 5.9B).

The responses to *Hp*-VAL-1, *Hp*-VAL-2, *Hp*-VAL-3 or *Hp*-VAL-4 were also evaluated in terms of CD154 expression, but were found not to differ from media alone cultures (Figure 5.9C). This shows that that CD40L or CD154 is not a good marker of recent T cell activation, perhaps as it is too quickly turned over and degraded. A similar pattern was seen in Tregs (data not shown). As a result, CD154 was not pursued further as a marker of CD4+ T cell activation.

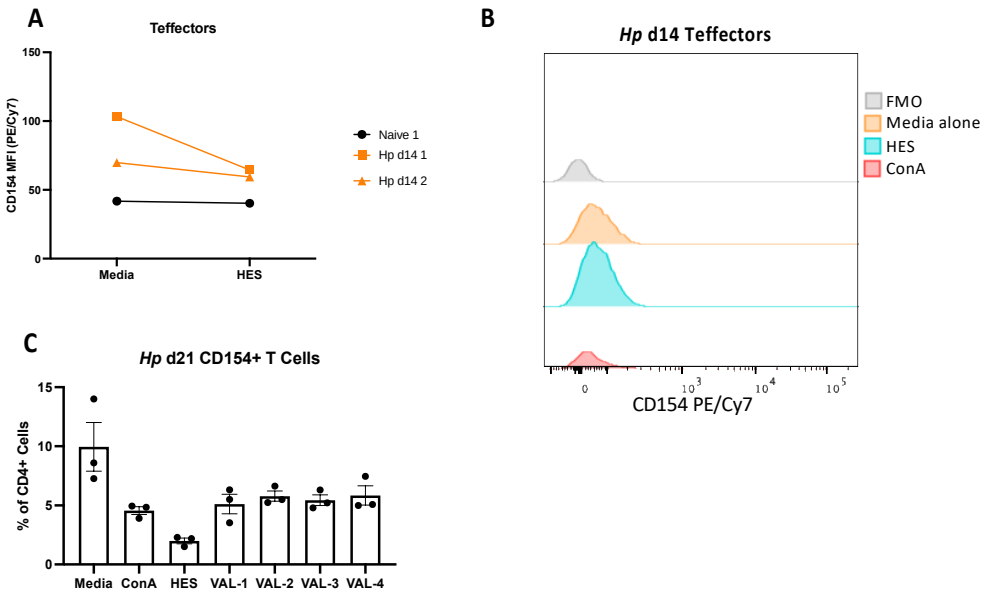

Figure 5.9 The expression of CD154 on Teffector cells after 16 hours restimulation with HES and some components. C57BL/6 mice were infected with 200 L3 *H. polygyrus* for 14 days before *in vitro* restimulation for 16 hours. (A) The average expression of CD154 on Teffector cells after 16 hours *in vitro* in CD4+ T cells from naïve mice (black circles) or *H. polygyrus* d14 mice (orange squares and triangles). (B) Histogram showing representative CD154 expression on Teffector cells from *H. polygyrus d14* infected mice in response to HES (blue), ConA (red), media alone (orange) and the FMO control (grey). (C) Bar graph showing the proportion of Teffector cells from *H. polygyrus* d14 mice expressing CD154 in response to 16 hour restimulation with media alone, 1ug/ml ConA, 10ug/ml HES, 1ug/ml VAL-1, 1ug/ml VAL-2, 1ug/ml VAL-3 and 1ug/ml VAL-4. Data representative of 3 experiments. Each point represents a replicate well from the same mouse. Error bars represent the standard error of the mean.

5.3.9 Nr4a3-Tocky mice as a marker of T cell restimulation in vitro

Nr4a3 is a gene product related to Nur77 (Nr4a1), a common TCR engagement marker. However, Nr4a3 is a more sensitive marker of TCR engagement than Nur77 which is dependent on NFAT signalling and Nr4a3 has lower background than Nurr77. This means that Nr4a3 can be used as a clear and NFAT-dependent marker of T cell activation (Bending, Martín, et al., 2018; Jennings et al., 2020). To evaluate this, the expression of CD69 and the Nr4a3-Timer protein was first compared in cultures stimulated with ConA or HES, and analysing CD69 expression among cells responding or not responding through expression of Nr4a3.

In this analysis, cells which have responded to antigen any time in the last 27 hours (New, Persistent and Arrested), were found to express varying levels of CD69 (Figure 5.10A, Figure 5.10B). Within the population responding to ConA (Figure 5.10A), it was notable that expression of CD69 is not limited to cells which express the Nr4a3 reporter gene, there are also Timer-negative cells (in the lower left quadrant of Fig 5.10 A) which express CD69, suggesting that Nr4a3-Timer protein dynamics give a better insight into TCR engagement than in the case of CD69 than the mutated mCherry Timer protein (Figure 5.10A). Figure 3.10C shows the percentage of CD4+ T cells isolated from an *H. polygyrus* infected mouse expressing CD69 in the Timer– (non-responders), New and Arrested quadrants after 16 hours of culture with ConA. There is a higher percentage of CD4+ T cells in the New and Arrested populations compared to the Timer– cells (Figure 5.10C). When cultured with HES, there is a trend towards an increase in the proportion of CD69+ T cells in the New and Arrested populations compared to the Timer– population. However, in both cases, there is a high proportion of Timer– CD4+ T cells expressing CD69, suggesting that CD69 does not mark newly TCR stimulated T cells with as high specificity as the Timer system. When looking at the MFI of CD69, there is little difference in expression in New, Arrested and Timer– cells cultured in HES for 16 hours (Figure 5.10D). When cultured in ConA, there is an increase in the MFI of CD69 in the Arrested population and a varied increase in the New population. This shows that MFI of CD69 can separate responders and non-responders when cultured in ConA but

not when cultured with HES, making it an unsuitable marker when compared to the Nr4a3-Tocky mouse system.

In cells cultured with HES, and in accordance with the earlier results (Figure 5.7, 5.8), CD69 levels are much lower than seen with ConA stimulation; notably, around 20% of Timer+ cells do not express high levels of CD69 (Figure 5.10C). This observation casts further doubt on the use of CD69 as an activation maker, as these cells would have been discounted if that was the only read-out. Taken together, these results show that the new Nr4a3-Timer model is more sensitive and gives more insight into the antigen recognition of T cells than the previous markers discussed here.

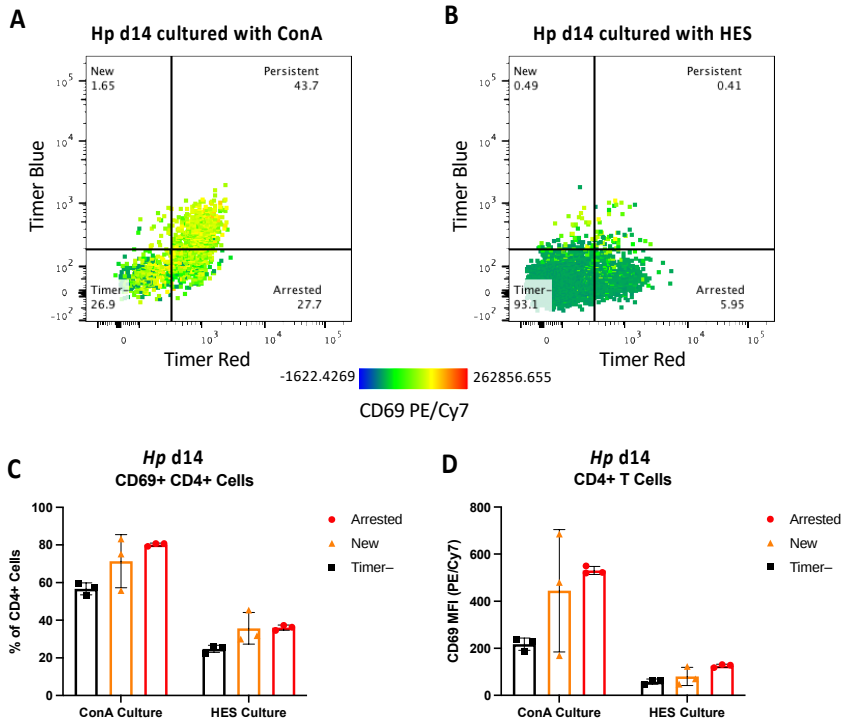

Figure 5.10 The expression of CD69 and Timer proteins in CD4+ T cells . C57BL/6 mice were infected with 200 L3 *H. polygyrus* for 14 days before *in vitro* restimulation for 16 hours. (A) An overlaid scatterplot of Timer blue against Timer red with the expression of CD69 overlaid as a heatmap in *H polygyrus* d14 cells cultured with ConA. The quadrants show the timer negative cells as well as the new, persistent and arrested quadrants. (B) An overlaid scatterplot of Timer blue against Timer red with the expression of CD69 overlaid as a heatmap in *H polygyrus* d14 cells cultured with HES. The quadrants show the timer negative cells as well as the new, persistent and arrested quadrants. (C-D) Bar graphs showing (C) the percentage of CD4+ T cells expressing CD69 and (D) the MFI of CD69 in cells from the Timer– (black), New (orange) and arrested (black) populations when cultured with 1ug/ml ConA or 10ug/ml HES for 16 hours. Data representative of 2 experiments. Each point represents a replicate well from the same mouse. Error bars represent the standard error of the mean.

5.3.10 Restimulation of Nr4a3-Timer CD4+ T cells after 14 or 21 days of H. polygyrus infection

At around 9 days post-infection with *H. polygyrus,* the worm burrows out of the muscularis of the intestine to emerge into the lumen as adults. This means that at 14 days post-infection the murine host immune system has only had access to adult HES for around 5 days. To increase the number of days the T cells are exposed to HES, we compared the restimulation of T cells from d14 and d21 *H. polygyrus* infected Nr4a3-timer mice. Regardless of the infection status of the mouse from which CD4+ T cells are isolated, culturing with the mitogen ConA causes an increase in new and persistent cells compared to media alone (Figure 5.11). CD4+ T cells from the d14 *H. polygyrus* infected mouse did not respond to HES *in vitro* as their expression of the blue variant of the protein is not increased when cultured with HES versus media alone (Figure 5.11). However, there is a small increase in the percentage of New CD4+ cells (Timer blue+, Timer red-) when cultured with HES versus media alone in the 21 day *H. polygyrus* infected mice (Figure 5.11). This suggests that there are a small number CD4+T cells in *Hp* d21 mice which recognise an antigen in HES. However, as was seen with CD69, T cells from naïve mice also respond to HES with expansion of the New timer population when cultured with HES versus media.

Together these data suggest that *H. polygyrus* infection induces T cells which recognise antigens found within HES, but even after 21 days' infection these only represent a very small proportion of the cells found within the MLN. Interpretation of the data is also confounded by the apparent responses of naïve T cells to HES, a phenomenon that requires further investigation to ascertain if it is dependent on Class II-mediated presentation or represents other biological activities in HES.

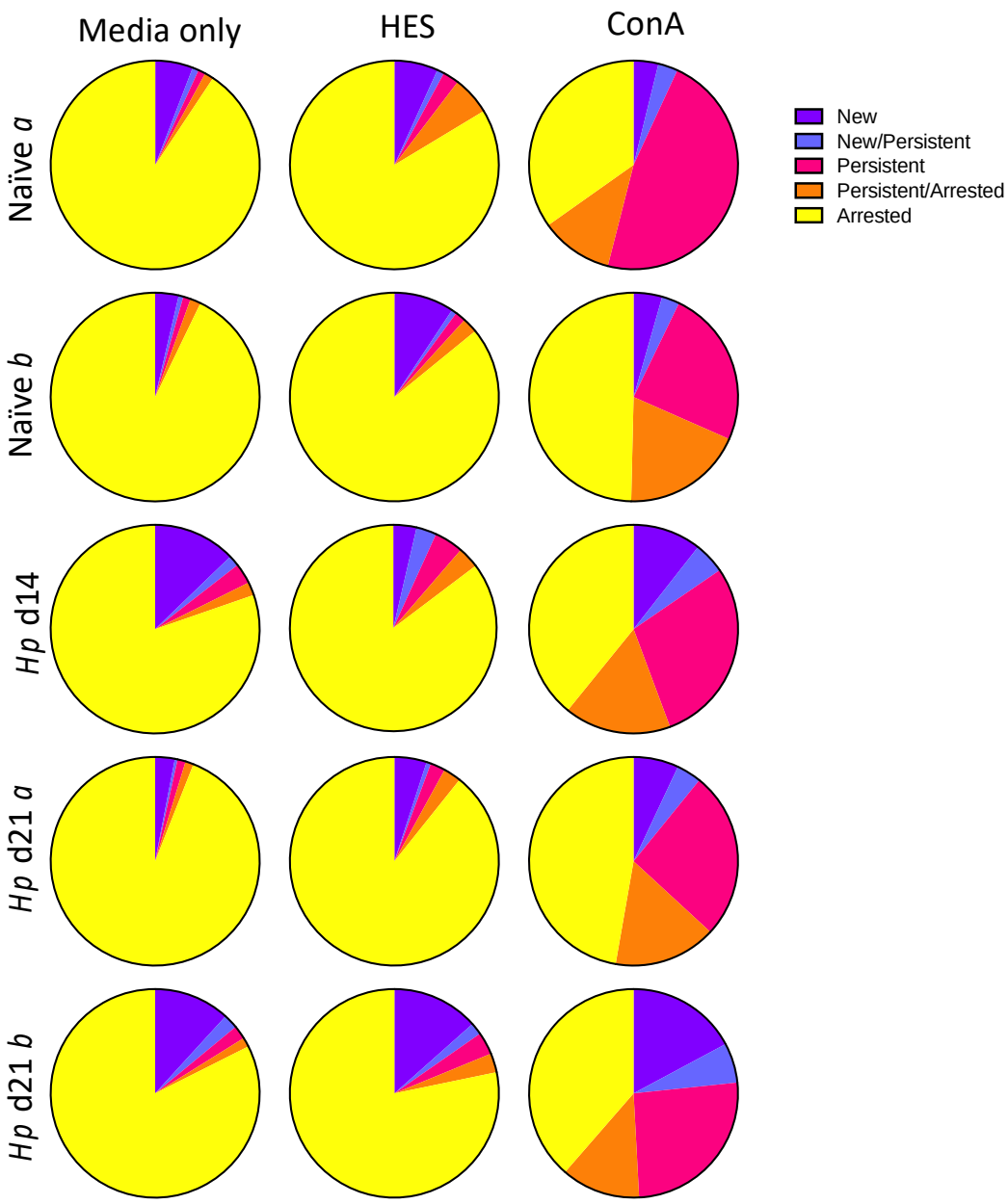

Figure 5.11 In vitro restimulation of d14 and d21 H. polygyrus infected MLN cells with HES. C57BL/6 mice were infected with 200 L3 *H. polygyrus* for 14 days or 21 days before *in vitro* restimulation for 16 hours. Pie charts show the proportions of cells in each timer phenotype as determined by bioinformatic analysis. Pie charts are shown for naïve (rows 1 and 2), *H. polygyrus* d14 (row 3) and *H. polygyrus* d21 infected mice (rows 4 and 5) when cultured for 16 hours in media alone (column 1), with 10ug/ml HES (column 2) or 1ug/ml ConA (Column 3). Data representative of 2 experiments.

5.3.11 Restimulation of Nr4a3-Timer CD4+ T cells after secondary infection with H. polygyrus

Secondary infection with most pathogens will lead to reactivation of memory CD4+ T cells which respond faster and more vigorously than naïve CD4+ T cells undergoing primary activation. As *H. polygyrus* establishes a chronic infection, most investigators study the secondary response in mice treated with anthelmintic drugs to clear the primary infection. By following a similar protocol, clearing the infection with *H. polygyrus* at day 14, and after 10 days; interval reinfecting for 7 days as seen in Figure 5.12, we hoped to see greater numbers of T cells responding to HES due to the more rapid activation and enhanced proliferation of memory T cells.

Figure 5.13 shows the proportion of Timer+ CD4+ T cells in the different timer quadrants from naïve and reinfected mice. The cells which have been recently restimulated are found in the quadrants with expression of the blue variant of the timer protein (New and Persistent). As found in the earlier experiments, some reactivity to HES was found in naïve T cells. Here, two of the naïve mice (*a* and *c*) responded to HES suggesting again that either there are epitopes in HES which can be recognised by naïve cells, or that HES contains nonspecific stimuli (Figure 5.13). Naïve mouse *b* had high levels of New and Persistent cells when cultured in media alone, possibly due to contamination or dysregulated calcineurin/NFAT signalling, which would obscure any response to antigen *in vitro* (Figure 5.13).

The reinfected mice show a high level of variation in the response to restimulation with HES; for example reinfected mouse *a* had a higher proportion of New and Persistent cells when cultured with HES versus media alone, while mice *b* and *c* did not expand either population under similar conditions (Figure 5.13). Hence, even during secondary infection, there is considerable variability in the proportion of *H. polygyrus* specific CD4+ T cells and their ability to respond *in vitro*. Of note is the low level of Timer+ cells within the cultures from this experiment which meant that the usual bioinformatic analysis could not be used to calculate the timer angle and this experiment was instead analysed using flow cytometric analysis and FlowJo.

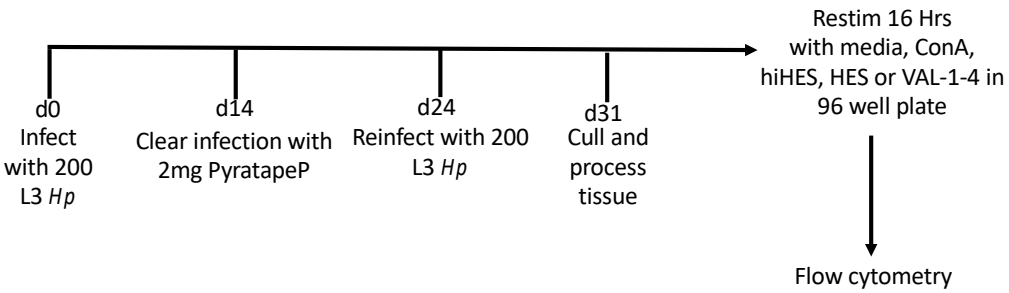

Figure 5.12 The experimental set up for H. polygyrus secondary infection and restimulation in vitro . C57BL/6 mice were infected with 200 L3 *H. polygyrus* for 14 days before clearing the infection with 2mg of Pyratape P. 10 days after clearance, the egg counts were checked for full clearance of the worm and the mice reinfected with 200 L3 *H. polygyrus* for 7 days before *in vitro* restimulation for 16 hours.

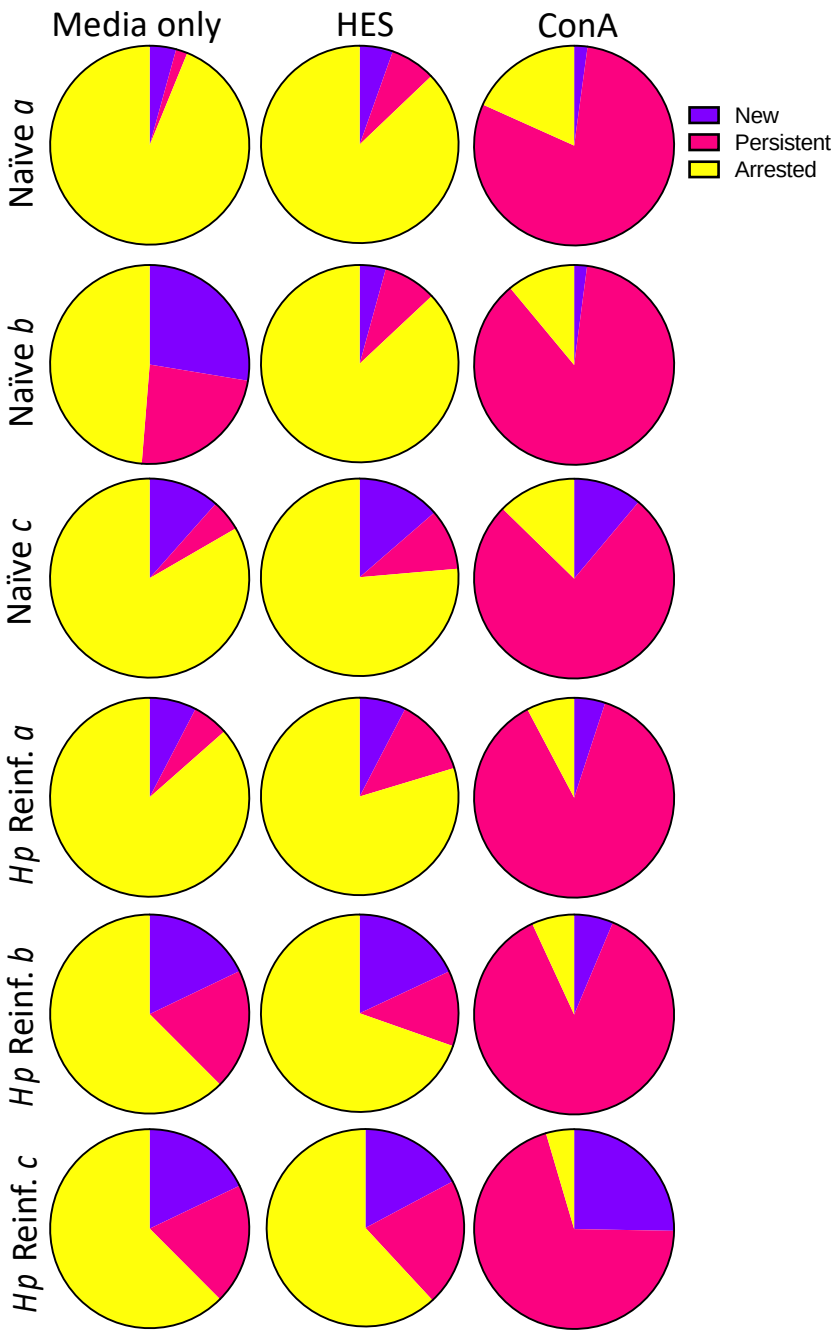

Figure 5.13 In vitro restimulation of MLN cells with HES from mice reinfected with H. polygyrus. C57BL/6 mice were infected with 200 L3 *H. polygyrus* for 14 days before clearance with Pyratape P and reinfected 10 days later for 7 days as in Figure 2.14 before *in vitro* restimulation for 16 hours. Pie charts show the proportions of cells in each timer phenotype as determined by flow cytometric analysis. Pie charts are shown for naïve (rows 1, 2 and 3) and *H. polygyrus* reinfected mice (rows 4, 5 and 6) when cultured for 16 hours in media alone (column 1), with 10ug/ml HES (column 2) or 1ug/ml ConA (Column 3).

5.3.12 Restimulation of Nr4a3-Timer CD4+ T cells after clearing H. polygyrus infection

As such a small proportion of CD4+ T cells isolated from the MLN responded by these assays of TCR restimulation, it was decided to try to isolate CD4+ T cells which form the memory response to *H. polygyrus* infection, and to collect cells from mice in the absence of active infection which might exert an immunosuppressive effect. To isolate memory cells, mice were infected with 200 L3 *H. polygyrus* larvae for 14 days before the infection was cleared by giving 2 mg of PyratapeP (pyrantel embonate) by gavage. Mice were then culled and their MLN collected 10 days post-clearance for *in vitro* analysis (Figure 5.14).

As shown in Figure 5.15, and as seen before, cells from naïve mice showed responses to varying degrees to components of HES. CD4+ T cells from reinfected mice also showed variation: those from mouse *a* showed clear expansion of the blue variant of the timer protein (New, New/Persistent, Persistent), suggesting recent TCR engagement and thus a response to HES (Figure 5.15). However, mouse *b* did not have such a large expansion of timer blue positive cells, although there was an increase in proportion of cells in the New quadrant (Figure 5.15). Cells in the New quadrant have no expression of the red variant and thus have only seen antigen in the plate (within the last 7 hours). This suggests that T cells from both reinfected mice responded to HES *in vitro* but to different levels of expansion (Figure 5.15).

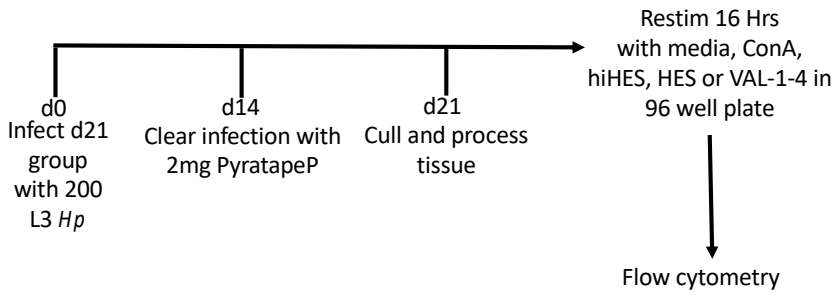

Figure 5.14 The experimental set up for H. polygyrus clearance and restimulation in vitro . C57BL/6 mice were infected with 200 L3 *H. polygyrus* for 14 days before clearing the infection with 2mg of Pyratape P before *in vitro* restimulation for 16 hours

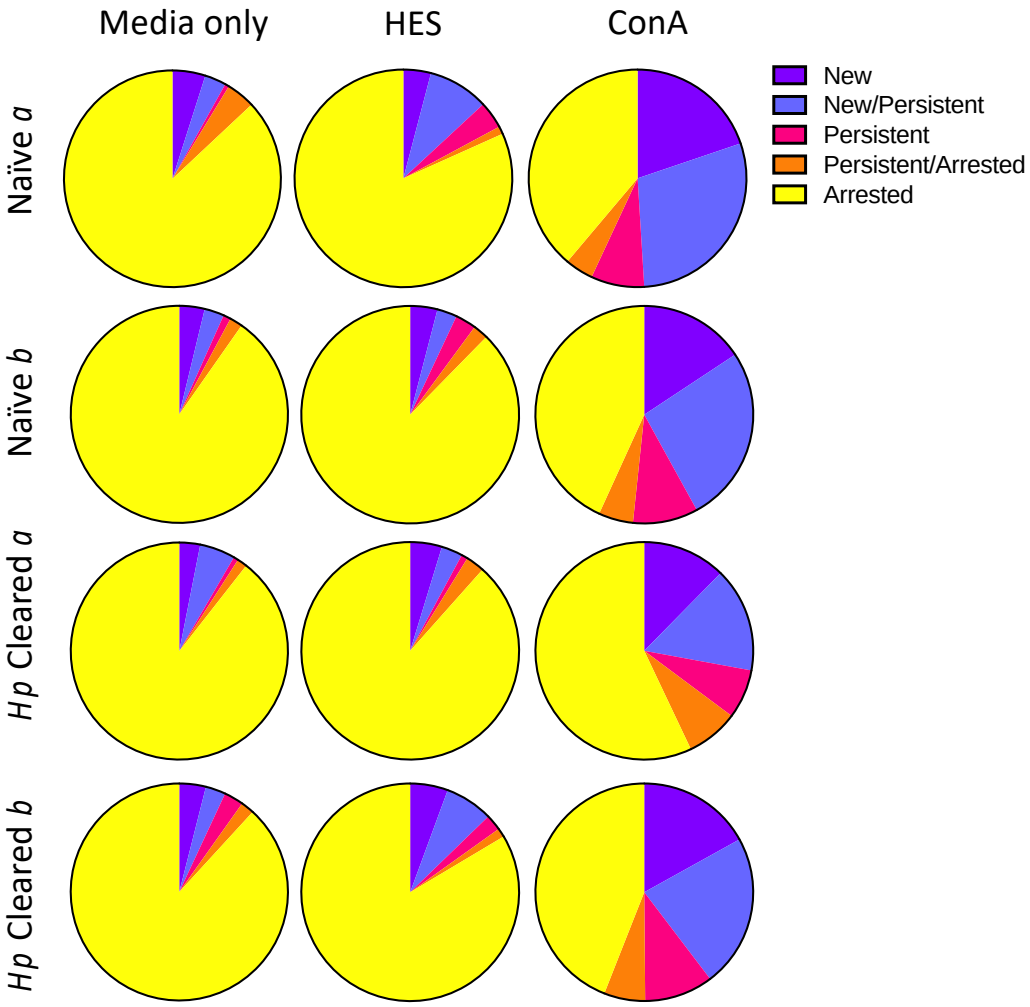

Figure 5.15 In vitro restimulation of MLN cells with HES from mice previously infected with H. polygyrus. C57BL/6 mice were infected with 200 L3 *H. polygyrus* for 14 days before clearance with Pyratape P and culled 10 days later as in Figure 5.12. Pie charts show the proportions of cells in each timer phenotype as determined by bioinformatic analysis. Pie charts are shown for naïve (rows 1 and 2) and *H. polygyrus* cleared mice (rows 3 and 4) when cultured for 16 hours in media alone (column 1), with 10ug/ml HES (column 2) or 1ug/ml ConA (Column 3).

5.3.13 Restimulation of Nr4a3-tocky CD4+ T cells with heat inactivated HES (hiHES)

HES has many molecules which are known to affect the function and activation of immune cells (Grainger et al., 2010; Coakley et al., 2017; Johnston et al., 2017; Osbourn et al., 2017; Smyth et al., 2018; Chauché et al., 2020). To test whether the variable responses seen when CD4+ T cells are restimulated *in vitro* with are due to an active molecule within HES altering the activation of the CD4+ T cells, HES was heat-inactivated for 30 minutes at 100°C. This hiHES was then used in the restimulation assay to test whether inactive HES is able to activate CD4+ T cells from *H. polygyrus* cleared mice (Figure 5.14).

As seen in Figure 5.16, there is very little response to hiHES by CD4+ T cells from naïve mice, suggesting that the component of HES which upregulated Nr4a3 and CD69 on naïve CD4+ T cells is heat-labile. However, there was also no recognition by CD4+ T cells from the *H. polygyrus* cleared mice (Figure 5.16). This may suggest that CD4+ T cells are activated by the same molecule which activates naïve CD4+ T cells. There is also a possibility that the epitopes which *H. polygyrus* specific CD4+ T cells recognise have been destroyed during the heat inactivation. Together this suggests that HES is able to alter the activation of T cells *in vitro* and this activity is lost when heat inactivated.

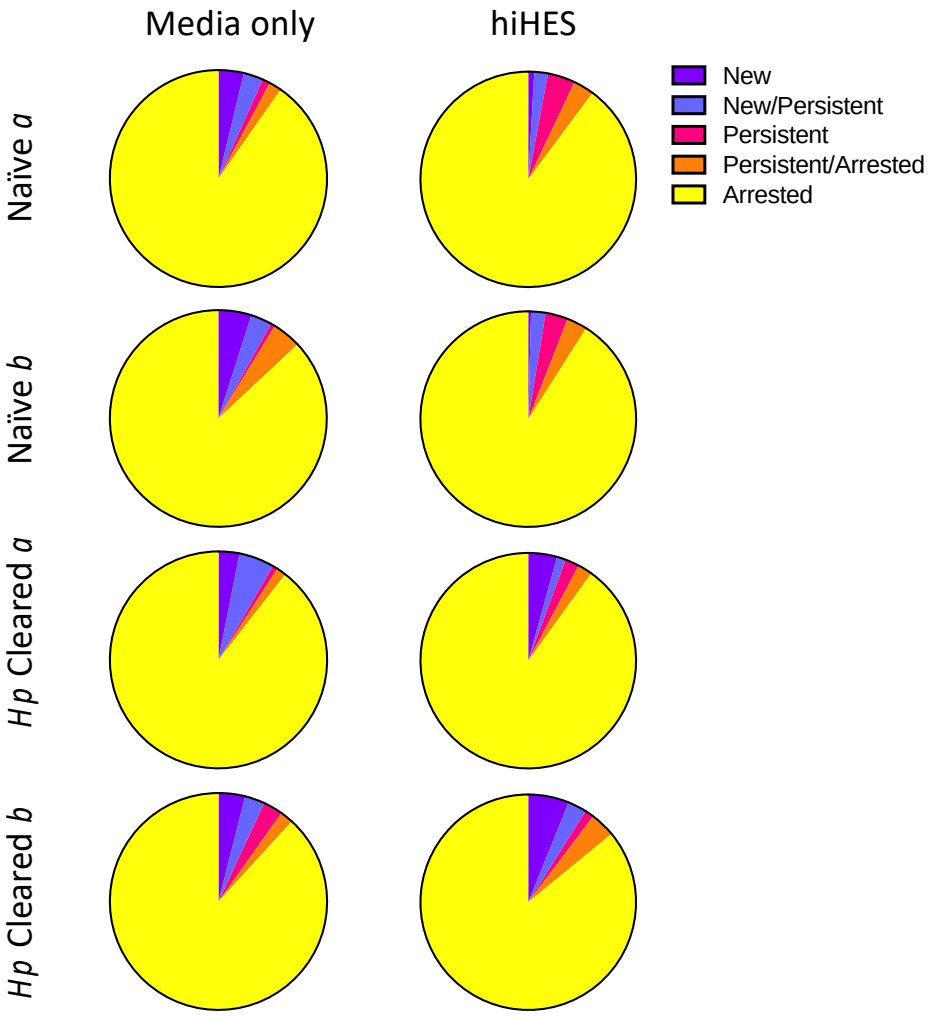

Figure 5.16 In vitro restimulation of MLN cells with heat inactivated HES (hiHES) from mice previously infected with H. polygyrus. C57BL/6 mice were infected with 200 L3 *H. polygyrus* for 14 days before clearance with Pyratape P and culled 10 days later as in Figure 5.12. Pie charts show the proportions of cells in each timer phenotype as determined by bioinformatic analysis. Pie charts are shown for naïve (rows 1 and 2) and *H. polygyrus* cleared mice (rows 3 and 4) when cultured for 16 hours in media alone (column 1) or with 10ug/ml of hiHES (column 2).

5.3.14 Restimulation of Nr4a3-tocky CD4+ T cells with various Hp-VAL proteins

In several assays, the response to *Hp*-VAL-1, *Hp*-VAL-2, *Hp*-VAL-3 and *Hp*-VAL-4 was measured, but was found to be small to negligible in both infected and naïve mice. Figure 5.17 shows the proportion of cells in the timer quadrants when cultured for 16 hours with each of the four *Hp*-VAL family members. Looking first at the naïve cells, there are varying levels of responses to *Hp*-VAL-1, *Hp*-VAL-2 and *Hp*-VAL-4 in the two naïve mice (Figure 5.17). This suggests that there are naïve CD4+ T cells which can respond to *Hp*-VAL-1, *Hp*-VAL-2 and *Hp*-VAL-4. In cultures of cells from the *H. polygyrus* infected and cleared mice, there is a response to *Hp*-VAL-1 in mouse *a* but not mouse *b* (Figure 5.17). There are also variable responses to *Hp*-VAL-2 in that mouse *a* shows a slight expansion of cells in the New quadrant suggesting there is a small response to *Hp*-VAL-2, whereas mouse *b* shows no recognition (Figure 5.17).

Consistently throughout every experiment, there is no response to *Hp*-VAL-3 in either the naïve or cleared CD4+ T cells, suggesting that *Hp*-VAL-3 is poorly, if at all, immunogenic (Figure 5.17, data not shown). Finally, *Hp*-VAL-4 is recognised by cleared mouse *a* but not mouse *b* (Figure 5.17). Together this suggests that the *Hp*-VAL-1, *Hp*-VAL-2 and *Hp*-VAL-4 are potentially immunogenic and recognised by cells from *H. polygyrus* infected mice whereas *Hp*-VAL-3 is likely not immunogenic. However, the recognition of *Hp*-VAL proteins is not consistent between replicate infected mice, suggesting differential responses to *H. polygyrus* even in inbred mouse lines.

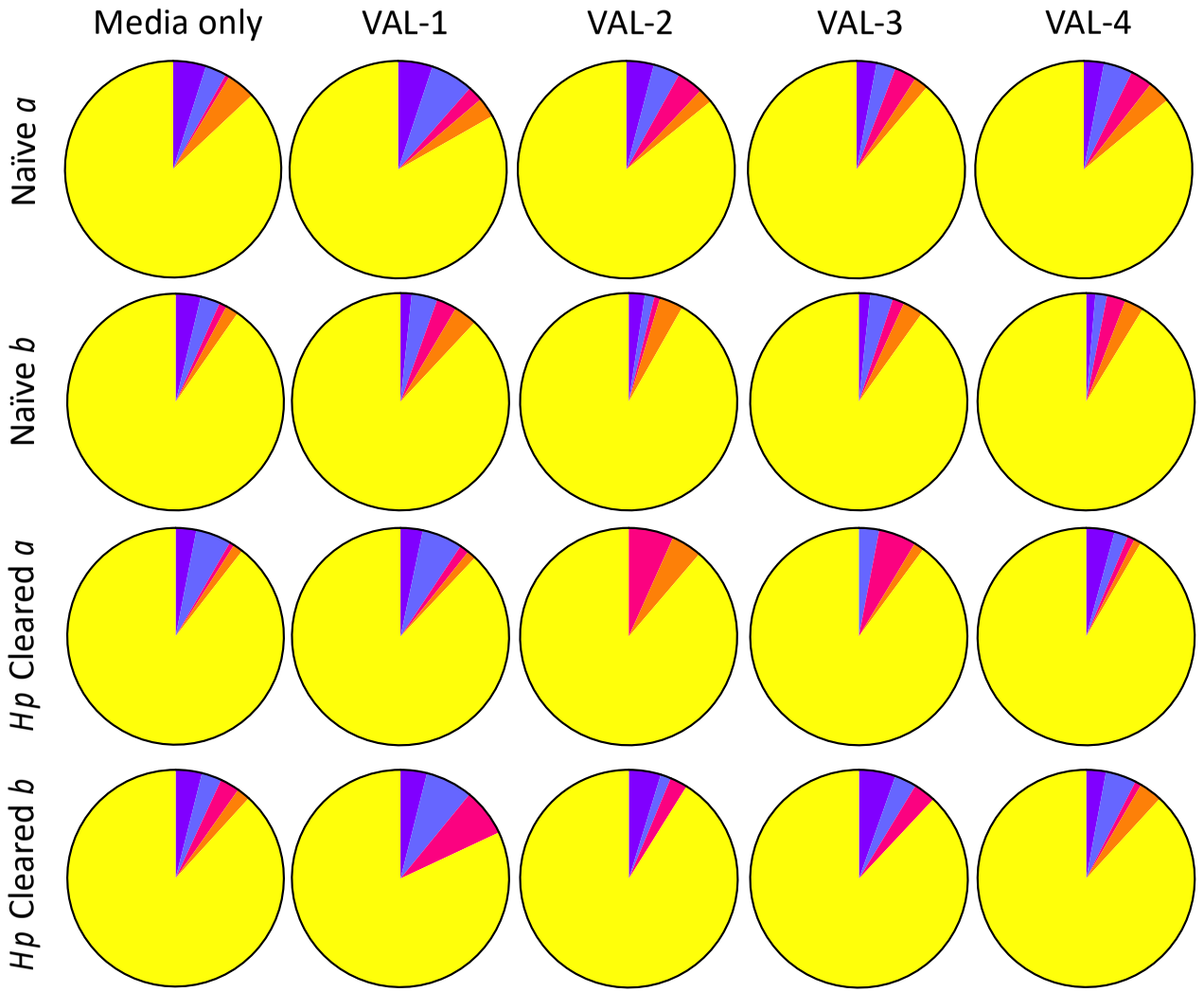

Figure 5.17 In vitro restimulation of MLN cells with Hp-VAL proteins from mice previously infected with H. polygyrus. C57BL/6 mice were infected with 200 L3 *H. polygyrus* for 14 days before clearance with Pyratape P and culled 10 days later as in Figure 5.12. Pie charts show the proportions of cells in each timer phenotype as determined by bioinformatic analysis. Pie charts are shown for naïve (rows 1 and 2) and *H. polygyrus* cleared mice (rows 3 and 4) when cultured for 16 hours in media alone (column 1), 1ug/ml *Hp*-VAL-1 (column 2), 1ug/ml *Hp*-VAL-2 (column 3), 1ug/ml *Hp*-VAL-3 (column 4) or 1ug/ml *Hp*-VAL-4 (Column 5). Data representative of 2 experiments.

5.4 Discussion

To better understand the adaptive immune response to *H. polygyrus*, it is important to know what aspect of infection is triggering the immune response. The T cell response is antigen dependent and is dependent on TCR recognition of peptide presented by MHC II. Once an epitope and its TCR are isolated, this information can be used as a vaccination target to assess whether boosting the natural immune response can lead to immunity and can be used to generate a *H. polygyrus* specific tetramer or transgenic TCR mouse. There are currently no TCR transgenic mice with specificity for a natural epitope found in nematode infection. The creation of such a line would not only facilitate better understanding of the response to that single epitope, but would also allow modelling of infection in ways that are currently unavailable. While this project has not produced an *H. polygyrus* specific TCR and its corresponding epitope, it demonstrates the scale and challenge of the operation needed to find a successful clone. With such a small proportion of cells in the MLN being specific to an antigen in HES, finding CD4+ T cells which respond to specific components of HES is like finding a needle in a haystack.

One approach to identify T cell epitopes is through informatics based on known peptide binding to individual MHC Class II proteins, scanning parasite protein sequences for high affinity peptides. However, although MHC II epitope prediction has been greatly improved in recent years with increasing sizes of peptide libraries and more advanced algorithms and neural networks, these predictions may not reflect real immunogenic T cell epitopes found within an *H. polygyrus* infected mouse (Nelson, Petzold and Unanue, 1994; Nielsen, Lundegaard and Lund, 2007; Wang et al., 2008; Nielsen and Lund, 2009; Nielsen et al., 2010; Zhang et al., 2012; Graham et al., 2018; Jensen et al., 2018; Reynisson et al., 2020). There are many stages of antigen processing which are not easily modelled artificially, such as antigen processing by APCs and competition with higher affinity epitopes.

First, antigen processing which leads to a peptide loaded onto class II MHC is dependent on enzymatic degradation of phagocytosed proteins into peptides which can be loaded onto MHC II (J. S. Blum et al., 2013; Gfeller & Bassani-

Sternberg, 2018; Vyas et al., 2008). Different APCs also have differences in their expression levels of enzymes and the internal pH of their lysosomes which regulates the activity of the enzymes and can lead to different APCs from the same host yielding distinct peptides loaded onto MHC II (J. S. Blum et al., 2013; Hoze, Tsaban, Maman, & Louzoun, 2013; Vyas et al., 2008). Currently, MHC II epitope prediction does not fully account for the pre-processing of proteins into peptides within the antigen presenting cells. It had been argued that a method should be employed to predict the peptides made naturally by antigen presenting cells and these predicted epitopes should then be fed into MHC II epitope prediction tools to predict their binding to class II MHC(Hoze *et al.*, 2013; Schneidman-Duhovny *et al.*, 2019). This approach is more likely to find a natural CD4+ T cell epitope that plays a role in an infected mouse.

There are also a wide variety of peptides that can be bound to MHC II and each of these peptides has its own binding affinity to MHC II. In fact, there is a hierarchy of binding strength in which the peptides with the highest binding affinity are known as immunodominant epitopes and can outcompete lower affinity peptides (Akram & Inman, 2012; Graham et al., 2018). This means that even if a peptide can be processed by APCs and loaded onto MHC II, it may not be presented for T cell recognition if it is outcompeted by other epitopes. This further restricts the pool of potential peptides in *H. polygyrus* infection.

Despite these limitations, the prediction algorithms offered several interesting insights; firstly, that the most likely epitopes in the most abundant antigens (*Hp*-VAL-1 and VAL-2) mapped exactly to regions of sequence polymorphism in the parasite. Examples of antigenic variation are rare in helminth parasites, but this may be one system worth investigating, eg whether VAL-1.1 immunization of mice would favour emergence of parasites expressing VAL-1.2. Another unexpected outcome was the greater number of predicted epitopes binding the MHC Class II of the more susceptible C57BL/6 strain, than was the case for the more resistant BALB/c strain. Whether this translates into a greater T cell response in C57BL/6 mice, or if these epitopes are recognised by Tregs rather than Teffectors, remains to be determined.

It is therefore important to include empirical methods to identify T cell antigens and epitopes, as for example in this chapter by *in vitro* restimulation of antigen-experienced CD4+ T cells with specific parasite antigens. From all the results of the various restimulation protocols summarised in this chapter, it is clear that there is a very small number of *H. polygyrus* antigen specific T cells within the MLN. It is possible that a better proportion of the *H. polygyrus* specific cells are found in the duodenal lamina propria and surrounding tissues where the adult worms reside. However, isolating cells from the small intestine lamina propria of *H. polygyrus* infected mice is difficult and usually yields low viability and low quality cells (Ferrer-Font et al., 2020; H. C. Webster et al., 2020). While different small intestine lamina propria protocols have been published recently, the resulting lamina propria cells would likely not survive a 16 hour culture and thus the MLN is the best tissue for recovering *H. polygyrus* specific T cells (Ferrer-Font et al., 2020; H. C. Webster et al., 2020).

As discussed in 5.1.42, the number of potential T cell epitopes presented during *H. polygyrus* is likely to be expansive. This makes finding clones with an *H. polygyrus* specific TCR and their corresponding epitope a very difficult challenge. An additional complication is the likely wound healing type 2 response in *H. polygyrus* infected mice that may stimulate TCRs which recognise indicators of damage and self-antigen or be indirectly induced by cytokine production from other cells (Gause et al., 2013). Infection with *H. polygyrus* leads to damage of the intestinal barrier when the larvae migrate through the intestinal epithelium to encyst in the muscularis, and again when they migrate back through the epithelial layer to mature into the adult stage (Johnston *et al.*, 2015). This damage to the intestinal epithelium releases antigens which can be recognised by CD4+ T cells as well as allowing translocation of intestinal bacteria into the intestinal lamina propria (C. C. Chen, Louie, McCormick, Walker, & Shi, 2005). Taking into account antigens that are created from the damage caused by helminth infection, the HES specific T cells may be outnumbered by those responding to the tissue disruption caused by *H. polygyrus* and thus contribute minimally to the anti-helminth response.

There is also a possibility that a component of HES is interfering with the activation of T cells *in vitro*. This is not unexpected as HES has been shown to

induce Tregs using *Hp*-TGM and using *Hp*-ARI to tether IL-33 to damaged cells to prevent alarmin responses (Grainger et al., 2010; Johnston et al., 2017; Osbourn et al., 2017; Smyth et al., 2018). When HES was heat inactivated as in Figure 5.16, there was loss of CD4+ T cell recognition, suggesting there is a heat-labile component of HES is acting on the pathway of activation or proliferation of T cells after activation, this would explain why very few T cells express activation markers when presented with hiHES or HES as an antigen. There could also be a mitogen in HES which activates CD4+ T cells independent of the TCR. An α-MHC class II antibody can be tested to block the TCR: MHC: peptide complex within the same assay set up and activation in the presence of this antibody would suggest there is a mitogen in HES. As discussed in the Introduction, *H. polygyrus* infection induces $CD11c^{lo}$ CD103- dendritic cells which are poorly responsive to TLR stimulus and induce lower levels of T cell activation *in vivo* (Katherine A. Smith et al., 2011). There is also evidence that *in vitro*, HES treated BMDCs can induce T cells which produce IL-10 and induce Foxp3+ Tregs, showing that HES is able to tolerise DCs and this impacts the activation of CD4+ T cells (A. M. Blum et al., 2012).

It has been shown that a naïve CD4+ T cells TCR and the TCR signalling they receive impacts their differentiation into different T helper subsets (Pacholczyk & Kern, 2008; Snook, Kim, & Williams, 2018). While the exact relationship between TCR affinity and TCR signalling with T helper differentiation is not fully understood, it is generally accepted that Teffector cells receive higher TCR signalling than Tregs and this signalling strength impacts whether a naïve CD4+ T cell becomes an effector cell or a regulatory cell (Bhattacharyya & Feng, 2020; Snook et al., 2018; Wolf, Emerson, Pingel, Buller, & DiPaolo, 2016). However, there is an overlap in the TCR repertoire in conventional T cells and Tregs which suggests that these cells received similar TCR signalling and ended up differentiating in separate directions (Pacholczyk & Kern, 2008). Using a transgenic mouse with a fixed TCRß chain and Foxp3 reporter, it was found that TCRs shared between Tregs and conventional T cells shared more than 90% of the TCR DNA sequence. This suggests that Tregs and conventional T cells which share the same TCR originate from the same CD4+ T cell clone (Wolf *et al.*, 2016). Performing TCR sequencing on Tregs and Teffectors from *H. polygyrus* infected mice would allow assessment of TCR repertoire overlap between Tregs

and Teffectors during infection. Changes in the proportion of Tregs and Teffector cells with overlapping TCRs can give insights into T cell activation dynamics during helminth infection and how activation is impacted by the presence of immunomodulatory molecules like *Hp*-TGM.

While the solution to these problems was not discovered throughout this project, there are many circumstances in which a *H. polygyrus* specific TgTCR could be used to develop our understanding of the adaptive immune response to *H. polygyrus*. For example, the role of Th cell skewing in clearance of the worm can be explored by culturing Th0 TgTCR cells into different Teffector and Treg subtypes before adoptively transferring into a mouse infected with *H. polygyrus*. The difference in the outcome of infection can be measured using parasitology and the impact of different Th subtypes on *H. polygyrus* infection can be elucidated. Another interesting idea is following the antigen specific T cells by transferring the cells into an *H. polygyrus* infected mouse with a different CD45 haplotype and looking for the transferred antigen specific cells in different tissues. This would allow tracking of the antigen specific response and may explain how *H. polygyrus* is able to enact suppression on compartments away from the duodenum. Finally, the effect of different worm burdens and antigen availability on the Th2 response can be studied *in vitro* by observing the difference in TgTCR T cells exposed to different doses of *H. polygyrus* antigen. This could explain the difference in immunopathology in those infected with few worms versus those infected with a high worm burden.

5.5 Summary

In summary, there are a small proportion of CD4+ T cells which recognise antigens found within HES and can be restimulated *in vitro*. On top of this, there is a high level of variation between inbred mice, suggesting that there are factors outside of genetics which impact the *H. polygyrus* specific T cell repertoire. There was very little response to the top VAL proteins from adult HES suggesting that although they are the most abundant proteins in HES, they have low CD4+ T cell immunogenicity. Finally, there are components within HES which are recognised by naïve CD4+ T cells after 16 hours in culture, this suggests that

there are immunogenic components to HES that have eluded us in the scope of this project.

- There are a small proportion of CD4+ T cells in the MLN which recognise components of HES
- There is high mouse to mouse variation in the CD4+ T cell response to HES
- Naïve mice are able to recognise components of HES after 16 hours in culture
- There is little to no response to the venom allergen like proteins found in HES

Chapter 6 Discussion

The dynamics and complexity of T cell responses to *H. polygyrus*, and the interplay of helper and regulatory cells, determine the balance between resistance and susceptibility to *Heligmosomoides polygyrus* infection (Filbey et al., 2014; K A Smith et al., 2016). The particular importance of Treg cell responses to infection is exemplified by the activation and expansion of this subset upon infection, and the presence of a TGF-ß mimic (TGM) found within *H. polygyrus* ES that can act directly to induce Treg differentiation (Johnston et al., 2017; Smyth et al., 2018, 2021; White et al., 2021).

It has been suggested that Tregs from *H. polygyrus*-infected mice may be distinct from, and more suppressive than, naïve Tregs due to the influence of the worm and its ES products, including more potent Treg induction by TGM versus TGF-ß (Bowron *et al.*, 2020; White *et al.*, 2021). Heightened Treg function could provide an explanation for the ability of *H. polygyrus* infection to inhibit a wide range of inflammatory disorders (Bashir et al., 2002; Kitagaki et al., 2006; Saunders et al., 2007; White, Johnston, et al., 2020; Wilson et al., 2005).

However, there has been contradicting information about the importance of the Treg response in resistance versus clearance. In experiments in which the Treg compartment is depleted, diphtheria toxin-treated Foxp3LuciDTR mice did not show decreased worm burdens, which would have been expected when Treg suppression is lifted (Smith et al., 2016). While in C57BL/6LuciDTR mice, there is an increase in IL-4 and IL-13 production when given diphtheria toxin suggesting a higher Th2 response, in *H. polygyrus*-infected BALB/c Foxp3LuciDTR mice, when diphtheria toxin is given, there is actually an increase in worm burden, due to an uncontrolled IFNγ response (Smith et al., 2016). However, the deletion of Tregs during *H. polygyrus* infection led to weight loss and increased pathology associated with infection, reiterating that Tregs are not only important for modulation of the response to helminthiases but also act to prevent immunopathology and maintain the health of the host (K A Smith et al., 2016).

In addition, the Finney laboratory showed that in early infection C57BL/6 Tregs from *H. polygyrus*-infected mice are suppressive but no more so than their naïve counterparts (Bowron et al., 2020). It has also been shown that iTregs induced by TGM are similar to those induced by TGF-ß, but that TGM signalling is more sustained (White et al., 2021). These findings open the question of whether Tregs primarily impair responses associated with clearance of *H. polygyrus*, leading to higher susceptibility as previously hypothesised. To understand the role of Tregs and their corresponding Teffector cells (Th2 cells), further characterisation of *H. polygyrus* CD4+ T cells was undertaken.

Using single cell sequencing, the CD4+ T cell response to *H. polygyrus* was compared in partially resistant BALB/c and fully susceptible C57BL/6 mice. It was clear that on a global level, Th2 cells were expressing the highest levels of TCR signalling, co-stimulation and cytokine signalling genes in the MLN. This suggests that the Th2 population is activated by and recognising antigens from *H. polygyrus* infection which is in keeping with the literature (Filbey et al., 2014). When the Th2 cell cluster data were isolated and re-clustered, transcriptionally distinct sub-populations of Th2 cells were identified, suggesting that they may be performing distinct functions during infection.

The proportions of the Th2 subclusters were different in BALB/c and C57BL/6 at homeostasis and differentially expanded upon infection in the two strains, which may explain the difference in the outcome of parasitology. Th2 cells have been shown to be heterogeneous and express different genes and proteins which can lead to different functions. For example, expression of PU.1 marks a sub population of Th2 cells which do not produce IL-4 (Chang *et al.*, 2005). Single cell sequencing of Th2 cells from *Nippostrongylus brasiliensis* infected mice also showed differential expression of *Il5* and *Il13* in the Th2 population, suggesting different Th2 cells function to upregulate different arms of the type 2 response (Radtke, Thuma, Kirchner, Ekici, & Voehringer, 2021). This is in line with the findings of Chapter 3 which show transcriptomically distinct clusters of Th2 cells during *H. polygyrus* infection. There is also evidence of increased IL-10 signalling in the Th2 cell population during *H. polygyrus* infection which suggests that the Th2 population is being modulated by IL-10. One of the main producers of IL-10

are Tregs which may imply that Th2 cells from *H. polygyrus* infected are being controlled by Tregs (Shevyrev & Tereshchenko, 2020).

Inspection of single cell sequencing data from the Treg cluster also reveals subtypes of Tregs during *H. polygyrus* infection, with different levels of TCR signalling, co-stimulation and cytokine signalling gene expression. This is in keeping with literature which shows that not only are there pTregs, nTregs and iTregs, there are also subsets of Tregs performing specialist functions (Shevyrev & Tereshchenko, 2020). Tregs can express a wide array of suppressive molecules including co-inhibitory receptors like CTLA-4, produce an array of cytokines and even co-express Foxp3 and transcription factors associated with other Teffector subtypes, showing that sub-populations of Tregs exist which exert their modulation of the immune system using different strategies and molecules (Eberl & Pradeu, 2017; L. Walker, 2013; Wing et al., 2008).

As with Th2 cells, the two mouse strains bore different proportions of the Treg subclusters at homeostasis, which differentially expanded in response to *H. polygyrus* infection. A very striking difference was seen in the Treg response to *H. polygyrus* in BALB/c versus C57BL/6 mice in terms of their expression of genes associated with TCR signalling, co-stimulation and cytokine signalling, which rise in BALB/c mice following *H. polygyrus* infection, suggesting that increased Treg activity compared to naïve BALB/c mice. However, in C57BL/6 mice, Tregs from *H. polygyrus* mice are strikingly less active than those from naïve C57BL/6 mice, suggesting that Tregs from *H. polygyrus* infected mice are not receiving high levels of TCR stimulation and activation. This may suggest that Tregs from C57BL/6 mice are not the main suppressors of the Th2 response and may not be responsible for the full susceptibility of C57BL/6 mice. However, all the data from single cell sequencing has to be assessed at the protein level and while this was done for CTLA-4, ICOS, Ly6E, Bcl2 and cMaf, more validation is required to confirm the changes seen in the gene expression and pathway analysis.

Changes in expression of key Treg molecules in Tregs from early *H. polygyrus* infection were also scrutinised at a protein level using flow cytometry. The co-inhibitory receptor families were of interest due to the suppression of Teffectors

by Tregs from *H. polygyrus* infected mice being dependent on CTLA-4 (Bowron *et al.*, 2020). On top of this, *Ctla4* was a significant gene hit in the single cell sequencing which showed changes during infection. CTLA-4, PD-1 and TIGIT were assessed in Foxp3+ Tregs and Foxp3- Teffectors from C57BL/6 mice. The proportion of Tregs expressing CTLA-4 increased during early *H. polygyrus* infection when stained extracellularly but not intracellularly as the majority of Tregs were CTLA-4+ intracellularly. This is in keeping with the finding that during early infection, Treg suppression is dependent on CTLA-4 (Bowron *et al.*, 2020). There is no increase in proportion of Tregs expressing PD-1 or TIGIT during *H. polygyrus* infection which implies that CTLA-4 may be acting alone in early infection and not in concert with other co-inhibitory receptors. However, the proportion of Th2 cells expressing either CTLA-4, PD-1 or TIGIT does increase upon infection with *H. polygyrus*. This shows that while these molecules are not important to the Treg response, they may play an important role in Teffector cells. This may imply that these cells are inhibited in terms of function and or expansion (Ovcinnikovs et al., 2019; Tai et al., 2012; L. Walker, 2013; Wing et al., 2008).

Foxp3+ Tregs which co-express transcription factors associated with other Th subtypes like GATA3, T-Bet and RORγt have been described and play different roles during homeostasis and inflammation (Koch et al., 2009; Wang, Su and Wan, 2011; Wohlfert et al., 2011; Ohnmacht et al., 2015; Sefik et al., 2016; Yang et al., 2016; Levine et al., 2017). The majority of research shows that Th types are likely better suppressed by their Treg counterpart, for example, GATA3+ Tregs may be more efficient at suppressing Th2 cells (Koch et al., 2009; Levine et al., 2017; Ohnmacht et al., 2015). The data shown in Chapter 4 suggests that Th subtypes are upregulated in proportion with the upregulation of their Treg counterparts, suggesting that this paradigm may be correct. With Th2 cells being the effector type associated with *H. polygyrus* infection, it is also true that the proportion of GATA3hi Tregs expands during infection. This further backs the hypothesis but more work is required to further phenotype this population and ideally use of a $GATA3^{fl/fl}Foxp3^{Cre}$ mouse line to assess the parasitology when GATA3 expression in Tregs alone is deleted.

Of particular interest in the case of *H. polygyrus* are RORγt+ Tregs, as RORγt$^{fl/fl}$Foxp3^{Cre} mice clear the worm more efficiently than their BALB/c counterparts (Ohnmacht et al., 2015). This is interesting as Th17 cells are not thought to be important to worm clearance, and modulation of these cells should not be consequential to outcome of infection. However, there was no significant expansion of the proportion of RORγt+ Tregs in the MLN during *H. polygyrus* infection which suggests that these cells may also not be important to the immune response against the parasite, although there is an increase in numbers so it cannot be excluded that they are playing a role during infection.

There is similar parasitological outcome of *H. polygyrus* infection of RORγt$^{fl/fl}$Foxp3^{Cre} mice and IL-6 knockout mice where the transgenic mice clear their infection more efficiently than wild type counterparts (Ohnmacht et al., 2015; Katherine A. Smith & Maizels, 2014). On top of this, IL-6 is the cytokine which induces RORγt expression in Th17 cells, which may imply a role in RORγt expression in Tregs (Dienz & Rincon, 2009). It was hypothesised that the outcome of infection may be due to loss of RORγt expression in the absence of IL-6 signalling. However, when IL-6 was blocked using a monoclonal antibody, the RORγt expression by Tregs or Th17 cells was unchanged compared to naïve mice with IL-6 blocked. This may be explained by the compensation in IL-6 production seen in the whole MLN restimulation with α-CD3. An IL-6 knockout mouse which cannot produce IL-6 will be required to assess the impact of complete loss of IL-6 on RORγt+ Tregs as these cells cannot compensate for lack of IL-6. However, during IL-6 blockade, there is still an increased Th2 response to *H. polygyrus* infection as seen in expansion of Th2 numbers and increased IL-4 production which may imply that if the infection was continued to a later point in infection, there may be increased clearance of the worm. In addition, there is a loss of CD44, an activation marker, on Tregs from IL-6 blocked mice when infected with *H. polygyrus* and an increase in CD44+ Teffector cells (Baaten et al., 2010; T. Liu et al., 2009; Vincent & Mechti, 2004). This suggests that the Tregs are becoming less active and suppressive and Teffector cells are becoming more active when this suppression is lost as a result of lack of IL-6. Again, if IL-6 levels are compensated by increased production, an IL-6 KO will be required to understand the importance of IL-6 KO in the expression of RORγt within Tregs.

Another major question in *H. polygyrus* infection is what antigens CD4+ T cells recognise during infection. There are thousands of potential epitopes from the worm itself and its excretory secretory products known as HES as well as the potential for bacterial translocation and damage to the intestine during worm burrowing into the muscularis to encyst (Johnston *et al.*, 2015). The antigenic diversity of helminths is very different to that of viruses which present a limited number of epitopes and few immunodominant molecules which have been successfully targeted to generate TgTCR mouse lines in the past (Barnden et al., 1998; Cho et al., 2020; Fernandez-Ruiz et al., 2017; S. J. McSorley et al., 2002; Stephens et al., 2005; Vanheerswynghels et al., 2018).

With such as volume of potential antigens from *H. polygyrus*, it became important to narrow down the targets using proteomic data and previous knowledge (Hewitson et al., 2013; Hewitson, Filbey, et al., 2011; Hewitson, Harcus, et al., 2011). As a result the venom allergen-like proteins or VAL proteins were obvious candidates due to their abundance in larval and adult *H. polygyrus* ES, as well as a dominant antibody response to these proteins, suggesting the presence of VAL-specific CD4+ T cells (Hewitson et al., 2013; Hewitson, Filbey, et al., 2011; Hewitson, Harcus, et al., 2011). If an immunogenic epitope can be found for *H. polygyrus*-infected mice, it would allow targeted vaccination studies to assess whether boosting the immune response against a known T cell epitope can lead to sterile immunity (Hewitson et al., 2013; Hewitson, Filbey, et al., 2011; Hewitson, Harcus, et al., 2011). This may lead to an effective vaccine against the laboratory strain and can inform the selection of epitopes for human vaccination (Hewitson & Maizels, 2014). If the TCR which recognises the epitope can be sequenced, it would allow generation of a TCR transgenic mouse against an *H. polygyrus* antigen (Vanheerswynghels *et al.*, 2018). This transgenic TCR mouse could be used to track the migration of antigen-specific T cells and allow *in vitro* differentiation of naïve tgTCR CD4+ T cells into different subtypes of Th cell before adoptively transferring into a naïve mouse to assess the outcome on infection (Barnden et al., 1998; Cho et al., 2020; S. J. McSorley et al., 2002; Vanheerswynghels et al., 2018). This would allow us to assess which Th cell types play roles in clearance versus susceptibility.

While an epitope and corresponding TCR were not found in the timeline of this project (Chapter 5), the study has given insight into the antigen-specific response to *H. polygyrus* in the MLN. It appears that very few HES specific CD4+ T cells are to be found within the MLN of *H. polygyrus* infected, reinfected or cleared mice, which makes finding a TCR and epitope significantly more difficult. One consideration is that the low number of responding cells may reflect the tissue sampled. The MLN is the lymphoid organ which drains the duodenum and is the site of T cell activation and priming (Bousso, 2008; Johnston et al., 2015); it also yields high numbers of viable cells which are readily cultured. However, most antigen-specific T cells are likely to be at the tissue site, exerting their effector function and not in the lymph node (Bousso, 2008). As seen in Chapter 3, lymph nodes contain mostly naïve CD4 T cells which enter the lymph node to interact with APCs and either become activated or recirculate through the lymphatics (M. C. Hunter, Teijeira, & Halin, 2016). As a result, the pool of antigen-specific T cells is diluted by the presence of these cells. However, it was not possible to culture small intestine lamina propria or Peyer's patch cells without high levels of death in culture after 16 hours (data not shown) and thus tissue site lymphocytes could not be used for this experiment.

Another point of discussion is the fact that in many experiments, T cells from naïve mice responded more strongly to HES than did those from *H. polygyrus*-experienced mice. This is surprising as the naïve mice should have very low frequencies of parasite-specific cells, and would be expected to take longer to respond to the antigen. However, the finding appears robust as both CD69 and Nr4a3 are directly downstream of TCR signalling, and recognition of peptide: MHC complexes alone upregulates these markers before lymphocytes are fully activated (Radulovic et al., 2013b; Cibrián and Sánchez-madrid, 2017; Jennings et al., 2020). While this added a hurdle to finding a T cell epitope in natural *H. polygyrus* infection, it reveals that there are naïve T cells which recognise epitopes in HES within 16 hours of exposure. This suggests that there are antigens within HES that are immunogenic or components which act as a mitogen or may activate CD4 T cells through an active molecule which is heat-labile.

While future work will require testing of different panels of possible antigens, it is important to first understand the response to whole HES. Use of an α-MHC II antibody would allow us to assess whether the activation is due to MHC interactions with the TCR or with an activating molecule or mitogen. If there is an activator or mitogen in HES, HES can be fractionated by size and charge and the fractions tested *in vitro* to track down the active molecule. If there is no mitogen and activator, HES can again be fractionated and tested in the restimulation assay to track down the immunogenic component of HES. This reverse engineering of the process may allow for faster identification of an immunogenic antigen.

Understanding the antigen specificity of CD4+ T cells during *H. polygyrus* infection may also lead to a better understanding of the relationships between the Th2 and Treg populations. For example, if the majority of Tregs recognise *H. polygyrus* antigens and are part of the anti-helminth response, their control of the anti-helminth response may lead to inhibition of the Th2 response, leading to susceptibility to the worm and limited clearance. However, if the Treg expansion shows recognition of the damage response, the Tregs are unlikely to be directly inhibiting the type 2 response against the worm, leading to increased clearance. This is an area of the immune response against *H. polygyrus* which requires greater study.

It is also worth noting that these experiments were carried out using a bolus infection where all larvae are given to the host at one time point, meaning the parasites are all in the same life cycle stage at any given moment. This is not the pattern of infection seen in the human population, where hosts are continuously reinfected with helminths, leading to parasites in different life stages in the same host (Behnke *et al.,* 2003; Brailsford and Behnke, 1992; Ariyaratne *et al*., 2020). In the laboratory, this infection pattern can be mimicked with a trickle infection, where small numbers of larvae are orally gavaged into host on multiple occasions (Behnke *et al.,* 2003; Brailsford and Behnke, 1992; Ariyaratne *et al*., 2020). Using trickle infection, the usually susceptible C57BL/6 mouse is able to partially clear infection like the BALB/c mouse (Ariyaratne *et al*., 2020). This may be due to the constant re-triggering of the immune response with smaller numbers of larvae allowing protective

immunity to form. Comparing the T cell response in C57BL/6 mice infected using the bolus or trickle method may give insights into the dynamics of Th2 and Treg responses and their interplay which allow clearance of the worm versus susceptibility to infection seen in the bolus infection.

To summarise, the CD4+ T cell response is pivotal in *H. polygyrus* infection and certainly determines the balance between clearance and susceptibility (Filbey *et al.*, 2014). Within the CD4+ population, suppression or activation of Th2 cells must be the primary factor in clearance of the worm. While it is clear that Th2 cells from *H. polygyrus*-infected mice are active and undertaking effector functions, they also show signs of being under suppression or dysregulated, particularly in the more susceptible C57BL/6 strain. Paradoxically, Tregs appear to be activated in early *H. polygyrus* infection of BALB/c but not in C57BL/6 counterparts. This may imply that Tregs are more central to the BALB/c response than to the C57BL/6 response to *H. polygyrus*, in which case other regulatory mechanisms may be operating in the latter strain (Figure 6.1). Further work will be required to further phenotype the Treg response to *H. polygyrus* in both strains to assess differences in their response and function and to elucidate the role of IL-6 in Treg function during infection. The HES specific CD4+ T cell response during *H. polygyrus* infection is complex and likely made up of thousands of antigens which makes finding immunodominant epitopes difficult. However, using the sensitivity of the Nr4a3-Tocky mouse model, assessing HES for an active molecule or mitogen and using a fractionation-based approach to antigen discovery, a transgenic TCR mouse against an immunodominant *H. polygyrus* antigen may be possible.

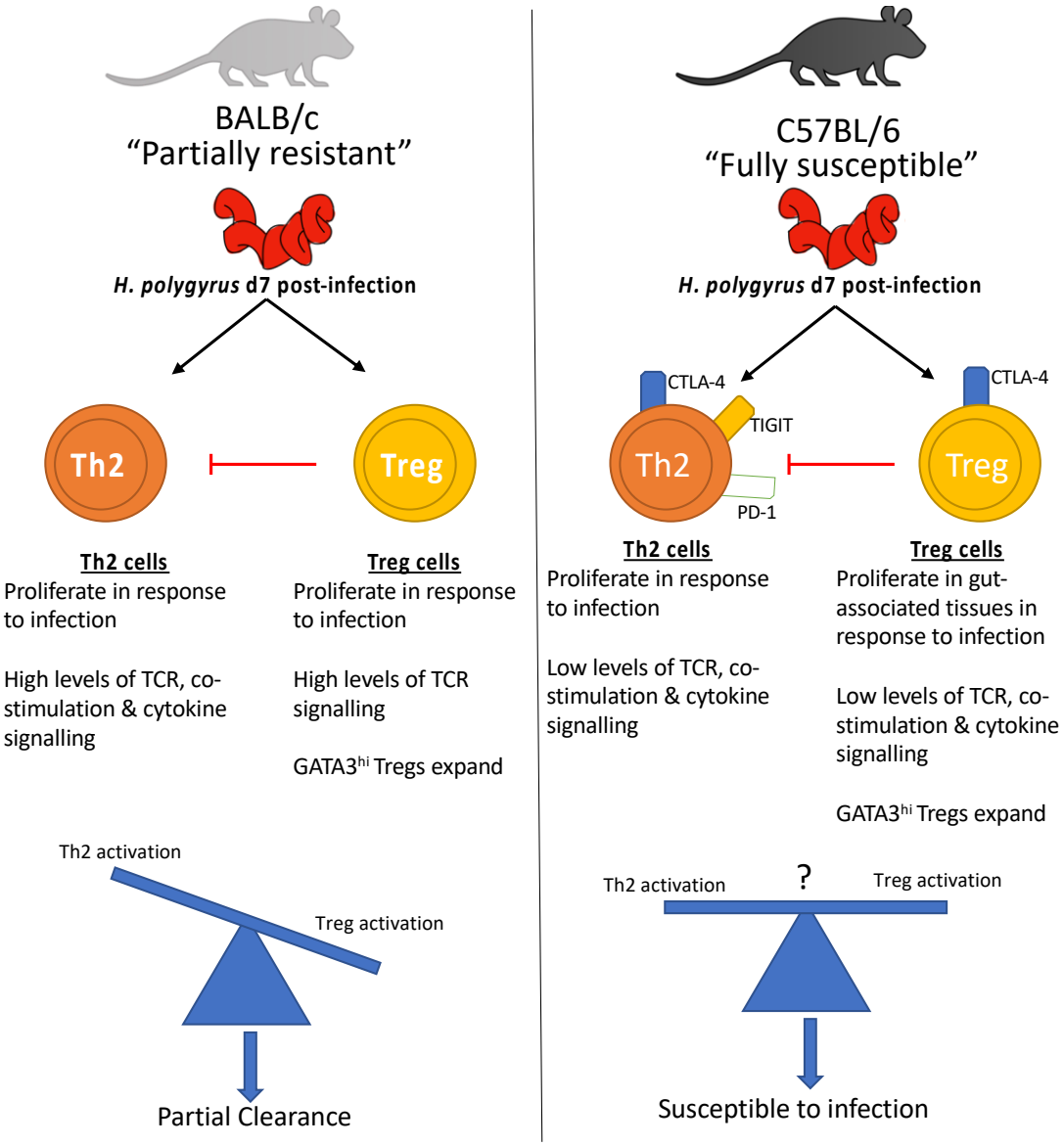

Figure 6.1 T cell response to H. polygyrus in BALB/c and C57BL/6 mice. Infection with *H. polygyrus* leads to expansion of both Th2 cells and Tregs in both partially resistant BALB/c mice (left) and susceptible C57BL/6 mice (right). However, their Th2 and Treg populations are distinct. BALB/c Th2 cells are more transcriptionally active in *Hp* infected mice, whereas Th2 cells from C57BL/6 mice are less active in *Hp* infected mice which may explain their difference in infection outcome. Tregs are able to suppress the Th2 response during infection and while BALB/c Tregs are transcriptionally active during *Hp* infection, C57BL/6 Tregs are distinctly inactive at the RNA level and are likely not the main suppressors of the Th2 response in C57BL/6 mice infected with *Hp*. The GATA3^{hi} Treg subpopulation of Tregs expands in both BALB/c and C57BL/6 mice upon infection with *Hp*.

Appendix

I. R script used for single cell RNA sequencing

```
####Load all required packages
library(Seurat)
library(magrittr)
library(dplyr)
library(cowplot)
library("ggplot2")
library(dittoSeq)
library(EnhancedVolcano)
library(DESeq2)
library(patchwork)
library(limma)
library(leidenbase)
library(monocle3)
library(garnett)
library(SeuratWrappers)
library(ggpubr)
library(ReactomeGSA)

#####Set output directory

setwd("path_to_folder")

#####Separate samples using demuxlet
#import naive data and add demux
naive.data <- Read10X(data.dir = "path_to_file")
naive <- CreateSeuratObject(counts = naive.data, project = "Naive",
min.cells = 3)
Demuxnaive = "path_to_file"

#Run the import
#Note: You can leave Lane.names blank
naive <- importDemux2Seurat(Seurat.name = naive,
                            Lane.info.meta = "orig.ident",
                            Demuxlet.best = Demuxnaive,
                            bypass.check = TRUE,
                            verbose = TRUE)

naive$sample <- "Naive"
naive$group <- "Naive1"
naive[["percent.mt"]] <- PercentageFeatureSet(object = naive, pattern =
"^mt-")
plot1 <- FeatureScatter(object = naive, feature1 = "nCount_RNA", feature2 =
"percent.mt")
plot2 <- FeatureScatter(object = naive, feature1 = "nCount_RNA", feature2 =
"nFeature_RNA")
CombinePlots(plots = list(plot1, plot2))

#Choose QC cut offs
naive <- subset(naive, subset = nFeature_RNA > 300 & nFeature_RNA < 2800 &
percent.mt < 5)
```

```
#run standard normalisation
naive <- NormalizeData(naive, normalization.method = "LogNormalize",
scale.factor = 10000)


### load the infected data
hpoly.data <- Read10X(data.dir = "path_to_file")
hpoly <- CreateSeuratObject(counts = hpoly.data, project = "Hp d7",
min.cells = 3)
Demuxhpoly = "path_to_file"

Demux
#Run the import
#Note: You can leave Lane.names blank
hpoly <- importDemux2Seurat(Seurat.name = hpoly,
                            Lane.info.meta = "orig.ident",
                            Demuxlet.best = Demuxhpoly,
                            bypass.check = TRUE,
                            verbose = TRUE)

hpoly$sample <- "hpoly1"
hpoly$group <- "hpoly"
hpoly[["percent.mt"]] <- PercentageFeatureSet(object = hpoly, pattern =
"^mt-")
plot1 <- FeatureScatter(object = hpoly, feature1 = "nCount_RNA", feature2 =
"percent.mt")
plot2 <- FeatureScatter(object = hpoly, feature1 = "nCount_RNA", feature2 =
"nFeature_RNA")
CombinePlots(plots = list(plot1, plot2))

#Choose QC cut offs
hpoly <- subset(hpoly, subset = nFeature_RNA > 300 & nFeature_RNA < 3000 &
percent.mt < 5)

#run standard normalisation
hpoly <- NormalizeData(hpoly, normalization.method = "LogNormalize",
scale.factor = 10000)

DefaultAssay(hpoly) <- "RNA"
hpoly <- NormalizeData(hpoly, normalization.method = "LogNormalize",
scale.factor = 10000)
hpoly$group <- "Hp"
naive <- NormalizeData(naive, normalization.method = "LogNormalize",
scale.factor = 10000)
naive$group <- "Naive"
hpoly <- FindVariableFeatures(hpoly, assay = "RNA")
naive <- FindVariableFeatures(naive, assay = "RNA")
Cell.anchors <- FindIntegrationAnchors(object.list = list(hpoly, naive),
scale = TRUE, anchor.features = 2000, dims = 1:50, assay = c("RNA", "RNA"))
all.genes <- rownames(x = hpoly)
Combined <- IntegrateData(anchorset = Cell.anchors, dims = 1:15,
features.to.integrate = all.genes)

#####Separate samples using CellHashing

#Read in the scseq library
Naive.umis <- Read10X("path_to_file")

#Create Seurat object
```

```
Naive.hashtags #Check Seurat object contains HTO columns
Naive.hashtags$sample <- "Naive"
Naive.hashtags$group <- "naive"

#####Quality control

##Naive

Naive.singlet[["percent.mt"]] <- PercentageFeatureSet(object =
Naive.singlet, pattern = "^mt-")
plot1 <- FeatureScatter(object = Naive.singlet, feature1 = "nCount_RNA",
feature2 = "percent.mt")
plot2 <- FeatureScatter(object = Naive.singlet, feature1 = "nCount_RNA",
feature2 = "nFeature_RNA")
CombinePlots(plots = list(plot1, plot2))

#Choose QC cut offs
Naive.umis <- subset(Naive.umis, subset = "nFeature_RNA" > 100 &
"nFeature_RNA" < 3500 & "percent.mt" < 15)

#####Integrate the UMI and CITE-seq

#Naive data

Naive.umis #Check the barcodes have the same format in UMI (scseq) and HTO
data

#Read in the HTO library
Naive.htos <- Read10X(data.dir = "/path_to_file", gene.column=1)
Naive.htos  #Check the barcodes have the same format in UMI (scseq) and HTO
data

#If the barcodes dont match and one has -1, remove -1 from barcodes to allow
proper pairing
colnames(Naive.umis) <- sub("-1", "", colnames(Naive.umis))

#Select barcodes found in both the RNA and HTO libraries
Naive.bcs <- intersect(colnames(Naive.umis), colnames(Naive.htos))
Naive.bcs

#Subset RNA and HTO by barcode
Naive.umis <- Naive.umis[,Naive.bcs]
Naive.htos <- as.matrix(Naive.htos[,Naive.bcs])

#Create Seurat object
Naive.hashtags <- CreateSeuratObject(counts = Naive.umis)
Naive.hashtags #Check Seurat object contains HTO columns
Naive.hashtags$sample <- "Naive"
Naive.hashtags$group <- "naive"

#Add the HTO as an independent assay
Naive.hashtags[["HTO"]] <- CreateAssayObject(counts = Naive.htos)

#Normalise data - set margin to 2 or you get lots of doublets - solution
found https://github.com/satijalab/seurat/issues/2383
Naive.hashtags <- NormalizeData(Naive.hashtags, assay = "HTO",
normalization.method = "CLR", margin = 2)

#Demultiplex samples using the HTOs
```

```
Naive.hashtags <- HTODemux(Naive.hashtags, assay = "HTO", positive.quantile
= 0.99)

#Summary of the HTO classifications
table(Naive.hashtags$HTO_classification.global)

#Visualise HTO classifications as ridge plots
Idents(Naive.hashtags) <- "HTO_maxID"
RidgePlot(Naive.hashtags, assay = "HTO", features =
rownames(Naive.hashtags[["HTO"]])[1:2], ncol = 2)

#Change the default assay to HTO
DefaultAssay(Naive.hashtags) <- "HTO"

#Create a scatter plot to show singlet classification inclusivity
FeatureScatter(Naive.hashtags, feature1 = "BALB/c", feature2 = "C57BL/6")

#Visualise the number of UMIs for singlets, doublets and negative cells in
violin plots
Idents(Naive.hashtags) <- "HTO_classification.global"
VlnPlot(Naive.hashtags, features = "nCount_RNA", pt.size = 0.1, log = TRUE)

# Remove negative cells
Naive.hashtags.subset <- subset(Naive.hashtags, idents = "Negative", invert
= TRUE)

# Calculate a distance matrix using HTO
hto.dist.mtx <- as.matrix(dist(t(GetAssayData(object =
Naive.hashtags.subset, assay = "HTO"))))

# Calculate tSNE embeddings
Naive.hashtags.subset <- RunTSNE(Naive.hashtags.subset, distance.matrix =
hto.dist.mtx, perplexity = 100)

DimPlot(Naive.hashtags.subset)
HTOHeatmap(Naive.hashtags, assay = "HTO", ncells = 50000)

# Extract the singlets
Naive.singlet <- subset(Naive.hashtags, idents = "Singlet")

# Select the top 1000 most variable features
Naive.singlet <- FindVariableFeatures(Naive.singlet, selection.method =
"mean.var.plot")


# Scale RNA data
Naive.singlet <- ScaleData(Naive.singlet, features =
VariableFeatures(Naive.singlet))

#Hp infected data

#Read in the scseq library
Hpoly.umis <- Read10X("path_to_file")
Hpoly.umis

#Read in the HTO library
Hpoly.htos <- Read10X(data.dir = "path_to_file", gene.column=1)

Hpoly.htos
```

```
#Remove -1 from barcodes to allow proper pairing
colnames(Hpoly.umis) <- sub("-1", "", colnames(Hpoly.umis))

#Select barcodes found in both the RNA and HTO libraries
Hpoly.bcs <- intersect(colnames(Hpoly.umis), colnames(Hpoly.htos))
Hpoly.bcs

#Subset RNA and HTO by barcode
Hpoly.umis <- Hpoly.umis[,Hpoly.bcs]
Hpoly.htos <- as.matrix(Hpoly.htos[,Hpoly.bcs])

#Create Seurat object
Hpoly.hashtags <- CreateSeuratObject(counts = Hpoly.umis)
Hpoly.hashtags #Check Seurat object contains HTO columns

#Add the HTO as an independent assay
Hpoly.hashtags[["HTO"]] <- CreateAssayObject(counts = Hpoly.htos)

#Normalise data
Hpoly.hashtags <- NormalizeData(Hpoly.hashtags, assay = "HTO",
normalization.method = "CLR", margin = 2)

#Demultiplex samples using the HTOs
Hpoly.hashtags <- HTODemux(Hpoly.hashtags, assay = "HTO", positive.quantile
= 0.99)

#Summary of the HTO classifications
table(Hpoly.hashtags$HTO_classification.global)

#Visualise HTO classifications as ridge plots
Idents(Hpoly.hashtags) <- "HTO_maxID"
RidgePlot(Hpoly.hashtags, assay = "HTO", features =
rownames(Hpoly.hashtags[["HTO"]])[1:2], ncol = 2)

#Change the default assay to HTO
DefaultAssay(Hpoly.hashtags) <- "HTO"

#Create a scatter plot to show singlet classification inclusivity
FeatureScatter(Hpoly.hashtags, feature1 = "BALB", feature2 = "C57")

#Visualise the number of UMIs for singlets, doublets and negative cells in
violin plots
Idents(Hpoly.hashtags) <- "HTO_classification.global"
VlnPlot(Hpoly.hashtags, features = "nCount_RNA", pt.size = 0.1, log = TRUE)

# Remove negative cells
Hpoly.hashtags.subset <- subset(Hpoly.hashtags, idents = "Negative", invert
= TRUE)

# Calculate a distance matrix using HTO
hto.dist.mtx <- as.matrix(dist(t(GetAssayData(object =
Hpoly.hashtags.subset, assay = "HTO"))))

# Calculate tSNE embeddings
Hpoly.hashtags.subset <- RunTSNE(Hpoly.hashtags.subset, distance.matrix =
hto.dist.mtx, perplexity = 100)
DimPlot(Hpoly.hashtags.subset)
```

```
HTOHeatmap(Hpoly.hashtags, assay = "HTO", ncells = 50000)

# Extract the singlets
Hpoly.singlet <- subset(Hpoly.hashtags, idents = "Singlet")

# Select the top 1000 most variable features
Hpoly.singlet <- FindVariableFeatures(Hpoly.singlet, selection.method =
"mean.var.plot")

# Scale RNA data
Hpoly.singlet <- ScaleData(Hpoly.singlet, features =
VariableFeatures(Hpoly.singlet))

####Integrate the samples using anchor points
DefaultAssay(Hpoly.singlet) <- "RNA"
Hpoly.singlet <- NormalizeData(Hpoly.singlet, normalization.method =
"LogNormalize", scale.factor = 10000)
Hpoly.singlet$group <- "Hp"
Naive.singlet<- NormalizeData(Naive.singlet, normalization.method =
"LogNormalize", scale.factor = 10000)
Naive.singlet$group <- "Naive"
Hpoly.singlet <- FindVariableFeatures(Hpoly.singlet, assay = "RNA")
Naive.singlet <- FindVariableFeatures(Naive.singlet, assay = "RNA")
Cell.anchors <- FindIntegrationAnchors(object.list = list(Hpoly.singlet,
Naive.singlet), scale = TRUE, anchor.features = 2000, dims = 1:50, assay =
c("RNA", "RNA"))
all.genes <- rownames(x = Hpoly.singlet)
Combined <- IntegrateData(anchorset = Cell.anchors, dims = 1:15,
features.to.integrate = all.genes)


Combined <- ScaleData(Combined, verbose = FALSE)
Combined <- RunPCA(Combined, npcs = 50, verbose = TRUE)
Combined <- RunUMAP(Combined, reduction = "pca", dims = 1:15, reduction.name
= "UMAP")
Combined <- FindNeighbors(Combined, reduction = "pca", dims = 1:15)
Combined <- FindClusters(Combined, resolution = 0.5)

Combined$status_strain<-paste(Combined$hash.ID, Combined$group, sep = "_")
DimPlot(Combined, reduction = "umap", label = FALSE)
DimPlot(Combined, reduction = "umap", split.by = 'status_strain', ncol = 2)

# Check gene expression of different populations via violin plot
DefaultAssay(Combined) <- "integrated"
VlnPlot(Combined, features = c("Cd3e", "Cd4", "Cd8a"))
VlnPlot(Combined, features = c("Gata3", "Foxp3", "Rorc"))
VlnPlot(Combined, features = c("Il4" , "Il10", "Tgfb1"))
FeaturePlot(Combined, features = c("Cd4", "Cd8a", "Gata3", "Rorc", "Foxp3"),
label = TRUE)
VlnPlot(Combined, features = c("Areg"))
VlnPlot(Combined, features = c("Il4", "Il5", "Il13","Il10","Tgfb1"))

saveRDS(Combined,"290721Combined.rds")

# find conserved markers for the clusters
Combined.markers <- FindAllMarkers(Combined, only.pos = TRUE, min.pct =
0.25, logfc.threshold = 0.25)
Combined.markers %>% group_by(cluster) %>% top_n(2)
```

```
#find top 10 exprressed genes for each cluster + export to csv
DefaultAssay(Combined) <- "integrated"
allclusterstop10 <- Combined.markers %>%
  group_by(cluster) %>%
  top_n(n = 10, wt = avg_log2FC)
DoHeatmap(
  Combined,
  features = allclusterstop10$gene,
  cells = NULL,
  group.by = "ident",
  group.bar = TRUE,
  group.colors = NULL,
  disp.min = -2.5,
  slot = "scale.data",
  assay = NULL,
  label = TRUE,
  size = 4,
  hjust = 0,
  angle = 0,
)+ NoLegend() + theme(axis.text.y = element_text(size = 6))

View(allclusterstop10)
write.csv(allclusterstop10,"290721allclusterstop10.csv", row.names = FALSE)

#find top 30 exprressed genes for each cluster + export to csv
DefaultAssay(Combined) <- "integrated"
allclusterstop30 <- Combined.markers %>%
  group_by(cluster) %>%
  top_n(n = 30, wt = avg_log2FC)

DoHeatmap(
  Combined,
  features = allclusterstop30$gene,
  cells = NULL,
  group.by = "ident",
  group.bar = TRUE,
  group.colors = NULL,
  disp.min = -2.5,
  disp.max = NULL,
  slot = "scale.data",
  assay = NULL,
  label = TRUE,
  size = 4,
  hjust = 0,
  angle = 0,
)+ NoLegend() + theme(axis.text.y = element_text(size = 6))
View(allclusterstop30)
write.csv(allclusterstop30,"290721allclusterstop30.csv", row.names = FALSE)

# plot frequencies
freq_table_sample <- as.data.frame(prop.table(x = table(Idents(Combined),
Combined@meta.data$status_strain), margin = 2))

ggplot(data=freq_table_sample, aes(x=freq_table_sample$Var2,
y=freq_table_sample$Freq, fill=freq_table_sample$Var1)) +
geom_bar(stat="identity", color="black") + labs(x="Sample", y="Proportion of
Cells", fill="Cluster")  + scale_x_discrete(limits =
rev(levels(freq_table_sample$Var2)))
```

```
#Name clusters
Combined <- SetIdent(Combined, value = Combined@meta.data$seurat_clusters)

Combined$status_strain<-paste(Combined$hash.ID, Combined$group, sep = "_")

new.cluster.ids <- c("Naivea", "Naiveb", "Tfh", "Th2", "Tregs", "IFN",
"Emerging", "APC", "Th2 stress", "B cell")
names(new.cluster.ids) <- levels(Combined)
Combined <- RenameIdents(object = Combined, new.cluster.ids)
DimPlot(Combined, reduction = "umap", label = TRUE, pt.size = 0.5) +
NoLegend()

######Remove the non CD4 T cells

#Select clusters containing Cd4+s
Combined.Cd4 <- subset(Combined, idents = c("Naivea", "Naiveb", "Tfh",
"Th2", "Tregs", "IFN", "Emerging"), invert = FALSE)
Combined.Cd4 <- RunUMAP(Combined.Cd4, reduction = "pca", dims = 1:50,
reduction.name = "UMAP")
DimPlot(Combined.Cd4, reduction = "umap", split.by = 'status_strain', ncol =
2)
DimPlot(Combined.Cd4, reduction = "umap")

DefaultAssay(Combined.Cd4) <- "integrated"
cd4top10 <- Combined.markers %>%
  group_by(cluster) %>%
  top_n(n = 10, wt = avg_log2FC)
DoHeatmap(
  Combined.Cd4,
  features = cd4top10$gene,
  cells = NULL,
  group.by = "ident",
  group.bar = TRUE,
  group.colors = NULL,
  disp.min = -2.5,
  disp.max = NULL,
  slot = "scale.data",
  assay = NULL,
  label = TRUE,
  size = 4,
  hjust = 0,
  angle = 0,
)+ NoLegend() + theme(axis.text.y = element_text(size = 6))

View(cd4top10)
write.csv(cd4top10,"290721Cd410.csv", row.names = FALSE)

# plot frequencies
freq_table_sample_Cd4 <- as.data.frame(prop.table(x =
table(Idents(Combined.Cd4), Combined.Cd4@meta.data$status_strain), margin =
2))
ggplot(data=freq_table_sample_Cd4, aes(x=freq_table_sample_Cd4$Var2,
y=freq_table_sample_Cd4$Freq, fill=freq_table_sample_Cd4$Var1)) +
geom_bar(stat="identity", color="black") + labs(x="Sample", y="Proportion of
Cells", fill="Cluster")  + scale_x_discrete(limits =
rev(levels(freq_table_sample_Cd4$Var2)))

#####Isolate the Th2s
```

```
#Select clusters containing Th2
Combined.th2 <- subset(Combined, idents = c("Th2"), invert = FALSE)
DimPlot(Combined.th2, reduction = "umap", split.by = "status_strain")

# re-clusterting, without the other cell types
DefaultAssay(object = Combined.th2) <- "integrated"
# Run the standard workflow for visualization and clustering
Combined.th2 <- ScaleData(object = Combined.th2, verbose = FALSE)
Combined.th2 <- RunPCA(object = Combined.th2, npcs = 50, verbose = FALSE)
# t-SNE and Clustering
Combined.th2 <- RunUMAP(object = Combined.th2, reduction = "pca", dims =
1:30)
Combined.th2 <- FindNeighbors(object = Combined.th2, reduction = "pca", dims
= 1:30)
Combined.th2 <- FindClusters(Combined.th2, resolution = 0.5)
DimPlot(object = Combined.th2, reduction = "umap")

DimPlot(Combined.th2, reduction = "umap", split.by = 'status_strain', label
= TRUE)
# find conserved markers for the clusters
Combined.th2.markers <- FindAllMarkers(Combined.th2, only.pos = TRUE,
min.pct = 0.25, logfc.threshold = 0.25)
Combined.th2.markers %>% group_by(cluster) %>% top_n(2)

#find top 10 exprressed genes for each cluster + export to csv
DefaultAssay(Combined.th2) <- "integrated"
Th2top10 <- Combined.th2.markers %>%
  group_by(cluster) %>%
  top_n(n = 10, wt = avg_log2FC)
DoHeatmap(
  Combined.th2,
  features = Tregtop10$gene,
  cells = NULL,
  group.by = "ident",
  group.bar = TRUE,
  group.colors = NULL,
  disp.min = -2.5,
  slot = "scale.data",
  assay = NULL,
  label = TRUE,
  size = 4,
  hjust = 0,
  angle = 0,
)+ NoLegend() + theme(axis.text.y = element_text(size = 6))

# plot frequencies
freq_table_sample <- as.data.frame(prop.table(x =
table(Idents(Combined.th2), Combined.th2@meta.data$status_strain), margin =
2))
ggplot(data=freq_table_sample, aes(x=freq_table_sample$Var2,
y=freq_table_sample$Freq, fill=freq_table_sample$Var1)) +
geom_bar(stat="identity", color="black") + labs(x="Sample", y="Proportion of
Cells", fill="Cluster")  + scale_x_discrete(limits =
rev(levels(freq_table_sample$Var2)))

#####Isolate the Tregs

#Select clusters containing Tregs
Combined.tregs <- subset(Combined, idents = c("Tregs"), invert = FALSE)
```

```
DimPlot(Combined.tregs, reduction = "umap", split.by = "status_strain")

# re-clusterting, without the other cell types
DefaultAssay(object = Combined.tregs) <- "integrated"
# Run the standard workflow for visualization and clustering
Combined.tregs <- ScaleData(object = Combined.tregs, verbose = FALSE)
Combined.tregs <- RunPCA(object = Combined.tregs, npcs = 50, verbose =
FALSE)
# t-SNE and Clustering
Combined.tregs <- RunUMAP(object = Combined.tregs, reduction = "pca", dims =
1:30)
Combined.tregs <- FindNeighbors(object = Combined.tregs, reduction = "pca",
dims = 1:30)
Combined.tregs <- FindClusters(Combined.tregs, resolution = 0.5)
DimPlot(object = Combined.tregs, reduction = "umap")

DimPlot(Combined.tregs, reduction = "umap", split.by = 'status_strain',
label = TRUE)
# find conserved markers for the clusters
Combined.treg.markers <- FindAllMarkers(Combined.tregs, only.pos = TRUE,
min.pct = 0.25, logfc.threshold = 0.25)
Combined.treg.markers %>% group_by(cluster) %>% top_n(2)

#find top 10 exprressed genes for each cluster + export to csv
DefaultAssay(Combined.tregs) <- "integrated"
Tregtop10 <- Combined.treg.markers %>%
  group_by(cluster) %>%
  top_n(n = 10, wt = avg_log2FC)
DoHeatmap(
  Combined.tregs,
  features = Tregtop10$gene,
  cells = NULL,
  group.by = "ident",
  group.bar = TRUE,
  group.colors = NULL,
  disp.min = -2.5,
  slot = "scale.data",
  assay = NULL,
  label = TRUE,
  size = 4,
  hjust = 0,
  angle = 0,
)+ NoLegend() + theme(axis.text.y = element_text(size = 6))

Combined$celltype.group <- Combined$name, Combined$status_strain, sep = "_")
Combined$celltype.group <- paste(Idents(Combined), Combined$status_strain,
sep = "_")
Combined$celltype <- Idents(Combined)
comparison="."

## Differential expression

############################ Th2 C57 vs BALB
#Set up gene matrix with average expression for MA plot
Treg.raw.data <- as.matrix(GetAssayData(Combined.tregs, slot = "counts",
assay = "RNA")[, WhichCells(Combined.th2)])
mean_exp_marker <- rowMeans( Treg.raw.data[ row.names(BalbNvHTreg.response),
] )
#Run FindMarkers to find differentially expressed genes
```

```
Idents(Combined.tregs) <- "status_strain"

#Run differential expression
BalbNvHTreg.response <- FindMarkers(Combined.tregs, ident.1 = "BALB_Naive",
ident.2 = "BALB_Hp",min.cells.group = 1, min.cells.feature = 1, verbose =
TRUE, min.pct = 1)
RidgePlot(Combined.tregs, features = "Ctla4", group.by = "status_strain")
#Combine FindMarkers output and average expression of each gene

BalbNvHTreg.response$baseMean <- mean_exp_marker
row.names(BalbNvHTreg.response)

#Rename the column headers to be ggmaplot compatible
BalbNvHTreg.response <- BalbNvHTreg.response %>%
  rename(
     padj = p_val_adj,
     log2FoldChange = avg_log2FC
  )
BalbNvHTreg.response <- BalbNvHTreg.response %>%
  rename(
    padj = p_val_adj,
    log2FoldChange = avg_log2FC
  )
names(BalbNvHTreg.response)[2] <-log2FoldChange

#Set up a gene list as an input for ggmaplot
Gene_list_b6vbalbHpolynTh2.response <- rownames(b6vbalbHpolyTreg.response)

#Run ggmaplot to plot the results
ggmaplot(b6vbalbHpolyTreg.response, main = expression("C57 Hp d7" %->% "BALB
Hp d7"),
         fdr = 0.05, fc = 1, size = 0.4,
         palette = c("#B31B21", "#1465AC", "darkgray"),
         genenames = as.vector(diff_express$rownames),
         select.top.method = "fc",
         legend = "top", top =1000,
         label.select = Gene_list_b6vbalbHpolynTh2.response,
         font.label = c("bold", 11),
         font.legend = "bold",
         font.main = "bold",
         ggtheme = ggplot2::theme_minimal())

EnhancedVolcano(b6vbalbHpolyTreg.response,
                lab = rownames(b6vbalbHpolyTreg.response),
                x = 'avg_log2FC',
                y = 'p_val_adj',
                xlim = c(-5, 8),
                title = 'Genes down- or up- regulated in d7 infected BALB/c
mice compared to d7 infected C57BL/6 mice',
                pCutoff = 10e-1,
                FCcutoff = 0.5,
                pointSize = 3.0,
                labSize = 4.5)

####Pathway analysis of all clusters
Combined.Cd4$names <- paste(Idents(Combined.Cd4))
Idents(Combined.tregs) <- "status_strain"
gsva_result_treg_status <- analyse_sc_clusters(Combined.tregs, verbose =
TRUE, create_reports = TRUE)
```

```
gsva_result
pathway_expression <- pathways(gsva_result)
colnames(pathway_expression) <- gsub("\\.Seurat", "",
colnames(pathway_expression))

pathway_expression[1:3,]

max_difference <- do.call(rbind, apply(pathway_expression, 1, function(row)
{
  values <- as.numeric(row[2:length(row)])
  return(data.frame(name = row[1], min = min(values), max = max(values)))
}))

max_difference$diff <- max_difference$max - max_difference$min

# sort based on the difference
max_difference <- max_difference[order(max_difference$diff, decreasing = T),
]

head(max_difference)

# limit to selected T cell related pathways
relevant_pathways <- c("R-HSA-388841", "R-HSA-202403", "R-HSA-389513", "R-
HSA-389356", "R-HSA-8877330", "R-HSA-3249367", "R-HSA-202424", "R-HSA-
6785807", "R-HSA-9020591", "R-HSA-9006936", "R-HSA-6783783", "R-HSA-
9014843")
plot_gsva_heatmap(gsva_result,
                  pathway_ids = relevant_pathways, # limit to these pathways
                  margins = c(15,30), # adapt the figure margins in
heatmap.2
                  dendrogram = "col", # only plot column dendrogram
                  scale = "row", # scale for each pathway
                  key = FALSE, # don't display the color key
                  lwid=c(0.1,4)) # remove the white space on the left
```

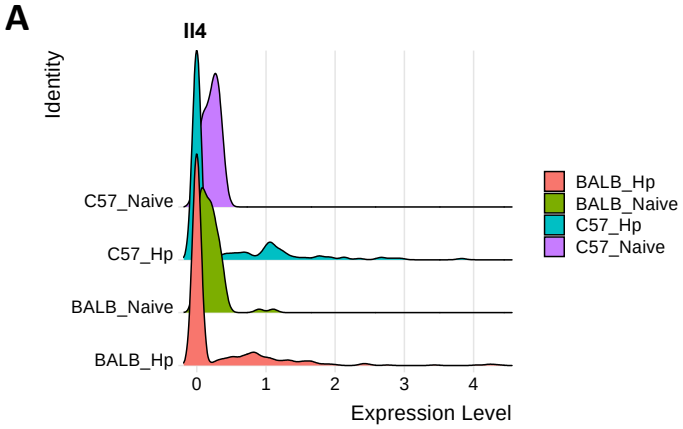

Supplementary Figure 3.1 Ridge plot showing the distribution of Th2 cells along the expression spectrum of Il4. (A) Ridge plot showing the expression of *Il4* in Th2 cells from naïve and *H. polygyrus* infected Foxp3^{GFP} C57BL/6 and Foxp3^{GFP} BALB/c mice.
Ridge plot generated using RidgePlot function in Seurat.

References

Adegnika, A.A., de Vries, S.G., Zinsou, F.J., Honkepehedji, Y.J., Dejon Agobé, J.C., Vodonou, K.G., Bikangui, R., Bouyoukou Hounkpatin, A., Bache, E.B., Massinga Loembe, M., van Leeuwen, R., Molemans, M., Kremsner, P.G., Yazdanbakhsh, M., Hotez, P.J., Bottazzi, M.E., Li, G., Bethony, J.M., Diemert, D.J., *et al.* (2021) Safety and immunogenicity of co-administered hookworm vaccine candidates Na-GST-1 and Na-APR-1 in Gabonese adults: a randomised, controlled, double-blind, phase 1 dose-escalation trial, *The Lancet Infectious Diseases*, 21(2), pp. 275–285.

Ahn, J. bin, Kang, S.A., Kim, D.H. and Yu, H.S. (2016) Activation and recruitment of regulatory T cells via chemokine receptor activation in Trichinella spiralis-infected mice, *Korean Journal of Parasitology*, 54(2), pp. 163–171.

Ajuebor, M.N., Hogaboam, C.M., Kunkel, S.L., Proudfoot, A.E.I. and Wallace, J.L. (2001) The Chemokine RANTES Is a Crucial Mediator of the Progression from Acute to Chronic Colitis in the Rat, *The Journal of Immunology*, 166(1), pp. 552–558.

Akram, A. and Inman, R.D. (2012) Immunodominance: A pivotal principle in host response to viral infections, *Clinical Immunology*, 143(2), pp. 99–115.

Albonico, M., Stoltzfus, R.J., Savioli, L., Tielsch, J.M., Chwaya, H.M., Ercole, E. and Cancrini, G. (1998) Epidemiological evidence for a differential effect of hookworm species, Ancylostoma duodenale or Necator americanus, on iron status of children, *International Journal of Epidemiology*, 27(3), pp. 530–537.

Alvarez, F., Fritz, J.H. and Piccirillo, C.A. (2019) Pleiotropic effects of IL-33 on CD4+ T cell differentiation and effector functions, *Frontiers in Immunology*, 10, p. Article-522.

Anbu, K.A. and Joshi, P. (2008) Identification of a 55 kDa Haemonchus contortus excretory/secretory glycoprotein as a neutrophil inhibitory factor, *Parasite Immunology*, 30, pp. 23–30.

Antas, P.R.Z., Oliveira, E.B., Milagres, A.S., Franken, K.C., Ottenhoff, T.H.M., Klatser, P., Sarno, E.N. and Sampaio, E.P. (2002) Kinetics of T cell-activation molecules in response to Mycobacterium tuberculosis antigens, *Memorias do Instituto Oswaldo Cruz*, 97(8), pp. 1097–1099.

Appleman, L.J. and Boussiotis, V.A. (2003) T cell anergy and costimulation, *Imm. Rev.*, 192, pp. 161–180.

Ariyaratne, A., Kim, S.Y., Pollo, S.M.J., de Cassia Luzzi, M., Bowron, J., Szabo, E., Wasmuth, J.D., Nair, M.G. and Finney, C.A.M. (2020). Host protection to intestinal worm infections: the importance of activated and armed innate effector cells at the host parasite interface. *BioRChiV preprint*.

Asiedu, S.O., Kwarteng, A., Amewu, E.K.A., Kini, P., Aglomasa, B.C. and Forkuor, J.B. (2021) Financial burden impact quality of life among lymphatic Filariasis patients, *BMC Public Health*, 21(1), pp. 1–10.

Athie-Morales, V., Smits, H.H., Cantrell, D.A. and Hilkens, C.M.U. (2004) Sustained IL-12 Signaling Is Required for Th1 Development, *The Journal of Immunology*, 172(1), pp. 61–69.

Baaten, B.J.G., Li, C.R. and Bradley, L.M. (2010) Multifaceted regulation of T cells by CD44, *Communicative and Integrative Biology*, 3(6), pp. 508–512.

Babu, B. v., Nayak, A.N. and Dhal, K. (2005) Epidemiology of episodic adenolymphangitis: A longitudinal prospective surveillance among a rural community endemic for bancroftian filariasis in coastal Orissa, India, *BMC Public Health*, 5, pp. 1–6.

Babu, S. and Nutman, T.B. (2014) Immunology of lymphatic filariasis, *Parasite Immunology*, 36(8), pp. 338–346.

Bacchetta, R., Barzaghi, F. and Roncarolo, M.G. (2016) From IPEX syndrome to FOXP3 mutation: A lesson on immune dysregulation, *Annals of the New York Academy of Sciences*, 1417(1), pp. 5–22.

Bager, P., Arnved, J., Rønborg, S., Wohlfahrt, J., Poulsen, L.K., Westergaard, T., Petersen, H.W., Kristensen, B., Thamsborg, S., Roepstorff, A., Kapel, C. and Melbye, M. (2010) Trichuris suis ova therapy for allergic rhinitis: A randomized, double-blind, placebo-controlled clinical trial, *Journal of Allergy and Clinical Immunology*, 125, pp. 1–3.

Bancroft, A., Else, K. and Grencis, R. (1994) Low-level infection with Trichuris muris significantly affects the polarization of the CD4 response, *Eur J Immunol*, 24, pp. 3113–3118.

Barnden, M.J., Allison, J., Heath, W.R. and Carbone, F.R. (1998) Defective TCR expression in transgenic mice constructed using cDNA- based α- and ß-chain genes under the control of heterologous regulatory elements, *Immunology and Cell Biology*, 76(1), pp. 34–40.

Bashir, M.E.H., Andersen, P., Fuss, I.J., Shi, H.N. and Nagler-Anderson, C. (2002) An Enteric Helminth Infection Protects Against an Allergic Response to Dietary Antigen, *The Journal of Immunology*, 169(6), pp. 3284–3292.

Behnke, J.M., Lowe, A., Clifford, S. and Wakelin, D. (2003). Cellular and serological responses in resistant and susceptible mice exposed to repeated infection with Heligmosomoides polygyrus. *Parasite Immunol,* 25, pp. 333-340.

Belkaid, Y. (2007) Regulatory T cells and infection: A dangerous necessity, *Nature Reviews Immunology*, 7(11), pp. 875–888.

Bending, D., Martín, P.P., Paduraru, A., Ducker, C., Marzaganov, E., Laviron, M., Kitano, S. and Miyachi, H. (2018) A timer for analyzing temporally dynamic changes in transcription during differentiation in vivo, *Journal of Cell Biology*, 217(8), pp. 2931–2950.

Bending, D., Paduraru, A., Ducker, C.B., Martín, P.P. and Crompton, T. (2018) A temporally dynamic Foxp 3 autoregulatory transcriptional circuit controls the effector Treg programme, *The EMBO Journal*, 37, p. e99013.

Benson, M.J., Pino-Lagos, K., Rosemblatt, M. and Noelle, R.J. (2007) All-trans retinoic acid mediates enhanced T reg cell growth, differentiation, and gut homing in the face of high levels of co-stimulation, *Journal of Experimental Medicine*, 204(8), pp. 1765–1774.

Bethony, J., Brooker, S., Albanico, M., Geiger, S., Loukas, A., Diemert, D. and Hotez, P. (2006) Soil-transmitted helminth infections: ascariasis, trichuriasis, and hookworm, *Lancet*, 367, pp. 1521–1532.

Bettini, M.L., Bettini, M. and Vignali, D.A.A. (2012) T-cell receptor retrogenic mice: A rapid, flexible alternative to T-cell receptor transgenic mice, *Immunology*, 136(3), pp. 265–272.

Bhattacharyya, N.D. and Feng, C.G. (2020) Regulation of T Helper Cell Fate by TCR Signal Strength, *Frontiers in Immunology*, 11, p. Article-624.

Bhaumik, S., Mickael, M.E., Moran, M., Spell, M. and Basu, R. (2021) RORγt Promotes Foxp3 Expression by Antagonizing the Effector Program in Colonic Regulatory T Cells, *The Journal of Immunology*, 207(8), pp. 2027–2038.

Blaxter, M.L., Dorris, M., Frisse, L.M., Vida, J.T. and Thomas, W.K. (1998) A molecular evolutionary framework for the phylum Nematoda, *Nature*, 392, pp. 71–75.

Blum, A.M., Hang, L., Setiawan, T., Urban, J.P., Stoyanoff, K.M., Leung, J. and Weinstock, J. V. (2012) Heligmosomoides polygyrus bakeri Induces Tolerogenic Dendritic Cells that Block Colitis and Prevent Antigen-Specific Gut T Cell Responses , *The Journal of Immunology*, 189(5), pp. 2512–2520.

Blum, J.S., Wearsch, P.A. and Cresswell, P. (2013) Pathways of antigen processing, *Annual Review of Immunology*, pp. 443–473.

Bour-Jordan, H., Esensten, J.H., Martinez-Llordella, M., Penaranda, C., Stumpf, M. and Bluestone, J.A. (2011) Intrinsic and extrinsic control of peripheral T-cell tolerance by costimulatory molecules of the CD28/B7 family, *Immunological Reviews*, 241(1), pp. 180–205.

Bousso, P. (2008) T-cell activation by dendritic cells in the lymph node: Lessons from the movies, *Nature Reviews Immunology*, 8(9), pp. 675–684.

Bowron, J., Ariyaratne, A., Luzzi, M. de C., Szabo, E. and Finney, C.A.M. (2020) Suppressive mechanisms by Heligmosomoides polygyrus-induced Tregs in C57BL/6 mice change over time and differ to that of naïve mice, *European Journal of Immunology*, 50(8), pp. 1167–1173.

Bradbury, R.S. and Graves, P.M. (2016) Current WHO protocols for mass drug administration in helminth control, *Microbiology Australia*, 37(1), p. 10.

Brailsford, T.J. and Behnke, J.M. (1992). The dynamics of trickle infections with Heligmosomoidespolygyrus in syngeneic strains of mice. *Int. J. Parasitol,* 22, pp. 351–359.

Broomfield, M.A., Doyle, E.K., Kahn, L.P., Smith, W.D. and Walkden-Brown, S.W. (2020). A simplified Barbervax vaccination regimen in lambs to evoke immunological protection to Haemonchus contortus. *Vet Par,* 287, Article-109243.

Buch, T., Heppner, F.L., Tertilt, C., Heinen, T.J.A.J., Kremer, M., Wunderlich, F.T., Jung, S. and Waisman, A. (2005). A Cre-inducible diphtheria toxin receptor mediates cell lineage ablation after toxin administration. *Nature Methods*, 2(6), pp. 419-426.

Buck, A.H., Coakley, G., Simbari, F., McSorley, H.J., Quintana, J.F., le Bihan, T., Kumar, S., Abreu-Goodger, C., Lear, M., Harcus, Y., Ceroni, A., Babayan, S.A., Blaxter, M., Ivens, A. and Maizels, R.M. (2014) Exosomes secreted by nematode parasites transfer small RNAs to mammalian cells and modulate innate immunity, *Nature Communications*, 5, p. Article-5488.

Bundy, D.A.P., Cooper, E.S., Thompson, D.E., Didier, J.M., Anderson, R.M. and Simmons, I. (1987) Predisposition to Trichuris trichiura infection in humans, *Epidemiology and Infection*, 98(1), pp. 65–71.

Burke, M.L., Jones, M.K., Gobert, G.N., Li, Y.S., Ellis, M.K. and McManus, D.P. (2009) Immunopathogenesis of human schistosomiasis, *Parasite Immunology*, 31(4), pp. 163–176.

Butler, A., Hoffman, P., Smibert, P., Papalexi, E. and Satija, R. (2018) Integrating single-cell transcriptomic data across different conditions, technologies, and species, *Nature Biotechnology*, 36(5), pp. 411–420.

Cabreira-Cagliari, C., Dias, N.D.C., Bohn, B., Fagundes, D.G.D.S., Margis-Pinheiro, M., Bodanese-Zanettini, M.H. and Cagliari, A. (2018) Revising the PLAC8 gene family: From a central role in differentiation, proliferation, and apoptosis in mammals to a multifunctional role in plants, *Genome*, 61(12), pp. 857–865.

Campbell, C.H. (1955) The Antigenic Role of the Excretions and Secretions of Trichinella spiralis in the Production of Immunity in Mice, *Source: The Journal of Parasitology*, 41(5), pp. 483–491.

Cançado, G.G.L., Fiuza, J.A., de Paiva, N.C.N., Lemos, L.D.C.D., Ricci, N.D., Gazzinelli-Guimarães, P.H., Martins, V.G., Bartholomeu, D.C., Negrão-Corrêa, D.A., Carneiro, C.M. and Fujiwara, R.T. (2011) Hookworm products ameliorate dextran sodium sulfate-induced colitis in BALB/c mice, *Inflammatory Bowel Diseases*, 17(11), pp. 2275–2286.

Cao, X., Cai, S.F., Fehniger, T.A., Song, J., Collins, L.I., Piwnica-Worms, D.R. and Ley, T.J. (2007) Granzyme B and Perforin Are Important for Regulatory T Cell-Mediated Suppression of Tumor Clearance, *Immunity*, 27(4), pp. 635–646.

Centre for Disease Control (2021) *Neglected Tropical Diseases*. Date accessed:19/08/2021, Available online: https://www.cdc.gov/globalhealth/ntd/diseases/index.html

Chang, H.C., Zhang, S., Thieu, V.T., Slee, R.B., Bruns, H.A., Laribee, R.N., Klemsz, M.J. and Kaplan, M.H. (2005) PU.1 expression delineates heterogeneity in primary Th2 cells, *Immunity*, 22(6), pp. 693–703.

Chattopadhyay, P.K., Yu, J. and Roederer, M. (2006) Live-cell assay to detect antigen-specific CD4+ T-cell responses by CD154 expression, *Nature Protocols*, 1(1), pp. 1–6.

Chauché, C., Vacca, F., Chia, S.L., Richards, J., Gregory, W.F., Ogunkanbi, A., Wear, M. and McSorley, H.J. (2020) A Truncated Form of HpARI Stabilizes IL-33, Amplifying Responses to the Cytokine, *Frontiers in Immunology*, 11(June), pp. 1–10.

Chauhan, S.K., Saban, D.R., Lee, H.K. and Dana, R. (2009) Levels of Foxp3 in regulatory T cells reflect their functional status in transplantation 1, *J Immunol*, 182(1), pp. 148–153.

Chen, C.C., Louie, S., McCormick, B., Walker, W.A. and Shi, H.N. (2005) Concurrent infection with an intestinal helminth parasite impairs host resistance to enteric Citrobacter rodentium and enhances Citrobacter-induced colitis in mice, *Infection and Immunity*, 73(9), pp. 5468–5481.

Chen, F., Wu, W., Millman, A., Craft, J.F., Chen, E., Patel, N., Boucher, J.L., Urban, J.F., Kim, C.C. and Gause, W.C. (2014) Neutrophils prime a long-lived effector macrophage phenotype that mediates accelerated helminth expulsion, *Nature Immunology*, 15(10), pp. 938–946.

Chen, L. and Flies, D.B. (2013) Molecular mechanisms of T cell co-stimulation and co-inhibition, *Nature Reviews Immunology*, 13(4), pp. 227–242.

Chen, T., Hou, X., Ni, Y., Du, W., Han, H., Yu, Y. and Shi, G. (2018) The imbalance of FOXP3/GATA3 in regulatory T cells from the peripheral blood of asthmatic patients, *Journal of Immunology Research*, 2018, pp. 1–10.

Chen, W. and ten Dijke, P. (2016) Immunoregulation by members of the TGFß superfamily, *Nature Reviews Immunology*, 16(12), pp. 723–740.

Chen, W.J., Jin, W., Hardegen, N., Lei, K.J., Li, L., Marinos, N., McGrady, G. and Wahl, S.M. (2003) Conversion of Peripheral CD4+CD25- Naive T Cells to CD4+CD25+ Regulatory T Cells by TGF-ß Induction of Transcription Factor Foxp3, *Journal of Experimental Medicine*, 198(12), pp. 1875–1886.

Cheng, J., Liao, J., Shao, X., Lu, X. and Fan, X. (2021) Multiplexing Methods for Simultaneous Large-Scale Transcriptomic Profiling of Samples at Single-Cell Resolution, *Advanced Science*, 8(17), p. 2101229.

Cho, Y. bin, Lee, I.G., Joo, Y.H., Hong, S.H. and Seo, Y.J. (2020) Tcr transgenic mice: a valuable tool for studying viral immunopathogenesis mechanisms, *International Journal of Molecular Sciences*, 21(24), pp. 1–12.

Choi, Y.S., Eto, D., Yang, J.A., Lao, C. and Crotty, S. (2013) Cutting Edge: STAT1 Is Required for IL-6–Mediated Bcl6 Induction for Early Follicular Helper Cell Differentiation, *The Journal of Immunology*, 190(7), pp. 3049–3053.

Cibrián, D. and Sánchez-madrid, F. (2017) CD69 : from activation marker to metabolic gatekeeper, *European Journal of Immunology*, 47(6), pp. 946–953.

Coakley, G., McCaskill, J.L., Borger, J.G., Simbari, F., Robertson, E., Millar, M., Harcus, Y., McSorley, H.J., Maizels, R.M. and Buck, A.H. (2017) Extracellular Vesicles from a Helminth Parasite Suppress Macrophage Activation and Constitute an Effective Vaccine for Protective Immunity, *Cell Reports*, 19(8), pp. 1545–1557.

Cook, L., Reid, K.T., Häkkinen, E., de Bie, B., Tanaka, S., Smyth, D.J., White, M.P.J., Wong, M.Q., Huang, Q., Gillies, J.K., Ziegler, S.F., Maizels, R.M. and Levings, M.K. (2021) Induction of stable human FOXP3+ Tregs by a parasite-derived TGF-ß mimic, *Immunology and Cell Biology*, 99(8), pp. 833–847.

Croft, A.M., Bager, P. and Garg, S.K. (2012) Helminth therapy (worms) for allergic rhinitis, *Cochrane Database of Systematic Reviews*, 4, p. CD009238.

Crotty, S. (2014) T Follicular Helper Cell Differentiation, Function, and Roles in Disease, *Immunity*, 41(4), pp. 529–542.

Crotty, S. (2015a) A brief history of T cell help to B cells, *Nature Reviews Immunology*, 15(3), pp. 185–189.

Culpepper, G.A., Wysocka, M., Trinchieri, G., Murphy, K.M., E Macatonia, A.S., Hosken, N.A., Litton, M., Vieira, P. and Hsieh, C.S. (1995) T Dendritic cells produce IL-12 and direct the development of Th1 cells from naive CD4+ T cells, *J Immunol*, 154, pp. 5071–5079.

Dainichi, T., Maekawa, Y., Ishii, K., Zhang, T., Fawzy Nashed, B., Sakai, T., Takashima, M. and Himeno, K. (2001) Nippocystatin, a cysteine protease inhibitor from Nippostrongylus brasiliensis, inhibits antigen processing and modulates antigen-specific immune response, *Infection and Immunity*, 69(12), pp. 7380–7386.

Daveson, A.J., Jones, D.M., Gaze, S., McSorley, H., Clouston, A., Pascoe, A., Cooke, S., Speare, R., Macdonald, G.A., Anderson, R., McCarthy, J.S., Loukas, A. and Croese, J. (2011) Effect of hookworm infection on wheat challenge in celiac disease - a randomised double-blinded placebo controlled trial, *PLoS ONE*, 6(3), p. e17366.

Diemert, D.J., Pinto, A.G., Freire, J., Jariwala, A., Santiago, H., Hamilton, R.G., Periago, M.V., Loukas, A., Tribolet, L., Mulvenna, J., Correa-Oliveira, R., Hotez, P.J. and Bethony, J.M. (2012) Generalized urticaria induced by the Na-ASP-2 hookworm vaccine: Implications for the development of vaccines against helminths, *Journal of Allergy and Clinical Immunology*, 130(1), pp. 169-176.e6.

Dienz, O. and Rincon, M. (2009) The effects of IL-6 on CD4 T cell responses, *Clinical Immunology*, 130(1), pp. 27–33.

Domogalla, M.P., Rostan, P. v., Raker, V.K. and Steinbrink, K. (2017) Tolerance through education: How tolerogenic dendritic cells shape immunity, *Frontiers in Immunology*, 8, p. Article-1764.

Drurey, C., Coakley, G. and Maizels, R.M. (2020) Extracellular vesicles: new targets for vaccines against helminth parasites, *International Journal for Parasitology*, 50(9), pp. 623–633.

Eberl, G. and Pradeu, T. (2017) Towards a General Theory of Immunity?, *Trends in Immunology*, 39(4), pp. 261–263.

Efimova, O. v. and Kelley, T.W. (2009) Induction of granzyme B expression in T-cell receptor/CD28-stimulated human regulatory T cells is suppressed by inhibitors of the PI3K-mTOR pathway, *BMC Immunology*, 10, pp. 1–13.

Ehsan, M., Hu, R.S., Liang, J.L., Song, X., Yan, R., Zhu, X.Q. and Li, X. (2020). Advances in the Development of Anti-Haemonchus contortus Vaccines: Challenges, Opportunities, and Perspectives. *Vaccines*, 8, Article-8030555.

Eisenbarth, S.C. (2019) Dendritic cell subsets in T cell programming: location dictates function, *Nature Reviews Immunology*, 19(2), pp. 89–103.

Elgueta, R., Benson, M.J., De Vries, V.C., Wasiuk, A., Guo, Y. and Noelle, R.J. (2009) Molecular mechanism and function of CD40/CD40L engagement in the immune system, *Immunological Reviews*, 229(1), pp. 152–172.

Elliott, D.E., Setiawan, T., Metwali, A., Blum, A., Urban, J.F. and Weinstock, J. v. (2004) Heligmosomoides polygyrus inhibits established colitis in IL-10-deficient mice, *European Journal of Immunology*, 34(10), pp. 2690–2698.

Esensten, J.H., Helou, Y.A., Chopra, G., Weiss, A. and Bluestone, J.A. (2016) CD28 costimulation: from mechanism to therapy, *Immunity*, 30(45), pp. 6347–6358.

Esser-von Bieren, J., Mosconi, I., Guiet, R. Piersgilli, A., Volpe, B., Chen, F., Gause, W.C., Seitz, A., Verbeek, J.S. and Harris, N.L. (2013). Antibodies Trap Tissue Migrating Helminth Larvae and Prevent Tissue Damage by Driving IL-4Ra-Independent Alternative Differentiation of Macrophages. *PLoS Pathogens*, 9(11), e1003771.

Eto, D., Lao, C., DiToro, D., Barnett, B., Escobar, T.C., Kageyama, R., Yusuf, I. and Crotty, S. (2011) IL-21 and IL-6 are critical for different aspects of B cell immunity and redundantly induce optimal follicular helper CD4 T cell (Tfh) differentiation, *PLoS ONE*, 6(3), p. e17739.

Evans, H. and Mitre, E. (2015) Worms as therapeutic agents for allergy and asthma: Understanding why benefits in animal studies have not translated into clinical success, *Journal of Allergy and Clinical Immunology*, 135(2), pp. 343–353.

Fallarino, F., Grohmann, U., Hwang, K.W., Orabona, C., Vacca, C., Bianchi, R., Belladonna, M.L., Fioretti, M.C., Alegre, M.L. and Puccetti, P. (2003) Modulation of tryptophan catabolism by regulatory T cells, *Nature Immunology*, 4(12), pp. 1206–1212.

Faustino, L.D., Griffith, J.W., Rahimi, R.A., Nepal, K., Hamilos, D.L., Cho, J.L., Medoff, B.D., Moon, J.J., Vignali, D.A.A. and Luster, A.D. (2020) Interleukin-33 activates regulatory T cells to suppress innate γδ T cell responses in the lung, *Nature Immunology*, 21(11), pp. 1371–1383.

Feng, T., Cao, A.T., Weaver, C.T., Elson, C.O. and Cong, Y. (2011) Interleukin-12 converts Foxp3+ regulatory T cells to interferonγ-producing Foxp3+ T cells that inhibit colitis, *Gastroenterology*, 140(7), pp. 2031–2043.

Fernandez-Ruiz, D., Lau, L.S., Ghazanfari, N., Jones, C.M., Ng, W.Y., Davey, G.M., Berthold, D., Holz, L., Kato, Y., Enders, M.H., Bayarsaikhan, G., Hendriks, S.H., Lansink, L.I.M., Engel, J.A., Soon, M.S.F., James, K.R., Cozijnsen, A., Mollard, V., Uboldi, A.D., *et al.* (2017) Development of a Novel CD4(+) TCR Transgenic Line That Reveals a Dominant Role for CD8(+) Dendritic Cells and CD40 Signaling in the Generation of Helper and CTL Responses to Blood-Stage Malaria., *Journal of immunology (Baltimore, Md. : 1950)*, p. ji1700186.

Ferreira, I., Smyth, D., Gaze, S., Aziz, A., Giacomin, P., Ruyssers, N., Artis, D., Laha, T., Navarro, S., Loukas, A. and McSorleya, H.J. (2013) Hookworm excretory/secretory products induce interleukin-4 (il-4)+ il-10+ cd4+ t cell responses and suppress pathology in a mouse model of colitis, *Infection and Immunity*, 81(6), pp. 2104–2111.

Ferrer-Font, L., Mehta, P., Harmos, P., Schmidt, A.J., Chappell, S., Price, K.M., Hermans, I.F., Ronchese, F., le Gros, G. and Mayer, J.U. (2020) High-dimensional analysis of intestinal immune cells during helminth infection, *eLife*, 9, pp. 1–16.

Filbey, K.J., Grainger, J.R., Smith, K.A., Boon, L., van Rooijen, N., Harcus, Y., Jenkins, S., Hewitson, J.P. and Maizels, R.M. (2014) Innate and adaptive type 2 immune cell responses in genetically controlled resistance to intestinal helminth infection, *Immunology and Cell Biology*, 92(5), pp. 436–448.

Filbey, K.J., Varyani, F., Harcus, Y., Hewitson, J.P., Smyth, D.J., McSorley, H.J., Ivens, A., Nylén, S., Rottenberg, M., Löser, S. and Maizels, R.M. (2019) Macrophage migration inhibitory factor (MIF) is essential for type 2 effector cell immunity to an intestinal helminth parasite, *Frontiers in Immunology*, 10, p. Article-2375.

Finney, C.A.M., Taylor, M.D., Wilson, M.S. and Maizels, R.M. (2007) Expansion and activation of CD4+CD25+ regulatory T cells in Heligmosomoides polygyrus infection, *European Journal of Immunology*, 37(7), pp. 1874–1886.

Fleming, J.O. and Weinstock, J. v. (2015) Clinical trials of helminth therapy in autoimmune diseases: Rationale and findings, *Parasite Immunology*. Blackwell Publishing Ltd, pp. 277–292.

Fontenot, J.D., Rasmussen, J.P., Williams, L.M., Dooley, J.L., Farr, A.G. and Rudensky, A.Y. (2005). Regulatory T Cell Lineage Specification by the Forkhead Transcription Factor Foxp3. *Immunity*, 22 pp. 329-341.

Francisco, L.M., Salinas, V.H., Brown, K.E., Vanguri, V.K., Freeman, G.J., Kuchroo, V.K. and Sharpe, A.H. (2009) PD-L1 regulates the development, maintenance, and function of induced regulatory T cells, *Journal of Experimental Medicine*, 206(13), pp. 3015–3029.

Fransen, F., Zagato, E., Mazzini, E., Fosso, B., Manzari, C., Aidy, S.E., Chiavelli, A., D'Erchia, A.M., Sethi, M.K., Pabst, O., Marzano, M., Moretti, S, Romani, L., Penna, G., Pesole, G. and Rescigno, M. (2015). BALB/c and C57BL/6 Mice Differ in Polyreactive IgA Abundance, which Impacts the Generation of Antigen-Specific IgA and Microbiota Diversity. *Immunity*, 43, pp. 527-540.

Frew, J.W. (2019) The hygiene hypothesis, old friends, and new genes, *Frontiers in Immunology*, 10, p. Article-388.

Friedman, J.F., Mital, P., Kanzaria, H.K., Olds, G.R. and Kurtis, J.D. (2007) Schistosomiasis and pregnancy, *Trends in Parasitology*, 23(4), pp. 159–164.

Fujimoto, M., Nakano, M., Terabe, F., Kawahata, H., Ohkawara, T., Han, Y., Ripley, B., Serada, S., Nishikawa, T., Kimura, A., Nomura, S., Kishimoto, T. and Naka, T. (2011) The Influence of Excessive IL-6 Production In Vivo on the Development and Function of Foxp3 + Regulatory T Cells , *The Journal of Immunology*, 186(1), pp. 32–40.

Gabriel, S.S., Bon, N., Chen, J., Wekerle, T., Bushell, A., Fehr, T. and Cippà, P.E. (2016) Distinctive expression of Bcl-2 factors in regulatory T cells determines a pharmacological target to induce immunological tolerance, *Frontiers in Immunology*, 7(MAR), p. Article-73.

Garg, S.K., Croft, A.M. and Bager, P. (2014) Helminth therapy (worms) for induction of remission in inflammatory bowel disease, *Cochrane Database of Systematic Reviews*, 1, p. CD009400.

Gause, W.C., Wynn, T.A. and Allen, J.E. (2013) Type 2 immunity and wound healing: Evolutionary refinement of adaptive immunity by helminths, *Nature Reviews Immunology*, 13(8), pp. 607–614.

George, P.J., Anuradha, R., Kumar, N.P., Kumaraswami, V., Nutman, T.B. and Babu, S. (2012) Evidence of Microbial Translocation Associated with Perturbations in T Cell and Antigen-Presenting Cell Homeostasis in Hookworm Infections, *PLoS Neglected Tropical Diseases*, 6(10), p. e1830.

Gfeller, D. and Bassani-Sternberg, M. (2018) Predicting antigen presentation-What could we learn from a million peptides?, *Frontiers in Immunology*. Frontiers Media S.A., pp. 1–17.

di Giovangiulio, M., Rizzo, A., Franzè, E., Caprioli, F., Facciotti, F., Onali, S., Favale, A., Stolfi, C., Fehling, H.J., Monteleone, G. and Fantini, M.C. (2019) Tbet Expression in Regulatory T Cells Is Required to Initiate Th1-Mediated Colitis, *Frontiers in Immunology*, 10, p. Article-2158.

Girgis, N., Mahesh Gundra, U. and Loke, P. (2013) Immune Regulation during Helminth Infections, *PLoS Pathogens*, 9(4), p. e1003250.

Goronzy, J.J. and Weyand, C.M. (2008) T-cell co-stimulatory pathways in autoimmunity, *Arthritis Research and Therapy*, 10, p. S3.

Graham, D.B., Luo, C., O'Connell, D.J., Lefkovith, A., Brown, E.M., Yassour, M., Varma, M., Abelin, J.G., Conway, K.L., Jasso, G.J., Matar, C.G., Carr, S.A. and Xavier, R.J. (2018) Antigen discovery and specification of immunodominance hierarchies for MHCII-restricted epitopes, *Nature Medicine*, 24(11), pp. 1762–1772.

Grainger, J.R., Smith, K.A., Hewitson, J.P., McSorley, H.J., Harcus, Y., Filbey, K.J., Finney, C.A.M., Greenwood, E.J.D., Knox, D.P., Wilson, M.S., Belkaid, Y., Rudensky, A.Y. and Maizels, R.M. (2010) Helminth secretions induce de novo T cell Foxp3 expression and regulatory function through the TGF-ß pathway, *Journal of Experimental Medicine*, 207(11), pp. 2331–2341.

Griss, J., Viteri, G., Sidiropoulos, K., Nguyen, V., Fabregat, A. and Hermjakob, H. (2020) ReactomeGSA - Efficient Multi-Omics Comparative Pathway Analysis, *Molecular and Cellular Proteomics*, 19(12), pp. 2115–2124.

Groth, B., Smith, A. and Higgins, C. (2004) T cell activation: in vivo veritas, *Immunology and cell biology*, 82(3), pp. 260–268.

Gumly, T.P., Mckenzie, I.F. and Sandrin, M.S. (1995) Tissue expression, structure and function of the murine Ly-6 family of molecules, *Immunology and Cell Biology*, 73(4), pp. 277–296.

Hadaschik, E.N., Wei, X., Leiss, H., Heckmann, B., Niederreiter, B., Steiner, G., Ulrich, W., Enk, A.H., Smolen, J.S. and Stummvoll, G.H. (2015) Regulatory T cell-deficient scurfy mice develop systemic autoimmune features resembling lupus-like disease, *Arthritis Research and Therapy*, 17(1), pp. 1–12.

Hagan, P., Behnke, J. and Parish, H. (1981) Stimulation of immunity to Nematospiroides dubius in mice using larvae attenuated by cobalt 60 irradiation, *Parasite Immunology*, 3, pp. 149–156.

Hang, L., Setiawan, T., Blum, A.M., Urban, J.F., Stoyanoff, K.M., Arihiro, S., Reinecker, H.-C. and Weinstock, J. v. (2010a) Heligmosomoides polygyrus infection can inhibit colitis through direct interaction with innate immunity, *J Immunol*, 185(6).

Hang, L., Setiawan, T., Blum, A.M., Urban, J.F., Stoyanoff, K.M., Arihiro, S., Reinecker, H.-C. and Weinstock, J. v. (2010b) Heligmosomoides polygyrus

infection can inhibit colitis through direct interaction with innate immunity, *J Immunol*, 185(6), pp. 3184–3189.
Haque, A., Engel, J., Teichmann, S.A. and Lönnberg, T. (2017) A practical guide to single-cell RNA-sequencing for biomedical research and clinical applications, *Genome Medicine*. BioMed Central Ltd., pp. 1–12.
Harnett, M.M., Deehan, M.R., Williams, D.M. and Harnett, W. (1998) Induction of signalling anergy via the T-cell receptor in cultured Jurkat T cells by pre-exposure to a filarial nematode secreted product, *Parasite Immunology*, 20, pp. 551–563.
Harnett, W., Worms, M.J., Kapil, A., Grainger, M. and Parkhousef, R.M.E. (1989) Origin, kinetics of circulation and fate in vivo of the major excretory-secretory product of Acanthocheilonema viteae, *Parasitology*, 99, pp. 229–239.
Harriman, S.G.R., Kunimoto, D.Y., Elliott, J.F. and Paetkau, V. (1988) The role of IL-5 in IgA B cell differentiation, *J Immunol*, 140, pp. 3033–3039.
Hartmann, S., Kyewski, B., Sonnenburg, B. and Lucius, R. (1997) A filarial cysteine protease inhibitor down- regulates T cell proliferation and enhances interleukin-10 production, *Eur. J. Immunol.*, 27, pp. 2253–2260.
Hartmann, W., Brunn, M.L., Stetter, N., Gagliani, N., Muscate, F., Stanelle-Bertram, S., Gabriel, G. and Breloer, M. (2019) Helminth Infections Suppress the Efficacy of Vaccination against Seasonal Influenza, *Cell Reports*, 29(8), pp. 2243-2256.e4.
Hartmann, W., Marsland, B.J., Otto, B., Urny, J., Fleischer, B. and Korten, S. (2011) A Novel and Divergent Role of Granzyme A and B in Resistance to Helminth Infection, *The Journal of Immunology*, 186(4), pp. 2472–2481.
Hata, A.N., Engelman, J.A. and Faber, A.C. (2015) The BCL2 family: Key mediators of the apoptotic response to targeted anticancer therapeutics, *Cancer Discovery*, 5(5), pp. 475–487.
Helmby, H. (2015) Human helminth therapy to treat inflammatory disorders-where do we stand?, *BMC Immunology*, 16(1), pp. 1–5.
Hewitson, J., Filbey, K.J., Esser-von Bieren, J., Camberis, M., Schwartz, C., Murray, J., Reynolds, L.A., Blair, N., Robertson, E., Harcus, Y., Boon, L., Huang, S.C.C., Yang, L., Tu, Y., Miller, M.J., Voehringer, D., le Gros, G., Harris, N. and Maizels, R.M. (2015) Concerted Activity of IgG1 Antibodies and IL-4/IL-25-Dependent Effector Cells Trap Helminth Larvae in the Tissues following Vaccination with Defined Secreted Antigens, Providing Sterile Immunity to Challenge Infection, *PLoS Pathogens*, 11(3), pp. 1–22.
Hewitson, J., Filbey, K.J., Grainger, J.R., Dowle, A.A., Pearson, M., Murray, J., Harcus, Y. and Maizels, R.M. (2011) Heligmosomoides polygyrus Elicits a Dominant Nonprotective Antibody Response Directed against Restricted Glycan and Peptide Epitopes, *The Journal of Immunology*, 187(9), pp. 4764–4777.
Hewitson, J., Harcus, Y., Murray, J., van Agtmaal, M., Filbey, K.J., Grainger, J.R., Bridgett, S., Blaxter, M.L., Ashton, P.D., Ashford, D.A., Curwen, R.S., Wilson, R.A., Dowle, A.A. and Maizels, R.M. (2011) Proteomic analysis of secretory products from the model gastrointestinal nematode Heligmosomoides polygyrus reveals dominance of Venom Allergen-Like (VAL) proteins, *Journal of Proteomics*, 74(9), pp. 1573–1594.
Hewitson, J., Ivens, A.C., Harcus, Y., Filbey, K.J., McSorley, H.J., Murray, J., Bridgett, S., Ashford, D., Dowle, A.A. and Maizels, R.M. (2013) Secretion of Protective Antigens by Tissue-Stage Nematode Larvae Revealed by

Proteomic Analysis and Vaccination-Induced Sterile Immunity, *PLoS Pathogens*, 9(8), p. e1003492.
Hewitson, J. and Maizels, R.M. (2014) Vaccination against helminth parasite infections, *Expert Review of Vaccines*, 13(4), pp. 473–487.
Hicks, S.C., Townes, F.W., Teng, M. and Irizarry, R.A. (2018) Missing data and technical variability in single-cell RNA-sequencing experiments, *Biostatistics*, 19(4), pp. 562–578.
Hoogerwerf, M.-A., Coffeng, L.E., Brienen, E.A., Janse, J.J., Langenberg, M.C., Kruize, Y.C., Gootjes, C., Manurung, M.D., Dekker, M., Becker, L., Erkens, M.A., van der Beek, M.T., Ganesh, M.S., Feijt, C., Winkel, B.M., Westra, I.M., Meij, P., Loukas, A., Visser, L.G., *et al.* (2019) New insights into the kinetics and variability of egg excretion in controlled human hookworm infections, *The Journal of Infectious Diseases*, 220(6), pp. 1044–1048.
Hoogerwerf, M.A., Koopman, J.P.R., Janse, J.J., Langenberg, M.C.C., van Schuijlenburg, R., Kruize, Y.C.M., Brienen, E.A.T., Manurung, M.D., Verbeek-Menken, P., van der Beek, M.T., Westra, I.M., Meij, P., Visser, L.G., van Lieshout, L., de Vlas, S.J., Yazdanbakhsh, M., Coffeng, L.E. and Roestenberg, M. (2021) A Randomized Controlled Trial to Investigate Safety and Variability of Egg Excretion after Repeated Controlled Human Hookworm Infection, *Journal of Infectious Diseases*, 223(5), pp. 905–913.
Hotez, P.J., Bethony, J.M., Diemert, D.J., Pearson, M. and Loukas, A. (2010) Developing vaccines to combat hookworm infection and intestinal schistosomiasis, *Nature Reviews Microbiology*, 8(11), pp. 814–826.
Hotez, P.J., Brooker, S., Bethony, J.M., Bottazzi, M.E., Loukas, A. and Xiao, S. (2004) Hookworm Infection, *The New England Journal of Medicine*, 351, pp. 799–807.
Hotez, P.J., Diemert, D., Bacon, K.M., Beaumier, C., Bethony, J.M., Bottazzi, M.E., Brooker, S., Couto, A.R., da Silva Freire, M., Homma, A., Lee, B.Y., Loukas, A., Loblack, M., Morel, C.M., Oliveira, R.C. and Russell, P.K. (2013) The human hookworm vaccine, *Vaccine*, 31(SUPPL2), pp. 227–232.
Hou, T.Z., Qureshi, O.S., Wang, C.J., Baker, J., Young, S.P., Walker, L.S.K. and Sansom, D.M. (2015) A Transendocytosis Model of CTLA-4 Function Predicts Its Suppressive Behavior on Regulatory T Cells, *The Journal of Immunology*, 194(5), pp. 2148–2159.
Hoze, E., Tsaban, L., Maman, Y. and Louzoun, Y. (2013) Predictor for the effect of amino acid composition on CD4+ T cell epitopes preprocessing, *Journal of Immunological Methods*, 391(1–2), pp. 163–173.
Hunter, C.A. and Jones, S.A. (2015) IL-6 as a keystone cytokine in health and disease, *Nature Immunology*, 16(5), pp. 448–457.
Hunter, M.C., Teijeira, A. and Halin, C. (2016) T cell trafficking through lymphatic vessels, *Frontiers in Immunology*, 7, p. Article-613.
Imbratta, C., Hussein, H., Andris, F. and Verdeil, G. (2020) c-MAF, a Swiss Army Knife for Tolerance in Lymphocytes, *Frontiers in Immunology*, 11, p. Article-206.
Iwai, Y., Ishida, M., Tanaka, Y., Okazaki, T., Honjo, T. and Minato, N. (2002) Involvement of PD-L1 on tumor cells in the escape from host immune system and tumor immunotherapy by PD-L1 blockade, *PNAS*, 99(19), pp. 12293–12297.
Jarrett, E., Mackenzie, S. and Bennich, H. (1980) Parasite-induced “nonspecific” IgE does not protect against allergic reactions., *Nature*, 283, pp. 302–304.

Jenkins, M.K., Khoruts, A., Ingulli, E., Mueller, D.L., Mcsorley, S.J., Reinhardt, R.L., Itano, A. and Pape, K.A. (2001) In vivo activation of antigen specific CD4 T cells, *Annu Rev Immunol*, 19, pp. 23–45.

Jennings, E., Elliot, T.A.E., Thawait, N., Kanabar, S., Yam-Puc, J.C., Ono, M., Toellner, K.M., Wraith, D.C., Anderson, G. and Bending, D. (2020) Nr4a1 and Nr4a3 Reporter Mice Are Differentially Sensitive to T Cell Receptor Signal Strength and Duration, *Cell Reports*, 33(5), p. 108328.

Jensen, K.K., Andreatta, M., Marcatili, P., Buus, S., Greenbaum, J.A., Yan, Z., Sette, A., Peters, B. and Nielsen, M. (2018) Improved methods for predicting peptide binding affinity to MHC class II molecules, *Immunology*, 154(3), pp. 394–406.

Jia, T.W., Melville, S., Utzinger, J., King, C.H. and Zhou, X.N. (2012) Soil-transmitted helminth reinfection after drug treatment: A systematic review and meta-analysis, *PLoS Neglected Tropical Diseases*, 6(5), p. e1621.

Johnston, C.J.C., Robertson, E., Harcus, Y., Grainger, J.R., Coakley, G., Smyth, D.J., McSorley, H.J. and Maizels, R. (2015) Cultivation of Heligmosomoides Polygyrus: An Immunomodulatory Nematode Parasite and its Secreted Products, *Journal of Visualized Experiments*, 98, pp. 1–10.

Johnston, C.J.C., Smyth, D.J., Kodali, R.B., White, M.P.J., Harcus, Y., Filbey, K.J., Hewitson, J.P., Hinck, C.S., Ivens, A., Kemter, A.M., Kildemoes, A.O., le Bihan, T., Soares, D.C., Anderton, S.M., Brenn, T., Wigmore, S.J., Woodcock, H. v., Chambers, R.C., Hinck, A.P., *et al.* (2017) A structurally distinct TGF-β mimic from an intestinal helminth parasite potently induces regulatory T cells, *Nature Communications*, 8(1), p. 1741.

Joller, N., Lozano, E., Burkett, P.R., Patel, B., Xiao, S., Zhu, C., Xia, J., Tan, T.G., Sefik, E., Yajnik, V., Sharpe, A.H., Quintana, F.J., Mathis, D., Benoist, C., Hafler, D.A. and Kuchroo, V.K. (2014) Treg cells expressing the coinhibitory molecule TIGIT selectively inhibit proinflammatory Th1 and Th17 cell responses, *Immunity*, 40(4), pp. 569–581.

Jung, C., Hugot, J.-P. and Barreau, F. (2010) Peyer's Patches: The Immune Sensors of the Intestine, *International Journal of Inflammation*, 19, pp. 1–12.

Junttila, I.S. (2018) Tuning the cytokine responses: An update on interleukin (IL)-4 and IL-13 receptor complexes, *Frontiers in Immunology*, 9, p. Article-888.

Kang, H.M., Subramaniam, M., Targ, S., Nguyen, M., Maliskova, L., McCarthy, E., Wan, E., Wong, S., Byrnes, L., Lanata, C.M., Gate, R.E., Mostafavi, S., Marson, A., Zaitlen, N., Criswell, L.A. and Ye, C.J. (2018) Multiplexed droplet single-cell RNA-sequencing using natural genetic variation, *Nature Biotechnology*, 36(1), pp. 89–94.

Kanobana, K., Koets, A., Kooyman, F.N.J., Bakker, N., Ploeger, H.W. and Vervelde, L. (2003). B cells and antibody response in calves primary-infected or re-infected with Cooperia oncophora: influence of priming dose and host responder type. *Int J Parasitol*, 33, pp. 1487-1502.

Karwacz, K., Bricogne, C., MacDonald, D., Arce, F., Bennett, C.L., Collins, M. and Escors, D. (2011) PD-L1 co-stimulation contributes to ligand-induced T cell receptor down-modulation on CD8 + T cells, *EMBO Molecular Medicine*, 3(10), pp. 581–592.

Keane, T.M., Goodstadt, L., Danecek, P., White, M.A., Wong, K., Yalcin, B., Heger, A., Agam, A., Slater, G., Goodson, M., Furlotte, N.A., Eskin, E., Nellåker, C., Whitley, H., Cleak, J., Janowitz, D., Hernandez-Pliego, P., Edwards, A., Belgard, T.G., *et al.* (2011) Mouse genomic variation and its effect on phenotypes and gene regulation, *Nature*, 477(7364), pp. 289–294.

King, C.H. (2015) Health metrics for helminth infections, *Acta Tropica*, 141(Part B), pp. 150–160.

King, I.L. and Mohrs, M. (2009) IL-4-producing CD4+ T cells in reactive lymph nodes during helminth infection are T follicular helper cells, *Journal of Experimental Medicine*, 206(5), pp. 1001–1007.

Kitagaki, K., Businga, T.R., Racila, D., Elliott, D.E., Weinstock, J. v. and Kline, J.N. (2006) Intestinal Helminths Protect in a Murine Model of Asthma, *The Journal of Immunology*, 177(3), pp. 1628–1635.

Kitz, A., Marcken, M., Gautron, A., Mitrovic, M., Hafler, D.A. and Dominguez-Villar, M. (2016) AKT isoforms modulate Th1-like Treg generation and function in human autoimmune disease , *EMBO reports*, 17(8), pp. 1169–1183.

Klementowivz, J.E., Travis, M.A., Grencis, R.K. (2012). Trichuris muris: a model gastrointestinal parasite infection. *Semin Immunopathol,* 34(6), pp. 815-828.

Kloosterman, A., Parmentier, H.K. and Ploeger, H.W. (1992). Breeding cattle and sheep for resistance to gastrointestinal nematodes. *Parasitology today*, 8(10), pp. 330-337.

Knipper, J.A., Ivens, A. and Taylor, M.D. (2019) Helminth-induced Th2 cell dysfunction is distinct from exhaustion and is maintained in the absence of antigen, *PLoS Neglected Tropical Diseases*, 13(12), p. e0007908.

Koch, M.A., Tucker-Heard, G., Perdue, N.R., Killebrew, J.R., Urdahl, K.B. and Campbell, D.J. (2009) The transcription factor T-bet controls regulatory T cell homeostasis and function during type 1 inflammation, *Nature Immunology*, 10(6), pp. 595–602.

Komada, H., Nakabayashi, H., Hara, M. and Izutsu, K. (1996) Early Calcium Signaling and Calcium Requirements for the IL-2 Receptor Expression and IL-2 Production in Stimulated Lymphocytes, *CELLULAR IMMUNOLOGY*, 173, pp. 215–220.

Konkel, J.E., Frommer, F., Leech, M.D., Yagita, H., Waisman, A. and Anderton, S.M. (2010) PD-1 signalling in CD4+ T cells restrains their clonal expansion to an immunogenic stimulus, but is not critically required for peptide-induced tolerance, *Immunology*, 130(1), pp. 92–102.

Kotze, A.C. and Prichard, R.K. (2016) Anthelmintic Resistance in Haemonchus contortus. History, Mechanisms and Diagnosis., *Advances in Parasitology*, 93, pp. 397–428.

Kourepini, E., Paschalidis, N., Simoes, D.C.M., Aggelakopoulou, M., Grogan, J.L. and Panoutsakopoulou, V. (2016) TIGIT Enhances Antigen-Specific Th2 Recall Responses and Allergic Disease, *The Journal of Immunology*, 196(9), pp. 3570–3580.

Kumar, P., Bhattacharya, P. and Prabhakar, B.S. (2018) A comprehensive review on the role of co-signaling receptors and Treg homeostasis in autoimmunity and tumor immunity, *Journal of Autoimmunity*, 95(July), pp. 77–99.

Kumari, A.K., Harichandrakumar, K.T., Das, L.K. and Krishnamoorthy, K. (2005) Physical and psychosocial burden due to lymphatic filariasis as perceived by patients and medical experts, *Tropical Medicine and International Health*, 10(6), pp. 567–573.

Kusunoki, T., Sugai, M., Katakai, T., Omatsu, Y., Iyoda, T., Inaba, K., Nakahata, T., Shimizu, A. and Yokota, Y. (2003) TH2 dominance and defective development of a CD8+ dendritic cell subset in Id2-deficient mice, *Journal of Allergy and Clinical Immunology*, 111(1), pp. 136–142.

Lanningham-foster, L., Green, C.L., Langkamp-henken, B., Davis, B.A., Nguyen, K.T., Bender, B.S., Cousins, R.J. and Langkamp-Henken, B. (2002) Overexpression of CRIP in transgenic mice alters cytokine patterns and the immune response, *Am J Physiol Endocrinol Metab*, 282, pp. 1197–1203.

Lee, P.Y., Wang, J.-X., Parisini, E., Dascher, C.C. and Nigrovic, P.A. (2013) Ly6 family proteins in neutrophil biology, *Journal of Leukocyte Biology*, 94(4), pp. 585–594.

Lesley, J., Howes, N., Perschl, A. and Hyman, R. (1994) Hyaluronan Binding Function of CD44 Is Transiently Activated on T Cells during an In Vivo Immune Response, *J. Exp. Med.*, 180, pp. 383–387.

Levine, A.G., Medoza, A., Hemmers, S., Moltedo, B., Niec, R.E., Schizas, M., Hoyos, B.E., Putintseva, E. v., Chaudhry, A., Dikiy, S., Fujisawa, S., Chudakov, D.M., Treuting, P.M. and Rudensky, A.Y. (2017) Stability and function of regulatory T cells expressing the transcription factor T-bet, *Nature*, 546(7658), pp. 421–425.

Li, C., DiSpirito, J.R., Zemmour, D., Spallanzani, R.G., Kuswanto, W., Benoist, C. and Mathis, D. (2018) TCR Transgenic Mice Reveal Stepwise, Multi-site Acquisition of the Distinctive Fat-Treg Phenotype, *Cell*, 174(2), pp. 285-299.e12.

Li, D.Y. and Xiong, X.Z. (2020) ICOS+ Tregs: A Functional Subset of Tregs in Immune Diseases, *Frontiers in Immunology*, 11, p. Article-2104.

Linsley, P.S., Brady, W., Urnes, M., Grosmaire, L.S., Damle, N.K. and Ledbetter, J.A. (1991) CTLA4 Is a Second Receptor for the B Cell Activation Antigen B7, *J Exp Med*, 174, pp. 561–569.

Liu, Q., Dwyer, G.K., Zhao, Y., Li, H., Mathews, L.R., Chakka, A.B., Chandran, U.R., Demetris, J.A., Alcorn, J.F., Robinson, K.M., Ortiz, L.A., Pitt, B.R., Thomson, A.W., Fan, M.H., Billiar, T.R. and Turnquist, H.R. (2019) IL-33–mediated IL-13 secretion by ST2+ Tregs controls inflammation after lung injury, *JCI Insight*, 4(6), p. e123919.

Liu, T., Soong, L., Liu, G., König, R. and Chopra, A.K. (2009) CD44 expression positively correlates with Foxp3 expression and suppressive function of CD4+Tregcells, *Biology Direct*, 4, p. 40.

Loebbermann, J., Thornton, H., Durant, L., Sparwasser, T., Webster, K.E., Sprent, J., Culley, F.J., Johansson, C. and Openshaw, P.J. (2012) Regulatory T cells expressing granzyme B play a critical role in controlling lung inflammation during acute viral infection, *Mucosal Immunology*, 5(2), pp. 161–172.

Loukas, A., Hotez, P.J., Diemert, D., Yazdanbakhsh, M., McCarthy, J.S., Correa-Oliveira, R., Croese, J. and Bethony, J.M. (2016) Hookworm infection, *Nature Reviews Disease Primers*, 2, p. Article-16088.

Louten, J. (2016) Virus Structure and Classification, in *Essential Human Virology.*, pp. 19–29.

Lucca, L.E. and Dominguez-Villar, M. (2020) Modulation of regulatory T cell function and stability by co-inhibitory receptors, *Nature Reviews Immunology*, 20(11), pp. 680–693.

Luckheeram, R.V., Zhou, R., Verma, A.D. and Xia, B. (2012) CD4 +T cells: Differentiation and functions, *Clinical and Developmental Immunology*, 2012, p. 925135.

Lustigman, S., Brotman, B., Huima, T., Prince, A.M. and McKerrow, J.H. (1992) Molecular cloning and characterization of onchocystatin, a cysteine proteinase inhibitor of Onchocerca volvulus, *Journal of Biological Chemistry*, 267(24), pp. 17339–17346.

Lyons, J.J., Liu, Y., Ma, C.A., Yu, X., O'Connell, M.P., Lawrence, M.G., Zhang, Y., Karpe, K., Zhao, M., Siegel, A.M., Stone, K.D., Nelson, C., Jones, N., DiMaggio, T., Darnell, D.N., Mendoza-Caamal, E., Orozco, L., Hughes, J.D., McElwee, J., *et al.* (2017) ERBIN deficiency links STAT3 and TGF-ß pathway defects with atopy in humans, *The Journal of experimental medicine*, 214(3), pp. 669–680.

Maeda, K., Almofty, S.A., Singh, S.K., Eid, M.M.A., Shimoda, M., Ikeda, T., Koito, A., Pham, P., Goodman, M.F. and Sakaguchi, N. (2013) GANP Interacts with APOBEC3G and Facilitates Its Encapsidation into the Virions To Reduce HIV-1 Infectivity, *The Journal of Immunology*, 191(12), pp. 6030–6039.

Mahajan, S., Cervera, A., MacLeod, M., Fillatreau, S., Perona-Wright, G., Meek, S., Smith, A., MacDonald, A. and Gray, D. (2007) The role of ICOS in the development of CD4 T cell help and the reactivation of memory T cells, *European Journal of Immunology*, 37(7), pp. 1796–1808.

Maizels, R.M. (2021) Identifying novel candidates and configurations for human helminth vaccines, *Expert Review of Vaccines*, 20(11), pp. 1389–1393.

Maizels, R.M., Hewitson, J.P., Murray, J., Harcus, Y.M., Dayer, B., Filbey, K.J., Grainger, J.R., McSorley, H.J., Reynolds, L.A. and Smith, K.A. (2012) Immune modulation and modulators in Heligmosomoides polygyrus infection, *Experimental Parasitology*, 132(1), pp. 76–89.

Maizels, R.M., Mcsorley, H.J. and Smyth, D.J. (2014) Helminths in the hygiene hypothesis: Sooner or later?, *Clinical and Experimental Immunology*, 177(1), pp. 38–46.

Maizels, R.M. and Smith, K.A. (2011) Regulatory T Cells in Infection, *Advances in Immunology*. 1st edn, 112, pp. 73–136.

Maizels, R.M., Smits, H.H. and McSorley, H.J. (2018) Modulation of Host Immunity by Helminths: The Expanding Repertoire of Parasite Effector Molecules, *Immunity*, 49(5), pp. 801–818.

Malarkannan, S. (2020) NKG7 makes a better killer, *Nature Immunology*, 21, pp. 1139–1140.

Manoury, B., Gregory, W.F., Maizels, R.M. and Watts, C. (2001) Bm-CPI-2, a cystatin homolog secreted by the filarial parasite Brugia malayi, inhibits class II MHC-restricted antigen processing Bé né dicte, *Current Biology*, 11, pp. 447–451.

Maruszewska-Cheruiyot, M., Donskow-Lysoniewska, K. and Doligalska, M. (2018) Helminth therapy: Advances in the use of parasitic worms against Inflammatory Bowel Diseases and its challenges, *Helminthologia (Poland)*, 55(1), pp. 1–11.

McFarland, J.M., Paolella, B.R., Warren, A., Geiger-Schuller, K., Shibue, T., Rothberg, M., Kuksenko, O., Colgan, W.N., Jones, A., Chambers, E., Dionne, D., Bender, S., Wolpin, B.M., Ghandi, M., Tirosh, I., Rozenblatt-Rosen, O., Roth, J.A., Golub, T.R., Regev, A., *et al.* (2020) Multiplexed single-cell transcriptional response profiling to define cancer vulnerabilities and therapeutic mechanism of action, *Nature Communications*, 11(1), p. Article-4296.

McSorley, H.J., Blair, N.F., Smith, K.A., McKenzie, A.N.J. and Maizels, R.M. (2014) Blockade of IL-33 release and suppression of type 2 innate lymphoid cell responses by helminth secreted products in airway allergy, *Mucosal Immunology*, 7(5), pp. 1068–1078.

McSorley, H.J., Gaze, S., Daveson, J., Jones, D., Anderson, R.P., Clouston, A., Ruyssers, N.E., Speare, R., McCarthy, J.S., Engwerda, C.R., Croese, J. and

Loukas, A. (2011) Suppression of inflammatory immune responses in celiac disease by experimental hookworm infection, *PLoS ONE*, 6(9), p. e24092.
McSorley, H.J., Harcus, Y.M., Murray, J., Taylor, M.D. and Maizels, R.M. (2008) Expansion of Foxp3 + Regulatory T Cells in Mice Infected with the Filarial Parasite Brugia malayi , *The Journal of Immunology*, 181(9), pp. 6456–6466.
McSorley, H.J., O'Gorman, M.T., Blair, N., Sutherland, T.E., Filbey, K.J. and Maizels, R.M. (2012) Suppression of type 2 immunity and allergic airway inflammation by secreted products of the helminth Heligmosomoides polygyrus, *European Journal of Immunology*, 42(10), pp. 2667–2682.
McSorley, S.J., Asch, S., Costalonga, M., Reinhardt, R.L. and Jenkins, M.K. (2002) Tracking Salmonella-specific CD4 T cells in vivo reveals a local mucosal response to a disseminated infection, *Immunity*, 16(3), pp. 365–377.
Mei, C. (2020) Progress on Immunopathogenesis of Hepatic Fibrosis by Schistosome Infections, *Science Journal of Public Health*, 8(5), p. 141.
Mellor, A.L. and Munn, D.H. (2004) IDO expression by dendritic cells: Tolerance and tryptophan catabolism, *Nature Reviews Immunology*, pp. 762–774.
Mikami, N., Kawakami, R., Chen, K.Y., Sugimoto, A., Ohkura, N. and Sakaguchi, S. (2020) Epigenetic conversion of conventional T cells into regulatory T cells by CD28 signal deprivation, *PNAS*, 117(22), pp. 12258–12258.
Miller, T.A. (1964) Effect of X-Irradiation upon the Infective Larvae of Ancylostoma caninum and the Immunogenic Effect in Dogs of a Single Infection with 40 kr-Irradiated Larvae, *Source: The Journal of Parasitology*, 50(6), pp. 735–742.
Miragaia, R.J., Gomes, T., Chomka, A., Jardine, L., Riedel, A., Hegazy, A.N., Whibley, N., Tucci, A., Chen, X., Lindeman, I., Emerton, G., Krausgruber, T., Shields, J., Haniffa, M., Powrie, F. and Teichmann, S.A. (2019) Single-Cell Transcriptomics of Regulatory T Cells Reveals Trajectories of Tissue Adaptation, *Immunity*, 50(2), pp. 493-504.e7.
Mohrs, K., Harris, D.P., Lund, F.E. and Mohrs, M. (2005) Systemic Dissemination and Persistence of Th2 and Type 2 Cells in Response to Infection with a Strictly Enteric Nematode Parasite, *The Journal of Immunology*, 175(8), pp. 5306–5313.
Montaño, K.J., Cue, C. and Sotillo, J. (2021) Rodent Models for the Study of Soil-Transmitted Helminths : A Proteomics Approach, *Front. Cell. Infect. Microbio.*, 11, p. Article-639573.
Morante-Palacios, O., Fondelli, F., Ballestar, E. and Martínez-Cáceres, E.M. (2021) Tolerogenic Dendritic Cells in Autoimmunity and Inflammatory Diseases, *Trends in Immunology*, 42(1), pp. 59–75.
Mortimer, K., Brown, A., Feary, J., Jagger, C., Lewis, S., Antoniak, M., Pritchard, D. and Britton, J. (2006) Dose-ranging study for trials of therepeutic infection with Necator americanus in humans, *Am. J. Med. Hyg.*, 75(5), pp. 914–920.
Mosconi, I., Dubey, L.K., Volpe, B., Esser-von Bieren, J., Zaiss, M.M., Lebon, L., Massacand, J.C. and Harris, N.L. (2015) Parasite proximity drives the expansion of regulatory T cells in Peyer's patches following intestinal helminth infection, *Infection and Immunity*, 83(9), pp. 3657–3665.
Mpairwe, H., Tweyongyere, R. and Elliott, A. (2014) Pregnancy and helminth infections, *Parasite Immunology*, 36(8), pp. 328–337.
Nakajima, T., Kanno, T., Yokoyama, S., Sasamoto, S., Asou, H.K., Tumes, D.J., Ohara, O., Nakayama, T. and Endo, Y. (2021) ACC1-expressing pathogenic T

helper 2 cell populations facilitate lung and skin inflammation in mice, *Journal of Experimental Medicine*, 218(12), p. e20210639.
Nelson, C.A., Petzold, S.J. and Unanue, E.R. (1994) Peptides determine the lifespan of MHC class II molecules in the antigen-presenting cell, *Nature*, 371, pp. 250–252.
Neumann, C., Blume, J., Roy, U., Teh, P.P., Vasanthakumar, A., Beller, A., Liao, Y., Heinrich, F., Arenzana, T.L., Hackney, J.A., Eidenschenk, C., Gálvez, E.J.C., Stehle, C., Heinz, G.A., Maschmeyer, P., Sidwell, T., Hu, Y., Amsen, D., Romagnani, C., *et al.* (2019) c-Maf-dependent Treg cell control of intestinal TH17 cells and IgA establishes host–microbiota homeostasis, *Nature Immunology*, 20(4), pp. 471–481.
Ng, S.S., de Labastida Rivera, F., Yan, J., Corvino, D., Das, I., Zhang, P., Kuns, R., Chauhan, S.B., Hou, J., Li, X.Y., Frame, T.C.M., McEnroe, B.A., Moore, E., Na, J., Engel, J.A., Soon, M.S.F., Singh, B., Kueh, A.J., Herold, M.J., *et al.* (2020) The NK cell granule protein NKG7 regulates cytotoxic granule exocytosis and inflammation, *Nature Immunology*, 21(10), pp. 1205–1218.
Nielsen, M. and Lund, O. (2009) NN-align. An artificial neural network-based alignment algorithm for MHC class II peptide binding prediction, *BMC Bioinformatics*, 10, p. 296.
Nielsen, M., Lund, O., Buus, S. and Lundegaard, C. (2010) MHC Class II epitope predictive algorithms, *Immunology*, pp. 319–328.
Nielsen, M., Lundegaard, C. and Lund, O. (2007) Prediction of MHC class II binding affinity using SMM-align, a novel stabilization matrix alignment method, *BMC Bioinformatics*, 8, pp. 1–12.
Nusse, Y.M., Savage, A.K., Marangoni, P., Rosendahl-Huber, A.K.M., Landman, T.A., de Sauvage, F.J., Locksley, R.M. and Klein, O.D. (2018) Parasitic helminths induce fetal-like reversion in the intestinal stem cell niche, *Nature*, 559(7712), pp. 109–113.
Nutman, T.B. (2015) Looking beyond the induction of Th2 responses to explain immunomodulation by helminths, *Parasite Immunology*, pp. 304–313.
Ohkura, N. and Sakaguchi, S. (2020) Transcriptional and epigenetic basis of Treg cell development and function: its genetic anomalies or variations in autoimmune diseases, *Cell Research*. Springer Nature, pp. 465–474.
Ohnmacht, C., Park, J.-H., Cording, S., Wing, J.B., Atarashi, K., Obata, Y., Gaboriau-Routhiau, V., Marques, R., Dulauroy, S., Fedoseeva, M., Busslinger, M., Cerf-Bensussan, N., Boneca, I.G., Voehringer, D., Hase, K., Honda, K., Sakaguchi, S. and Eberl, G. (2015) The microbiota regulates type 2 immunity through RORγt+ T cells, *Science*, 349(6251), pp. 989–993.
Okada, H., Kuhn, C., Feillet, H. and Bach, J.F. (2010) The “hygiene hypothesis” for autoimmune and allergic diseases: An update, *Clinical and Experimental Immunology*, 160(1), pp. 1–9.
Oldenhove, G., Bouladoux, N., Wohlfert, E.A., Hall, J.A., Chou, D., dos santos, L., O’Brien, S., Blank, R., Lamb, E., Natarajan, S., Kastenmayer, R., Hunter, C., Grigg, M.E. and Belkaid, Y. (2009) Decrease of Foxp3+ Treg Cell Number and Acquisition of Effector Cell Phenotype during Lethal Infection, *Immunity*, 31(5), pp. 772–786.
Osbourn, M., Soares, D.C., Vacca, F., Cohen, E.S., Scott, I.C., Gregory, W.F., Smyth, D.J., Toivakka, M., Kemter, A.M., le Bihan, T., Wear, M., Hoving, D., Filbey, K.J., Hewitson, J.P., Henderson, H., Gonzàlez-Cìscar, A., Errington, C., Vermeren, S., Astier, A.L., *et al.* (2017) HpARI Protein Secreted by a Helminth Parasite Suppresses Interleukin-33, *Immunity*, 47(4), pp. 739-751.e5.

Ovcinnikovs, V., Ross, E.M., Petersone, L., Edner, N.M., Heuts, F., Ntavli, E., Kogimtzis, A., Kennedy, A., Wang, C.J., Bennett, C.L., Sansom, D.M. and Walker, L.S.K. (2019) CTLA-4-mediated transendocytosis of costimulatory molecules primarily targets migratory dendritic cells, *Science Immunology*, 4(35), p. eaaw0902.

Pacholczyk, R. and Kern, J. (2008) The T-cell receptor repertoire of regulatory T cells, *Immunology*, pp. 450–458.

Pastille, E., Frede, A., McSorley, H.J., Gräb, J., Adamczyk, A., Kollenda, S., Hansen, W., Epple, M., Buer, J., Maizels, R.M., Klopfleisch, R. and Westendorf, A.M. (2017) Intestinal helminth infection drives carcinogenesis in colitis-associated colon cancer, *PLoS Pathogens*, 13(9), pp. 1–22.

Patsoukis, N., Li, L., Sari, D., Petkova, V. and Boussiotis, V.A. (2013) PD-1 Increases PTEN Phosphatase Activity While Decreasing PTEN Protein Stability by Inhibiting Casein Kinase 2, *Molecular and Cellular Biology*, 33(16), pp. 3091–3098.

Peixoto, T.V., Carrasco, S., Botte, D.A.C., Catanozi, S., Parra, E.R., Lima, T.M., Ugriumov, N., Soriano, F.G., de Mello, S.B.V., Rodrigues, C.M. and Goldenstein-Schainberg, C. (2019) CD4+CD69+ T cells and CD4+CD25+FoxP3+ Treg cells imbalance in peripheral blood, spleen and peritoneal lavage from pristane-induced systemic lupus erythematosus (SLE) mice, *Advances in rheumatology (London, England)*, 59(1), p. 30.

Pompa-Mera, E.N., Yépez-Mulia, L., Ocaña-Mondragón, A., García-Zepeda, E.A., Ortega-Pierres, G. and González-Bonilla, C.R. (2011) Trichinella spiralis: Intranasal immunization with attenuated Salmonella enterica Carrying a gp43 antigen-derived 30mer epitope elicits protection in BALB/c mice, *Experimental Parasitology*, 129(4), pp. 393–401.

Pritchett-Corning, K.R. and Clifford, C.B. (2012) Parasitic Infections of Laboratory Mice, *The Laboratory Mouse*, pp. 503–518.

Progatzky, F., Shapiro, M., Chng, S.H., Garcia-Cassani, B., Classon, C.H., Sevgi, S., Laddach, A., Bon-Frauches, A.C., Lasrado, R., Rahim, M., Amaniti, E.M., Boeing, S., Shah, K., Entwistle, L.J., Suárez-Bonnet, A., Wilson, M.S., Stockinger, B. and Pachnis, V. (2021) Regulation of intestinal immunity and tissue repair by enteric glia, *Nature*, 599(7883), pp. 125–130.

Puel, A. and Casanova, J.L. (2019) The nature of human IL-6, *The Journal of experimental medicine*, 216(9), pp. 1969–1971.

Qiao, X., Pham, D.N.T., Luo, H. and Wu, J. (2010) Ran overexpression leads to diminished T cell responses and selectively modulates nuclear levels of c-Jun and c-Fos, *Journal of Biological Chemistry*, 285(8), pp. 5488–5496.

Qureshi, O.S., Zheng, Y., Nakamura, K., Attridge, K., Manzotti, C., Schmidt, E.M., Baker, J., Jeffery, L.E., Kaur, S., Briggs, Z., Hou, T.Z., Futter, C.E., Anderson, G., Walker, L.S.K. and Sansom, D.M. (2011) Trans-Endocytosis of CD80 and CD86: A Molecular Basis for the Cell-Extrinsic Function of CTLA-4, *Science*, 332, pp. 600–603.

Radtke, D., Thuma, N., Kirchner, P., Ekici, A.B. and Voehringer, D. (2021) Th2 single-cell heterogeneity and clonal interorgan distribution in helminth-infected mice, *BioRxiv Preprint*, pp. 1–27.

Radulovic, K., Manta, C., Rossini, V., Holzmann, K., Kestler, H.A., Wegenka, U.M., Nakayama, T. and Niess, J.H. (2012) CD69 Regulates Type I IFN-Induced Tolerogenic Signals to Mucosal CD4 T Cells That Attenuate Their Colitogenic Potential, *The Journal of Immunology*, 188(4), pp. 2001–2013.

Radulovic, K., Rossini, V., Manta, C., Holzmann, K., Kestler, H.A. and Niess, J.H. (2013b) The Early Activation Marker CD69 Regulates the Expression of

Chemokines and CD4 T Cell Accumulation in Intestine, *PLoS ONE*, 8(6), p. e65413.

Rausch, S., Huehn, J., Kirchhoff, D., Rzepecka, J., Schnoeller, C., Pillai, S., Loddenkemper, C., Scheffold, A., Hamann, A., Lucius, R. and Hartmann, S. (2008) Functional analysis of effector and regulatory T cells in a parasitic nematode infection, *Infection and Immunity*, 76(5), pp. 1908–1919.

Redpath, S.A., van der Werf, N., Cervera, A.M., Macdonald, A.S., Gray, D., Maizels, R.M. and Taylor, M.D. (2013) ICOS controls Foxp3+ regulatory T-cell expansion, maintenance and IL-10 production during helminth infection, *European Journal of Immunology*, 43(3), pp. 705–715.

Reynisson, B., Barra, C., Kaabinejadian, S., Hildebrand, W.H., Peters, B., Peters, B., Nielsen, M. and Nielsen, M. (2020) Improved Prediction of MHC II Antigen Presentation through Integration and Motif Deconvolution of Mass Spectrometry MHC Eluted Ligand Data, *Journal of Proteome Research*, 19(6), pp. 2304–2315.

Reynolds, L.A., Filbey, K.J. and Maizels, R.M. (2012) Immunity to the model intestinal helminth parasite Heligmosomoides polygyrus, *Seminars in Immunopathology*, 34(6), pp. 829–846.

Rieu, P., Ueda, T., Haruta, I., Sharma, C.E. and Amin Arnaout, M. (1994) The A-Domain of B2 Integrin CR3 (CD11b/CD18) Is a Receptor for the Hookworm-derived Neutrophil Adhesion Inhibitor NIF, *J. Cell. Bio.*, 127(6), pp. 2081–2091.

Riveau, G., Deplanque, D., Remoué, F., Schacht, A.M., Vodougnon, H., Capron, M., Thiry, M., Martial, J., Libersa, C. and Capron, A. (2012) Safety and immunogenicity of rSh28GST antigen in humans: Phase 1 randomized clinical study of a vaccine candidate against urinary schistosomiasis, *PLoS Neglected Tropical Diseases*, 6(7), p. e1704.

Rock, K.L., Reiser, H., Bamezai, A., Mcgrew, J. and Benacerraf, B. (1989) The LY-6 Locus: A Multigene FamilyEncoding Phosphatidylinositol-AnchoredMembrane Proteins Concerned withT-Cell Activation, *Immunological Reviews*, 111(111), pp. 195–224.

Rogers, P.R., Song, J., Gramaglia, I., Killeen, N. and Croft, M. (2001) *OX40 Promotes Bcl-xL and Bcl-2 Expression and Is Essential for Long-Term Survival of CD4 T Cells*, *Immunity*.

Rook, G.A.W. (2010) Darwinian medicine and the “hygiene” or “old friends” hypothesis, *Clinical and Experimental Immunology*, 160(1), pp. 70–79.

Rook, G.A.W. and Brunet, L.R. (2005) Microbes, immunoregulation, and the gut, *Gut*, 54(3), pp. 317–320.

van de Run, M., Heimfeld, S., Spangrude, G.J. and Weissman, I.L. (1989) Mouse hematopoietic stem-cell antigen Sca-1 is a member of the Ly-6 antigen family (ceil surface protein/polymerase chain reaction/immunohistology), *Proc. Nati. Acad. Sci. USA*, 86, pp. 4634–4638.

Ruyssers, N.E., de Winter, B.Y., de Man, J.G., Loukas, A., Pearson, M.S., Weinstock, J. v., van den Bossche, R.M., Martinet, W., Pelckmans, P.A. and Moreels, T.G. (2009) Therapeutic potential of helminth soluble proteins in TNBS induced colitis in mice, *Inflammatory Bowel Diseases*, 15(4), pp. 491–500.

Sakaguchi, S., Yamaguchi, T., Nomura, T. and Ono, M. (2008) Regulatory T Cells and Immune Tolerance, *Cell*, 133(5), pp. 775–787.

Sandborn, W.J., Elliott, D.E., Weinstock, J., Summers, R.W., Landry-Wheeler, A., Silver, N., Harnett, M.D. and Hanauer, S.B. (2013) Randomised clinical trial: The safety and tolerability of Trichuris suis ova in patients with

Crohn's disease, *Alimentary Pharmacology and Therapeutics*, 38(3), pp. 255–263.
Sanjabi, S., Oh, S.A. and Li, M.O. (2017) Regulation of the immune response by TGF-β: From conception to autoimmunity and infection, *Cold Spring Harbor Perspectives in Biology*, 9(6), p. a0222361.
Saunders, K.A., Raine, T., Cooke, A. and Lawrence, C.E. (2007) Inhibition of autoimmune type 1 diabetes by gastrointestinal helminth infection, *Infection and Immunity*, 75(1), pp. 397–407.
Schiering, C., Krausgruber, T., Chomka, A., Fröhlich, A., Adelmann, K., Wohlfert, E.A., Pott, J., Griseri, T., Bollrath, J., Hegazy, A.N., Harrison, O.J., Owens, B.M.J., Löhning, M., Belkaid, Y., Fallon, P.G. and Powrie, F. (2014) The alarmin IL-33 promotes regulatory T-cell function in the intestine, *Nature*, 513(7519), pp. 564–568.
Schneider, B., Jariwala, A.R., Periago, M.V., Gazzinelli, M.F., Bose, S.N., Hotez, P.J., Diemert, D.J. and Bethony, J.M. (2011) A history of hookworm vaccine development, *Human Vaccines*, 7(11), pp. 1234–1244.
Schneidman-Duhovny, D., Khuri, N., Dong, G.Q., Winter, M.B., Shifrut, E., Friedman, N., Craik, C.S., Pratt, K.P., Paz, P., Aswad, F. and Sali, A. (2019) Predicting CD4 T-cell epitopes based on antigen cleavage, MHCII presentation, and TCR recognition, *PLoS ONE*, 13(11), p. e0206654.
Scrivener, S., Yemaneberhan, H., Zebenigus, M., Tilahun, D., Girma, S., Ali, S., McElroy, P., Custovic, A., Woodcock, A., Pritchard, D., Venn, A. and Britton, J. (2001) Independent effects of intestinal parasite infection and domestic allergen exposure on risk of wheeze in Ethiopia: A nested case-control study, *Lancet*, 358(9292), pp. 1493–1499.
See, P., Lum, J., Chen, J. and Ginhoux, F. (2018) A single-cell sequencing guide for immunologists, *Frontiers in Immunology*, 9(OCT), p. Article-2425.
Sefik, E., Geva-zatorsky, N., Oh, S., Konnikova, L., Zemmour, D., Mcguire, A.M., Burzyn, D., Ortiz-lopez, A., Lobera, M., Yang, J., Ghosh, S., Earl, A., Snapper, S.B., Jupp, R., Mathis, D. and Benoist, C. (2016) Individual intestinal symbionts induce a distinct population of RORγ+ regulatory T cells, *Science*, 349(6251), pp. 993–997.
Segura, M., Su, Z., Piccirillo, C. and Stevenson, M.M. (2007) Impairment of dendritic cell function by excretory-secretory products: A potential mechanism for nematode-induced immunosuppression, *European Journal of Immunology*, 37(7), pp. 1887–1904.
Semple, K., Nguyen, A., Yu, Y., Wang, H., Anasetti, C. and Yu, X.Z. (2011) Strong CD28 costimulation suppresses induction of regulatory T cells from naive precursors through Lck signaling, *Blood*, 117(11), pp. 3096–3103.
Sharma, R., Sung, S.S.J., Fu, S.M. and Ju, S. te (2009) Regulation of multi-organ inflammation in the regulatory T cell-deficient scurfy mice, *Journal of Biomedical Science*, 16(1), pp. 1–8.
Sharpe, A.H. and Freeman, G.J. (2002) The B7-CD28 superfamily, *Nature Reviews Immunology*, 2(2), pp. 116–126.
Shevach, E.M. and Thornton, A.M. (2014) tTregs, pTregs, and iTregs: Similarities and differences, *Immunological Reviews*, 259(1), pp. 88–102.
Shevyrev, D. and Tereshchenko, V. (2020) Treg Heterogeneity, Function, and Homeostasis, *Frontiers in Immunology*, 10, p. Article-3100.
Shi, Q., Xu, R., Song, G., Lu, H., Xue, D., He, X. and Xia, Y. (2020) GATA3 suppresses human fibroblasts-induced metastasis of clear cell renal cell carcinoma via an anti-IL6/STAT3 mechanism, *Cancer Gene Therapy*, 27(9), pp. 726–738.

Siede, J., Fröhlich, A., Datsi, A., Hegazy, A.N., Varga, D. v., Holecska, V., Saito, H., Nakae, S. and Löhning, M. (2016) IL-33 receptor-expressing regulatory t cells are highly activated, Th2 biased and suppress CD4 T Cell proliferation through IL-10 and TGFß Release, *PLoS ONE*, 11(8), p. e0161507.

Slade, C.D., Reagin, K.L., Lakshmanan, H.G., Klonowski, K.D. and Watford, W.T. (2020) Placenta-specific 8 limits IFNγ production by CD4 T cells in vitro and promotes establishment of influenza-specific CD8 T cells in vivo, *PLoS ONE*, 15, p. e0235706.

Smallwood, T.B., Giacomin, P.R., Loukas, A., Mulvenna, J.P., Clark, R.J. and Miles, J.J. (2017) Helminth immunomodulation in autoimmune disease, *Frontiers in Immunology*, 8(APR), p. Article-453.

Smith, K.A., Filbey, K.J., Reynolds, L.A., Hewitson, J.P., Harcus, Y., Boon, L., Sparwasser, T., Hämmerling, G. and Maizels, R.M. (2016) Low-level regulatory T-cell activity is essential for functional type-2 effector immunity to expel gastrointestinal helminths, *Mucosal Immunology*, 9(2), pp. 428–443.

Smith, K.A., Hochweller, K., Hämmerling, G.J., Boon, L., MacDonald, A.S. and Maizels, R.M. (2011) Chronic Helminth Infection Promotes Immune Regulation In Vivo through Dominance of CD11c lo CD103 − Dendritic Cells, *The Journal of Immunology*, 186(12), pp. 7098–7109.

Smith, K.A. and Maizels, R.M. (2014) IL-6 controls susceptibility to helminth infection by impeding Th2 responsiveness and altering the Treg phenotype in vivo, *European Journal of Immunology*, 44(1), pp. 150–161.

Smith, W.D., Newlands, G.F.J., Smith, S.K., Pettit, D. and Skuce, P.J. (2003). Metalloendopeptidases from the intestinal brush border of Haemonchus contortus as protective antigens for sheep. *Parasite Immunology*, 25, pp. 313-323,.

Smyth, D.J., Harcus, Y., White, M.P.J., Gregory, W.F., Nahler, J., Stephens, I., Toke-Bjolgerud, E., Hewitson, J.P., Ivens, A., McSorley, H.J. and Maizels, R.M. (2018) TGF-ß mimic proteins form an extended gene family in the murine parasite Heligmosomoides polygyrus, *International Journal for Parasitology*, 48(5), pp. 379–385.

Smyth, D.J., Ren, B., White, M.P.J., McManus, C., Webster, H., Shek, V., Evans, C., Pandhal, J., Fields, F., Maizels, R.M. and Mayfield, S. (2021) Oral delivery of a functional algal-expressed TGF-ß mimic halts colitis in a murine DSS model, *Journal of Biotechnology*, 340(August), pp. 1–12.

Snook, J.P., Kim, C. and Williams, M.A. (2018) TCR signal strength controls the differentiation of CD4 + effector and memory T cells, *Sci. Immunol*, 3, p. 9103.

Sprouse, M.L., Scavuzzo, M.A., Blum, S., Shevchenko, I., Lee, T., Makedonas, G., Borowiak, M., Bettini, M.L. and Bettini, M. (2018) High self-reactivity drives T-bet and potentiates Treg function in tissue-specific autoimmunity, *JCI insight*, 3(2), pp. 1–14.

Stein, M.M., Hrusch, C.L., Gozdz, J., Igartua, C., Pivniouk, V., Murray, S.E., Ledford, J.G., Marques dos Santos, M., Anderson, R.L., Metwali, N., Neilson, J.W., Maier, R.M., Gilbert, J.A., Holbreich, M., Thorne, P.S., Martinez, F.D., von Mutius, E., Vercelli, D., Ober, C., *et al.* (2016) Innate Immunity and Asthma Risk in Amish and Hutterite Farm Children, *New England Journal of Medicine*, 375(5), pp. 411–421.

Stephens, R., Albano, F.R., Quin, S., Pascal, B.J., Harrison, V., Stockinger, B., Kioussis, D., Weltzien, H.U. and Langhorne, J. (2005) Malaria-specific transgenic CD4+T cells protect immunodeficient mice from lethal infection

and demonstrate requirement for a protective threshold of antibody production for parasite clearance, *Blood*, 106(5), pp. 1676–1684.
Stoeckius, M., Zheng, S., Houck-Loomis, B., Hao, S., Yeung, B.Z., Mauck, W.M., Smibert, P. and Satija, R. (2018) Cell Hashing with barcoded antibodies enables multiplexing and doublet detection for single cell genomics, *Genome Biology*, 19(1), pp. 1–12.
Stoltzfus, J.D., Pilgrim, A.A. and Herbert, D.B.R. (2017) Molecular & Biochemical Parasitology Perusal of parasitic nematode ' omics in the post-genomic era, *Molecular & Biochemical Parasitology*, 215, pp. 11–22.
Stone, K.D., Prussin, C. and Metcalfe, D.D. (2010) IgE, mast cells, basophils, and eosinophils, *Journal of Allergy and Clinical Immunology*, 125(2 Suppl 2), pp. s73–s80.
Strachan, D.P. (1989) Hay fever, hygiene, and household size, *BMJ*, 299, pp. 1259–1260.
Stuart, T., Butler, A., Hoffman, P., Hafemeister, C., Papalexi, E., Mauck, W.M., Hao, Y., Stoeckius, M., Smibert, P. and Satija, R. (2019) Comprehensive Integration of Single-Cell Data, *Cell*, 177(7), pp. 1888–1902.
Summers, R. (2003) Trichuris suis seems to be safe and possibly effective in the treatment of inflammatory bowel disease, *The American Journal of Gastroenterology*, 98(9), pp. 2034–2041.
Summers, R.W., Elliot, D.E., Urban, J.F., Thompson, R. and Weinstock, J. v. (2005) Trichuris suis therapy in Crohn's disease, *Gut*, 54(1), pp. 87–90.
Sun, Y., Liu, G., Li, Z., Chen, Y., Liu, Y., Liu, B. and Su, Z. (2013) Modulation of dendritic cell function and immune response by cysteine protease inhibitor from murine nematode parasite Heligmosomoides polygyrus, *Immunology*, 138(4), pp. 370–381.
Tai, X., Laethem, F. van, Pobezinsky, L., Guinter, T., Sharrow, S.O., Adams, A., Granger, L., Kruhlak, M., Lindsten, T., Thompson, C.B., Feigenbaum, L. and Singer, A. (2012) Basis of CTLA-4 function in regulatory and conventional CD4 T cells, *Blood*, 119(22), pp. 5515–5163.
Tan, C.L., Kuchroo, J.R., Sage, P.T., Liang, D., Francisco, L.M., Buck, J., Thaker, Y.R., Zhang, Q., McArdel, S.L., Juneja, V.R., Lee, S.J., Lovitch, S.B., Lian, C., Murphy, G.F., Blazar, B.R., Vignali, D.A.A., Freeman, G.J. and Sharpe, A.H. (2021) PD-1 restraint of regulatory T cell suppressive activity is critical for immune tolerance, *Journal of Experimental Medicine*, 218(1).
Tang, Q., Henriksen, K.J., Boden, E.K., Tooley, A.J., Ye, J., Subudhi, S.K., Zheng, X.X., Strom, T.B. and Bluestone, J.A. (2003) Cutting Edge: CD28 Controls Peripheral Homeostasis of CD4 + CD25 + Regulatory T Cells , *The Journal of Immunology*, 171(7), pp. 3348–3352.
Taylor, M.D., Harris, A., Babayan, S.A., Bain, O., Culshaw, A., Allen, J.E. and Maizels, R.M. (2007) CTLA-4 and CD4 + CD25 + Regulatory T Cells Inhibit Protective Immunity to Filarial Parasites In Vivo , *The Journal of Immunology*, 179(7), pp. 4626–4634.
Tesciuba, A.G., Shilling, R.A., Agarwal, M.D., Bandukwala, H.S., Clay, B.S., Moore, T. v, Weinstock, J. v, Welcher, A.A. and Sperling, A.I. (2008) ICOS Costimulation Expands Th2 Immunity by Augmenting Migration of Lymphocytes to Draining Lymph Nodes 1, *J Immunol*, 181(2), pp. 1019–1024.
Tesseur, I., Zou, K., Berber, E., Zhang, H. and Wyss-Coray, T. (2006). Highly sensitive and specific bioassay for measuring bioactive TGF-ß. *BMC*, 7(15).
Tibbitt, C.A., Stark, J.M., Martens, L., Ma, J., Mold, J.E., Deswarte, K., Oliynyk, G., Feng, X., Lambrecht, B.N., de Bleser, P., Nylén, S., Hammad, H.,

Arsenian Henriksson, M., Saeys, Y. and Coquet, J.M. (2019) Single-Cell RNA Sequencing of the T Helper Cell Response to House Dust Mites Defines a Distinct Gene Expression Signature in Airway Th2 Cells, *Immunity*, 51(1), pp. 169–184.

Tinkler, S.H. (2019) Preventive chemotherapy and anthelmintic resistance of soil-transmitted helminths – Can we learn nothing from veterinary medicine?, *One Health*, 9, p. 100106.

Tischner, D., Gaggl, I., Peschel, I., Kaufmann, M., Tuzlak, S., Drach, M., Thuille, N., Villunger, A. and Jan Wiegers, G. (2012) Defective cell death signalling along the Bcl-2 regulated apoptosis pathway compromises Treg cell development and limits their functionality in mice, *Journal of Autoimmunity*, 38(1), pp. 59–69.

Topalian, S.L., Hodi, F.S., Brahmer, J.R., Gettinger, S.N., Smith, D.C., McDermott, D.F., Powderly, J.D., Carvajal, R.D., Sosman, J.A., Atkins, M.B., Leming, P.D., Spigel, D.R., Antonia, S.J., Horn, L., Drake, C.G., Pardoll, D.M., Chen, L., Sharfman, W.H., Anders, R.A., *et al.* (2012) Safety, Activity, and Immune Correlates of Anti–PD-1 Antibody in Cancer, *New England Journal of Medicine*, 366(26), pp. 2443–2454.

Turner, J.D., Jackson, J.A., Faulkner, H., Behnke, J., Else, K.J., Kamgno, J., Boussinesq, M. and Bradley, J.E. (2008) Intensity of intestinal infection with multiple worm species is related to regulatory cytokine output and immune hyporesponsiveness, *Journal of Infectious Diseases*, 197(8), pp. 1204–1212.

Turner, K.J., Shannahan, K. and Holt, P.G. (1985) Suppression of Allergic Reactivity by Intestinal Helminths: Susceptibility Is a Function of IgE Responder Phenotype, *Archs Allergy appl. Immun*, 78, pp. 329–331.

Vanheerswynghels, M., Toussaint, W., Schuijs, M., Vanhoutte, L., Killeen, N., Hammad, H. and Lambrecht, B.N. (2018) The Generation and Use of Allergen-Specific TCR Transgenic Animals, *Type 2 Immunity*, 1799, pp. 183–210.

Velaga, S., Ukena, S.N., Dringenberg, U., Alter, C., Pardo, J., Kershaw, O. and Franzke, A. (2015) Granzyme a is required for regulatory T-cell mediated prevention of gastrointestinal graft-versus-host disease, *PLoS ONE*, 10(4), p. e0124927.

Venken, K., Hellings, N., Thewissen, M., Somers, V., Hensen, K., Rummens, J.L., Medaer, R., Hupperts, R. and Stinissen, P. (2008) Compromised CD4+ CD25high regulatory T-cell function in patients with relapsing-remitting multiple sclerosis is correlated with a reduced frequency of FOXP3-positive cells and reduced FOXP3 expression at the single-cell level, *Immunology*, 123(1), pp. 79–89.

Vercruysse, J., Levecke, B. and Prichard, R. (2012) Human soil-transmitted helminths: Implications of mass drug administration, *Current Opinion in Infectious Diseases*, 25(6), pp. 703–708.

Verma, N.D., Hall, B.M., Plain, K.M., Robinson, C.M., Boyd, R., Tran, G.T., Wang, C., Bishop, G.A. and Hodgkinson, S.J. (2014) Interleukin-12 (IL-12p70) promotes induction of highly potent Th1-like CD4+CD25+ T regulatory cells that inhibit allograft rejection in unmodified recipients, *Frontiers in Immunology*, 5, p. Article-190.

Vincent, I. and Mechti, N. (2004) IL-6 regulates CD44 cell surface expression on human myeloma cells, *Leukemia*, 18(5), pp. 967–975.

Vyas, J.M., van der Veen, A.G. and Ploegh, H.L. (2008) The known unknowns of antigen processing and presentation, *Nature Reviews Immunology*, 8(8), pp. 607–618.

Walker, L. (2013) Treg and CTLA-4: Two intertwining pathways to immune tolerance, *Journal of Autoimmunity*, 45, pp. 49–57.
Walker, L.S.K. and Sansom, D.M. (2015) Confusing signals: Recent progress in CTLA-4 biology, *Trends in Immunology*, 36(2), pp. 63–70.
Walsh, C.M., Smith, P. and Fallon, P.G. (2007) Role for CTLA-4 but not CD25+ T cells during Schistosoma mansoni infection of mice, *Parasite Immunology*, 29(6), pp. 293–308.
Walunas, T.L., Lenschow, D.J., Bakker, C.Y., Linsley, P.S., Freeman, G.J., Green, J.M., Thompson, C.B. and Bluestone, J.A. (1994) CTLA-4 Can Function as a Negative Regulator of T Cell Activation, *Immunity*, 1, pp. 405–413.
Wan, Y.Y. (2014) GATA3: A master of many trades in immune regulation, *Trends in Immunology*, 35(6), pp. 233–242.
Wang, P., Sidney, J., Dow, C., Mothé, B., Sette, A. and Peters, B. (2008) A systematic assessment of MHC class II peptide binding predictions and evaluation of a consensus approach, *PLoS Computational Biology*, 4(4), p. e1000048.
Wang, P., Sidney, J., Kim, Y., Sette, A., Lund, O., Nielsen, M. and Peters, B. (2010) Peptide binding predictions for HLA DR, DP and DQ molecules, *BMC Bioinformatics*, 11, p. Article-568.
Wang, Y., Su, M.A. and Wan, Y.Y. (2011) An Essential Role of the Transcription Factor GATA-3 for the Function of Regulatory T Cells, *Immunity*, 35(3), pp. 337–348.
Warunek, J., Jin, R.M., Blair, S.J., Garis, M., Marzullo, B. and Wohlfert, E.A. (2021) Tbet expression by Tregs is needed to protect against Th1-mediated immunopathology during Toxoplasma infection in mice, *BioRchiv Preprint*, pp. 1–39.
Watanabe, K., Mwinzi, P.N.M., Black, C.L., Muok, E.M.O., Karanja, D.M.S., Secor, W.E. and Colley, D.G. (2007) T Regulatory Cell Levels Decrease in People Infected With Schistosoma mansoni on Effective Treatment, *Am J Med Hyg*, 77(4), pp. 676–682.
Watanabe, M., Fujihara, C., Radtke, A.J., Chiang, Y.J., Bhatia, S., Germain, R.N. and Hodes, R.J. (2017) Co-stimulatory function in primary germinal center responses: CD40 and B7 are required on distinct antigenpresenting cells, *Journal of Experimental Medicine*, 214(9), pp. 2795–2810.
Watanabe, M., Watanabe, S., Hara, Y., Harada, Y., Kubo, M., Tanabe, K., Toma, H. and Abe, R. (2005) ICOS-Mediated Costimulation on Th2 Differentiation Is Achieved by the Enhancement of IL-4 Receptor-Mediated Signaling, *The Journal of Immunology*, 174(4), pp. 1989–1996.
Webster, H.C., Andrusaite, A.T., Shergold, A.L., Milling, S.W.F. and Perona-Wright, G. (2020) Isolation and functional characterisation of lamina propria leukocytes from helminth-infected, murine small intestine, *Journal of Immunological Methods*, 477, p. Article-112702.
Webster, K.E., Walters, S., Kohler, R.E., Mrkvan, T., Boyman, O., Surh, C.D., Grey, S.T. and Sprent, J. (2009) In vivo expansion of t reg cells with il-2-mab complexes: induction of resistance to eae and long-term acceptance of islet allografts without immunosuppression, *Journal of Experimental Medicine*, 206(4), pp. 751–760.
van der Werf, N., Redpath, S.A., Azuma, M., Yagita, H. and Taylor, M.D. (2013) Th2 Cell-Intrinsic Hypo-Responsiveness Determines Susceptibility to Helminth Infection, *PLoS Pathogens*, 9(3), p. e1003215.

Wheaton, J.D., Yeh, C.-H. and Ciofani, M. (2017) Cutting Edge: c-Maf Is Required for Regulatory T Cells To Adopt RORγt + and Follicular Phenotypes , *The Journal of Immunology*, 199(12), pp. 3931–3936.

White, M.P.J., Johnston, C.J.C., Grainger, J.R., Konkel, J.E., O'Connor, R.A., Anderton, S.M. and Maizels, R.M. (2020) The Helminth Parasite Heligmosomoides polygyrus Attenuates EAE in an IL-4Rα-Dependent Manner, *Frontiers in Immunology*, 11, pp. 1–14.

White, M.P.J., McManus, C.M. and Maizels, R.M. (2020) Regulatory T-cells in helminth infection: induction, function and therapeutic potential, *Immunology*, pp. 248–260.

White, M.P.J., Smyth, D.J., Cook, L., Ziegler, S.F., Levings, M.K. and Maizels, R.M. (2021) The parasite cytokine mimic Hp-TGM potently replicates the regulatory effects of TGF-ß on murine CD4+ T cells, *Immunology and Cell Biology*, 99(8), pp. 848–864.

Wikenheiser, D.J. and Stumhofer, J.S. (2016) ICOS co-stimulation: Friend or foe?, *Frontiers in Immunology*, 7(AUG), pp. 1–16.

Wildin, R.S., Ramsdell, F., Peake, J., Faravelli, F., Casanova, J.-L.-R., Buist, N., Levy-Lahad, E., Mazzella, M., Goulet, O., Perroni, L., Dagna Bricarelli, F., Byrne, G., Mceuen, M., Proll, S., Appleby, M. and Brunkow, M.E. (2000) The immune dysregulation,polyendocrinopathy, enteropathy,X-linked syndrome (IPEX) is causedby mutations of FOXP3, *Proc. Natl. Acad. Sci. USA*, 66, pp. 683–690.

Wilson, M.S., Taylor, M.D., Balic, A., Finney, C.A.M., Lamb, J.R. and Maizels, R.M. (2005) Suppression of allergic airway inflammation by helminth-induced regulatory T cells, *The Journal of Experimental Medicine*, 202(9), pp. 1199–1212.

Wing, K., Onishi, Y., Prieto-Martin, P., Yamaguchi, T., Miyara, M., Fehervari, Z., Nomura, T. and Sakaguchi, S. (2008) CTLA-4 control over Foxp3+ regulatory T cell function, *Science*, 322, pp. 271–275.

Wohlfert, E.A., Grainger, J.R., Bouladoux, N., Konkel, J.E., Oldenhove, G., Ribeiro, C.H., Hall, J.A., Yagi, R., Naik, S., Bhairavabhotla, R., Paul, W.E., Bosselut, R., Wei, G., Zhao, K., Oukka, M., Zhu, J. and Belkaid, Y. (2011) GATA3 controls Foxp3 + regulatory T cell fate during inflammation in mice, *Journal of Clinical Investigation*, 121(11), pp. 4503–4515.

Wohlleben, G., Trujillo, C., Müller, J., Ritze, Y., Grunewald, S., Tatsch, U. and Erb, K.J. (2004) Helminth infection modulates the development of allergen-induced airway inflammation, *International Immunology*, 16(4), pp. 585–596.

Wolf, K.J., Emerson, R.O., Pingel, J., Buller, R.M. and DiPaolo, R.J. (2016) Conventional and regulatory CD4+ T cells that share identical TCRs are derived from common clones, *PLoS ONE*, 11(4), pp. 1–14.

World Health Organisation (2021) *Neglected tropical diseases*. https://www.who.int/health-topics/neglected-tropical-diseases/

Wright, J.E., Werkman, M., Dunn, J.C. and Anderson, R.M. (2018) Current epidemiological evidence for predisposition to high or low intensity human helminth infection: A systematic review, *Parasites and Vectors*, 11(1), pp. 1–12.

Xu, K., Yang, W.Y., Nanayakkara, G.K., Shao, Y., Yang, F., Hu, W., Choi, E.T., Wang, H. and Yang, X. (2018) GATA3, HDAC6, and BCL6 regulate FOXP3+ Treg plasticity and determine Treg conversion into either novel antigen-presenting cell-like Treg or Th1-Treg, *Frontiers in Immunology*, 9(JAN), p. Article-45.

Yang, B., Hagemann, S., Mamareli, P., Lauer, U., Hoffmann, U., Beckstette, M., Fohse, L., Prinz, I., Pezoldt, J., Suerbaum, S., Sparwasser, T., Hamann, A., Floess, S., Huehn, J. and Lochner, M. (2016) Foxp3+ T cells expressing ROR g t represent a stable regulatory T-cell effector lineage with enhanced suppressive capacity during intestinal inflammation, *Nature*, 9(2), pp. 444–457.

Yang, I. v., Pedersen, B.S., Liu, A., O'Connor, G.T., Teach, S.J., Kattan, M., Misiak, R.T., Gruchalla, R., Steinbach, S.F., Szefler, S.J., Gill, M.A., Calatroni, A., David, G., Hennessy, C.E., Davidson, E.J., Zhang, W., Gergen, P., Togias, A., Busse, W.W., *et al.* (2015) DNA methylation and childhood asthma in the inner city, *Journal of Allergy and Clinical Immunology*, 136(1), pp. 69–80.

Yang, Y., Zhang, Z., Yang, J., Chen, X., Cui, S. and Zhu, X. (2010) Oral vaccination with Ts87 DNA vaccine delivered by attenuated Salmonella typhimurium elicits a protective immune response against Trichinella spiralis larval challenge, *Vaccine*, 28(15), pp. 2735–2742.

Yoo, J.K., Cho, J.H., Lee, S.W. and Sung, Y.C. (2002) IL-12 Provides Proliferation and Survival Signals to Murine CD4 + T Cells Through Phosphatidylinositol 3-Kinase/Akt Signaling Pathway , *The Journal of Immunology*, 169(7), pp. 3637–3643.

Yu, L., Yang, F., Zhang, F., Guo, D., Li, L., Wang, X., Liang, T., Wang, J., Cai, Z. and Jin, H. (2018) CD69 enhances immunosuppressive function of regulatory T-cells and attenuates colitis by prompting IL-10 production, *Cell Death and Disease*, 9(9), p. Article-905.

Yu, X., Harden, K., Gonzalez, L.C., Francesco, M., Chiang, E., Irving, B., Tom, I., Ivelja, S., Refino, C.J., Clark, H., Eaton, D. and Grogan, J.L. (2009) The surface protein TIGIT suppresses T cell activation by promoting the generation of mature immunoregulatory dendritic cells, *Nature Immunology*, 10(1), pp. 48–57.

Zakeri, A., Hansen, E.P., Andersen, S.D., Williams, A.R. and Nejsum, P. (2018) Immunomodulation by helminths: Intracellular pathways and extracellular vesicles, *Frontiers in Immunology*, 9, p. Article-2349.

Zaretsky, A.G., Taylor, J.J., King, I.L., Marshall, F.A., Mohrs, M. and Pearce, E.J. (2009) T follicular helper cells differentiate from Th2 cells in response to helminth antigens, *Journal of Experimental Medicine*, 206(5), pp. 991–999.

Zeldenryk, L.M., Gray, M., Speare, R., Gordon, S. and Melrose, W. (2011) The emerging story of disability associated with lymphatic filariasis: A critical review, *PLoS Neglected Tropical Diseases*, 5(12), p. e1366.

Zemmour, D., Zilionis, R., Kiner, E., Klein, A.M., Mathis, D. and Benoist, C. (2018) Single-cell gene expression reveals a landscape of regulatory T cell phenotypes shaped by the TCR article, *Nature Immunology*, 19(3), pp. 291–301.

Zhan, B., Beaumier, C.M., Briggs, N., Jones, K.M., Keegan, B.P., Bottazzi, M.E. and Hotez, P.J. (2014) Advancing a multivalent "Pan-anthelmintic" vaccine against soil-transmitted nematode infections, *Expert Review of Vaccines*, 13(3), pp. 321–331.

Zhang, L., Udaka, K., Mamitsuka, H. and Zhu, S. (2012) Toward more accurate pan-specific MHC-peptide binding prediction: A review of current methods and tools, *Briefings in Bioinformatics*. Oxford University Press, pp. 350–364.

Zhang, R., Huynh, A., Whitcher, G., Chang, J.H., Maltzman, J.S. and Turka, L.A. (2013) An obligate cell-intrinsic function for CD28 in Tregs, *Journal of Clinical Investigation*, 123(2), pp. 580–593.

Zhao, Jingxian, Zhao, Jincun and Perlman, S. (2012) Differential Effects of IL-12 on Tregs and Non-Treg T Cells: Roles of IFN-γ, IL-2 and IL-2R, *PLoS ONE*, 7(9), p. e46241.

Zheng, B., Zhang, J., Chen, H., Nie, H., Miller, H., Gong, Q. and Liu, C. (2020) T Lymphocyte-Mediated Liver Immunopathology of Schistosomiasis, *Frontiers in Immunology*, 11, p. Article-61.

Zhong, S.U. and Dobson, C. (1996) Heligmosomoides polygyrus: Resistance in Inbred, Outbred, and Selected Mice, *Experimental Parasitology*, 82, pp. 122–131.

Zhu, J., Yamane, H., Cote-Sierra, J., Guo, L. and Paul, W.E. (2006) GATA-3 promotes Th2 responses through three different mechanisms: Induction of Th2 cytokine production, selective growth of Th2 cells and inhibition of Th1 cell-specific factors, *Cell Research*, 16(1), pp. 3–10.

Zhu, J., Yamane, H. and Paul, W.E. (2010) Differentiation of effector CD4+ T cell populations, *Annual Review of Immunology*, 28(1), pp. 445–489.